

INFRARED PHOTOMETRIC SCANNING OF GALAXIES

A THESIS SUBMITTED FOR THE  
DEGREE OF DOCTOR OF PHILOSOPHY

by

JACK ABOLINS

Department of Astronomy  
University of Leicester

1980

UMI Number: U440684

All rights reserved

INFORMATION TO ALL USERS

The quality of this reproduction is dependent upon the quality of the copy submitted.

In the unlikely event that the author did not send a complete manuscript and there are missing pages, these will be noted. Also, if material had to be removed, a note will indicate the deletion.



UMI U440684

Published by ProQuest LLC 2015. Copyright in the Dissertation held by the Author.  
Microform Edition © ProQuest LLC.

All rights reserved. This work is protected against  
unauthorized copying under Title 17, United States Code.



ProQuest LLC  
789 East Eisenhower Parkway  
P.O. Box 1346  
Ann Arbor, MI 48106-1346



THESIS  
599994  
2 5 80

x752971793

## C O N T E N T S

	Page No.
SUMMARY	i
SURFACE BRIGHTNESS DISTRIBUTION IN GALAXIES - A BRIEF OUTLINE	iii
CHAPTER 1    A REVIEW OF NEAR INFRARED EXTRAGALACTIC ASTRONOMY	
Formative Years	1.1
Sources of Near Infrared Radiation in Galaxies	1.4
Techniques Available for Galaxy Research	1.10
The Near Infrared Emission of Normal Galaxies	1.14
Effect of Non-stellar Sources on Normal Continua	1.24
Active Galaxies, including QSO's, Seyferts, BL Lacs, Emission Line Galaxies, Radio Galaxies and Peculiar Galaxies	1.27
Spatial Distribution of Near Infrared Radiation in Galaxies	1.43
Addendum (1979 update)	1.50
References to Chapter One	
CHAPTER 2    INSTRUMENTATION AND OBSERVING TECHNIQUES	
Instrumentation	2.1
Observing Techniques	2.11
Data and Data Reduction	2.17
References to Chapter Two	
CHAPTER 3    TWO MICRON OBSERVATIONS OF THE NUCLEAR BULGE OF M31	
Introduction	3.1
Previous Infrared Observations of M31	3.2
Observations and Results	3.3

	Page No.
Discussion	3.5
a) 2.2 $\mu\text{m}$ Brightness Distribution	3.5
b) Colour Gradients in the Bulge	3.8
Conclusions	3.12
CHAPTER 4    MAPPING OF THE CORE AND INNER DISK OF M82 AT TWO MICRONS	
M82 - An Overview	4.1
The Infrared Emission of M82	4.6
Optical, Infrared and Radio Bright Features	4.7
The Case for Two Micron Mapping	4.9
Observations	4.11
Results	4.13
Discussion	4.19
a) Two Micron Morphology	4.19
b) Two Micron Luminosity of the Central 90 pc	4.23
c) Major Axis Brightness Profile	4.25
d) Extinction in the Major Dust Lane	4.27
e) Core in Relation to Other Features	4.28
f) Colour Indices	4.29
g) Conclusions - Nature of the Two Micron Source	4.32
References to Chapter Four	
CHAPTER 5    NEAR INFRARED OBSERVATIONS OF NGC 972	
Introduction	5.1
Observations	5.5
Data Reduction and Results	5.6

	Page No.
Discussion	5.8
a) Gross Features of the Map	5.8
b) Classification of NGC 972	5.11
c) A (B-K) Colour Gradient?	5.12
d) The Two Micron Luminosity	5.13
e) Slit Scans - JHK Colours	5.15
f) NGC 972 as an IO Galaxy	5.17
g) Comparison of the M82 and NGC 972 Observations	5.18
Conclusions	5.20
References to Chapter Five	

APPENDIX: PUBLISHED PAPER FROM THE M82 WORK

SUMMARY

Surface photometric observations at near infrared wavelengths (J, H and K wavebands) of the galaxies M31, M82 and NGC 972 are described and the results discussed in the light of other, recent literature. The techniques used in surface photometry of extended objects at near infrared wavelengths are described and, as an introduction, a detailed review of near infrared, extragalactic astronomy is given.

R.A. and Dec. scans through the centre of M31 show the two micron surface brightness distribution in the nuclear bulge follows the de Vaucouleurs law and that the V-K gradient within the central  $\pm 5$  arcmins is small,  $\Delta(V-K)_{r=5} < 0.1$ . Comparisons are made with other published data.

Photometric scans through the active, central region of M82 reveal that the two micron emission from the galaxy is concentrated within a very high surface brightness "core" source measuring approximately  $25'' \times 8''$  ( $375 \times 120$  pc). The core is surrounded by a disk measuring  $90''$  by  $35''$  ( $1350$  pc  $\times$   $525$  pc) which though of lower surface brightness is still much brighter than the corresponding region in other normal disk systems. Contour maps of the two regions are presented. The asymmetry in the brightness distribution along the major axis is attributed to obscuration by the major dust lane, from which it is inferred that the extinction produced by the lane is,  $A_V \sim 16$ . The two micron core is approximately coincident and co-extensive with the diffuse radio emission and the visible "hot-spot" region, and is probably associated with a burst of star formation near the centre of the galaxy.

Two micron scanning observations of NGC 972 yield a low resolution contour map of the whole galaxy which is similar in some respects to published blue-waveband maps. In particular, the similarity in the gross distribution of B and K light along the major axis suggests

the unusual structure seen at shorter wavelengths cannot be due to dust obscuration as was previously assumed. An exciting possibility arising from this work is that the secondary feature in the southeast of the system may be a small, previously unsuspected, interacting galaxy, which might account for the IO-type appearance of NGC 972. The two micron luminosity of the central region of the galaxy is unusually high for its low mass and young mean spectral type, and is comparable with that of M82. J, H and K slit aperture scans yielded J-H and H-K colour indices which suggest the presence of an extended source of free-free emission near the centre of the galaxy. These are the first reported observations of NGC 972 at infrared wavelengths.

SURFACE BRIGHTNESS DISTRIBUTION IN GALAXIES - A BRIEF OUTLINE

The various morphological types of galaxy and their characteristic surface brightness distributions are often mentioned in this thesis. It is necessary therefore to give a brief introduction to the terms and ideas which will be referred to in the following chapters.

Galaxies exist in three basic structural types: "spheroidal" systems, "disk" systems and "composite" systems, i.e. galaxies which contain both disk and spheroidal components. The purely spheroidal systems are the elliptical galaxies, E0 to E6, and the purely disk systems are the Magellanic Irregulars and the "late-type" spirals, Sc, Sd and Sm. The composite systems are the "early-type" spirals, Sa through Sb, and the lenticular or SO galaxies, and consist of a bright, inner, elliptical-like region (the spheroidal component) and an outer, flattened region of relatively low surface brightness (the disk component). The composite structure of these systems is best seen in the popular textbook photographs of edge-on spirals like the Sombrero galaxy, NGC 4565 and NGC 891.

At visible wavelengths, empirical laws which describe the distribution of brightness within the two components are well known. In the spheroidal region of galaxies, the radial brightness distribution is described by the "de Vaucouleurs  $r^{\frac{1}{4}}$  law" (de Vaucouleurs, 1958):

$$\log \left[ \frac{B(r)}{B(r_e)} \right] = -a \left[ \left( \frac{r}{r_e} \right)^{\frac{1}{4}} - 1 \right]$$

where  $a$  is a constant and  $r_e$  is the radius in which half the total light (of given wavelength) is emitted. This is often expressed as simply:  $\log B(r) \propto (-r^{\frac{1}{4}})$ . Other empirical formulae describing the brightness distribution in spheroidal components are known, but the de Vaucouleurs law is the formula most commonly referred to.

In disk regions the brightness distribution is exponential:

$$B(r) = B_0 e^{-\alpha r}$$

(e.g. Freeman, 1976)

where  $\alpha$  is a constant with units of reciprocal length. The length-scale of the disk,  $\alpha^{-1}$  is more frequently discussed and is quoted in units of kiloparsecs. The disk is sometimes referred to as "the exponential disk". In the work described in the following chapters, two disk galaxies (M82 and NGC 972) and a composite galaxy (M31) have been observed.

In multiaperture photometry the distribution of light in galaxies is often expressed in terms of the quantity  $A/D(0)$ , where  $A$  is the aperture diameter and  $D(0)$  is the diameter of the galaxy at a surface brightness level of  $25 \text{ m}_B/\square$ ". This quantity is frequently referred to in chapter 1 where infrared multiaperture observations are described.

A Review of Near Infrared Extragalactic Astronomy

## 1.1 FORMATIVE YEARS

In the first published measurements of the infrared radiation from galaxies Johnson (1966) discussed the  $1\ \mu\text{m}$  to  $3.5\ \mu\text{m}$  emission from the central 35 arc seconds of ten of the brightest galaxies. The honour of being the very first extragalactic object of any kind to be measured in the infrared, fell however to 3C 273 the brightest Q.S.O. (Johnson 1964, Low and Johnson 1965). The Q.S.O. measurements attracted a great deal of attention to the subject as they showed that 3C 273 radiated most of its energy at infrared wavelengths, so endowing even more prodigious energy to (cosmologically interpreted) Q.S.O.'s. In contrast, Johnson's measurements of colours of normal galaxy nuclei showed no large excesses. These colours could on the whole be interpreted in terms of a normal late type population, though stars of a far cooler nature than any previously believed to inhabit nuclei had to be invoked to fully account for the observed colours. Johnson commented on the (surprising) apparent uniformity of colours among the Hubble types, and upon the lack of exotic quasar-like colours, despite the inclusion of two peculiar galaxies in his sample (M82 and M87). These unexciting results provided a "quiet before the storm". A kindling of popular interest took place when a "mini-quasar" was believed to have been found in the nucleus of the Seyfert galaxy NGC 1068 (Pacholczyk and Wisniewski, 1967). This discovery stimulated intense professional interest in the infrared emission of Seyferts, and in peculiar galaxies generally. As a result the next few years saw a spate of papers on the subject (Oke et al. 1967, Fitch et al. 1967, Wisniewski and Kleinmann 1968, Pacholczyk and Weymann 1968, Moroz and Dibai 1968, Oke et al. 1969, 1970, Pacholczyk 1970, Zwicky et al. 1970, Low and Kleinmann 1968, 1970a,b). The objects studied by these workers included most of the "classical Seyferts" (Seyfert 1943), a number of Q.S.O.'s, BL Lac, some Zwicky compact

galaxies and some non-Seyfert peculiar objects. The general conclusion of all these papers was that Seyfert galaxy nuclei closely resembled Q.S.O.'s in their near infrared continua, and that several non-Seyfert galaxies, notably M82 and M87 showed near infrared excesses. (Not detected by Johnson, 1966!) In M82 the excess in the continuum was steeper than that in most Seyferts, and in M87 the excess originated in the "jet" seen on short exposure plates. The reason for Johnson's failure to detect the excess in M82 is unclear, as this excess is not localised (see chapter on M82) and so miscentring is an unlikely explanation. In M87 however the excess in the jet would have been swamped by the dominating normal galaxy component seen by his large beam. Included in the list of papers above were the first published observations of galaxies at longer infrared wavelengths,  $5 \mu\text{m}$  to  $22 \mu\text{m}$  (Low and Kleinmann, 1968). These showed that Seyfert galaxies exhibit infrared continua which rise, apparently smoothly, from  $1 \mu\text{m}$  to  $20 \mu\text{m}$ , so that most of the energy is located at the longer wavelengths. From the time of the first long wavelength publication, observations in the near infrared ( $1 - 3.5 \mu\text{m}$ ) have attracted less attention than the longer wavelength work. Recently this trend has been reversing somewhat.

During these early years detector sensitivity was such that poor signal to noise ratios were obtained on galaxies. Furthermore galaxies are notoriously difficult objects to centre upon, and the uncertainty introduced by these two factors led to some erroneous reports, usually concerned with variability. Kleinmann and Low (1970a) for instance suggested considerable variability in M82 at wavelengths as short as  $3.5 \mu\text{m}$ . The most infamous examples however were the reports of variability in NGC 1068 at  $2.2 \mu\text{m}$  by Pacholczyk and Co. (1968 and 1970). In both these cases the observers knew full well the limitations of their instruments and the difficulty of the observations and yet chose

to publish without confirmation. Since variable objects and high energy sources were very much in vogue these seem to be classic cases of "seeing what you want to see".

Although these formative years were full of intense activity and debate on the active galaxy side, near infrared research on normal galaxies proceeded at a more sedate pace. After Johnson's pioneer work the main effort in this area came from the Caltech people and included work on the Galactic centre (Becklin and Neugebauer, 1968) and the nucleus of M31 (Sandage, Becklin and Neugebauer, 1969). These papers presented the first description of instrumentation and techniques used in the mapping of extended objects at near infrared wavelengths. The observations of the Galactic centre were the first at wavelengths at which the stellar content could be investigated. This is impossible at visible wavelengths since line-of-sight dust totally obscures light from the centre. Previously the Galactic centre had only been observed at radio wavelengths, but these signals come primarily from HII regions near the centre, not the stellar nucleus. A comparison between the spatial distribution of the  $2.2 \mu\text{m}$  emission from the Galactic centre and that from the nucleus of M31 revealed a close similarity which suggested that the Galaxy has a morphology nearer to Sb than the previously suspected Sc.

The efficacy of infrared observations for seeing through dust was further shown to great advantage when observations of the highly obscured object Maffei 1 at  $1.6 \mu\text{m}$  and  $2.2 \mu\text{m}$  revealed it to be a previously unknown, yet nearby, normal giant elliptical galaxy, comparable in size to the Galaxy and M31 and probably a member of the local group (Spinrad et al., 1971). The infrared continuum of M31 and the (de-reddened) continua of the Galactic centre and Maffei 1 appeared to be very similar to those of other normal galaxies (Johnson, 1966).

By the end of 1971 a total of twenty-six papers had been published containing near infrared observations of galaxies. Twenty-two of these were concerned mainly or exclusively with active galaxies, and only four were devoted to normal galaxies. Poor detector sensitivity restricted useful techniques to broad band photometry, and even with this, galaxy data were accurate to only  $\sim 10-20\%$ . Since 1971 detector sensitivity has been greatly improved and consequently spectrometric and polarimetric measurements are now possible. Accuracy in photometry is nowadays much better and more detailed work, such as the determination of small radial colour changes in galaxies, can now be undertaken.

The following sections of this chapter will review the various observational techniques currently used for galaxy research in the near infrared, and the results achieved with these. Both normal and active galaxies will be discussed. A synopsis of probable sources of near infrared radiation in galaxies is first given and later the effect of non-stellar components on the integrated stellar continuum is considered.

## 1.2 SOURCES AND FEATURES OF NEAR INFRARED RADIATION FROM GALAXIES

The continuum flux from galaxies in the spectral region  $1-4\ \mu\text{m}$  will probably be dominated by the contribution from cool stars (see below). These will almost certainly comprise the sole source in this spectral region from gas-free, radio-quiet ellipticals. However in objects exhibiting such features as a hot, young stellar population, dust, gaseous emission lines or known peculiarities at other wavelengths, a non-stellar contribution can be expected and may even dominate. Possible non-stellar sources include thermal re-radiation from heated dust, and emission processes such as synchrotron radiation and free-free radiation. Inverse-Compton radiation is unlikely to be a source at low energies and will not be discussed. Line and/or band features may

also be seen and are described below.

### Stellar Radiation

THE CONTINUUM: If we consider stars to be black bodies, then Wien's displacement law,  $\lambda_{\max} \propto 1/T_{\text{EFF}}$  gives the wavelength of peak emission ( $T_{\text{EFF}}$  is the effective temperature of the star). Table 1.1a gives a list of stellar types from O to M with their corresponding  $\lambda_{\max}$ . Table 1.1b gives a rough guide to the relative flux  $f(\lambda)/f(\lambda_{\max})$  which each spectral type contributes at the effective wavelength of the V, J, H, K and L bands. From these tables it is evident that cool stars radiate most of their energy in the near infrared, whereas for hot stars the infrared contribution to their total emission is negligible. Conversely stars cooler than  $\sim 3000^{\circ}\text{K}$  contribute relatively little to the visible waveband and consequently the contribution from these stars to the integrated light of galaxies will be more efficiently observed at near infrared wavelengths. Fig. 1.1a shows black body curves for a wide range of effective temperature. Fig. 1.1b represents the integrated continuum spectrum of a typical normal galaxy nucleus (M31, after Sandage et al., 1969).

STELLAR SPECTRAL FEATURES: These occur as lines or bands in absorption against the continuum background. Spinrad and Wing (1970) and more recently Merrill and Stein (1976a, 1976b) have reviewed this subject for the near infrared. In integrated galaxian spectra only the strongest of such features, probably those which occur in most late type stars, can be expected to be detectable. Molecular vibration-rotation bands are the most common in the infrared. Two molecular absorption bands have been detected in galaxies; they are the carbon monoxide feature seen at  $\sim 2.3 \mu\text{m}$  and the water vapour feature seen at

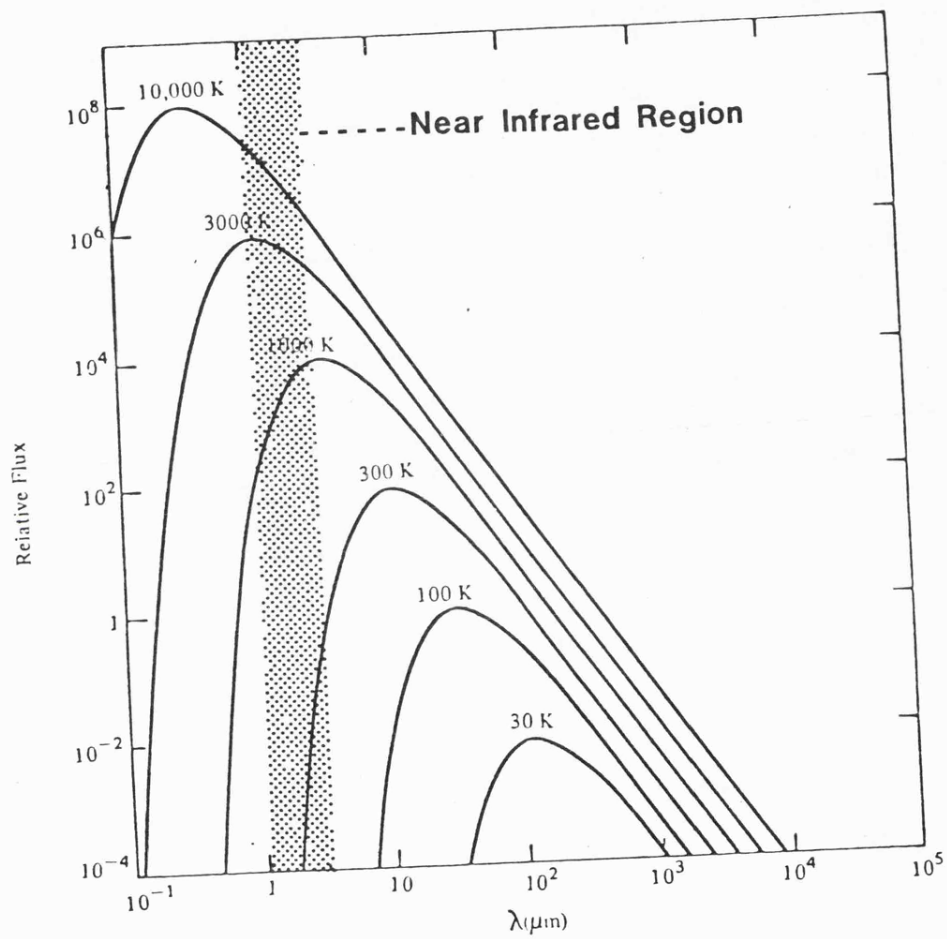


Fig. 1.1a: Black Body Curves and the Near Infrared Region

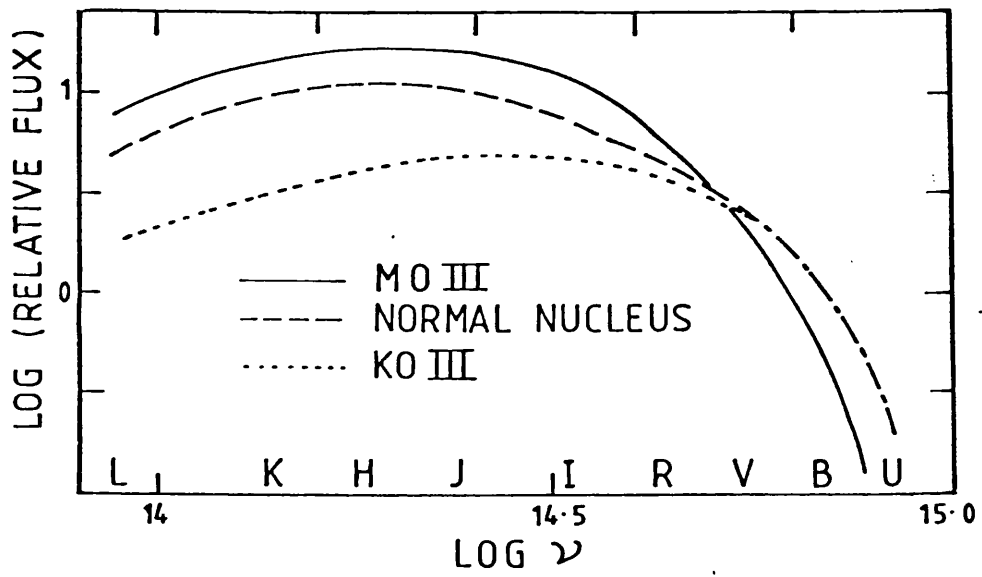


Fig. 1.1b: Continuum of Normal Galaxy Nucleus

Table 1.1a

$T_{\text{eff}}$ ( $^{\circ}\text{K}$ )	40,000	30,000	10,000	6,000	5,000	4,500	4,000	3,500	3,000	2,800	2,500
Mean Sp. Type*	O5	B0	A2	G0	G5	K0	K5	K8	M2	M5	M7
$\lambda_{\text{max}}$ ( $\mu\text{m}$ )	0.07	0.10	.29	.48	.58	.64	.72	.83	.97	1.04	1.16

\* These are rough guides only, usually the means of classes I, II, III are given.

Table 1.1b

$T_{\text{eff}}$	$f(\lambda)/f(\lambda_{\text{max}})$										
	$.36 \mu\text{m(U)}$	$.55 \mu\text{m(V)}$	$1.25 \mu\text{m(J)}$	$1.65 \mu\text{m(H)}$	$2.2 \mu\text{m(K)}$	$3.5 \mu\text{m(L)}$					
40,000	0.03	0.01	$\sim 10^{-4}$	-	-	-	-	-	-	-	-
30,000	0.06	0.03	$\sim 10^{-3}$	-	-	-	-	-	-	-	-
10,000	0.9	0.46	0.04	0.02	0.01	-	-	-	-	-	-
6,000	0.79	0.96	0.21	0.09	0.04	0.01	-	-	-	-	-
5,000	0.52	0.99	0.34	0.16	0.07	0.01	-	-	-	-	-
4,500	0.36	0.94	0.43	0.22	0.09	0.02	-	-	-	-	-
4,000	0.21	0.82	0.56	0.30	0.13	0.03	-	-	-	-	-
3,500	0.1	0.62	0.70	0.41	0.20	0.05	-	-	-	-	-
3,000	0.03	0.39	0.87	0.57	0.3	0.08	-	-	-	-	-
2,800	0.02	0.29	0.92	0.64	0.35	0.10	-	-	-	-	-
2,500	0.01	0.17	0.99	0.77	0.46	0.14	-	-	-	-	-

$\sim 2.0 \mu\text{m}$ . The relevance of these features is discussed in section 1.4.

### Non Stellar Radiation

**BLACK BODY RADIATION FROM DUST:** The presence of dust in galaxies is often revealed by the obscuration of starlight that it causes. This effect is best seen in photographs of edge on spirals. Dust is found in the discs of spirals, throughout type I irregulars and most extensively in type II irregulars. Generally ellipticals are dust free, but it is seen in a few; it appears dramatically in the case of Cen A (NGC 5128) and relatively inconspicuously in NGC 205, for example.

To a first crude approximation dust radiates as a black or gray body (i.e. a black body with emissivity  $\epsilon(\lambda) = \text{a constant} \neq 1$ ). For a black or gray body Wien's Law holds; table 1.2a shows the wavelength of peak emission for a range of dust temperatures and table 1.2b shows the fraction  $f(\lambda)/f(\lambda_{\text{max}})$  contributed at the effective wavelength of each near infrared waveband. Dust in the temperature range  $200^\circ\text{K}$ - $400^\circ\text{K}$  is of major importance as a  $10 \mu\text{m}$  source and may contribute significantly to the L band if present in sufficient quantity. Dust hotter than  $\sim 600^\circ\text{K}$  begins to contribute to the K band. Any very hot dust present,  $\sim 800^\circ\text{K}$ , could possibly dominate the near infrared continuum. The temperature to which dust can survive, before vaporisation, has been discussed several times in the context of galaxies (e.g. Rieke 1976, Allen 1976) and depends upon grain composition. Typically expected dust grains include silicate types which are identified by the  $10 \mu\text{m}$  absorption band "signature" (Kleinmann et al. 1976, Gillett et al. 1975, Rieke 1976), and graphite types (Allen 1976, Rees et al. 1969). The black/gray body approximation is naive but gives a "rule of thumb" guide to  $\lambda_{\text{max}}$ . Examples of physically more

Table 1.2a

$T_{\text{eff}} (^{\circ}\text{K})$	1500	1200	1000	800	600	400	200
$\lambda_{\text{max}} (\lambda \text{ m})$	1.93	2.42	2.9	3.62	4.83	7.25	14.5

Table 1.2b

$T_{\text{eff}} (^{\circ}\text{K})$	$f(\lambda)/f(\lambda_{\text{max}})$						
	$.55 \mu\text{m}(\text{V})$	$1.25 \mu\text{m}(\text{J})$	$1.65 \mu\text{m}(\text{H})$	$2.2 \mu\text{m}(\text{K})$	$2.5 \mu\text{m}(\text{L})$	$10.0 \mu\text{m}(\text{N})$	
1500	$\sim 2 \times 10^{-3}$	0.58	0.94	0.96	0.50	0.02	
1200	$\sim 10^{-4}$	0.26	0.67	0.98	0.75	0.05	
1000	-	0.1	0.39	0.82	0.92	0.09	
800	-	0.02	0.13	0.48	$\sim 1.00$	0.18	
600	-	$\sim 5 \times 10^{-4}$	0.01	0.13	0.75	0.37	
400	-	-	$\sim 10^{-4}$	$4 \times 10^{-3}$	0.19	0.8	
200	-	-	-	-	$\sim 10^{-4}$	0.68	

realistic grain radiation likely to occur in galaxies are given in the references above, and also in Aaronson (1978a). These usually involve assumptions for grain absorption and emission efficiencies and for the wavelength dependence of grain emissivity.

PLASMA PROCESSES: Dust and high density gas in the form of stars are two common forms of matter found in space. The third is low density gas. This may be neutral, or ionized or a mixture of both. Whenever an ionized component is present the gas is usually referred to as a plasma. Two radiation processes which occur in plasma are of major importance in astrophysics generally, and may each be seen in emission from various types of active galaxy. The first of these, free-free radiation is a "thermal process" which occurs in kinetically hot gases, and the second, synchrotron radiation, is a "non-thermal process" which occurs when relativistic electrons interact with a magnetic field.

#### THERMAL PROCESSES

a) Free-free radiation: In a hot plasma the charged particles are in rapid thermal motion, Coulomb forces between electrons, and between electrons and positively charged nuclei produce a high degree of scattering, particularly in the low mass electrons. During the scattering the electrons undergo acceleration with a resultant emission of radiation. This is known as free-free radiation as the electron is free - of the nuclei - both before and after scattering. In most cases of astrophysical interest the first order approximation assumes the plasma to be 100% ionized hydrogen, and in this case the form of the free-free spectrum is given by:

$$j(\nu, T) = 5.443 \times 10^{-39} g N_e^2 T^{-\frac{1}{2}} \exp(-h\nu/kT)$$

$$(\text{erg sec}^{-1} \text{ster}^{-1} \text{Hz}^{-1} \text{cm}^{-3})$$

where  $j(\nu, T)$  = volume emissivity

$g$  = Quantum mechanical gaunt factor

$N_e$  = electron density

Other symbols take their standard meaning.

This reduces to:

$$j(\nu) = \text{constant}; \text{ for } h\nu \ll kT.$$

Therefore the spectrum is "flat" with a long wavelength tail off where the plasma become optically thick, and a high frequency cut off corresponding to the initial kinetic energy of the emitting electron, i.e.

$$\nu_{\text{max}} = mv^2/2h.$$

b) Line features: As well as the continuum process just described, discrete spectral features may arise, in an interstellar gas, which fall in the near infrared waveband. A few of these have proved bright enough to be measured by modern detectors. Some of the hydrogen Brackett lines have been seen in emission in two external galaxies and in the Galactic centre (M82 - Willner et al. 1977, NGC 1068 - Thompson et al. 1978, G.C. - Neugebauer et al. 1978). These lines are the result of bound-bound transitions ( $N \geq 5 \rightarrow N = 4$ ,  $N$  is the principal quantum number) in the neutral hydrogen atom.  $Br_\alpha$  ( $N = 5 \rightarrow N = 4$ ,  $\lambda = 4.05 \mu\text{m}$ ) has been in M82 and  $Br_\gamma$  ( $N = 7 \rightarrow N = 4$ ,  $\lambda = 2.17 \mu\text{m}$ ) has been seen in NGC 1068, the Galactic centre and possibly M82. The only other identified features seen to date are two hydrogen molecular ( $H_2$ ) lines and a HeI line - both in NGC 1068. A strong but as yet

unidentified emission feature has been seen in M82 at  $3.3 \mu\text{m}$ ; this is similar to a feature seen in galactic planetary nebulae.

#### NON THERMAL EMISSION:

**Synchrotron Radiation:** When a charged particle moves in a magnetic field with a velocity perpendicular to the field lines it experiences a force  $q\mathbf{v} \wedge \mathbf{B}$  which constrains it to move in a circle, or in a helix if there is a velocity component parallel to the field lines. As the particle is accelerated by the magnetic field there is a characteristic radiation emitted which is known as cyclotron radiation when the particle velocity is classical, or synchrotron radiation if the velocity is relativistic. In the case of cyclotron emission the radiation field is isotropic and the emitted frequencies are harmonics of the particle angular frequency. The properties of synchrotron radiation are quite different however. In the case of single particles the emitted radiation is restricted to a pencil beam within a cone centred on the instantaneous velocity vector. The spectrum is continuous but exhibits a maximum at a frequency determined by the electron energy and the field strength. The emission is highly polarized. Generally the synchrotron radiation from protons and other charged nuclei is negligible as these are far more massive than the electrons and hence their acceleration is comparatively small.

In situations commonly encountered in astrophysical plasmas an ensemble of electrons with a range of energies must be considered. In many cases an energy spectrum of the form  $N(E)dE = KE^{-\alpha}dE$  is expected, and in a uniform magnetic field this ensemble will produce a radiation spectrum of the form  $f(\nu) \propto \nu^{-(\alpha-1)/2}$ , i.e. a power law. The ensemble radiation is also polarized, the degree of polarization  $D$ , is given by:  $D = \frac{(\alpha + 1)}{(\alpha + 7/3)}$ . Note that the power law spectrum is a function

of the ensemble energy spectrum, a different energy spectrum would produce a different radiation spectrum.

\*  $N(\epsilon)$  is the number of electrons of energy  $\epsilon$ ,  $K$  is a constant and  $\alpha$  is the (energy) spectral index,  $f(\nu)$  is the flux at frequency  $\nu$ .

### 1.3 TECHNIQUES AVAILABLE FOR GALAXY RESEARCH

The instrumental techniques which may be used successfully in a given branch of astronomy are limited by such factors as detector sensitivity and the brightness of the object observed in the waveband, aperture size or polarization mode etc., of interest. Thus, for example, an extremely faint quasar could be measured photometrically with a long integration time, but it will remain practically impossible to say, obtain a high resolution spectrum until a more sensitive detector becomes available. There is of course a third restriction, which is that an instrument capable of performing a certain task may not exist or may not have been developed for a particular waveband. This is currently the situation as regards imaging in the infrared. Photographic emulsions and photomultipliers are sensitive only as far as  $1.1 \mu\text{m}$ . At present mapping or contouring of extended objects in the infrared can only be achieved by scanning the object across the detector. Imaging systems using detector arrays or multiplex techniques are under development.

With the above factors in mind, the various techniques outlined below are restricted to those which are currently in common use for near infrared observations of galaxies.

#### 1.3.1 Broad Band Photometry

Photometry is the most basic quantitative technique available.

It entails simply measuring the integrated flux, from the star or galaxy etc., in a precisely defined waveband. In near infrared astronomy these wavebands are qualitatively defined by the four atmospheric windows in the 1-4  $\mu\text{m}$  region, and are quantitatively defined by the passbands of the J,H,K and L interference filters in common use. The so-called "effective wavelength",  $\lambda_0$  of each waveband is defined as:

$$\lambda_0 = \frac{\int \lambda \phi(\lambda) d\lambda}{\int \phi(\lambda) d\lambda}$$

where  $\lambda$  is the wavelength and  $\phi(\lambda)$  is the product of the filter response function and atmospheric transmission. To a first order approximation broad band photometry is equivalent to monochromatic photometry at wavelength  $\lambda_0$ , and so photometric observation at several different passbands may be used to determine the shape of continuum emission, but can not be used to distinguish emission or absorption features narrower than the filter passbands. Table 1.3 gives the characteristics of the standard wavebands in frequent use today. The J,H and K bands seem to be universally agreed upon, but the L band seems to vary slightly from research group to research group. Effective wavelengths of 3.5  $\mu\text{m}$  or 3.6  $\mu\text{m}$  are frequently seen in the literature. Johnson's (1966a) original L band had an effective wavelength of 3.4  $\mu\text{m}$ . The characteristics for L given in Table 1.3 are those most commonly quoted in the literature by the more prolific authors.

Absolute photometric measurement in infrared astronomy is difficult to achieve, so calibration relative to a system of standard stars is the normal procedure. Details of calibration methods etc., can be found in Chapter 2.

Determining the shape of continuum spectra is one application of photometry. It has three other uses in observations of galaxies.

**Table 1.3 : Standard JHKL Filter Passbands**

---

	J	H	K	L
$\lambda_{\circ} (\mu\text{m})$	1.25	1.65	2.22	3.5
$\Delta_{\lambda} (\mu\text{m})$	0.3	0.3	0.4	0.6

i) TIME MONITORED MEASUREMENTS: These are to look for variability in active nuclei, Q.S.O.'s and BL Lacs. Searches for variability in galaxies may be on time scales of  $\sim$  hours to years. These studies are limited by such factors as the brightness of the object and the period and magnitude of the variation. The fundamental limit for the detection of short period variations, which is set by the response time of the detector, is of little concern to observers of galaxies since variations on time scales less than hours are highly unlikely on the basis of light travel time arguments.

ii) MULTIAPERTURE ANALYSIS: By observing extended objects through a range of aperture sizes some first order knowledge of radial distribution of brightness and colour may be obtained.

iii) PHOTOMETRIC SCANNING: Far more detailed information on the spatial distribution of brightness and colour can be obtained by scanning an aperture across the galaxy. Photometric scanning is the main subject of the thesis and is to be discussed fully in the following chapters.

### 1.3.2 Polarimetry

Over the last four years or so photometric polarimetry has been used more and more in infrared galaxy research, particularly in observations of active galaxies. (E.g. Knacke and Capps 1974, Knacke et al. 1976, Kemp et al. 1977, Lebofsky et al. 1978, Capps and Knacke 1978). Published polarimetric observations of normal galaxies are restricted to M31 (Jameson and Hough 1978) and the Galactic centre (Adams and Hough 1977, and Capps and Knacke (1976).

Polarimetric techniques may yield information which distinguishes between thermal and non thermal processes in active nuclei, and may be useful for determining magnetic field properties of spiral galaxies via

observation of grain alignment in the dust lanes of edge on spirals.

### 1.3.3 Spectrometry

Unlike photometry, which may give a knowledge of the continuum spectrum, spectrometry reveals individual spectral features; lines and bands in absorption or emission. Three different techniques, which give three different levels of spectral resolution, have been used to date in galaxy research at near infrared wavelengths; the first two are really just extensions of ordinary broadband techniques to narrower and narrower wavebands. The third is a multiplex technique which has only recently (1978) reached a development level where useful research on faint objects like galaxies can be achieved.

1) **ABSORPTION BAND PHOTOMETRY:** Late type stars show absorption bands in their spectra due to the CO molecule at  $2.3\ \mu\text{m}$  and the  $\text{H}_2\text{O}$  molecule at  $2.0\ \mu\text{m}$ . These two features have proved to be very useful in understanding the nature of the late type population in normal galaxy nuclei (see section 1.4). The CO and  $\text{H}_2\text{O}$  colour indices (defined below) correlate strongly with the strength of the  $\text{H}_2\text{O}$  and CO absorption features (see Baldwin et al. 1973a,b and references therein for details). In turn the strengths of these features correlate with luminosity and temperature respectively. The CO band strength correlates in a positive sense with the luminosity of stars later than K0, i.e. the feature is stronger in giants than in dwarfs of the same spectral type. The  $\text{H}_2\text{O}$  band strength, again for stars cooler than K0, correlates in a negative sense with temperature, i.e. the cooler the stars the stronger the feature. Furthermore, for stars with spectral type between M0 and M6 it depends strongly on luminosity, but in the opposite sense to that of the CO index, i.e. the  $\text{H}_2\text{O}$  index is stronger in dwarfs than in giants.

In practice the CO and H<sub>2</sub>O indices are measured using standard photometric observing techniques in conjunction with narrow band interference filters with effective wavelengths and full-widths-at-half-maximum of 2.00  $\mu\text{m}$  (0.08  $\mu\text{m}$ ), 2.20  $\mu\text{m}$  (0.11  $\mu\text{m}$ ) and 2.36  $\mu\text{m}$  (0.08  $\mu\text{m}$ ). The narrow band  $\overline{2.36 \mu\text{m}}$  and  $\overline{2.20 \mu\text{m}}$  filters define the CO index =  $\overline{2.36 \mu\text{m}} - \overline{2.20 \mu\text{m}}$ , and the  $\overline{2.20 \mu\text{m}}$  and  $\overline{2.00 \mu\text{m}}$  define the H<sub>2</sub>O index =  $\overline{2.20 \mu\text{m}} - \overline{2.00 \mu\text{m}}$ , (Frogel et al. 1978, Aaronson et al. 1978). In principle this technique could be applied to other absorption or emission features.

ii) CVF SPECTROMETRY: Continuously Variable Filter wheels have been used for galaxy research since about 1974. They consist of a rotating wheel interference filter, the passband of which is a function of  $\theta$ , the angle of rotation.

A spectral resolution of  $\Delta\lambda/\lambda \sim 0.015$  is commonly obtained for  $\lambda = 1.9 \mu\text{m}$  to  $2.5 \mu\text{m}$  and  $\Delta\lambda/\lambda \sim 0.02$  from  $2.8 \mu\text{m}$  to  $4.2 \mu\text{m}$ .

In the near infrared this technique has been used in work on M82 (Willner et al. 1977) and the Galactic centre (Neugebauer et al. 1976b and 1978), NGC 253 and IC 342 (Becklin, private comm., 1979).

iii) FOURIER TRANSFORM SPECTROSCOPY: The techniques involved in FTS are too involved for discussion here; it will suffice to say that they have been used successfully for a bright galaxy in the waveband 2.0 - 2.5  $\mu\text{m}$  with spectral resolution equivalent to  $\Delta\lambda/\lambda \sim 0.002 - .0017$  (NGC 1068, Thompson et al. 1978).

#### 1.4 THE NEAR INFRARED EMISSION OF NORMAL GALAXIES

##### The JHK Plane

When the colours of normal galaxies are plotted on the UBV colour-colour diagram a definite correlation with Hubble type is apparent.

This is known as the colour-morphology sequence and is illustrated in fig. 1.2a (de Vaucouleurs, 1961). The correlation can be understood in terms of the differences in stellar population in the various Hubble types. The idea of colour-colour plots has been extended to near infrared photometry where the analogous diagrams are the JHK plane and the HKL plane. The pioneer photometry of Johnson (1966) and later that of Sandage et al. on M31 (1969), Penston (1973) and Glass (1973) has shown that normal galaxies appear to lie in very localized regions of the JHK and HKL diagrams. The mean positions are  $J-H \approx 0.73$ ,  $H-K \approx 0.25$  and  $K-L \approx 0.5$ , with a scatter  $\sim \pm 0.1$  about the central mean. Figs. 1.2b and 1.2c show the infrared colour-colour diagrams for normal galaxies. In 1.2b the loci of giant and dwarf stars of each spectral type are shown, and in fig. 1.2c the region where most normal stars are to be found is shown.

The infrared colours we see for normal galaxies cannot be fully explained in terms of those stars which, on the basis of UBV colours alone, were previously believed to synthesise the population in the central regions of galaxies (Arp 1965, quoted in Johnson 1966). Considerable numbers of stars of a far cooler nature than any previously believed to occur widely in galactic nuclei are required to explain the IR colours, particularly H-K and K-L. Such cool stars would contribute negligibly to the integrated visible light and hence would have remained undetected if only visible techniques had been used. The composite nature of galactic nuclei is evident in the infrared colour diagrams: the mean J-H colour corresponds roughly to mid K giants, the mean H-K colour to early M giants and the K-L colour to late M types. However, although these colours may be synthesised from a mixture of K and M giants, they could equally well be fitted by giants and later type dwarfs. The broad band colours alone cannot therefore give precise

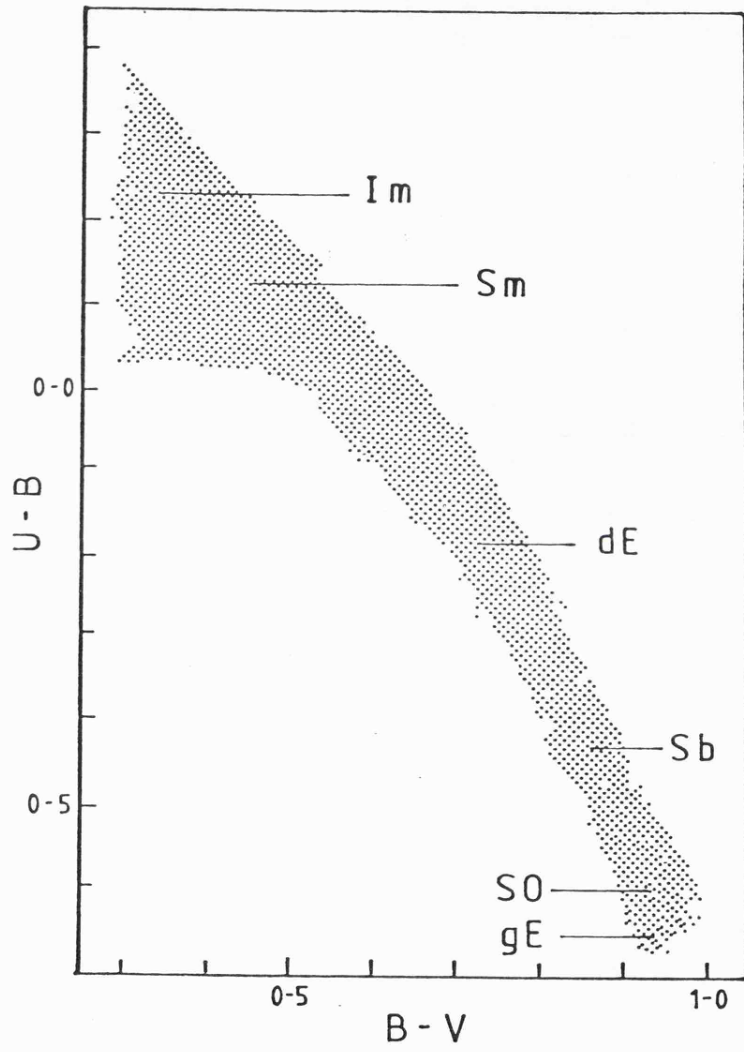


Fig. 1.2a: Normal Galaxies on the UBV Plane

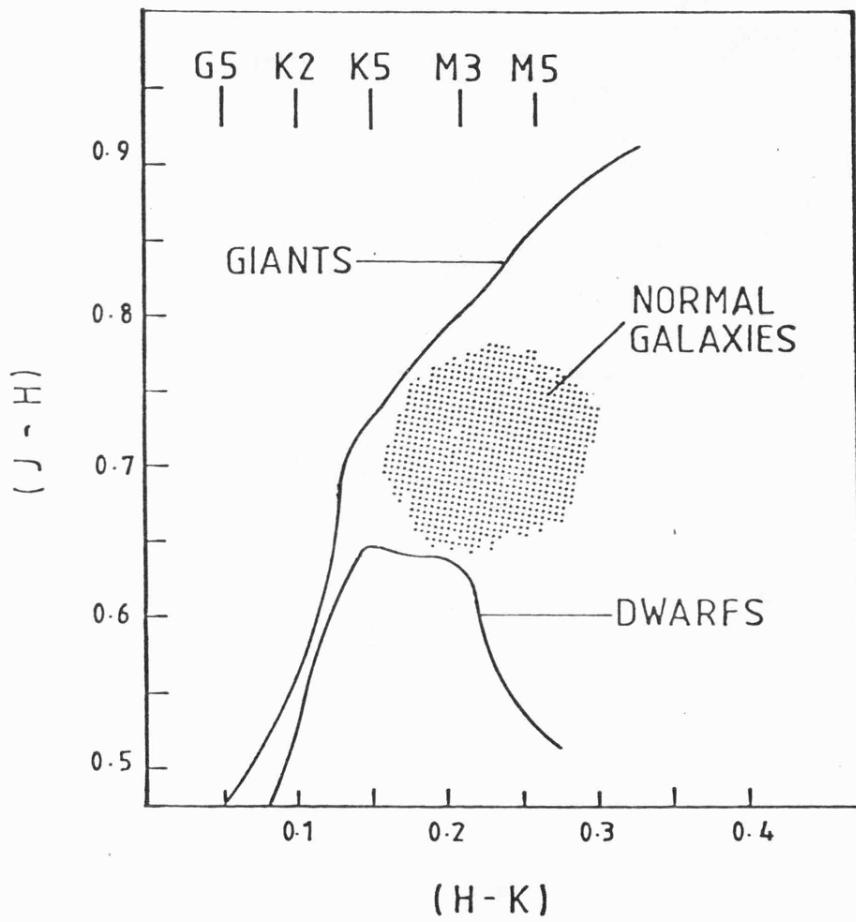


Fig. 1.2b: Normal Galaxies and Stars on the JHK Plane

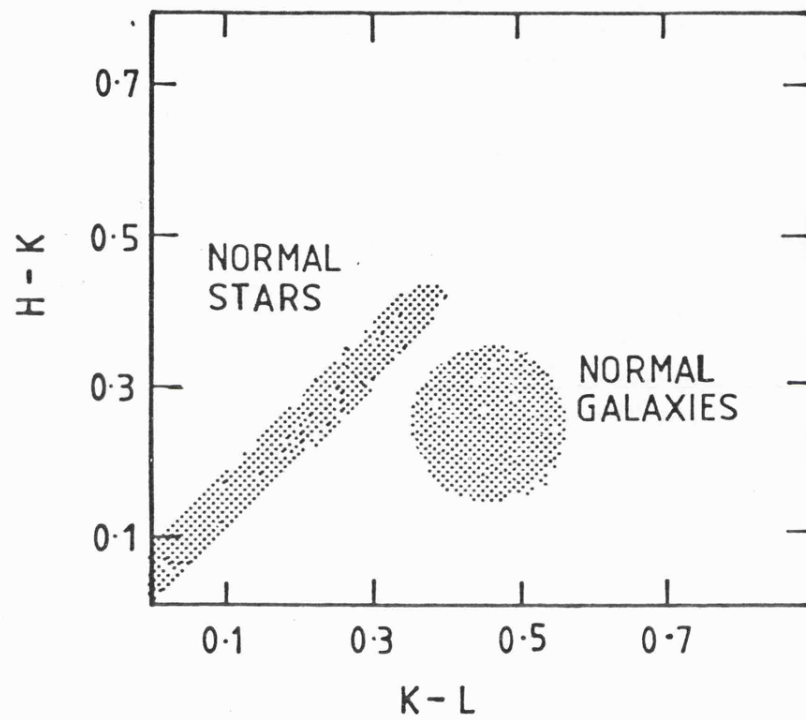


Fig. 1.2c : Normal Galaxies on the HKL plane

information concerning the late type luminosity function (Glass 1975).

Fig. 1.2b illustrates clearly why this is so.

Unfortunately, as Faber (1972) has emphasised, optical broad band and narrow band data are insufficient to uniquely determine the relative numbers of giant and dwarf stars in spectral types later than  $\sim$  K0. In particular she stressed that only near infrared data could provide the necessary constraints on the late type luminosity function in stellar population models.

The information summarised in the JHK diagram represents our first order knowledge of infrared colours of galaxies. In 1974 this was more or less all that was known on the subject. Many questions had still to be answered, but detector sensitivity limited the amount of available data. Only a few elliptical galaxies had been observed, no type I irregulars had been measured and the sum total of data which was available covered, randomly, a wide range of A/D(O). The immediate observational tasks for near infrared galaxy research were quite clear. These are summarised below.

- i) The existence of any correlation between Hubble type and infrared colours had to be determined, at constant A/D(O). The A/D(O) needed to be large so as to include most of the main body of the galaxies - and hence maximise the effect of differences between systems with a hot young population and those without.
- ii) Variation of colour with radius, within galaxies needed to be investigated. There was evidence that some galaxies, which appeared otherwise quite normal, showed excesses at small A/D(O).
- iii) Variation of colour with absolute magnitude between galaxies, at constant A/D(O), needed investigation.

iv) As Faber pointed out a method for distinguishing between the contribution from late type giants and that from late type dwarfs in integrated light was urgently required to assist in the synthesis of model populations for galactic nuclei.

Over the last few years all of these research problems have been tackled to some extent, especially for early type systems. In particular the increase in detector sensitivity has enabled narrow band techniques to be applied to the luminosity function problem. The remainder of this section will be taken up with a description of the extent of current knowledge.

#### Ellipticals and Lenticulars

The first attempt to systematically survey the infrared colours of elliptical galaxies was due to Grasdalen (1975). He obtained multiaperture (V-K) colours for a sample of fourteen ellipticals, and concluded that for a given A/D(0) there is very little cosmic dispersion in this colour index, but that within elliptical galaxies large V-K colour gradients exist. The latter conclusion was apparently confirmed by more detailed observations of M87 in which V and K measurements were made with the aperture displaced further and further from the centre of this galaxy. A colour variation was claimed amounting to  $0.9^m$  in V-K from the centre of the galaxy to the edge. A short time later Frogel et al. (1975c) published results which were exactly opposite to those of Grasdalen, i.e. a large scatter in V-K was seen among ellipticals, but no significant radial variation of V-K within E galaxies was established. The authors of this second paper indicated that discussions with Grasdalen had shown their conclusions to be correct. Unfortunately, no indication was given as to where the errors in Grasdalen's observations/reduction arose. A reading of his

observational procedure, his precautions to ensure good centring on the galaxy and his allowances for reference beam contamination make it difficult to see where his error(s) could have been.

The results of Frogel et al. were part of a massive venture to quantitatively determine the nature of the late type stellar population in E and SO systems. In a series of papers stretching over five years (Baldwin et al. 1973a, 1973b, Frogel et al. 1975a, 1975b, 1975c, Frogel et al. 1978, Aaronson et al. 1978, Persson et al. 1978) a large team of Harvard/Caltech astronomers measured the J, H and K colours and CO and H<sub>2</sub>O indices of over 50 elliptical and lenticular systems. The work involved in this project can be gauged by considering that in one year alone eighty observing nights were spent on various Mount Wilson and Mount Palomar telescopes plus unspecified amounts of time on various KPNO, Cerro Tololo and Las Campanas telescopes (Frogel et al. 1978). This is easily the biggest project undertaken in near infrared extragalactic studies. Hereinafter this project will be referred to as FPAM after the main authors (Frogel, Persson, Aaronson and Matthews).

#### Variation of IR Colour among Early Type Galaxies

Initially, work on colour variations from galaxy to galaxy proved inconclusive (Frogel et al. 1975c). A statistical analysis of subsequent data obtained with improved detector sensitivity revealed a weak but definite correlation of galaxy broad band colours, particularly V-K, with absolute magnitude. The sense of the correlation is that the more luminous the galaxy the redder the colour becomes. Although the FPAM sample contained only two dwarf E systems the correlation is particularly evident as one moves from these dwarfs (NGC 205 and NGC 404,  $M_V = -16.6$  and  $-16.08$  respectively) to the bulk of the rest of the sample ( $M_V \lesssim -20.0$ ); the dwarf galaxies are considerably bluer.

For the bright galaxies ( $M_V \lesssim -20.0$ ) there is no significant correlation established between CO or  $H_2O$  index with luminosity, although the dwarf galaxies have significantly weaker CO indices than the giant systems. This behaviour needs further investigation, particularly for  $-16 \gtrsim M_V \gtrsim -19$ . No  $H_2O$  indices have been published for dwarf systems.

#### Radial Variations of Infrared Colours within Early Type Galaxies

Multiaperture data are not ideal for a study of colour gradients within galaxies since such gradients are likely to be small, and photometric measurement is never better than a few percent (Frogel et al. 1975c, 1978). A better approach is to displace the measuring aperture from the centre of the galaxy (see data in this thesis and the technique of Strom et al. 1978 on the early type galaxies NGC 3115 and NGC 2768). Nevertheless a suitably large data set, such as that of FPAM may be treated statistically. Analysis of this sort reveals that the centres of E and SO galaxies are redder than their outer regions in J-K colour. Dependence of V-K colour upon radius has not been well established, although there is evidence that such gradients exist. It should be noted however that any V-K gradient can be entirely accounted for by that in J-K. The CO and  $H_2O$  indices show no radial variation greater than the measuring error (for  $1.0 \gtrsim A/D(0) \gtrsim 0.1$ ).

An interesting point arises out of the conclusions above. It seems that stellar population changes within galaxies are more evident at J-K and yet changes between galaxies are more evident at V-K. This implies that radial variations in stellar population, whether they are due to luminosity function changes or metallicity changes, are more apparent at wavelengths  $\gtrsim 1.2 \mu m$ , whereas the differences from galaxy

to galaxy are more apparent at wavelengths  $< 1.2 \mu\text{m}$ .

### Stellar Population Models

Although the CO and  $\text{H}_2\text{O}$  indices show no correlation with galaxy luminosity (for  $M_V \lesssim -20$ ), nor any radial gradient within galaxies, they have been of crucial importance in determining the late type stellar luminosity function in the nuclei of early type galaxies. Recent attempts by O'Connell (1976) and Tinsley and Gunn (1976) at synthesising elliptical galaxy nuclei have proved to be among the best models to date at reproducing observed visible data ( $\lambda < 1 \mu\text{m}$ ). However predictions based on these models for the major contributors to integrated infrared light differ dramatically, thus emphasising the limitations of visible data alone for investigating the cool component in galaxies. For example, the Tinsley and Gunn model predicts that M6III stars should contribute 12% of the  $2 \mu\text{m}$  light whereas O'Connell's model suggests that this population is more dominant and provides 35% of the K light. The CO and  $\text{H}_2\text{O}$  indices of the FPAM galaxies show that O'Connell's model gives a better representation of the observed infrared data. The Tinsley and Gunn model has (V-K) colours which are too blue and  $\text{H}_2\text{O}$  and CO indices which are too weak. The O'Connell model on the other hand, agrees almost exactly with the observed mean V-K colour and mean CO and  $\text{H}_2\text{O}$  indices of normal giant ellipticals and lenticulars. The O'Connell model and the infrared data together show that the main contributors to the  $2.2 \mu\text{m}$  light are K0III to M5III stars with 42% and M6III stars with 37%. The remaining 21% comes mainly from a range of dwarf stars. In particular the observed CO and  $\text{H}_2\text{O}$  indices and H-K colour require the contribution from the latest giants.

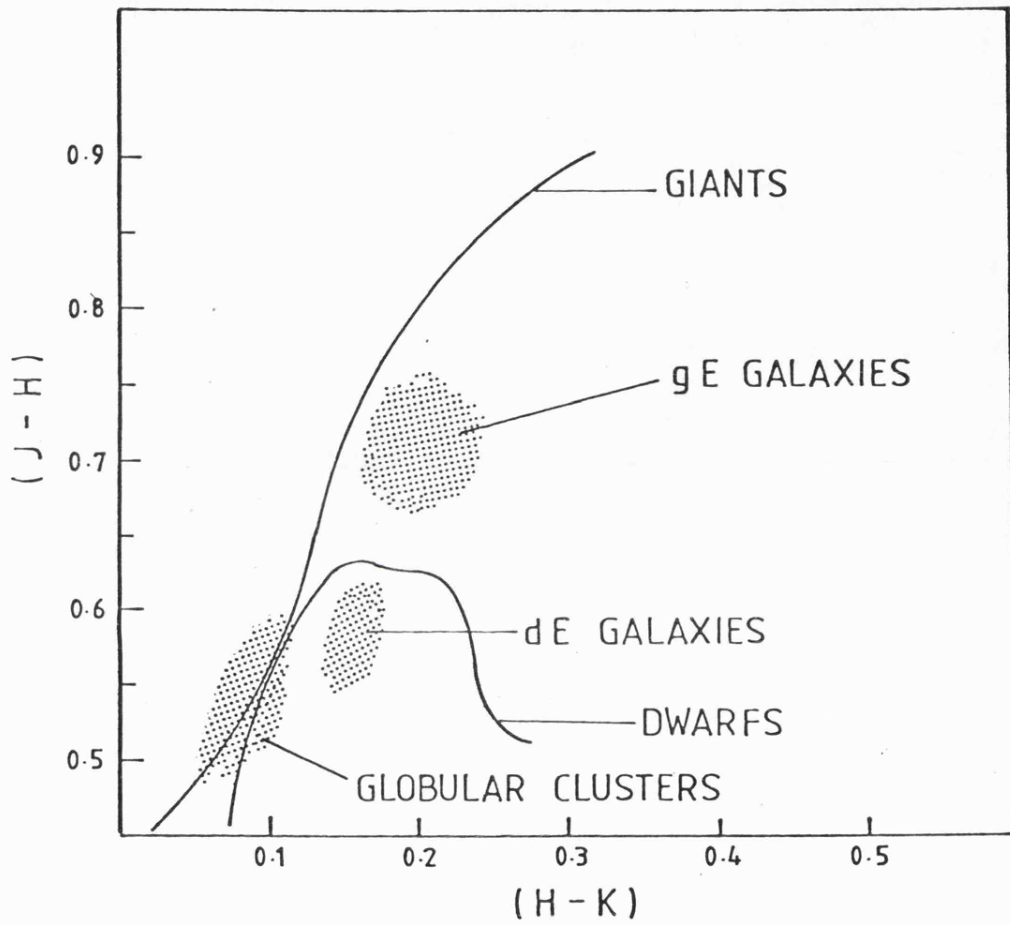


Fig. 1.3: Globular Clusters and Ellipticals on the JHK Plane

### Ellipticals and Globular Clusters

Globular clusters are known to show a wide range of metallicity, from extremely metal deficient systems through to those with only small metal deficiencies (Sandage 1970, Hartwick and Sandage 1968). If the infrared colours of a sample of globular clusters, in which there is a range of metallicity, are plotted on the JHK diagram it can be seen that the reddest are also the most metal rich (FPAM). This suggests that the colour difference between globular clusters is metallicity driven. When the range of the globular cluster JHK diagram is extended to include dwarf and giant elliptical galaxies, a correlation between colour and luminosity is apparent, with the colours of dwarf galaxies overlapping with those of the reddest globular clusters (see fig. 1.3). These facts strongly suggest that colour variations from galaxy to galaxy are also metallicity driven, and therefore as the most luminous systems are the reddest, they are probably the most metal rich. This result confirms similar conclusions made by McClure and Van den Bergh (1968), and Faber (1973), on the basis of optical data.

### Spiral and Irregular Galaxies

Published JHK data on spiral and irregular galaxies, particularly irregulars, are still few, and are far less extensive than those now available for early type galaxies. However, with the limited information available, there is no evidence for significant differences between spiral galaxy nuclei and elliptical galaxy nuclei. In fact Aaronson's (1978a) mean late type spiral (a mean of eight Sc-Scd spirals, as yet unpublished individually; no A/D(O) specified) has infrared colours which differ by only  $\sim 0.03$  from the mean elliptical of FPAM. This difference is of the order of the uncertainty in the measurements.

Most of the data available (Johnson 1966, Penston 1973, Glass

1973, Pacholczyk and Tarenghi 1975) are for measurements at small  $A/D(0)$  and it appears, at least with these small apertures, that (a) there is a large scatter in the infrared colours of spiral nuclei and (b) a relatively large number show a modest infrared excess especially at K-L (Glass 1973, 1975, Pacholczyk and Tarenghi 1975). The first of these points is similar to the behaviour in ellipticals, but the second is quite different from anything seen in these. How widespread the slight infrared excess at small  $A/D(0)$  actually is among spirals has not been extensively studied, and needs closer attention especially with even smaller apertures. We do know that systems like M31 do not seem to show any such behaviour. A number of the Glass galaxies apparently do however, and of those the majority appear to be "slightly active" galaxies, showing some narrow emission line activity. A number are "hot spot" galaxies (Sersic and Pastoriza 1965).

Aaronson (1978b) has obtained U-V and V-K colours for about fifty spiral and irregular (Im) galaxies, and U-V colours for the early type galaxies of FPAM for which V-K colours were already known. He has shown that for  $A/D(0) > 0.2$  there exists a well defined colour-morphology relation for Hubble types in the UVK plane. This is analogous to the similar relationship in the UBV plane mentioned earlier. Previously this UVK relationship was unknown. Pacholczyk and Tarenghi (1975) investigated the UVK behaviour of galaxies but failed to establish any correlation as their data was restricted to small apertures  $0.07 \lesssim A/D(0) \lesssim 0.17$ .

The UVK colour-morphology sequence is shown in fig. 1.4. Aaronson emphasises that although previous authors (Grasdalen 1975 and Pacholczyk and Tarenghi 1975) reported large dispersion in V-K for spirals and irregulars, for large  $A/D(0)$  the dispersion in V-K for a given Hubble type is comparable to the dispersion in U-V. The mean E/SO

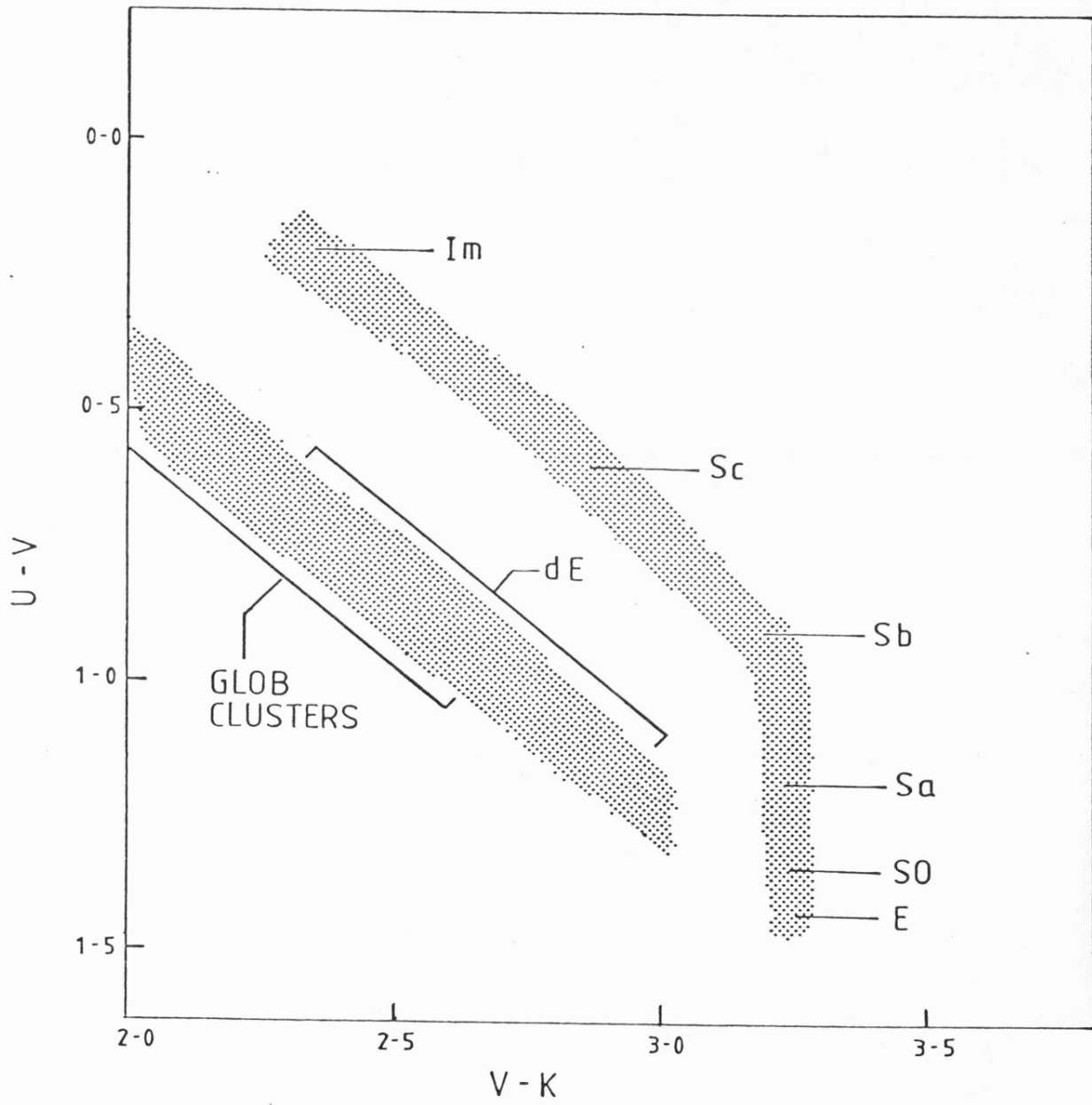


Fig. 1.4: Galaxies on the UVK Plane (Aaronson 1978b).

colours were adopted (minus the dE's), and the colour-magnitude effect was ignored. Over the range  $-19 < M_V < -23$  spirals did not show any significant correlation between infrared colour and  $M_V$ . Fig. 1.4 also shows the metallicity driven globular cluster-elliptical galaxy/colour sequence discussed above. Note that this sequence is quite separate from the galaxy morphology/colour sequence; in this respect the UVK plane is more useful than the UBV plane in which metallicity effects are essentially parallel to the galaxy morphology sequence.

The different loci for spiral-elliptical and globular cluster-elliptical sequences suggests that any metallicity differences between ellipticals and spirals are small. The colour-morphology sequence in the UVK plane may instead be understood in terms of an increase in the influence of young hot stars along the sequence E-S-Im, Morgan and Osterbrock (1969). This may be demonstrated qualitatively by mixing the light from an AO dwarf and an MO giant (say) and slowly varying the relative proportions of each. A range of 80% V light due to the A star through to 20% due to the M star adequately reproduces the sequence Im  $\rightarrow$  E in the UVK plane (Aaronson, 1978b). Even when the A star is contributing 80% of the V light, the M star provides 90% of the K light.

#### SUMMARY:

The majority of normal galaxies have very similar VJHK colours; significant differences between Hubble types are apparent only in the mean V-K colour of Sc/Im and E/Sa systems. The broad band data alone are insensitive to the relative numbers of dwarf and giant stars contributing to the integrated infrared light of galaxies, but the H-K, CO and H<sub>2</sub>O indices together indicate that M giants are the dominating component in E systems and probably in S systems also. The paucity of JHK photometric data for spirals and irregulars is the biggest gap in our knowledge, although Aaronson possesses multiaperture data for a number of these

galaxies which will hopefully be published soon.

#### 1.5 EFFECT OF NON STELLAR SOURCES ON THE INTEGRATED STELLAR CONTINUUM

A galaxy is usually considered to have normal colours if these are in agreement with its Hubble type mean colours which are explained purely in terms of integrated stellar content. Whenever a galaxy shows infrared colours that are redder than the mean expected for its morphological type it is said to have an infrared "excess". Apparent "deficits" of infrared light, i.e. colours which are bluer than those of its Hubble type mean, are rare, but may arise from a relative excess of hot young stars which presumably are due to an abnormally high rate of star formation compared to that seen in otherwise similar systems. There is however something rather paradoxical about the infrared colours of systems in which star formation is known to be actively continuing. In systems of this type where this phenomenon is considered normal, e.g. the Magallenic irregulars, the infrared colours are as expected; considerably bluer than other Hubble types. In contrast, in systems where there is intense star formation which is considered to be anomalous, e.g. Cen A and M82, the infrared colours are far redder than normal. These systems contain large quantities of dust, yet this dust cannot account for the red colour if simple reddening (after Van de Hulst, Johnson) is solely responsible. A near infrared contribution from warm/hot dust may explain this anomaly. The giant late type spiral NGC 253 is a system in which considerable star formation is expected, however unlike the Magallenic irregulars this galaxy shows very red colours similar to those in M82. Aaronson (1978b) has found ~ 7 systems which show substantial excesses at two microns which cannot be explained by reddening. This group includes M82 and NGC 253. This interesting phenomenon is worthy of a detailed study.

There are two common explanations given to account for infrared excesses. The first is interstellar reddening within the galaxy itself, the second is the presence of a non-stellar contribution to the near infrared light. The non-stellar sources most frequently considered are thermal re-radiation from warm dust, synchrotron radiation and free-free radiation.

#### Apparent Excesses due to Reddening

Extinction of starlight by dust in the interstellar medium is, roughly speaking, inversely proportional to wavelength. This has the effect of "reddening" transmitted light, hence the term "interstellar reddening". Thus, if the light from, say, the nucleus of another galaxy encounters a large optical depth of dust en route to a telescope on Earth, then the observed colour indices will be redder than the original intrinsic indices, so falsely giving the impression of an infrared excess. Such "excesses" then are purely apparent and can be corrected. Corrections are discussed in Chapter II.

#### Excesses due to Non-Stellar Sources

Several discussions on the effect of non-stellar contributions to the integrated infrared light of galaxies have appeared in the literature from time to time. Pacholczyk (1967) and Penston et al. (1974) have discussed the effect of Q.S.O. colours as these increasingly contaminate those of a normal galaxy. Neugebauer et al. (1976a) have synthesised infrared continua for a typical stellar nucleus (M31) plus (a) a power law spectrum and (b) a  $200^{\circ}\text{K}$  black body, both for cases where the non-stellar component flux is of the order of that from the galaxy and also when it dominates the galaxy. Glass (1975) has shown the effect of an  $800^{\circ}\text{K}$  black body on a "mean nucleus" of K5III stars.

Finally Allen (1976) has briefly discussed the influence of synchrotron radiation, non-stellar black body radiation and free-free radiation on normal galaxy colours.

Fig. 1.5 summarises the infrared colours of normal galaxies, the infrared colours of non-stellar sources and the effect of the latter on the former. The colours of a simple power law synchrotron source ( $f(\nu) \propto \nu^{-\alpha}$ ) are represented by the line marked P.L., the ticks indicate the changing values of spectral index. The locus of black body colours for different  $T_{\text{eff}}$  is shown by the curve B.B. Note that normal galaxies lie slightly to the left of the black body line and not on it. This may be explained by the H band opacity minimum in the atmospheres of late type stars. The dashed line from the normal galaxy region to the power law line represents the locus of the displayed colours when a normal galaxy becomes increasingly contaminated by synchrotron radiation of  $f(\nu) \propto \nu^{-2}$ . Similarly the dotted-and-dashed line indicates the range of colours for a K5III star plus an  $800^{\circ}\text{K}$  black body as the latter slowly dominates. This diagram illustrates why it is not always easy to determine the nature of an infrared excess from JHK data only. Further data taken at  $3.5 \mu\text{m}$  can sometimes distinguish between thermal and non-thermal excesses. Figs. 1.6a and 6b help in understanding why this may be so. Notice that at  $3.5 \mu\text{m}$  the continuum from the power law exceeds that from the black body. It must be emphasized however that although this is so in this particular case, different physical conditions may arise, e.g. hotter or more dust, or a different power law spectral index, which could produce continua which are very much alike. Glass (1973) has remarked on the possible importance of a free-free contribution to the infrared light of galaxies with emission lines similar to those seen in galactic HII regions (i.e. non-Seyfert). Optically thin free-free emission in

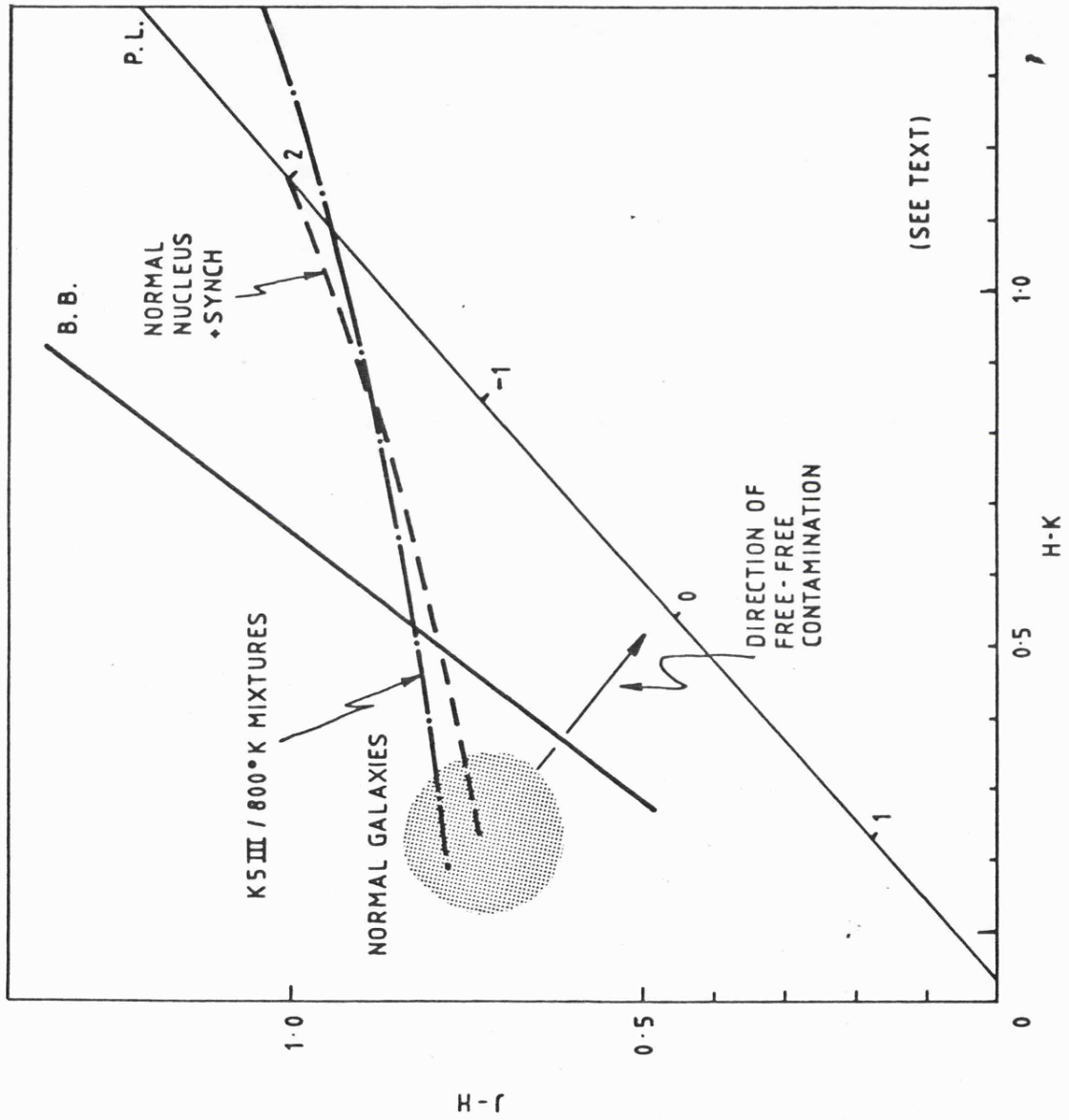
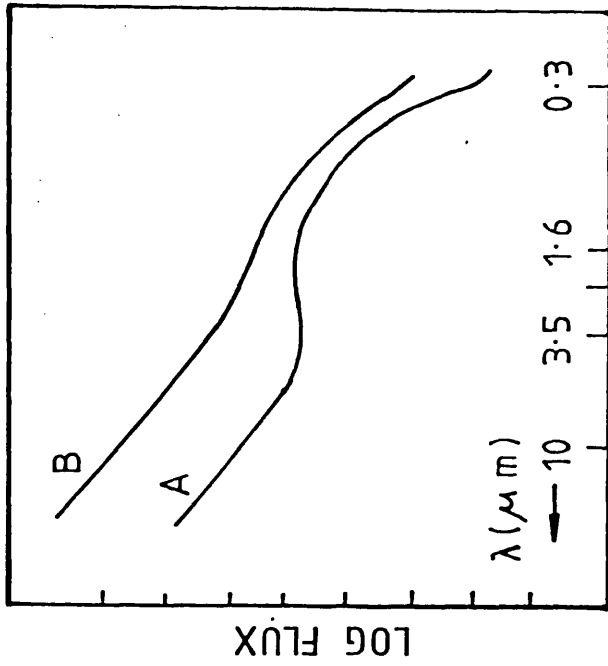


Fig. 1.5: Effect of Non-stellar Sources on Normal Galaxy Colours

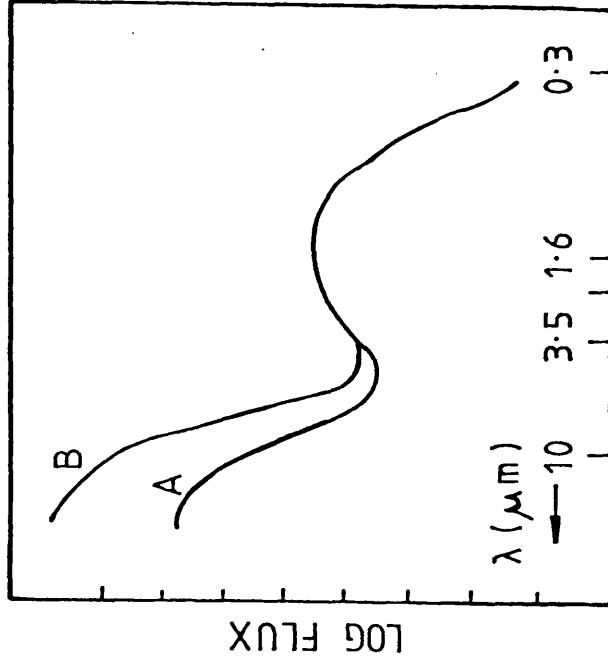
a) Normal Nucleus + Power Law ( $f_\nu \propto \nu^{-1.7}$ )



Curve A: Power law flux at  $3.5 \mu\text{m}$  equal to that of normal nucleus.

Curve B: Power law flux at  $3.5 \mu\text{m}$  is 10 times that of normal nucleus.

b) Normal Nucleus +  $200^\circ\text{K}$  B.B.



Curve A: BB flux at  $3.5 \mu\text{m}$  is  $10^{-5}$  that of normal nucleus.

Curve B: BB flux at  $3.5 \mu\text{m}$  is  $10^{-4}$  that of normal nucleus.

Fig. 1.6: Synthetic Energy Distributions (after Neugebauer et al. 1976a).

the near infrared approximates to  $f_{\nu} = \text{constant}$ , and therefore in terms of fig. 1.5 can be considered as a special case of the power law (P.L.) line with  $\alpha = 0$ . Therefore free-free may contribute to galaxies exhibiting H-K excesses, but J-H deficits. Free-free contamination could not explain the large near infrared excesses of most of the active galaxies described in the next section.

The ideas given above present only a simple introduction to the weird world of excesses. In reality behaviour more complex than the ideal cases outlined above can be expected, e.g. black body radiation from dust clouds which show a spatial variation of temperature, or synchrotron radiation from electrons with an unusual energy spectrum. These two examples are probably the most obvious; a combination of both is not out of the question.

## 1.6 ACTIVE GALAXIES

### Q.S.O.'s

The only systematic near infrared study of Q.S.O.'s published to date<sup>\*</sup> is that of Oke et al. (1970), who measured the forty-three brightest Q.S.O.'s at  $2.2 \mu\text{m}$  and obtained spectrophotometric ultraviolet and visible data for most of these. The main conclusions of the survey were that Q.S.O.'s have power law spectra from the ultraviolet through to  $2.2 \mu\text{m}$  with spectral indices in the range  $-1.6 \leq \alpha \leq -0.2$ , and secondly that there is no characteristic of the  $0.3 \mu\text{m}$  to  $2.2 \mu\text{m}$  spectrum which distinguishes radio quiet from radio active Q.S.O.'s. Other than the statement on power law continua, implying a non thermal source, no firm conclusion concerning the energy source was drawn. Rieke and Low (1972) measured a number of Q.S.O.'s out to  $10 \mu\text{m}$  and found that not all of these had such steep spectral indices from  $1 \mu\text{m}$  to  $10 \mu\text{m}$  as that of 3C 273 (Low and Johnson, 1965). Since the early

<sup>\*</sup> See addendum, p. 1.51.

seventies no  $1 \mu\text{m} - 4 \mu\text{m}$  data on Q.S.O.'s (as a class) has appeared in the major journals, however Becklin et al. have a major ongoing program to measure all quasi-stellar-sources brighter than  $m_v = 17$ , from  $0.3 \mu\text{m}$  to  $10 \mu\text{m}$  (Hale Obs. Report 1976-77). No paper has been published yet but preliminary results contradict the findings of Oke et al., and show that:

- a) The flux density of Q.S.O.'s does rise from the visible into the near infrared but there are several different types of continuum, which cannot be characterized by single, simple power laws.
- b) Though some quasars emit most of their energy at wavelengths  $> 10 \mu\text{m}$ , not all of them do. In fact a significant number reach a maximum at  $\sim 3 \mu\text{m}$ .

The nature of the infrared radiation mechanism is being closely studied, the new data are being checked for the presence of thermal re-radiation from dust as well as for the usually suggested non thermal sources. The conclusions of the new survey summarise the extent of current knowledge on the infrared continua of Q.S.O.'s.

**POLARIZATION:** Recent measurements of 3C 273 in the visible and infrared ( $2.2 \mu\text{m}$ ), (Kemp et al. 1977) show a very low degree of polarization in both wavebands which suggests either that the source is almost unpolarized or some depolarizing mechanism is working. 3C 273 is the only Q.S.O. measured polarimetrically to date.

**VARIABILITY:** In the near infrared and at  $10 \mu\text{m}$  possible variation in the flux from Q.S.O.'s has not been extensively monitored. Measurements of 3C 273 at  $2.2 \mu\text{m}$  in 1964-65 (Low and Johnson), 1968 (Low), 1970 (Oke et al.), 1972 (Rieke and Low) and 1976 (Allen) show that there has been no large amplitude variation during the last decade

or so. In the 1970 survey of Oke et al. the four large amplitude visible variables in the sample showed no sensible energy distribution changes (from the ultra violet through to  $2.2 \mu\text{m}$ ) during the variation, i.e. the variations at U and K followed those at V. No evidence for variability at K or other wavebands was found for the rest of the sample.

SPECTROMETRY: Very recently two Q.S.O.'s, 3C 273 and PG 0026 + 129, have been observed spectrophotometrically (Grasdalen 1976, Puetter et al. 1978). Measurements of the redshifted  $P\alpha$  line, at  $\sim 2.15 \mu\text{m}$ , are being used together with optical line data to study the peculiar recombination line ratios found in Q.S.O.'s.

### Seyfert Galaxies

Seyfert nuclei have been studied closely at near infrared wavelengths, notably by Penston et al. (1974) who concentrated on the classical Seyferts, and by Neugebauer et al. (1976) and Allen (1976) who examined the brighter Markarian Seyferts. Also, Stein and Weedman (1976) have observed thirty-nine Seyferts at  $0.3 \mu\text{m}$  and  $3.5 \mu\text{m}$ ; their sample included most of the bright classical and Markarian Seyferts.

THE NEAR INFRARED CONTINUUM: Penston et al. showed that the conclusion of Pacholczyk (1967), i.e. that the V to  $3.5 \mu\text{m}$  continuum from the nucleus of NGC 1068 resembled that of a normal galaxy nucleus plus an underluminous quasar, can be extended to include all the Seyfert nuclei in their sample. Ironically their data show that NGC 1068's colours gave the worst fit to this model as its near infrared spectral index was too steep. In this respect the spectrum of NGC 1068 more closely resembled the spectra of non Seyfert "infrared galaxies" (Low 1970, 1972) such as M82 and NGC 253, whereas the other Seyferts closely

mimicked 3C 273. At the time Weedman's spectral classification, which split Seyferts into two categories, was not widely referred to (at least among the infrared community) and Penston et al. made no mention of NGC 1068 being a type 2 Seyfert to explain their findings. Two years later however Stein and Weedman, and Neugebauer et al. drew attention to differences in the continua of the two classes. Stein and Weedman concluded that the nuclei of class 1 Seyferts contained a strong non thermal component which closely followed a power law of index  $\alpha = -1.3 \pm .3$ , and that class 2 nuclei, if typified by NGC 1068, contained a non stellar component which was almost certainly thermal re-radiation from heated dust. Neugebauer et al. were more cautious. They observed only five type 1 and 3 type 2 (cf. Stein and Weedman with 30 type 1 and 9 type 2) but had more extensive infrared data, and warned against over generalization regarding the shape of type 1 and type 2 continua. The  $1 \mu\text{m} - 10 \mu\text{m}$  spectra of Mkn 6, 9, 10, 79 and 124 (Neugebauer et al.'s type 1 sample) showed considerable differences from one to the next, in particular Mkn 124 showed a plateau between  $3.5 \mu\text{m}$  and  $10 \mu\text{m}$  and Mkn 10 showed a slight inflection around  $3.5 \mu\text{m}$ . So, although the Mkn 6, 9, and 79 spectra could be approximately fitted by power laws the other two couldn't. Neugebauer et al.'s data for type 2 Seyferts was in broad agreement with the predictions of Stein and Weedman, however their measurements of Mkn 34 showed evidence of a possible power law contribution to the continuum flux around  $3.5 \mu\text{m}$  and in the U.V.

The latest data on this subject have just, at the time of writing, become available (Rieke, December 1978). This paper presents new and more extensive data on the infrared continua of Seyfert galaxies. A total of forty-nine of these have been measured at JHKL with additional photometry at  $10 \mu\text{m}$  for all but three. The major conclusion

is that type 1 Seyferts cannot be considered simply as a power law plus stellar continuum, and moreover there may be an overlap in the shape of the infrared continua of type 1 and type 2 systems. A selection of type 1 and 2 spectra are shown in fig. 1.7. It is clear from this diagram that a great variety of spectral forms exist within the class 1 variety, and also that some type 1 spectra are remarkably similar to those of type 2. Several features in the spectra shown are worth pointing out.

- a) 3C 120, II Zw 136 and Mkn 509 show flux deficiencies at  $1 \mu\text{m}$ .
- b) Mkn 231 and NGC 1068 have been observed more closely, and in narrower wavebands than the rest of the sample, and it can be seen from their spectra that broad band photometry can substantially underestimate the spectral structure present.
- c) The continua of the type 1 Seyferts NGC 3227 and NGC 6814 and those of type 2, particularly Mkn 1 and Mkn 3 show clear similarities.

The  $1 \mu\text{m}$  deficiency is a newly discovered phenomenon and requires further study. The continuum substructure in Mkn 231 and NGC 1068 is discussed at length in Rieke, 1976 and Rieke and Low, 1975b respectively. Rieke is continuing to study detailed structure in other Seyferts. The similarity in the continuum shape of some of the two classes and the fact that dust is known to be present in at least one type 1, Mkn 231 - note the  $10 \mu\text{m}$  silicate absorption feature - is strong circumstantial evidence that in some type 1's re-radiation by warm dust plays a part in their infrared emission. In the case of Mkn 231 this could dominate (Rieke 1976, Joyce et al. 1975). Stoner and Ptak (1978) have even suggested that heated dust is the prime source in all type 1 Seyferts.

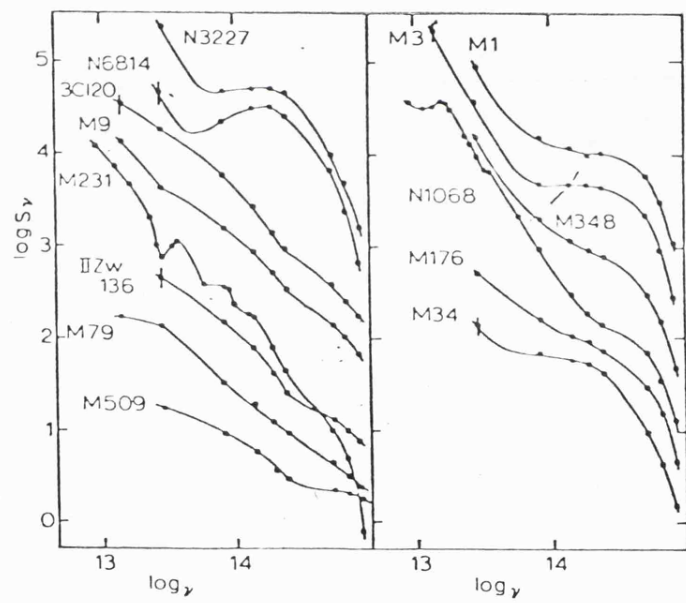


Fig. 1.7: Seyfert Energy Distributions (Rieke 1978).

VARIABILITY, SIZE OF NON STELLAR SOURCE: Variation in the luminosity of a source, at a given wavelength, sets a limit on the size of the region emitting that wavelength, since no complete changes can fully take place in less time than it takes light to traverse the region, i.e.  $R(\lambda) \lesssim c \tau_\lambda$ , where  $\tau_\lambda$  is the period of the variation at wavelength  $\lambda$ , and  $R$  is the linear size of the <sup>source</sup>. The finite speed of light has the effect of smoothing out temporal changes. Possible short term (i.e.  $\sim$  months) variations in the near infrared flux from Seyferts has been claimed, and not subsequently discredited (see section 1), for only two galaxies NGC 4151 and NGC 5548 (Penston et al. 1971, Penston et al. 1974). The evidence for variability in NGC 5548 was weak and will not be discussed further. In the case of NGC 4151 the  $2.2 \mu\text{m}$  luminosity was seen to change by a factor  $\sim 1.6$  during a period of about four months. Furthermore a variation  $\sim 50\%$  in the  $10 \mu\text{m}$  flux over a similar time scale has been claimed (Stein et al. 1974). If accepted, these variations limit the size of the infrared source to  $\lesssim 0.1 \text{ pc}$ . It should be pointed out that these observational results have not been independently confirmed.

No short term variation has been seen in the two or ten micron radiation of NGC 1068, the archetypal class 2 Seyfert. In fact the ten micron emitting region has been resolved at  $1''$  (Becklin et al. 1973b) which corresponds to  $\sim 100 \text{ pc}$  for a Hubble constant  $\sim 50 \text{ km s}^{-1} \text{ Mpc}^{-1}$ , therefore no variation in the ten micron flux can be expected during time scales  $< 300 \text{ years}$ . If the two micron non-stellar source is the same as the ten micron source, the same conclusion holds. The infrared luminosity of the  $100 \text{ pc}$  region can be accounted for by a highly luminous population of hot stars embedded in a dust cloud. Harwit and Pacini (1975) have discussed the physical conditions in this type of environment. No similar data are available yet for other type 2

Seyferts.

The recent work of Rieke (1978) casts some doubt upon possible near infrared variability in Seyferts. He shows that with only four exceptions there is no evidence for variability greater than measuring uncertainty between his results and previous data, over times of a year or more. Even among the exceptions, NGC 4051, 3C 120, Mkn 6 and Mkn 509 the data is insufficient and no firm conclusion can be made concerning short term variability on time scales  $\lesssim$  1 year. However there is evidence that the luminosity of 3C 120 appears to have decreased by a factor two over ten years.

In conclusion it must be emphasised that a systematic survey of infrared variability in Seyferts is required. Rieke's recent data (and the data of others) are inadequate and allow for variations  $< 20\%$  to go unnoticed. Positive evidence of short term variability would be the most direct demonstration that the infrared continua were of non-thermal origin, since the small diameter source demanded by such variations could not thermally produce, at plausible temperatures given the spectra, the required flux densities. The observed slow change in 3C 120 is consistent with the shortest time scales that might be observed from a thermal source (Rieke and Lebofsky 1979, quoted in Rieke 1978).

POLARIZATION; Polarization information for type 1 Seyferts is still somewhat limited but this situation should change in the next year or so. The available data comes from Kemp et al. (1977) who found very low polarization in the near infrared for NGC 4151, Mkn 231 and NGC 1275. (NGC 1275 is in fact a type 2, but like type 1 galaxies it is an X-ray source.) This low polarization was something of a surprise as synchrotron radiation was believed to be a probable major source of the near infrared

emission of these galaxies. The only conclusion that can be drawn at this stage is the same as that for 3C 273 given earlier, i.e. the near infrared source is either unpolarized or some depolarizing mechanism (e.g. Faraday Rotation) must be working.

NGC 1068 has been closely studied polarimetrically (Knacke and Capps 1974 and Lebofsky et al. 1978). Relatively large polarization compared to that found in those of type 1 was detected in the near infrared. Knacke and Capps observing at  $3.5 \mu\text{m}$  and  $10 \mu\text{m}$  concluded that their data could not distinguish between thermal and non thermal sources, and moreover could not rule out the possibility that both were present. The new near infrared observations at  $1.25 \mu\text{m}$ ,  $1.6 \mu\text{m}$ ,  $2.2 \mu\text{m}$  and  $3.5 \mu\text{m}$  of Lebofsky et al. have provided some fascinating data. High resolution, multiaperture photometry and polarimetry revealed a small nuclear source,  $< 4''$  - and very probably much smaller, which is responsible for the polarized flux. Furthermore, this source can only be directly observed in the wavelength range  $1 \mu\text{m} - 5 \mu\text{m}$ , since at shorter wavelengths the dust obscuration is too great and at longer wavelengths dust re-radiation dominates the spectrum. A bewildering variety of models was considered in an attempt to explain the results of the infrared photometry and polarimetry, these included a range of different black bodies at different temperatures superimposed on each other, power laws plus reddening and combinations of each. They concluded that a highly obscured, polarized power law spectrum is the most straightforward explanation of their high resolution data, but that complex combinations of thermal sources are also a possibility. According to Lebofsky et al. linear and circular polarization observations at  $5 \mu\text{m}$  may distinguish between these two models.

SEYFERT SUMMARY: The sum total data reviewed above tells us that Seyfert galaxies appear to be very individualistic in their infrared

emission, and although there is a rough correlation between infrared properties and Seyfert class this does not distinguish between the two as well as Weedman's spectroscopic (defining) criterion. More polarimetric data would be useful to see if the degrees of polarization seen in NGC 4151 and NGC 1068 are common to the other members of their respective classes and particularly to see if other type 2 Seyferts also have small, possibly non thermal, sources hidden in their nuclei.

The number of type 1 Seyferts containing dust in their nucleus is unknown. As dust re-radiation may play an important role in some of these galaxies it would clearly be of great interest to search for the silicate absorption feature in the brighter Seyferts. Future models must consider combinations of thermal and non thermal sources as well as just one or the other.

#### BL Lacertae Objects

Among the thirty or so known BL Lacs (Stein et al. 1976) useful work at infrared wavelengths has been confined to five of the brightest, BL Lac itself, OJ287, AP LIB, Mkn 421 and Mkn 501. Of these, all but OJ 287 are known or suspected to be embedded in a galaxy, probably an elliptical. The objects measured to date all show JHKL colours redder than normal galaxies, yet these range from only small excesses in Mkn 421 and Mkn 501 (Allen, 1976) to large excesses in BL Lac (Oke et al. 1968, Rieke 1972), OJ 287 at  $3.5 \mu\text{m}$  (Dyck et al. 1971) and AP LIB (Andrews et al. 1974). The three with large excesses have UV to near infrared continua which are steeper than those of the average Q.S.O., but are rather similar in this respect to the more variable Q.S.O.'s. The flatter spectra of Mkn 421 and 501 suggest either differences in physical conditions from one BL Lac to the next, or a range in the dominance of the central (BL Lac) source over the

surrounding galaxy.

Variations in the near infrared have been detected in OJ 287 and probably in BL Lac (Epstein et al. 1972), the variations in BL Lac are definite at  $10 \mu\text{m}$  (Rieke 1972). Andrews et al. have monitored small variations at H and K in AP LIB which indicate that the continuum is steeper when the source is fainter. Allen has seen a variation of order 50% at H, K and L in Mkn 421 over a period of two months. No variation in the infrared has been reported for Mkn 501. The variations seen in OJ 287, BL Lac, AP LIB and Mkn 421 have all been on similar time scales, i.e.  $\sim$  months; intraday variation has been seen in OJ 287 but a search for this in BL Lac proved negative. None of the others have been examined for this behaviour. The spectral indices and rapid variability of these sources suggest a non-thermal, probably synchrotron, emission mechanism (Oke et al. 1968, Rieke 1972, Andrews et al. 1974). In their recent review article Stein et al. (1976) called for more polarization measurements, particularly at  $\lambda = 2.2 \mu\text{m}$ , to provide a key to the understanding of physical conditions in BL Lacs. Since then several successful attempts have been made to measure this property in BL Lac itself (Knacke et al. 1976), OJ 287 and BL Lac (Rudnick et al. 1978) and AP LIB (Capps and Knacke 1978). All three have shown high percentage polarization (between 3% and 17%), in marked contrast to the very low polarization in Q.S.O. 3C 273. The degree of polarization and the observed absence of the reddening expected if the polarization was due to grain alignment seem to rule out dust as the cause of the polarization, but are consistent with a synchrotron source.

To summarise, the limited infrared data available, like that from optical and radio observations, suggests that most BL Lacs are probably non-thermal in nature. Where coordinated optical-infrared-radio

observations exist (Epstein et al. 1972, Rudnick et al. 1978) there is some evidence, particularly for OJ 287, that the optical through radio continuum comes from the same source component, though this is not conclusive for BL Lac (Olsen 1969) and has not been investigated for the others. Future work will probably be concentrated on obtaining simple photometric (J,H,K,L and  $10\ \mu\text{m}$ ) data on as many BL Lacs as possible in order to gauge the homogeneity of the class, and on coordinating infrared observations with optical, radio and perhaps X-ray observations in searches for intraday and longer variations in flux, degree of polarization and polarization position angle, to tie down the nature of physical conditions existing in these puzzling objects.

#### Emission Line Galaxies (ELG's)

Rieke and Low (1972) measured a few of these, IIZw 23, NGC 3690, NGC 4194, NGC 3504 and NGC 4385 and found that although their near infrared emission was essentially only that of normal galaxies, the ten micron luminosity - of their small sample at least - rivalled that of the average Seyferts. In his JHKL survey of southern galaxies Glass (1973, 1976) included a number of objects known to have peculiar nuclei containing "hot spots" (Sersic and Pastoriza 1965), or HII regions close to their nuclei. Seven of these, all known ELG's, NGC 613, NGC 1365, NGC 1672, NGC 1808, NGC 5253, NGC 7552 and NGC 7582, showed large K-L excesses, as large or even larger than those of many Seyferts. Unlike the Seyferts however only three of these, NGC 1365, NGC 5253 and NGC 7582 showed any significant excess at JHK. The presence of an excess shortward of  $3.5\ \mu\text{m}$  may be correlated with the level of excitation, in the sense that galaxies with high excitation emission lines show excesses at shorter wavelengths than those with only lower excitation lines. This behaviour has not been systematically investigated,

however it is worth noting that NGC 1365, NGC 5253 and NGC 7582 do show lines more highly excited than most of the rest of the Glass sample, and furthermore NGC 5506, an ELG X-ray source exhibiting lines as highly excited as  $\overline{\text{Fe VII}}$  has the reddest J-H and H-K colours of any ELG yet measured (Glass 1978). On the other hand M82 (not usually considered primarily as an ELG) does not show lines as highly excited as those seen in NGC 5506, and is not such a strong X-ray source, yet has JHK colours equally as red. The presence, extent and temperature of warm dust almost certainly plays a major role in the near infrared continua of those ELG's with JHK excesses.

More recently work by Allen (1976) and Neugebauer et al. (1976) has taken the number of ELG's measured in the infrared to over forty. Allen observed twenty two, taken mainly from the Markarian non-Seyfert galaxies, of which only Mkn 171 (a,b), Mkn 201 and Mkn 266 showed any excess at wavelengths of  $3.5 \mu\text{m}$  or less, though Allen emphasised that Mkn 52 showed a strong excess at  $8.4 \mu\text{m}$  yet had none at J,H,K or L. Neugebauer and Co. included ten "intergalactic HII region" galaxies in the UV to  $2.2 \mu\text{m}$  spectrophotometric/photometric study of Markarian galaxies. All ten were measured at  $1.6 \mu\text{m}$  and  $2.2 \mu\text{m}$ , Mkn 33 and Mkn 52 were measured at  $10 \mu\text{m}$  and marginal detections of Mkn 59 and Mkn 67 were obtained at  $10 \mu\text{m}$ . The infrared light from these galaxies comes from diffuse irregular patches of high surface brightness; generally no pronounced dominant central condensation (i.e. a nucleus) was observed in any of these galaxies. The irregular and extended nature of this type of source complicates photometry as centring becomes subjective, and therefore comparison of independent measurements can be reliably made only when centring positions, relative to nearby field stars, are well known and in agreement. The intrinsic, i.e. reddening corrected, UV to  $2.2 \mu\text{m}$  energy distributions

found in the intergalactic HII regions are remarkably flat. Although it is tempting to attribute this to a dominant free-free source, Neugebauer et al. claim that the observed  $H\beta$  intensity implies, for reasonable temperature, that the  $2.2\ \mu\text{m}$  flux density exceeds that expected from free-free emission by a factor of ten or more. The near infrared flux is therefore envisaged as arising from either M and K supergiants and warm dust intermingled with young ionizing stars, or from a (visually) inconspicuous population of old M and K giants. In the few cases where  $10\ \mu\text{m}$  measurements were obtained they were consistent with the flux expected from dust of temperature  $\sim 200^\circ\text{K}$ . In general the character of the infrared emission from Neugebauer et al.'s sample is not unlike that from Galactic HII regions.

The majority of emission line galaxies observed so far show no significant excesses, relative to normal galaxies, shortward of  $3.5\ \mu\text{m}$ , yet the case of Mkn 52 shows that this does not rule out excesses at longer infrared wavelengths. In general, where JHK excesses exist they are small but are accompanied by larger excesses at L. This however is not exclusively so, as the case of NGC 5506 proves. This heterogeneous group of galaxies needs further investigation at all wavelengths to establish which of the many members are in fact physically related.

### Radio Galaxies

Here the term "radio galaxy" refers to those "strong" radio sources defined by Matthews, Morgan and Schmidt (1964); "weak" sources, such as 3C 231 (M82) and 3C 71 (NGC 1068) are not included as radio galaxies for the purpose of this discussion, but have been described elsewhere under more pertinent section headings. Five classic radio sources have been measured at infrared wavelengths, Virgo A (M87),

Centaurus A (NGC 5128), Cygnus A, Fornax A (NGC 1316) and Perseus A (NGC 1275). Two of these, Virgo A (Frogel et al. 1978) and Fornax A (Glass 1973) show no near infrared excess in the main body of the galaxy, although Virgo A shows near infrared synchrotron emission in its famous jet (Wieniewski and Kleinmann, 1968). Rieke and Low (1972) include M87 in the "moderate excess" subcategory of their  $10 \mu\text{m}$  extragalactic source survey. The multiaperture photometry of Frogel and Co. suggests a possible bluening of the J-H and H-K colours in an aperture of  $7''$  relative to larger apertures; if real this may be related to the supermassive object now believed to exist at the centre of M87. There is no published near infrared data for Cygnus A, but it is well known that this radio source has a huge  $10 \mu\text{m}$  excess and has been dubbed an "ultra-high luminosity galaxy" by Rieke and Low (1972) along with such galaxies as Mkn 231. Cygnus A is a very faint, distant galaxy ( $\sim 300 \text{ Mpc}$ ) but long exposure photographic plates suggest it may be similar to Cen A, as it appears to show a dark central lane. The strong  $10 \mu\text{m}$  source in Cen A is known to be embedded in the famous dust lane which seems to split the galaxy in two. It was Becklin et al. (1971) who first discovered this source and identified it with the hot spot of Kunkel and Bradt (1971). Later Grasdalen and Joyce (1976) confirmed the results of Becklin et al. and further showed that the  $10 \mu\text{m}$  excess of the small central source is also clearly apparent at wavelengths as short as  $1.6 \mu\text{m}$ , and that it was in fact  $\lesssim 3''$  in diameter, so improving upon the ( $\lesssim 7''$ ) estimate of Becklin et al. In their paper Grasdalen and Joyce concentrated their attention upon the small source and concluded that it was of non thermal origin and probably related to the X-ray source of Grindlay et al. (1975). Unfortunately they neglected to point out that their multiaperture data clearly show that the extended region ( $\sim 12''$ ) surrounding the central

source also has a near infrared excess which, furthermore, cannot be explained simply by reddening. Emission from warm dust is the most likely explanation. Very recently Telesco (1978) has shown the presence of regions of  $10 \mu\text{m}$  emission as far as  $80''$  from the nucleus. Mapping of the central  $\pm 2$  arc minutes of Cen A at  $1.6 \mu\text{m}$ ,  $2.2 \mu\text{m}$  and  $10 \mu\text{m}$  would surely produce some fascinating results.

Perseus A is a strong radio source showing variability and a complex core structure embedded in an extensive halo. This structure is quite unlike the simple bi-lobed sources of the other galaxies in this section. It should be made clear at this point that the infrared flux from the previous galaxies is associated with the visible central galaxy, no infrared emission has yet been detected from the giant radio lobes. Perseus A has very red near infrared colours, is extremely luminous at  $10 \mu\text{m}$  and has been detected out as far as  $34 \mu\text{m}$  (Rieke and Low 1975b). It is also a Seyfert galaxy of the type 2 class, so whether the infrared flux, at the various wavelengths, is related to its Seyfert properties or to its radio properties is uncertain. It may not even be a "true" Seyfert; it certainly isn't a spiral galaxy as most, and possibly all, other Seyferts are, and although it spectroscopically resembles type 2's it is a stronger X-ray source than most type 1's. Had it not been included in Seyfert's original study, Seyfert 1943, it probably would not have been grouped with galaxies called Seyferts today, but would more likely be considered as a peculiar radio source (Weedman 1976). This uncertainty is not confined to Per A, Cen A could be considered as a dusty peculiar galaxy (see next section) or an X-ray galaxy. Is the infrared flux in such objects related to the X-rays, to the radio properties, to the bursts of star formation observed or are they all inter-related? Certainly bi-lobed radio structure is not always accompanied by bursts of star formation as witnessed by the many

morphologically normal radio ellipticals. A near infrared to  $10\ \mu\text{m}$  survey of strong radio sources to look for any correlation between infrared character and such properties as (i) radio structure, i.e. core-halo, bi-lobed or complex, and (ii) morphological peculiarities such as dust lanes, hot spots, etc., would clearly help our understanding. Indeed the whole future study of active and peculiar galaxies hinges on such surveys, which should, ideally, cover the whole electromagnetic spectrum.

### Dusty, Peculiar Galaxies

This final category of abnormal galaxies is again almost certainly non-homogeneous, although there are probably sub groups which are physically related. Krienke and Hodge (1974) collated and reviewed the visible and radio data available for the most well known northern dusty galaxies. These were mainly of the IO type but some dusty spirals and lenticulars were included. Three subclasses of dusty, peculiar objects were suggested (i) M82 type,  $H\alpha$  filaments present, possibly exploding, (ii) interacting galaxies, e.g. NGC 5195 in the M51 system, (iii) dusty galaxies with no  $H\alpha$  activity and showing no evidence of any interaction - possibly older remnants of (i). More recently Cottrell (1977) has suggested that all galaxies of this ilk are the product of an interaction of some sort, past or present. This must be investigated further. Only a few of these have been studied at infrared wavelengths, which is unfortunate as this would enable us to see through the dust which prevents detailed optical investigation. The few for which data is available, M82, NGC 3077 and NGC 5195 all show a  $10\ \mu\text{m}$  excess. In M82 this excess is on a par with those seen in the Seyferts whereas in NGC 5195 and NGC 3077 the  $10\ \mu\text{m}$  flux is midway between that of a normal galaxy and that of an average Seyfert. Only M82 however shows an excess

at near infrared wavelengths ( $\lambda < 3.5 \mu\text{m}$ ). This is possibly a further example of the heterogeneous nature of IO galaxies as a class, but the extent of JHK and  $10 \mu\text{m}$  excesses in dusty galaxies generally is yet to be fully investigated. Further discussion of the infrared properties of dusty, peculiar systems is given in Chapters 4 and 5.

### 1.7 THE STUDY OF THE SPATIAL DISTRIBUTION OF NEAR INFRARED RADIATION IN GALAXIES

We have at present only very limited information on the spatial distribution of infrared light in galaxies. This must be improved as knowledge of this kind is important for several reasons:

- (i) Luminosity profiles provide important constraints on theoretical dynamical models of galaxies (e.g. Freeman, 1976). Near infrared profiles may furnish a means of checking the distribution of mass held in the very cool population that is virtually undetectable at visible wavelengths.
- (ii) Multiwaveband profiles, preferably all of UBVR<sub>I</sub>JHKL, covering as much of a galaxy as possible, are necessary for a full understanding of the distribution of stellar populations. Unusual colour gradients in active and peculiar galaxies would obviously help in understanding the sources involved.
- (iii) In galaxies which contain large quantities of widely distributed dust, the underlying stellar population is often partly or completely hidden to optical scrutiny. As stars generally do not emit significantly in the X-ray, far infrared ( $\lambda < 5 \mu\text{m}$ ) or radio regions of the spectrum, the only way of studying the obscured stars directly is by observing at near infrared wavelengths ( $1.2 \mu\text{m} \lesssim \lambda \lesssim 2.2 \mu\text{m}$ ).
- (iv) Our knowledge of the presence and distribution of hot

( $700^{\circ}\text{K} \lesssim T_{\text{EFF}} \lesssim 1500^{\circ}\text{K}$ ) dust in galaxies is very scanty, but may be furthered by observations in the  $1\text{--}3.5\mu\text{m}$  region. The black body radiation at these shorter wavelengths, from dust in this temperature range, will far outweigh that at  $\sim 10\mu\text{m}$ , and would be apparent as a colour excess (relative to integrated starlight) which could not be explained by interstellar reddening.

In the majority of cases multiaperture photometry provides the only data available at present which describes the spatial distribution of near infrared radiation. As mentioned earlier in this chapter (1.4) Frogel and Co. have emphasised the inadequacy of the multiaperture technique for studying, for instance, radial colour gradients. Infrared instruments capable of imaging very faint extended sources have yet to be fully developed, consequently the only way of mapping or measuring luminosity profiles of galaxies is by moving the source across the detector field of view. This can be achieved by scanning the telescope itself, or the secondary mirror, or by means of a focal plane scanning mirror housed in the photometer (see Chapter 2). At the time of writing published data obtained using scanning techniques exists for only a handful of extragalactic objects; detailed work is limited to the Galactic centre and M31, although some data is available for NGC 3115 and 2768 (S0 and E5 respectively), NGC 253 (Sc), NGC 4631 (Scd), NGC 6946 (Sc) and IC 342 (Scd).

#### M31 and the Galactic Centre

The Caltech pair Gerry Neugebauer and Eric Becklin pioneered scanning photometry at infrared wavelengths in the late sixties. In 1968 they presented maps of the central  $\sim 150$  pc of the Galaxy (Becklin and Neugebauer, 1968), and a little later with Alan Sandage they published the two micron luminosity profile of the central  $400$  pc ( $\pm 2$  arcmins)

of M31 (Sandage et al., 1969). The data presented in these two papers revealed a close similarity in the two micron profiles of the two systems which suggested the Hubble type of the galaxy was closer to Sb, like that of M31, than to Sc as radio studies of the spiral arms had previously suggested. Remember that this was the first time that the stars of the Galactic centre had been directly observed (section 1.1). Later work (Becklin and Neugebauer, 1975) at higher resolution, and including maps at both two and ten microns, revealed the astonishing complexity of the central 3 pc of our Galaxy. The two and ten micron contour maps are on the whole quite dissimilar, indicating that different sources are responsible for the emission at the two different wavelengths. The observed two micron emission results from the output of three main components: about one third from a very bright point source (a luminous foreground star), one third from fifteen fainter discrete sources and the rest from the extended unresolved stellar background. The ten micron emission in the same region comes from nine discrete sources, an extended ridge, probably heated dust, and the rest from a low surface brightness background. The discrete sources which appear only at  $2.2 \mu\text{m}$  are believed to be late type supergiant stars (Neugebauer et al., 1976b) brighter than any previously expected to inhabit the nucleus. The discrete  $10 \mu\text{m}$  sources are variously thought to be luminous, dust embedded, late type stars, planetary nebulae or compact dusty HII regions (Borgmann et al., 1974). The  $2.2 \mu\text{m}$  discrete source no. 16 of Becklin and Neugebauer is definitely extended and is coincident with the radio point source of Balick and Brown (1974); it is probably the Galaxy's stellar density maximum, i.e. the nucleus.

After the early Sandage, Becklin, Neugebauer paper there was no further work on M31 at infrared wavelengths until recently when Iijima et al. (1976) compared the  $1.0 \mu\text{m}$  and  $2.2 \mu\text{m}$  profiles of the central

$\pm 8'$  with a resolution of  $1.8'$ , Abolins and Adams (1976, this thesis) measured the  $2.2 \mu\text{m}$  profile of the central  $\pm 6'$  with a resolution of  $45''$ , Matsumoto et al (1977) presented a  $2.2 \mu\text{m}$  contour map for the central  $\pm 10'$  and Abolins and Adams (1978, this thesis) measured the V-K gradient in the central  $\pm 5'$ . Further discussion is left until Chapter 3 where the Leicester research on M31 is described in full.

### IC 342

The nucleus of this late-type spiral has been mapped by Becklin et al. at  $1.6 \mu\text{m}$ ,  $2.2 \mu\text{m}$  and  $10 \mu\text{m}$ , with a resolution of  $3''$  ( $\approx 80 \text{ pc}$ ). No publication has yet appeared as data reduction and interpretation is not yet complete (Becklin, private communication). Preliminary analysis shows that the  $2.2 \mu\text{m}$  and  $10 \mu\text{m}$  centroids are definitely not coincident; the  $2.2 \mu\text{m}$  distribution is similar to that in the Galaxy and M31, and the ten micron source is quite bright and extended, and is believed to be associated with giant HII regions.

### NGC 4631

A  $2.2 \mu\text{m}$  scan along the edge-on axis of this Scd galaxy revealed that the peak at this wavelength was not coincident with the brightest visible region (Aaronson, 1978a). The closer proximity of the infrared peak (cf. the visible) to both the peak radio intensity (Pooley 1969) and the geometric centre of the galaxy suggests the infrared peak is probably the true position of the nucleus as defined by the stellar density maximum. The bright visible region is believed to be a foreground HII region. Aaronson believes the observed H-K excess seen in the nucleus of the galaxy is due to hot dust ( $T \sim 700^\circ\text{K}$ ).

NGC 2768 and NGC 3115

Strom et al. (1978) have obtained  $2.2\ \mu\text{m}$  minor axis brightness profiles of the early type galaxies NGC 2768 (E5) and NGC 3115 (E7/S0). By combining these with similar scans at V to obtain V-K gradients, and then comparing the results with the globular cluster and elliptical galaxy metallicity versus VJHK colour data of Frogel et al. (1978) (see section 1.4), Strom and Co. conclude that if metal abundance variations are mainly responsible for the colour differences between globular cluster galaxies and elliptical galaxies, then they are also the likely cause of intragalaxian colour changes in early type galaxies if typified by those in NGC 2768 and NGC 3115.

Strom et al.'s data exclude the possibility that NGC 2768 and NGC 3115 have massive halos made up of very cool dwarf stars ( $\sim M8V$ ) since the observed V-K index grows monotonically bluer, even at the outskirts of the galaxies, whereas a massive halo of very red dwarfs would produce a reddening of the V-K index at the greatest radial distances. (Strom and Strom in "Structure and Properties of Nearby Galaxies", I.A.U. Symposium No. 77, 1977).

NGC 253

NGC 253 does not fall neatly into any of the active/peculiar galaxy categories given above. Its optical appearance is that of a perfectly normal Sc galaxy whereas its near infrared excess,  $10\ \mu\text{m}$  excess and nuclear emission lines mark it as distinctly abnormal. Despite the extended  $10\ \mu\text{m}$  nuclear emission no corresponding near infrared map has been published, but Becklin et al. (1973a) and Rieke and Low (1975a) have obtained  $2.2\ \mu\text{m}$  strip scans through the  $10\ \mu\text{m}$  region with 5 arcsecond resolution. The infrared emission of NGC 253 is very similar to that of M82 which is fully described in Chapter 4.

NGC 5128 (Cen A)

Though no true scanning work has been published on Cen A, Becklin et al. (1971) examined the radial distribution of  $2.2 \mu\text{m}$  emission along a north-south line through the centre, and found that at radial distances  $> 50''$ , i.e. well away from the active nucleus, the surface brightness distribution resembled that at visual wavelengths in the outer regions of M31 (de Vaucouleurs 1958). This would seem to imply that there is a disc component in the galaxy. More recent observations (Adams, 1979, priv. comm.) suggest that there is a north-south asymmetry in the  $2.2 \mu\text{m}$  contours. Preliminary analysis of the Adams' contour map (Abolins and Adamson) has shown that to the north the distribution follows the  $r^{-\frac{1}{4}}$  law for  $r \lesssim 50''$ , but to the south there is an additional component which may possibly be  $2.2 \mu\text{m}$  emission from the recently discovered bright  $\text{H}\alpha$  region named "Knot X" (Graham, 1979). Future confirmatory observations should be undertaken as soon as possible.

NGC 6946

Optical observations of the face-on spiral galaxy NGC 6946 give no indication of the presence of large amounts of obscuring dust in the galaxy's centre, yet the  $2.2 \mu\text{m}$  map of the region (Lebofsky and Rieke, 1979) shows that the centroid at this wavelength is not coincident with the visually brightest spot, i.e. the true nucleus is so heavily obscured that it is not seen at visible wavelengths. This phenomenon might be expected a priori in edge-on galaxies such as NGC 4631 (see above), but it was previously unsuspected in relatively normal looking, face-on spirals. V and K surface photometry shows that the nucleus of M31 is relatively free of dust (see Chapter 3) and Adams and Hough (1978) suggest that most of the obscuring matter lying between the sun and the Galactic centre is not within the near vicinity of the nucleus but is

associated with the intervening spiral arms. The  $2.2\ \mu\text{m}$  observations of NGC 6946 show that in at least some apparently normal galaxies large quantities of dust lie very close to the nucleus.

### ADDENDUM

Since the major part of the review given in Chapter 1 was completed by early Spring, 1979, several comments are slightly out of date, and a few subsequent publications of some significance have not been mentioned. To amend this situation the highlights of 1979 are summarised below.

### PHOTOMETRY OF NORMAL GALAXIES

Aaronson's Ph.D. thesis (Harvard University, 1978) is now available on microfilm from the British Lending Library. It is the most comprehensive and accurate survey to date of the near infrared colours of normal galaxies and contains all the data in the FPAM series of papers as well as new JHK data for 91 galaxies distributed along the Hubble sequence from Sa to Im. (The new data fills the data gap mentioned in section 1.4). The major conclusions drawn from the new data for spirals and irregulars are as follows:

- 1) The near infrared light of the centre of all galaxies from E to Sc is dominated by mid to late M giants. In later types, Scd to Im, there is some evidence of a decrease in the influence of these stars, particularly in the J-H colour of Im systems.
- 2) Elliptical colours correlate more strongly with luminosity than those of spirals.
- 3) No significant radial gradient in the JHK colours was found for spiral galaxies generally, although V-K colour gradients do exist between the red bulge component and the blue disk component.

Frogel et al. (1979) have extended their JHK survey of early type galaxies; new data have been listed for 80 field galaxies, 35 Virgo cluster galaxies and 22 Coma cluster galaxies which span a large range (6 magnitudes) in absolute magnitude. No analysis of the data is given

but a paper is in preparation which will discuss any differences between field and cluster galaxy infrared colours.

#### SPECTRAL FEATURES IN NGC 253 AND M82

CVF observations of the CO and Br $\gamma$  features have been made for NGC 253 (Wyn-Williams et al., 1979). The strength of these features indicates that although the total mass of stars in the nucleus is about half that of our own galaxy the number of OB stars is about thirty times larger.

Measurement of the Br $\alpha$ /Br $\gamma$  ratio in the nucleus of M82 has been made using a cooled grating spectrometer with resolution  $\Delta\lambda/\lambda \sim 0.002$  (Simon et al., 1979). The observed variation in the ratio over an angular distance of only seven arcseconds indicates the extremely patchy nature of the obscuration within the nucleus (see Chapter 4).

#### ACTIVE GALAXY OBSERVATIONS

Neugebauer et al. (1979) have now published the 0.3 - 10  $\mu\text{m}$  survey of Q.S.O.'s mentioned in section 1.6. The energy distributions of 24 of the brightest Q.S.O.'s are given. The conclusions are basically the same as those outlined in the Hale Observatories report for 1977 which were given in section 1.6, but to these the following can now be added:

- a) The luminosity at 0.3  $\mu\text{m}$  of the Q.S.O.'s studied is similar to that at 3  $\mu\text{m}$  and is significantly greater than that at 1  $\mu\text{m}$ .
- b) No correlation is observed between the strength of the radio continuum and the infrared flux.
- c) For the quasars which are highly variable, the variations in the visible and infrared are correlated.
- d) Though the dominant radiation mechanism producing the visible to

ten micron flux is non-thermal a contribution from heated dust cannot be ruled out, particularly in those objects which seem to show an excess at  $3 \mu\text{m}$ .

Infrared observations of Seyfert galaxies and emission line galaxies continue with great gusto, yet in general no particularly new results have been unearthed. Two papers worth noting however are Danks et al. (1979) and Glass et al. (1979). In the former the nucleus of the extreme Seyfert 1 galaxy Fairall-9 is unambiguously shown to be a Q.S.O., and in the latter the relationship between the  $3.4 \mu\text{m}$  flux and the X-ray flux for emission line galaxies and Seyferts, first tentatively suggested by Elvis et al. (1978), is confirmed by a much larger sample.

#### INFRARED LUMINOSITY/HI VELOCITY - WIDTH RELATION

Aaronson et al. (1979) have discovered a tight correlation between the H magnitude of normal late type cluster galaxies and their global twenty-one centimetre line velocity-width. The constancy of the slope of the relation for the Virgo cluster, the Coma cluster and for several nearby galaxies suggests that it is universal in nature. By using a provisional calibration based upon the distances of Sandage and Tammann for local galaxies, values for the distance moduli of the Virgo and Coma clusters have been obtained and a mean value for the Hubble constant of  $H_0 = 61 \pm 4 \text{ km s}^{-1} \text{ Mpc}^{-1}$  follows from the preliminary results. The authors believe the infrared magnitude/velocity-width relation is now the most powerful tool available for determining red-shift independent distances to the adjacent great clusters.

## REFERENCES

- Aaronson, M. 1978a, P.A.S.P., 90, 28.
- Aaronson, M. 1978b, Ap. J., 221, L103.
- Aaronson, M. 1978c, Ph.D. Thesis, Harvard University.
- Aaronson, M., Frogel, J.A., and Persson, S.E. 1978, Ap. J., 220, 442.
- Aaronson, M., Huchra, J. and Mould, J. 1979, Ap. J., 229, 1.
- Adams, D.J. and Hough, J. 1977, M.N., 179, 73p.
- Allen, D.A. 1976, Ap. J., 207, 367.
- Andrews, P.J., Glass, I.S., Howarden, T.G. 1974, M.N., 168, 7p.
- Arp, H. 1965, Ap. J., 141, 43.
- Baldwin, J.R., Danziger, I.J., Frogel, J.A. and Persson, S.E. 1973a,  
Ap. L., 14, 1.
- Baldwin, J.R., Frogel, J.A. and Persson, S.E. 1973b, Ap. J., 184, 427.
- Balick, B. and Brown, R.L. 1974, Ap. J., 194, 265.
- Becklin, E.E. and Neugebauer, G. 1968, Ap. J., 151, 145.
- Becklin, E.E., Frogel, J.A., Kleinmann, D.E., Neugebauer, G., Ney, E.P.  
and Strecker, D.W. 1971, Ap. J., 170, L15.
- Becklin, E.E., Fomalont, E.B. and Neugebauer, G. 1973(a), Ap.J., 181, L27.
- Becklin, E.E., Matthews, K. and Neugebauer, G. 1973(b), Ap.J., 186, L69.
- Borgman, J., Koornneef, J. and de Vries, M. 1974, in 8th ESLAB  
Symposium, p. 229.
- Capps, R.W. and Knacke, R.F. 1976, Ap. J. 210, 76.
- Capps, R.W. and Knacke, R.F. 1978, Ap. L., 19, 113.
- Cottrell, G.A. 1978, M.N., 184, 259.
- Danks, A.C., Wamsteker, W., Vogts, N., Salinari, P., Tarenghi, M. and  
Duerbeck, H.W. 1979, Ap. J., 227, L59.
- Dyck, H.M., Kinman, T.D. and Lockwood, G.W. 1971, Nat. Phys. Sci., 234, 71.
- Epstein, E.E. and 21 others 1972, Ap. J., 178, L51.

- Faber, S.M. 1972, *Astron. and Ap.*, 20, 361.
- Faber, S.M. 1973, *Ap. J.*, 179, 423 and 731.
- Fitch, W.S., Packolczyk, A.G. and Weymann, R.J. 1967, *Ap. J.*, 150, L67.
- Freeman, K. 1976, in 6th Advanced Course, Swiss Society of Astronomy and Astrophysics, and references therein (Geneva Obs.).
- Frogel, J.A., Persson, S.E., Aaronson, M., Becklin, E.E. and Matthews, K. 1975a, Tercentenary Symposium, RGO.
- Frogel, J.A., Persson, S.E., Aaronson, M., Becklin, E.E., Matthews, K. and Neugebauer, E. 1975b, *Ap. J.*, 195, L15.
- Frogel, J.A., Persson, S.E., Aaronson, M., Becklin, E.E., Matthews, K. and Neugebauer, G. 1975c, *Ap. J.*, 200, L123.
- Frogel, J.A., Persson, S.E., Aaronson, M. and Matthews, K. 1978, *Ap. J.*, 220, 75.
- Gillett, F.C., Kleinmann, D.E., Wright, E.L. and Capps, R.W. 1975, *Ap. J.*, 198, L65.
- Glass, I.S. 1973, *M.N.*, 164, 155.
- Glass, I.S. 1976, *M.N.*, 175, 191.
- Glass, I.S. 1978, *M.N.*, 184, 85p.
- Glass, I.S. 1979, *M.N.*, 186, 29p.
- Graham, J.A. 1979, *Ap. J.*, 232, 60.
- Grasdalen, G.L. 1975, *Ap. J.*, 195, 605.
- Grasdalen, G.L. 1976, *Ap. J.*, 208, L11.
- Grasdalen, G.L. and Joyce, R.R. 1976, *Ap. J.*, 208, 317.
- Grindley, J.E., Schnapper, H., Schrier, E.J., Gursky, H. and Parsignault, D.R. 1975, *Ap. J.*, 201, 133.
- Hartwick, F.D.A. and Sandage, A. 1968, *Ap. J.*, 153, 715.
- Harwit, M. and Pacini, F. 1975, *Ap. J.*, 200, L27.
- Iijima, T., Ito, K., Matsumoto, T. and Uyama, K. 1976, *P.A.S.J.*, 28, 27.
- Jameson, R.F. and Hough, J. 1978, *M.N.*, 182, 179.

Johnson, H.L. 1964, Ap. J., 139, 1022.

Johnson, H.L. 1966a, Ann. Rev. Astron. and Ap.

Johnson, H.L. 1966, Ap. J., 143, 187.

Johnson, H.L. 1968, in "Stars and Stellar Systems" Vol. VII, p.167.

Joyce, R.R., Knacke, R.F., Simon, M. and Young, E. 1975, P.A.S.P., 87, 683.

Kemp, J.C., Rieke, G.H., Lebofsky, M.J. and Coyne, S.J. 1977, Ap. J., 215,  
L107.

Kleinmann, D.E. and Low, F.J. 1970a, Ap. J., 159, L165.

Kleinmann, D.E. and Low, F.J. 1970b, Ap. J., 161, L203.

Knacke, R.F. and Capps, R.W. 1974, Ap. J., 192, L19.

Knacke, R.F., Capps, R.W. and Johns, M. 1976, Ap. J., 210, L69.

Krienke, O.K. and Hodge, P.W. 1974, A.J., 79, 1242.

Kunkel, W.E. and Bradt, H.V. 1971, Ap. J., 170, L7.

Lebofsky, M.J., Rieke, G.H. and Kemp, J.C. 1978, Ap. J., 222, 95.

Lebofsky, M.J. and Rieke, G.H. 1979, Ap. J., 229, 111.

Low, F.J. 1968, Infrared Astronomy, Gordon and Breach (New York).

Low, F.J. and Johnson, H.L. 1965, Ap. J., 141, 336.

Low, F.J. and Kleinmann, D.E. 1968, A. J., 73, 868.

Matsumoto, T., Murakami, H. and Hamajima, K. 1977, P.A.S.J., 29, 583.

Matthews, T.A., Morgan, W.W. and Schmidt, M. 1964, Ap. J., 140, 35.

McClure, R.D. and van den Bergh, S. 1968, A. J., 73, 313.

Merrill, K.M. and Stein, W.H. 1967a, P.A.S.P., 88, 285.

Merrill, K.M. and Stein, W.H. 1967b, P.A.S.P., 88, 874.

Morgan, W.W. and Osterbrock, D.E. 1969, A. J., 74, 1969.

Moroz, V.I. and Dibai, E.A. 1968, Sov. Astron., 12, 184.

Neugebauer, G., Becklin, E.E., Oke, J.B. and Searle, E. 1976a, Ap. J.,  
205, 29.

Neugebauer, G., Becklin, E.E., Beckwith, S., Matthews, K. and Wyn-Williams,  
C.G. 1976b, Ap. J., 205, L139.

- Neugebauer, G., Becklin, E.E., Matthews, K. and Wyn-Williams, C.G.  
1978, Ap. J., 220, 149.
- Neugebauer, G., Oke, J.B., Becklin, E.E. and Matthews, K. 1979, Ap. J.,  
230, 79.
- O'Connell, R.W. 1976, Ap. J., 206, 370.
- Oke, J.B., Sargent, W.L.W., Neugebauer, G. and Becklin, E.E. 1967,  
Ap. J., 150, L173.
- Oke, J.B., Neugebauer, G. and Becklin, E.E. 1969, Ap. J., 156, L41.
- Oke, J.B., Neugebauer, G. and Becklin, E.E. 1970, Ap. J., 159, 341.
- Olsen, E.T. 1969, Nature, 224, 1008.
- Pacholczyk, A.G. and Weymann, R.J. 1968, A. J., 73, 870.
- Pacholczyk, A.G. and Wisniewski, W.I. 1967, Ap. J., 147, 394.
- Pacholczyk, A.G. 1970, Ap. J., 161, L207.
- Pacholczyk, A.G. and Tarengi, M. 1975, Mem. Soc. Ast. Ital., 46, 199.
- Penston, M.V. 1973, M. N., 162, 359.
- Penston, M.V., Penston, M.J., Neugebauer, G., Tritton, K.P., Becklin,  
E.E. and Visvanathan, N. 1971, M.N., 153, 29.
- Penston, M.V., Penston, M.J., Selmes, R.A., Becklin, E.E. and Neugebauer,  
G. 1974, M.N., 169, 357.
- Persson, S.W., Frogel, J.A. and Aaronson, M. 1979, Ap. J., Suppl. S.,  
39, 61.
- Pooley, G.G. 1969, M.N., 144, 143.
- Puetter, R.C., Smith, H.E. and Willner, S.P. 1979, Ap. J., 227, L5.
- Rees, M.J., Silk, J.I., Weemer, M.W. and Wickramasinghe, N.C. 1969,  
Nature, 223, 788.
- Rieke, G.H. 1972, Ap. J., 176, L61.
- Rieke, G.H. and Low, F.J. 1972, Ap. J., 176, L95.
- Rieke, G.H. and Low, F.J. 1975a, Ap. J., 197, 17.
- Rieke, G.H. and Low, F.J. 1975b, Ap. J., 200, L67.

- Rieke, G.H. 1976, Ap. J., 210, L5.
- Rieke, G.H. 1978, Ap. J., 226, 550.
- Rieke, G.H. and Lebofsky, M.J. 1979, Ap. J., 227, 710.
- Rudnick, F.N., Owen, N., Jones, T.W., Puschell, J.J. and Stein, W.A.  
1978, Ap. J., 225, L5.
- Sandage, A.R., Becklin, E.E. and Neugebauer, G. 1969, Ap. J., 157, 55.
- Sandage, A.R. 1970, Ap. J., 162, 841.
- Sersic, J.L. and Pastoriza, M. 1965, P.A.S.P., 77, 287.
- Seyfert, C.K. 1943, 97, 28.
- Simon, M., Simon, T. and Joyce, R.R. 1979, Ap. J., 227, 64.
- Spinrad, H. and Wing, R.F. 1969, Ann. Rev. Astron. and Ap.
- Spinrad, H., Sargent, W.L.W., Oke, J.B., Neugebauer, G., Landau, R.,  
King, I.R., Gunn, J.E., Garmino, G. and Dieter, N.H. 1971,  
Ap. J., 163, L25.
- Stein, W.A., Gillett, F.C. and Merrill, K.M. 1974, Ap. J., 187, 213.
- Stein, W.A. and Weedman, D.W. 1976, Ap. J., 205, 44.
- Stoner, R. and Ptak, R. 1977, Ap. J., 217, 940.
- Strom, K.M. and Strom, S.E. 1977, I.A.U. Symposium No. 77 Conf. Proc.  
Reidel Publishing.
- Strom, K.M., Strom, S.E. and Wells, D.C. 1978, Ap. J., 220, 62.
- Telesco, C.M. 1978, Ap. J., 226, L125.
- Thompson, R.I., Lebofsky, M.J. and Rieke, G.H. 1978, Ap. J., 222, L49.
- Tinsley, B.M. and Gunn, J.E. 1976, Ap. J., 203, 52.
- Van de Hulst, H.C. 1949, Rech. astr. Obs. Utrecht, 11, 1.
- Vaucouleurs, G. de, 1958, Ap. J., 128, 465.
- Willner, S.P., Soifer, B.T., Russell, R.W., Joyce, R.R. and Gillett, F.C.  
1977, Ap. J., 217, L121.
- Wisniewski, W.Z. and Kleinmann, D.E. 1968, A. J., 73, 866.

Wyn-Williams, C.G., Becklin, E.E., Matthews, K. and Neugebauer, G.

1979, M. N., 189, 163.

Zwicky, F., Oke, J.B., Neugebauer, G., Sargent, W.L.W. and Fairall, A.P.

1970, P.A.S.P., 82, 93.

**Instrumentation and Observing Techniques**

## 2.1 INSTRUMENTATION

### DETECTORS

The astronomer must appreciate the sensitivity of his detector in order to gauge whether or not a given faint object can be usefully observed. This is particularly true in off-nucleus photometric observations of galaxies where the very low surface brightnesses encountered require the detector to be pushed to its limits. Although a detailed account of the theory and operation of infrared detectors is beyond the scope of this thesis it is pertinent to include here a brief discussion of detector sensitivity.

The detectors currently used by the Leicester Infrared Group are indium antimonide (InSb) photovoltaic devices. When operated in the manner described by Hall et al. (1975) these detectors are the best commercially available at present for astronomical measurements in the J, H and K wavebands. With the exception of the 1976 observations of M31 (see chapter 3), which were made with a detector supplied by Barnes Engineering Co. of Connecticut, all other observations were made with a Santa Barbara Research Center (SBRC) detector. Prior to the InSb detectors, SBRC lead sulphide (PbS) photoconductive detectors were used by the Leicester group. (Akinci, 1978; Longmore, 1975). Fig. 2.1 illustrates the improvements in the signal-to-noise ratio of our InSb detectors over the past few years. At the top is a profile from a scan through Cen A, made in 1975 using a 40 inch telescope with a 30 arcsecond aperture. The bottom profile is from a scan made in 1979 through the same galaxy with the same telescope and a 26 arcsecond aperture.

### INDIUM ANTIMONIDE PHOTODIODES

Indium antimonide is an intrinsic photodetector with a forbidden energy gap (i.e. valence band to conduction band) of 0.22 eV at liquid

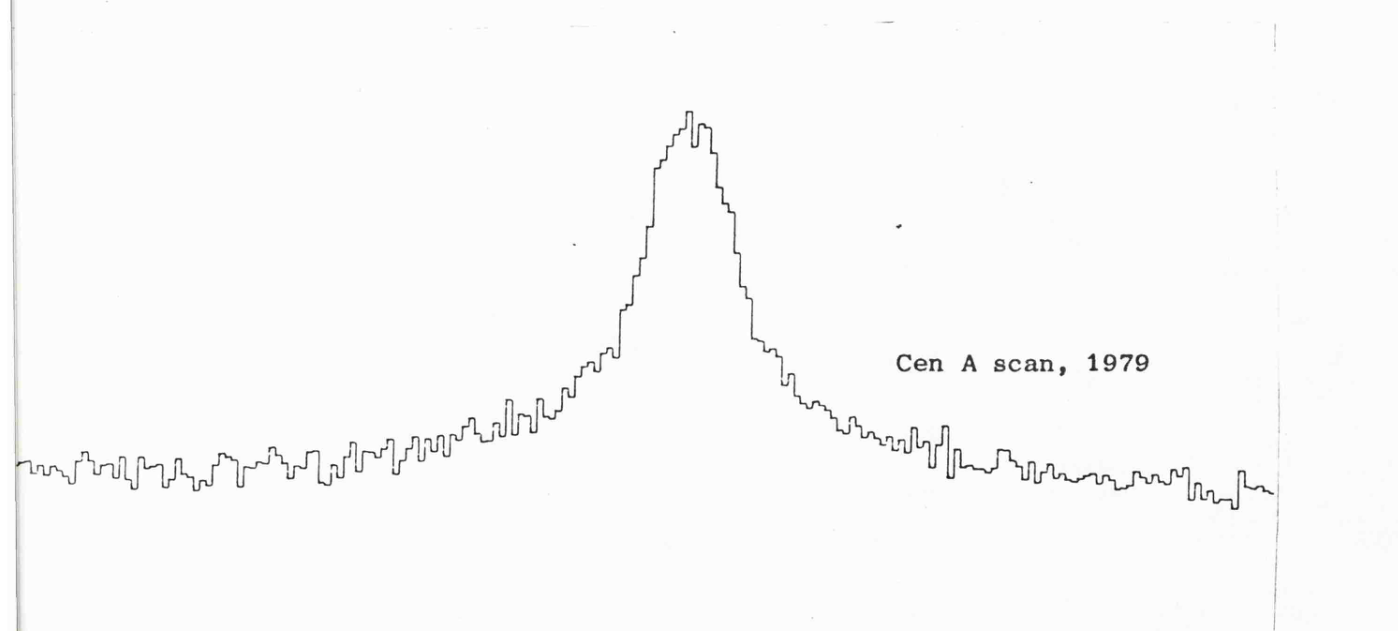
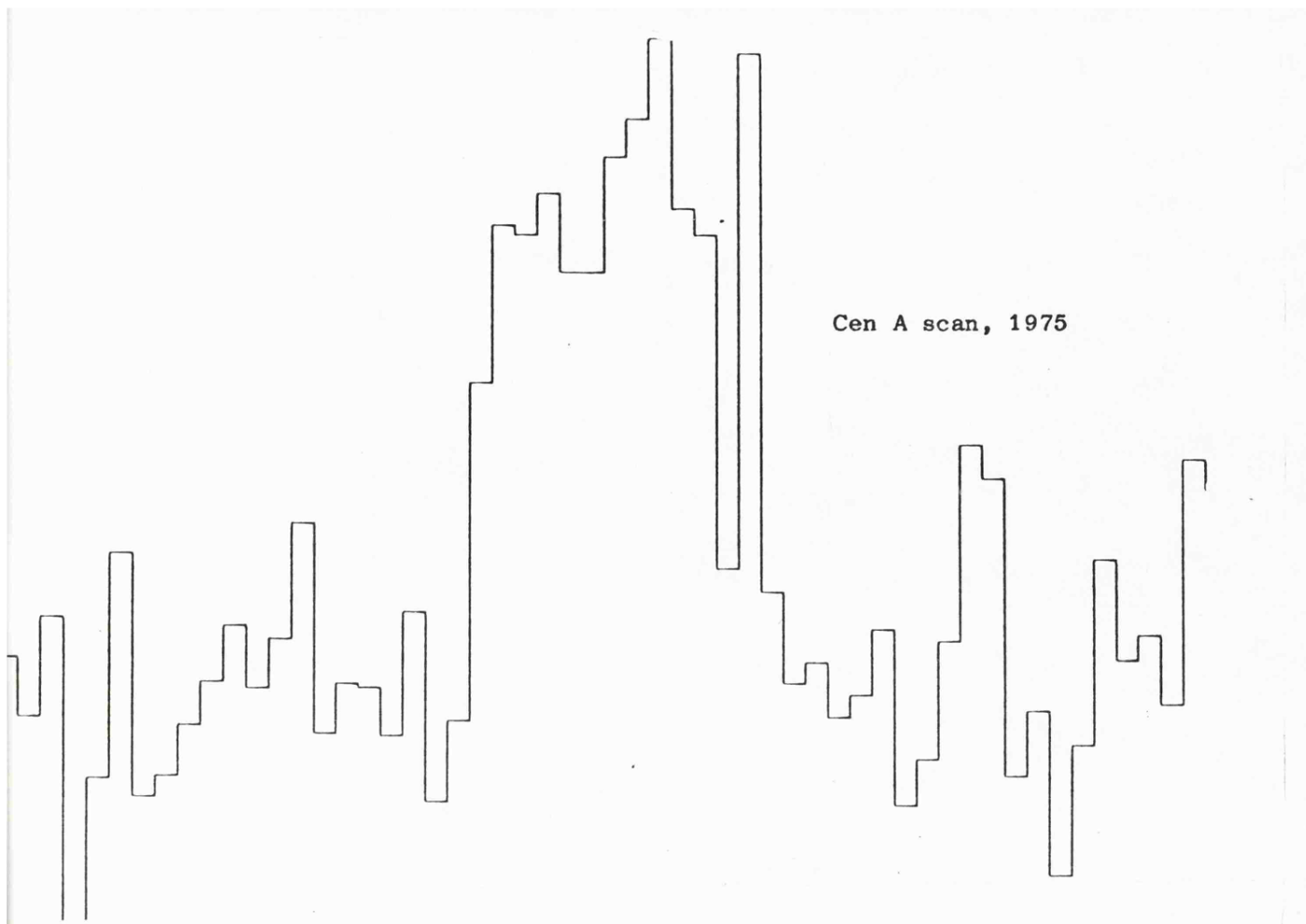


Fig. 2.1: Illustration of Detector Improvement since 1975

nitrogen temperatures, and thus impinging photons of wavelength  $\lambda < 5.5 \mu\text{m}$  are required to create an electron-hole pair. An InSb photovoltaic detector consists of adjacent zones of p and n doped material which together form a photodiode. Incident near infrared photons are absorbed at the junction creating an electron-hole pair which is separated by the junction field and appears as charge at the electrodes. In the absence of radiation the detector has the electrical characteristics of a normal diode. The various possible modes of operation of InSb photovoltaic devices are discussed in most standard texts, e.g. Hudson, 1969.

#### JOHNSON NOISE LIMITED OPERATION

The limiting sensitivity of any detector is determined by the intrinsic noise at its outputs (when background noise is negligible). The types of noise inherent in InSb photodiode systems are random thermal electron motion, i.e. Johnson noise,  $1/f$  or current noise and generation-recombination noise, the semiconductor equivalent of shot noise. The two latter noise sources are functions of the D.C. current through the detector (e.g. see Handbook of Military Infrared Technology) whereas the Johnson noise current is a function of only temperature and detector impedance. Thus when no D.C. current flows in a detector, Johnson noise will be the only type of noise present. In astronomical photometry the detected signal is typically very small and must be amplified immediately to prevent noise pickup along lengthy transmission cables. Hall et al. (1975) have described a preamplifier design with which Johnson noise limited operation of InSb photodiodes is realised. This design has been used for the Leicester preamplifiers used by the author.

The Johnson noise current is given by  $\Delta i \propto \sqrt{T/R}$ , where T is

the detector temperature and  $R$  is the system resistance. Thus to minimize the noise we must attempt to maximize  $R$  and minimize  $T$ .

Indium antimonide detectors are normally cooled by being placed in thermal contact with a bath of liquid nitrogen. At normal pressure the temperature of liquid nitrogen is  $77^\circ\text{K}$ , but it is nowadays common to cool the detector to "pumped" nitrogen temperatures, i.e.  $T \sim 64^\circ\text{K}$ , since this leads to a considerable increase in the detector resistance,  $R_D$ .

#### HYPERSENSITIZATION (FLASHING)

The system resistance,  $R$ , mentioned above is given by  $R_F R_D / (R_F + R_D)$  where  $R_D$  is the detector resistance and  $R_F$  is the preamplifier feedback resistance. At  $77^\circ\text{K}$  the typical resistance of SBRC InSb detectors is a few hundred megohms, whereas the feedback resistor is typically  $\sim 10^{10} \Omega$ , and so the system noise is limited by the detector resistance. By using a mysterious hypersensitizing process known commonly as "J-flashing" or simply "flashing" it is possible to increase the detector resistance by an order of magnitude or even more (MacGregor, 1977), so decreasing the system noise substantially. Flashing entails exposing the detector to extremely intense  $1.2 \mu\text{m}$  radiation (usually from an ordinary light bulb, J-filtered) for several minutes. The exact mechanism involved in flashing is poorly understood, but according to Matthews, quoted in Aaronson, 1978, it removes a surface charge layer that builds up on the protective oxide coating of the InSb crystal, thereby eliminating a spurious conduction current from the oxide to the p/n junction. Following MacGregor (1977) we find that the best procedure is to cool the detector to  $77^\circ\text{K}$ , flash, pump it to  $64^\circ\text{K}$ , and to flash again. The detector resistance increases at each stage.

## THEORETICAL DETECTOR LIMITS

The sensitivity of infrared detectors is commonly quoted in terms of Noise Equivalent Power, or N.E.P., which is defined as that radiant power for which the signal is equal to the RMS noise in a 1 Hz bandpass. MacGregor (1977) gives the theoretical N.E.P. at 64°K for InSb photodiodes as:

$$\text{N.E.P.}_{\text{LIM}} = \frac{7.5 \times 10^{-11}}{R^{\frac{1}{2}} \eta \lambda} \text{ W Hz}^{-\frac{1}{2}}$$

where  $\eta$  is the detector quantum efficiency. Thus for  $\eta = 1$ ,  $\lambda = 2.2 \mu\text{m}$  and  $R = 10^{10} \Omega$ , the best possible N.E.P. is  $3.4 \times 10^{-16} \text{ W Hz}^{-\frac{1}{2}}$ . The corresponding figure for the detector used by the author (for most of the observations described in the following chapters) is  $9.6 \times 10^{-16} \text{ W Hz}^{-\frac{1}{2}}$ , this is for an effective quantum efficiency  $\sim 0.5$ , and  $R = 5 \times 10^9 \Omega$ . The limiting performance of a detector described in terms of N.E.P. is difficult to visualize. A more easily appreciated quantity is the one sigma noise, in a one second integration, expressed as a magnitude (for a telescope of given size). On this basis the N.E.P. figures given above correspond to K magnitudes of 13.8 and 12.7 respectively, for a 1.5 m telescope. (Theoretical limits are compared to observed limits in section 2.3.)

## SKY SHOT NOISE LIMITATIONS

Even if intrinsically noiseless detectors were available the infrared astronomer would still be noise limited by sky shot noise. The limits imposed by shot noise at Tenerife, with the flux-collector, have been discussed quantitatively by MacGregor (1977). He concluded that in practice observers are currently detector limited at H and K, but with a small increase in detector sensitivity, or a decrease in system losses, background limited operation would be achieved, especially at K.

At J shot noise is the limiting factor.

Table 2.1 summarises the noise limitations at  $2.2 \mu\text{m}$  for InSb detectors, with values of  $\eta$  and R as discussed above, when used with the 1.5 m flux-collector at Tenerife (after MacGregor). In comparison the Caltech InSb detector systems are background limited at all apertures down to five arcseconds diameter on the 5 metre telescope, at K (Neugebauer, priv. comm. 1978).

#### IMPLICATIONS FOR THE SURFACE PHOTOMETRY OF GALAXIES

In an average textbook photograph of a galaxy (e.g. M31 in chapter 3) the V surface brightness in the outer regions is  $\sim 22 \text{ m}_V / \square''$ . Previously photometric measurement of these regions at wavelengths  $\lambda > 1 \mu\text{m}$  were, practically speaking, impossible. The only limitation in the near future will be the sky noise. What then will be the integration time necessary to make reasonable, near infrared photometric observations of the outer regions of galaxies? Assuming that in the outer regions of galaxies  $V-K \sim 2.0 - 2.5$  (a value suggested by Aaronson's photometry of Magellanic irregulars, i.e. the bluest galaxies and probably similar to spiral arm regions in their integrated broad band colours), then the expected K surface brightness will be  $\mu_K \sim 19.5 - 20 \text{ m}_K / \square''$ . Thus, from the figures in table 2.1, it should be possible for background limited systems to measure, photometrically at K, the outer regions of galaxies to the  $3\sigma$  level in approximately thirty-five to forty seconds or to the  $10\sigma$  level in approximately four hundred seconds, with a twenty-arcsecond aperture and a 1.5 m flux collector, i.e. near infrared surface photometry of galaxies from the nucleus out to the visible extremities is now possible.

Table 2.1 : Noise Limitations at 2.2  $\mu\text{m}$  with InSb Detectors on 1.5 m Telescope

Aperture	Noise Magn's, $1\sigma$ in 1 sec		Limiting Noise Factor	
	Detector, Case A $\eta = 1, R = 10^{10} \Omega$	Detector, Case B $\eta = 0.5, R = 5 \times 10^9$	In Case A	In Case B
20"	13.8	12.7	Background	Detector
15"	13.8	12.7	Background	Detector
10"	13.8	12.7	Background & Detector	Detector
5"	13.8	12.7	Detector	Detector

\* Tenerife, photometric conditions (MacGregor, 1977)

## THE CRYOSTAT

The primary function of a cryostat is to house the detector and maintain it at the necessary low temperature by providing a mounting in excellent thermal contact with the coolant, which is usually liquid nitrogen in near infrared systems. Most modern cryostats also house and cool other components; the Leicester cryostats contain filters, aperture stops, a Fabry lens and part of the preamplifier circuitry. Cooling of the filters and apertures minimizes their thermal emission and cooling of part of the preamplifier circuitry is essential for its high performance operation. The purpose of the Fabry lens is to <sup>image</sup> the <sup>primary</sup> light over the detector area thereby reducing noise introduced when seeing, guiding errors and local vibrations cause the focussed image to wander randomly over the (non-uniform) detector surface. The cryostat most frequently used in this research contains standard "UKIRT batch" J, H, K and L filters, (Table 2.2), four circular apertures (diameters: 0.5, 1, 2, 4.5 mm) and two slit apertures (0.5 and 1.0 x 4.5 mm). A detailed description of the cryostat structure is given in Akinci (1978), and a diagram is given in fig. 2.2.

Table 2.2: System Filters

	J	H	K	L
$\lambda_{\text{eff}} (\mu\text{ m})$	1.25	1.65	2.22	3.8
$\Delta \lambda (\mu\text{ m})$	0.3	0.3	0.4	0.7

## CHOPPING AND CHOPPERS

Modulating or "chopping" of the infrared radiation impinging on a detector performs one or both of two main functions; the first is to ensure an alternating output from the detector, as it is easier to amplify A.C. than D.C. signals, and the second is to enable cancellation

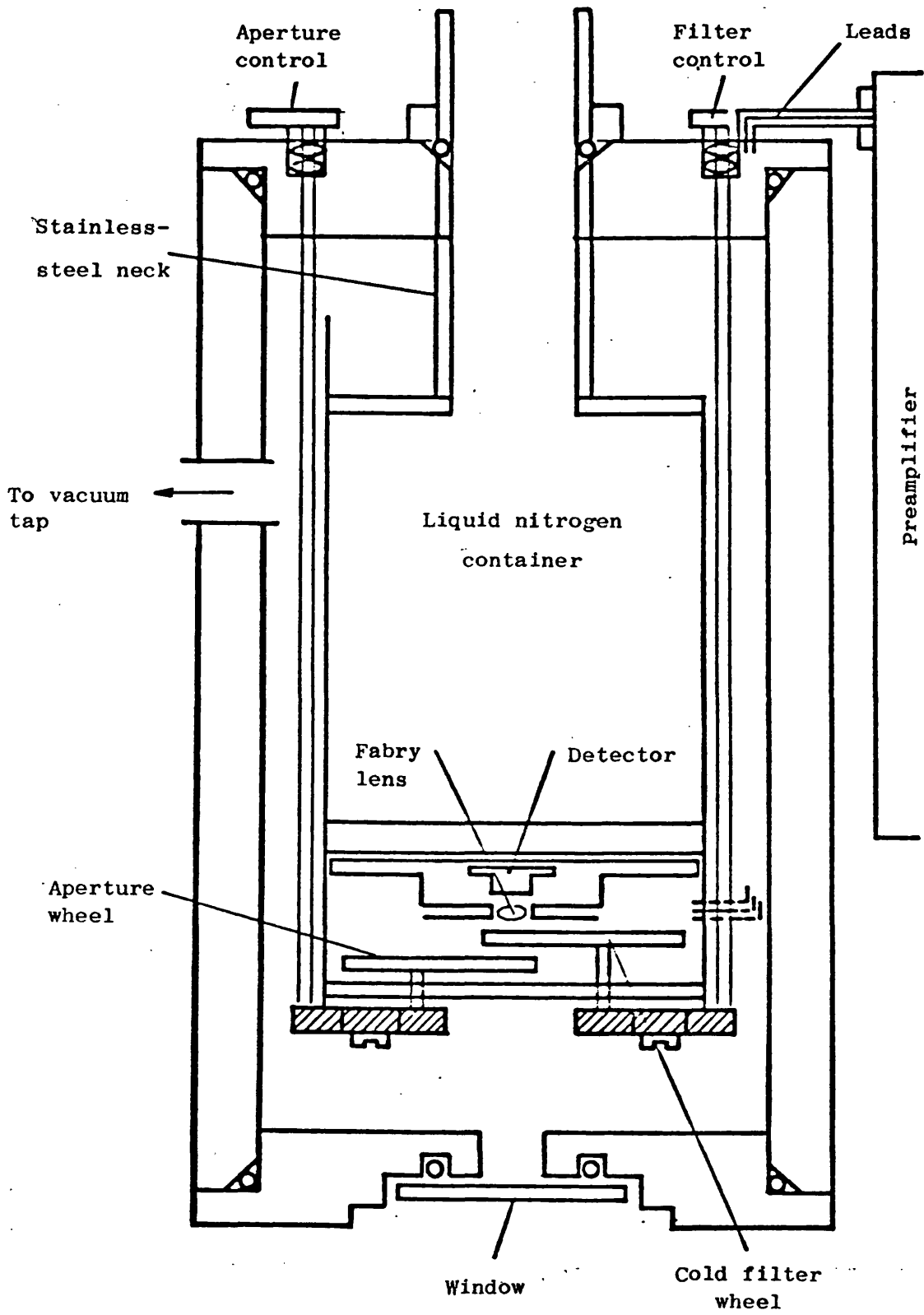


Fig. 2.2: Cryostat

of the high background signal\* which exists at wavelengths,  $\lambda > 1 \mu\text{m}$ . At wavelengths  $\lambda \gtrsim 3.5 \mu\text{m}$  and for faint sources at  $\lambda \lesssim 2.2 \mu\text{m}$ , the chopping technique used must incorporate background cancellation. However for bright sources at wavelengths  $\lambda \lesssim 2.2 \mu\text{m}$  the chopping technique need not provide direct background cancellation. In infrared astronomy the commonest method of chopping is "sky-chopping", sometimes known as "dual-beam chopping", and it is this technique which provides direct background cancellation. Two other methods of chopping have been used by the author, the first is the established technique known as "black-body chopping" and the other is a novel method involving rotating and stationary polaroids. Both of these are "single beam" techniques in which sky cancellation is not automatically achieved. Each method will now be briefly outlined, and is illustrated in fig. 2.3.

#### SKY-CHOPPING

In sky chopping the detector is exposed alternately to two neighbouring patches of sky ("beams"), the first of which (the source-beam) contains the object of interest plus an area of bright sky and the second (the reference-beam) contains just an equal area of sky. The difference between the two beams, i.e. the signal from the source of interest alone, can then be obtained by phase-sensitive rectification. Sky-chopping can be achieved by wobbling the secondary-mirror or by using focal plane devices such as vibrating mirrors or rotating, segmented mirrors.

---

\* At visible wavelengths the sky brightness is approximately  $23 \text{ m}_V/\square''$  at good sites on a moonless night, whereas at  $3.6 \mu\text{m}$ ,  $2.2 \mu\text{m}$ ,  $1.65 \mu\text{m}$  and  $1.25 \mu\text{m}$  the sky brightness is approximately 3.3, 10.5, 13.0 and 8.0 mags/ $\square''$  respectively. In an aperture of 20" diameter this amounts to  $m_L \sim -2.9$ ,  $m_K \sim 4.4$ ,  $m_H \sim 6.9$  and  $m_J \sim 1.9$

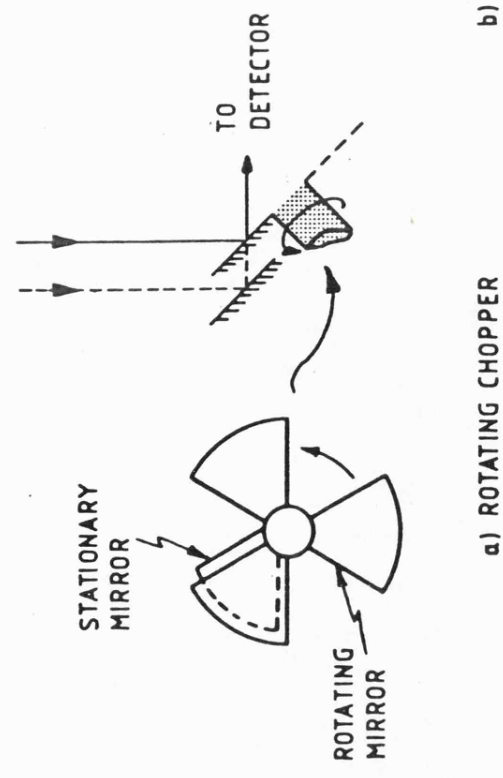
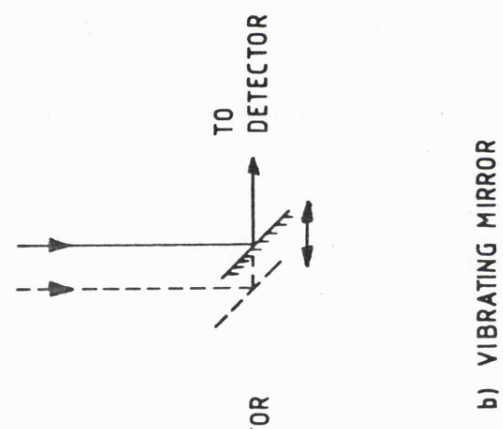
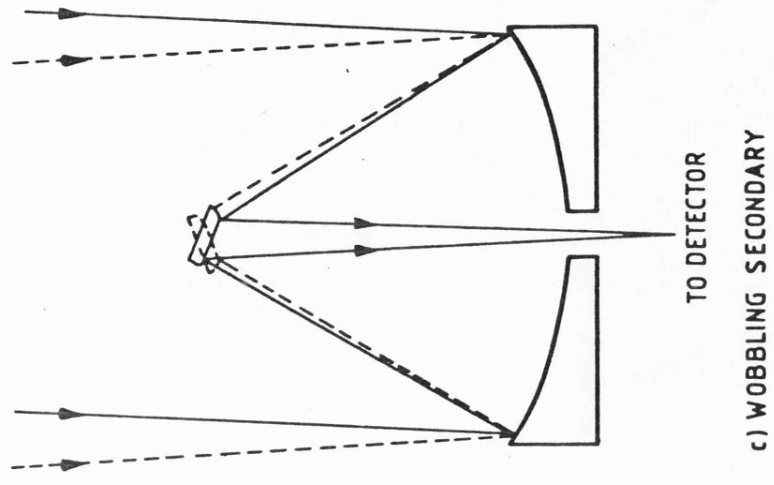
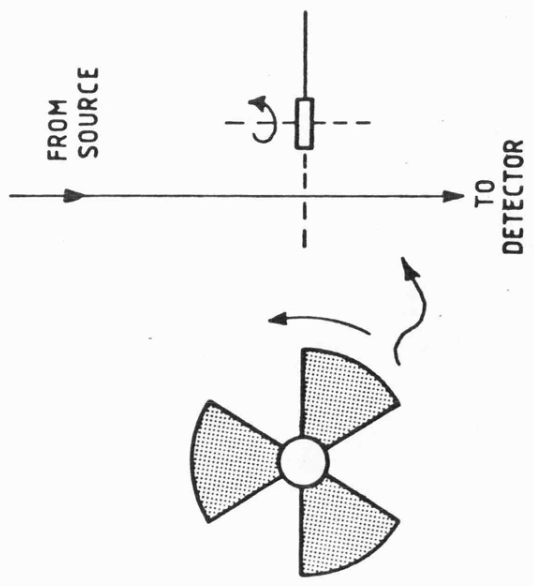
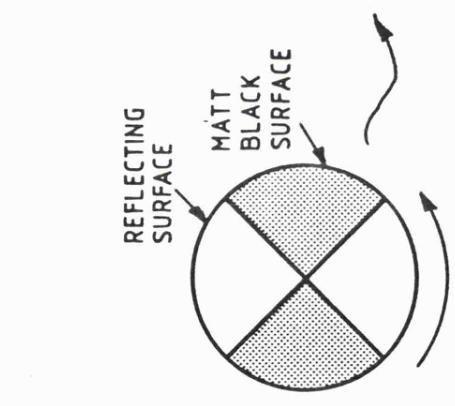


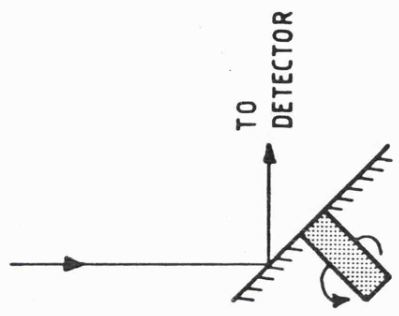
Fig. 2.3a: Sky choppers



a) "WARM" B-B CHOPPER (i)  
ROTATING, SEGMENTED BLACK DISC



b) "WARM" B-B CHOPPER (ii)  
ROTATING, SEGMENTED MIRROR/B-B



c) COLD B-B CHOPPER  
ROTATING, SEGMENTED MIRROR  
+ STATIONARY, 77°K B-B

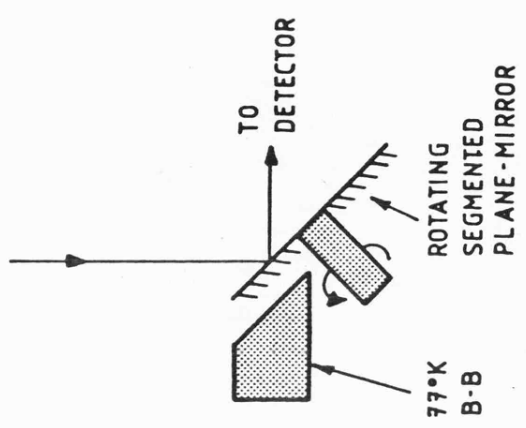


Fig. 2.3b: Black Body (B-B) Choppers

## BLACK-BODY CHOPPING

In black-body chopping the source beam is the only sky-beam (hence "single-beam") since the reference in this technique is a constant temperature black-body. The alternating output signal from the detector is then proportional to  $S - (S_{bb} - S_{bg})$ ,\* and therefore  $(S_{bb} - S_{bg})$  must be separately determined by observation of a nearby "empty" patch of sky. The simplest black-body choppers are rotating segmented, matt-black discs placed in the optical path to the detector, or rotating discs consisting of alternate segments of plane mirror and matt black surface. Temperature changes in these "warm" black-body choppers introduce drifts into the signal, as do sky brightness variations. More elaborate systems involve chopping against a matt black surface cooled to liquid nitrogen temperatures (Becklin and Neugebauer, 1968). These "cold" black-body choppers are unaffected by small temperature changes.

## MODULATION USING ROTATING AND STATIONARY POLAROIDS

The modulation in this case is a result of the varying net transmission which occurs when two similar polaroid sheets are placed in the optical path to the detector and one of the sheets is rotated. As with black-body chopping the background signal must be determined by observation of an "empty" patch of sky, however in photometric scanning both single beam techniques are convenient since the signal from the source of interest is seen "directly" as a peak above an otherwise constant background. The main points to note with the polaroid technique are i) the source of interest must be unpolarized, otherwise corrections must be made to the observed signal strength, which requires the objects

---

\*  $S$  = source of interest signal,  $S_{bb}$  = black-body signal,  $S_{bg}$  = background signal.

polarization parameters to be known, and ii) there is a two-thirds nett loss of signal due to the intervening polaroids and so the technique can only be used for bright sources.

#### PHOTOMETERS

A photometer can be considered as the detector-telescope interface, and as such it must consist of a) a cryostat mounting, b) the chopping mechanism, c) other associated optical components, e.g. mirrors, beam-splitter etc., and d) a means of attachment to the telescope backplate. Possible additional facilities include an off-axis guider, an incorporated visible channel and an image intensifier. The infrared group at Leicester possesses two near infrared photometers; the first, henceforth referred to as the version I photometer, was designed primarily with the photometry of stars in mind, and the second, henceforth referred to as the version II photometer, was designed for photometric scanning of extended objects. Unfortunately the version II instrument was extensively required for development of a near infrared multiplex imaging instrument and was not used by the author for any of the work described in the following chapters. The main advantage of the version II photometer is that it incorporates a "wide angle chopper" (of the rotating-segmented mirror variety) which provides a beam separation of several minutes of arc. In most cases a chopper throw of this order will set the reference beam clear of the detectable emission of the object of interest, and thus "reference beam contamination" is not a problem. A third instrument, the Hatfield Polarimeter, was used by the author and co-workers for the observations of M82, described in chapter 4. The polarimeter was used in the photometric scanning mode, the basic principle of which has been outlined above.

#### THE VERSION I PHOTOMETER

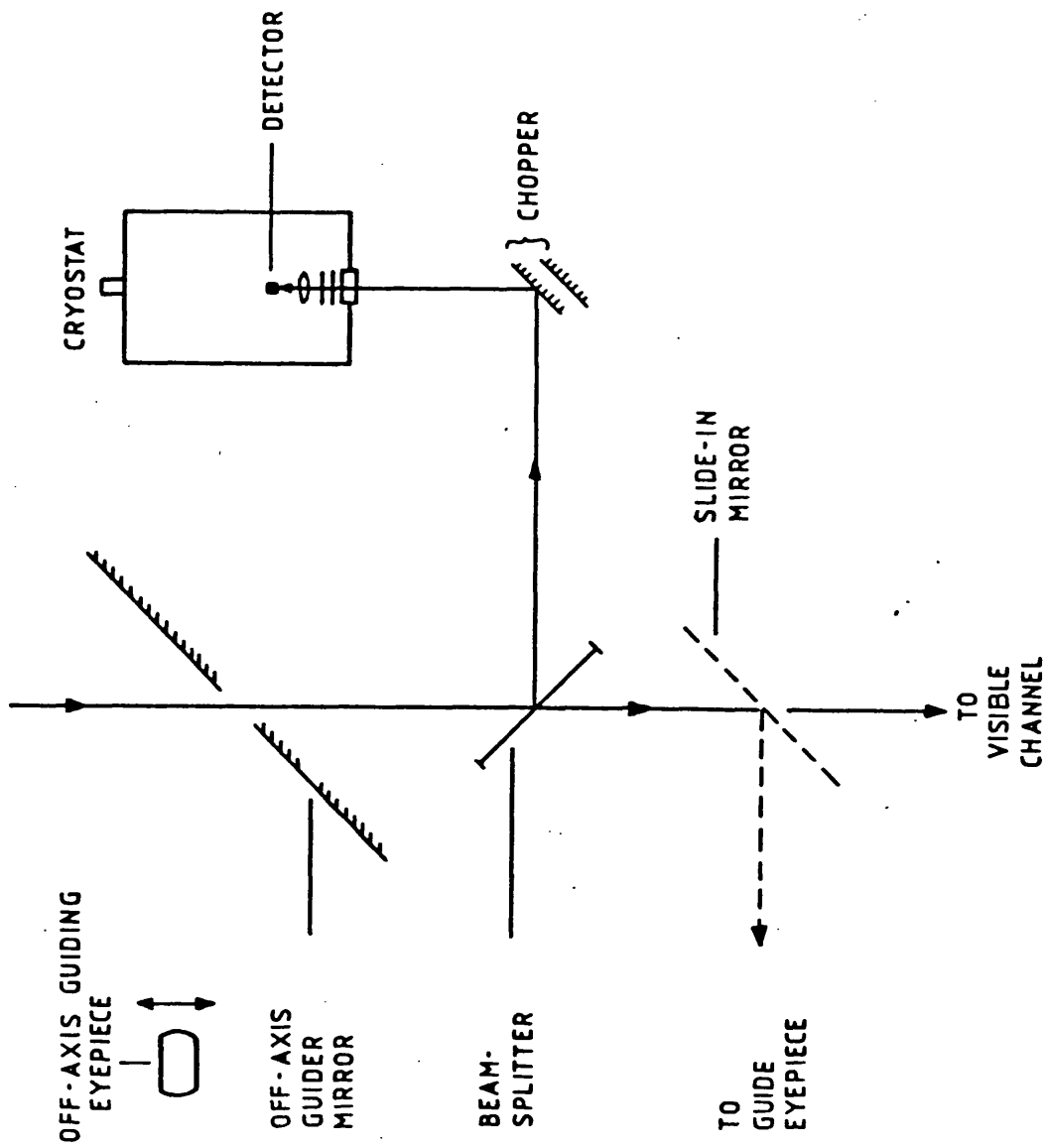
A schematic diagram of the photometer is given in fig. 2.4a, and structural details are described in Longmore (1975) and Akinci (1978). A crucial design feature of the photometer is the inclusion of the infrared/visible beam-splitter which transmits the visible light while reflecting the infrared light. This photometer can be used with either a vibrating mirror chopper or a black-body chopper. The maximum throw of the Leicester vibrating-mirror chopper is only 40 arcseconds at the Cassegrain focus of the Tenerife flux collector; as the diameter of most NGC galaxies is greater than this, reference beam flux is often a considerable problem when using this chopper. The method devised by the author to cope with this difficulty in the observations of NGC 972 is described in full in chapter five.

#### THE HATFIELD POLARIMETER

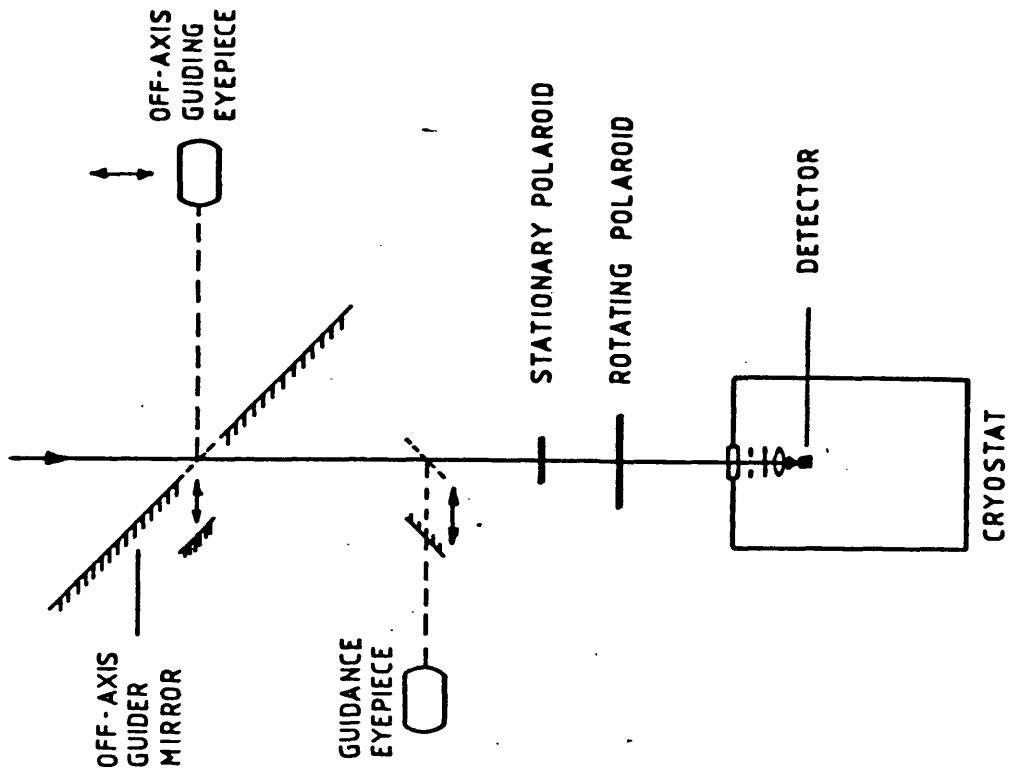
A schematic diagram of the polarimeter is given in fig. 2.4b; the instrument has been described in detail by Cox et al. (1978) and by McCall (1979). In the observations of M82 (chapter four) the photometer was initially to be used only for polarimetric measurements; its use as the photometric scanning instrument as well was due to equipment failure which prevented the intended use of the version I photometer.

#### SIGNAL PROCESSING ELECTRONICS

A block diagram of the processing electronics and data recording system is given in fig. 2.5. The arrangement of Hall preamplifier, P.S.D. and I.D.V.M. is now standard in infrared astronomy. The measured signal is immediately recorded either on magnetic tape or paper tape in the form of one second integrations.



(a) THE VERSION 1 PHOTOMETER



(b) THE HATFIELD POLARAMETER

Fig. 2.4

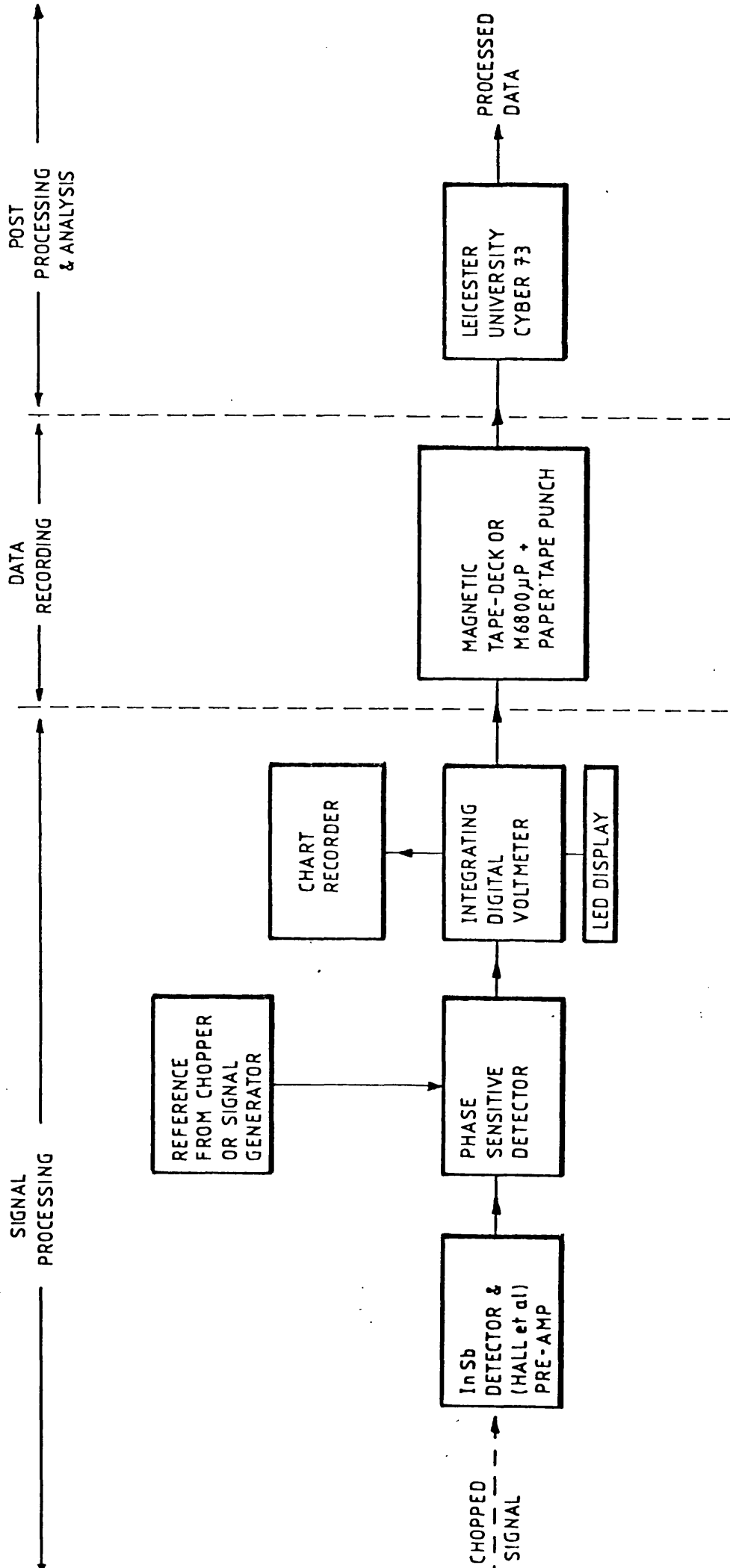


Fig. 2.5: Signal processing

## 2.2 OBSERVING TECHNIQUES

### INFRARED MAPPING OF GALAXIES

Until very recently<sup>\*</sup> no astronomically useful imaging instrument existed for wavelengths  $\lambda > 1 \mu\text{m}$ . The distribution of infrared light in extended sources has therefore only been studied using mapping techniques, i.e. photometric observations over the whole region of extended (detectable) emission to build up a surface brightness matrix from which an isophotal contour map can be drawn. This is achieved either by "point-by-point" photometry or using the less laborious scanning technique in which the surface brightness matrix is built up by moving the observing aperture across the source in a series of strip scans. Mathematically each strip scan provides the same amount of information as point-by-point photometry along the strip where each point is separated by half the aperture diameter (D), and the integration time at each point is  $D/2S$ , where S is the scan rate.

All near infrared maps of external galaxies and the Galactic Centre published to date (see chapter 1) have been obtained using the scanning technique. Point-by-point mapping is more convenient when the signal to noise is very low and the brightness gradient is small.

### METHODS OF SCANNING

Scanning of extended sources can be achieved by (i) moving the telescope pointing-axis, (ii) moving the secondary mirror (e.g. see Strom et al., 1978), or (iii) using a focal plane scanning system in the photometer (Baddily and Ring, 1977). As the Leicester/Hatfield instruments are of the basic standard design and as neither of the

---

\* Multiplex devices, and one and two dimensional detector arrays are currently reaching the stage in their development at which useful astronomical work can be done.

telescopes used are equipped with moving secondary mirrors all the observations described in the following chapters were made by scanning the telescope.

Maximum information is obtained with strip scans separated by half the beam width. Regions of high surface brightness gradient must be scanned in this way, but where the gradient is small, scans separated by one or two beam widths produce useful data. With scanning, increased resolution can only be achieved by reducing the size of the observing aperture, but reducing the aperture reduces the flux received, so the observer must compromise between signal strength and resolution. Conversely, wherever the surface brightness is low the biggest aperture must be used leading to an inevitable loss in resolution. This is not always a problem in the mapping of galaxies as it is the gross brightness distribution which is usually of interest in their faint outer regions where the surface brightness gradient is small.

With the points raised above in mind, the following sequence is given as the ideal procedure to follow when making mapping observations:

- i) With the largest aperture cover the whole detectable area with adjacent scans separated by one or two beam widths.
- ii) Regions of steep brightness gradient found in (i) should be scanned with first one, then half beam width separation between adjacent scans.
- iii) Fill in missing scans from (i).
- iv) Repeat (i) to (iii) scanning in a direction at right-angles to the first set of scans to confirm the general morphology.
- v) Reduce the aperture size and repeat (i) to (iv) over that part of the source which yields an adequate signal-to-noise.

#### CHOPPING IN GALAXY OBSERVATIONS

When using sky-chopping in observations of galaxies it is desirable to have the reference beam separated from the source beam by an amount greater than the extent of the object under observation,

otherwise the signal measured is proportional only to the difference in brightness between the two regions of galaxy caught in the source and reference beams. If the source concerned is very large, or the chopping mechanism used severely limits the angular size of the throw, the situation described may be unavoidable, in which case the signal from the region seen by the reference beam (the "reference beam flux") must be estimated using a brightness distribution law, or better still should be measured directly. In simple photometry of galaxies the first course of action is adopted, and is often an adequate first approximation, but in the mapping of galaxies this approach is unacceptable and direct measurement of the reference beam flux must be made. This may involve several steps, depending upon the relative sizes of the object of interest and the beam separation. This disadvantage of the sky-chopping approach may be compared with the drift problems encountered with black-body choppers, and the sensitivity loss experienced with the polaroid chopper (see fig. 2.6 and p. 2.16).

#### LOCATION DETERMINATION

Galaxies generally appear as hazy, diffuse objects when viewed directly, and with a few notable exceptions (e.g. the Seyferts and M31) are notoriously difficult to centre upon. Whenever off-nucleus observations are made, accurate location of the beam on any given region is a non-trivial problem. The only certain way of accurately locating the beam is to use a nearby, bright field star of known position as the origin of an R.A.-Declination grid system. The chosen star is "centred upon" and the telescope is offset in a pre-determined manner to the start of the scan. During the scan the apparent motion of the guide star is followed in the off-axis guider, and where possible (see pages 2.14/15) the handset controls are used to correct any deviations from the

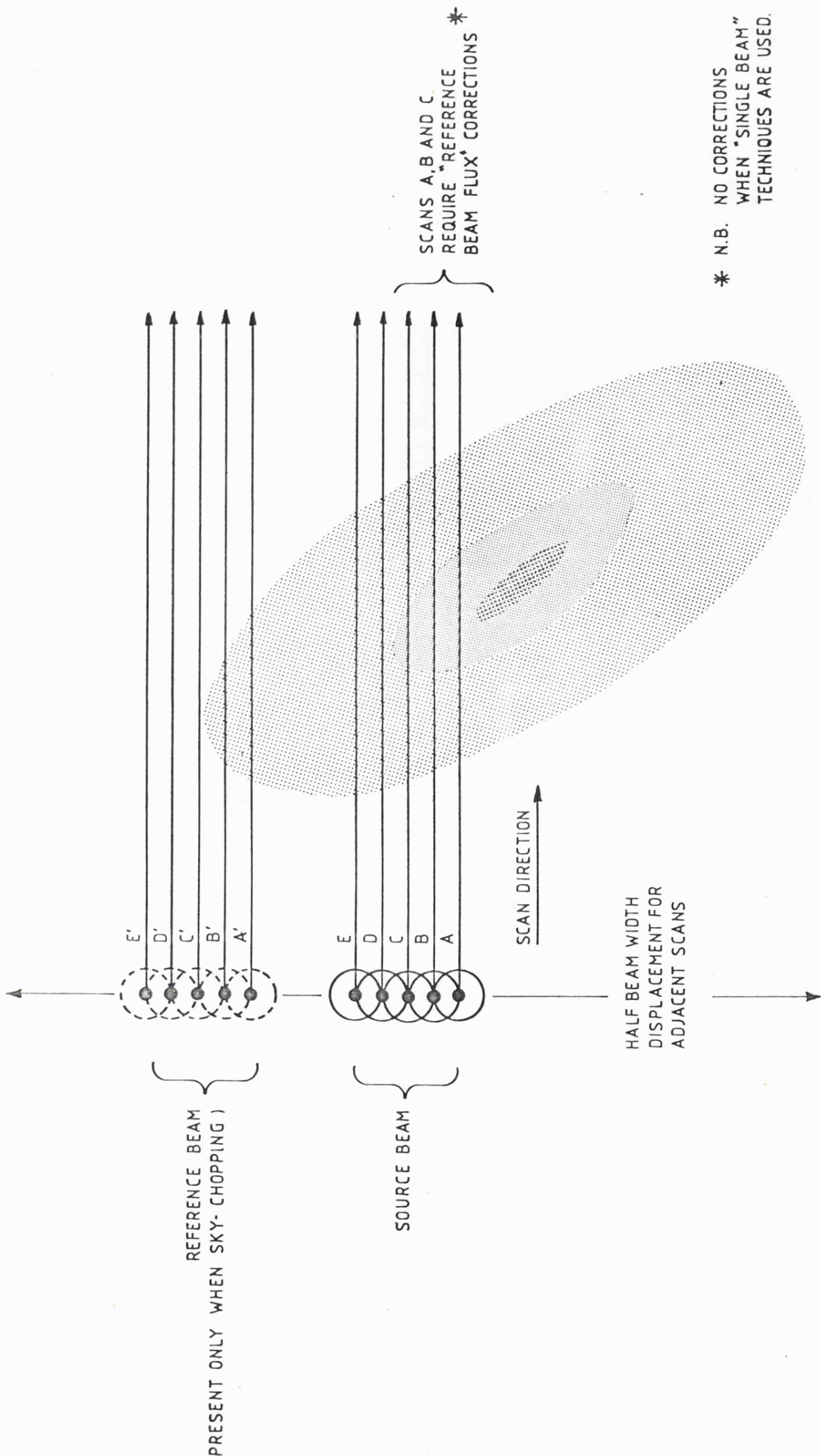


Fig. 2.6: Galaxy Scanning Observations

prescribed path. (Even when handset control is unavailable, following the guide star in the off-axis guider is essential as the observer needs to know if the telescope is deviating from its course, and if so, by how much.) Thus from the guide star position, and the known north-south and east-west scan lines, the final contour map can be drawn to the scale of sky plates, or other available photographs, and direct comparison with these can then be made.

#### TELESCOPE DRIFTING AND BACKLASH

Once a scan is set in motion the telescope should ideally follow the prescribed path exactly. Unfortunately this is not always the case, especially with the 1.5 m Tenerife telescope used for much of this work. Even when great care is taken with the initial balancing of this telescope it is frequently found to slip off its intended course by up to 20 arcseconds or so, particularly in R.A., and furthermore the degree of deviation from the intended course is not repeatable. The problem is particularly troublesome whenever a scan is intended to traverse a region of high surface brightness gradient such as the nucleus of a galaxy. Two years of having to work with this problem at Tenerife have shown that under certain conditions drift-free scanning is possible. If pre-observation balancing is painstakingly performed, the telescope does not drift perceptibly when the zenith angle of the pointing-axis is less than  $35^\circ$ . (Drifting occurs even at small zenith angles if the telescope is poorly balanced.) Between  $35^\circ$  and  $40^\circ$  the telescope begins to drift slowly during scans, and at zenith angles greater than  $45^\circ$  the drifting is severe; e.g. at zenith angles  $\sim 55^\circ$  scans have been observed to be fifteen to twenty arcseconds off course in the middle of five minute duration scans. This problem is particularly limiting at Tenerife as there is no observer guidance available when the

programmable scan facility is in operation since the handset controls are over-ridden for the duration of the scan.

Drifts of one to two arcseconds were noticed at the Isaac Newton telescope, but since handset guidance was available during a scan, compensation for small deviations from the prescribed path could immediately be made. It is worth noting that when observing with a telescope such as the INT which is equipped with an attached observing chair, the pointing is affected by an observer climbing into or out of the chair.

If a scan is to be made in the declination direction care must be taken to avoid positional uncertainty introduced by not taking up the "backlash" in the declination drive mechanism when the telescope motion changes direction. Thus whenever the telescope is moved to the start of a scan, the motion to the guide star, and then to the starting point must be in the same direction as that which will occur when the scan begins.

When making scanning observations with the Tenerife telescope it was found possible, by rigid adherence to backlash and telescope drift precautions, to maintain positional uncertainty to within 4 arcseconds. The corresponding figure for the INT was found to be 2 arcseconds.

#### PROFILE DATUM-LEVEL PROBLEMS

Ideally the profile obtained from a scan should include a sufficiently extensive region of steady background, on either side of the source peak, to provide a reliable datum level above which the signal can be measured (e.g. see figs. 2.9-11). Unfortunately, this was not always achieved, and during the course of the author's research several conditions have been experienced which have resulted in a

background level which was not stable.

a) BLACK-BODY CHOPPING DRIFTS

When using the black-body chopping technique, the temperature of the black-body and the sky brightness and transparency must remain constant for the duration of the scan, otherwise the quantity  $(S_{bb} - S_{bg})$  discussed above will not be constant and hence the background level in the profile obtained will drift with time. Drifting of this type occurred during observations of M31 made with a warm black-body chopper. In those observations of M31 which we describe in chapter three the background drifting was not a serious problem, drifts were  $\lesssim 10\%$  of the peak detection and appeared to be linear with time. Their effect could therefore be eliminated to first order by subtracting from the observed profile the least squares best fit to the apparent background slope. Becklin and Neugebauer (1978) have reported background drifts of a similar order in their observations of the Galactic Centre made with a cold black-body chopper, indicating that sky brightness variations are significant. Again the drifts were apparently linear with time and were removed from the data by the method just mentioned. It should be pointed out however that in other Leicester observations of M31, not reported here, drifts were sometimes  $\sim 50\%$  of the profile peak and occasionally were definitely non-linear.

It is interesting to note that in the other single beam technique used by the author, i.e. modulation using rotating and stationary polaroids, drifting of the background level was totally absent in all of the scans made. The reason for this is not fully understood but its consistent absence marks it as a major advantage of the technique.

b) P.S.D. DRIFTS

When sky-chopping is employed, temporal changes in sky brightness are unlikely to affect the background level since any such changes will

almost certainly be uniform over the relatively small distance between the two sky beams. Similarly any linear gradient in sky brightness will probably be on a very large scale compared to the beam separation, and so its effect on the profile background level will be negligible. However, consistent drifting of the background level has been occasionally observed by the author in series of scans obtained when using the sky-chopping technique. This was found to be due to drifting of the P.S.D. output signal which fortunately appeared to be linear with time, and was never more than 5% of the profile peak. Such drifting has occurred with more than one P.S.D.

It should be briefly mentioned that a considerable amount of the data obtained on two observing sessions (August 1978 and January 1979) was rendered effectively useless by irregular and sporadic background level variations associated with the signal processing electronics. This problem was not discovered until the data was plotted out back in Leicester, and was caused by an unstable reference phase shift circuit in a Brookdeal 9401 P.S.D. In the August 1978 data (NGC 972 and NGC 5195) there was also a curious low frequency modulation seen superimposed on the relatively high frequency detector noise. The mean amplitude of the modulation was several times that of the R.M.S. detector noise and so the data was too poor to use for analysis of radial variations in JHK colours as had been intended.

### 2.3 DATA AND DATA REDUCTION

With up to one thousand, one second integrations per scan, computer processing of the data is essential. The data originally stored on paper tape or magnetic (cassette) tape is therefore transferred to the Leicester University CDC Cyber 73 computer for reduction and analysis. The data is usually stored in related scan blocks, e.g. all

the  $2.2\ \mu\text{m}$  mapping scans of a galaxy made on a particular night, with each individual scan in the block separated from the next by a convenient and unambiguous delimiter, usually a negative number as all the data points are positive. Over the last three years software has been developed for the rapid, numerical processing of data blocks of this format and also for the graphical representation of raw or processed data. Several different types of data plotting are immediately available by simply changing the relevant parameter(s) in the software. Fig. 2.7 illustrates this by showing a typical profile (in this case from a scan through the nucleus of NGC 891 at  $2.2\ \mu\text{m}$ ) in four different ways: (i) the raw data in one second integration bins, (ii) the raw data averaged into ten second integration bins, (iii) the data after processing with a running mean over ten seconds and (iv) the data after processing with a polynomial, least squares equivalent, smoothing technique (Savitzky and Golay).

#### DATA EXAMPLES

Some examples are now given of the raw data obtained in the observations of M31, M82 and NGC 972 described in chapters 3, 4 and 5, respectively. The quality of this data is then briefly discussed in comparison to the theoretical limits given in section 2.1.

##### a) M31

Much of the M31 data was reduced before facilities to transfer data directly from magnetic tape to computer were available. The data had therefore to be transferred manually by copying four second integrations, read from the DVM, onto paper. Four seconds was found to be the shortest integration time which was possible to copy manually. Fig. 2.8 shows a profile from a typical scan through the nucleus. The profile was obtained with the  $1.5\ \text{m}$  Tenerife flux-collector with the

Version I photometer fitted with a black-body chopper and a Barnes InSb detector operated at  $77^{\circ}\text{K}$ . The one sigma, one second, noise in this profile, expressed as a magnitude, is  $m_K \sim 8.6$ . A better (modern) detector would improve the noise, but not the drifts.

b) M82

The M82 data was obtained with the 2.5 m Isaac Newton telescope at Herstmonceux, using the polaroid modulation technique described earlier, and a SBRC InSb detector operated at  $63^{\circ}\text{K}$ . Fig. 2.9 shows three examples of scans through or near the  $2.2\ \mu\text{m}$  centroid of the galaxy, with 6, 11 and 23 arcsecond apertures. The mean one sigma, one second noise magnitude in this data is  $\sim 9.5 - 9.8$ . On a 1.5 m telescope, the noise magnitude would be 8.4 to 8.7.

c) NGC 972

The NGC 972 data was obtained with the 1.5 m Tenerife flux-collector using the Version I photometer fitted with a vibrating mirror chopper and an SBRC InSb detector operated at  $63^{\circ}\text{K}$ . Fig.2.10 shows two examples of the  $2.2\ \mu\text{m}$  mapping observations. The one sigma, one second noise magnitude is  $m_K \sim 11.9$ . Fig.2.11a shows J, H and K slit scan profiles along an east-west line through the nucleus. Fig.2.11b gives examples of how summing the profiles from identically executed scans can improve the signal-to-noise. Each profile shown is the mean of the sum of three profiles, one which (at each wavelength) is shown in fig.2.11a.

Table 2.3 summarises the observed noise limits measured by the author and compares these to the theoretical limits for an InSb photovoltaic detector with an effective quantum efficiency of 50% and a resistance of  $5 \times 10^9\ \Omega$ . Observations of NGC 972 and NGC 5195 made by the author and observations of faint standard stars by M. Sherrington (priv. comm.) lead to limiting noise magnitudes which are in excellent

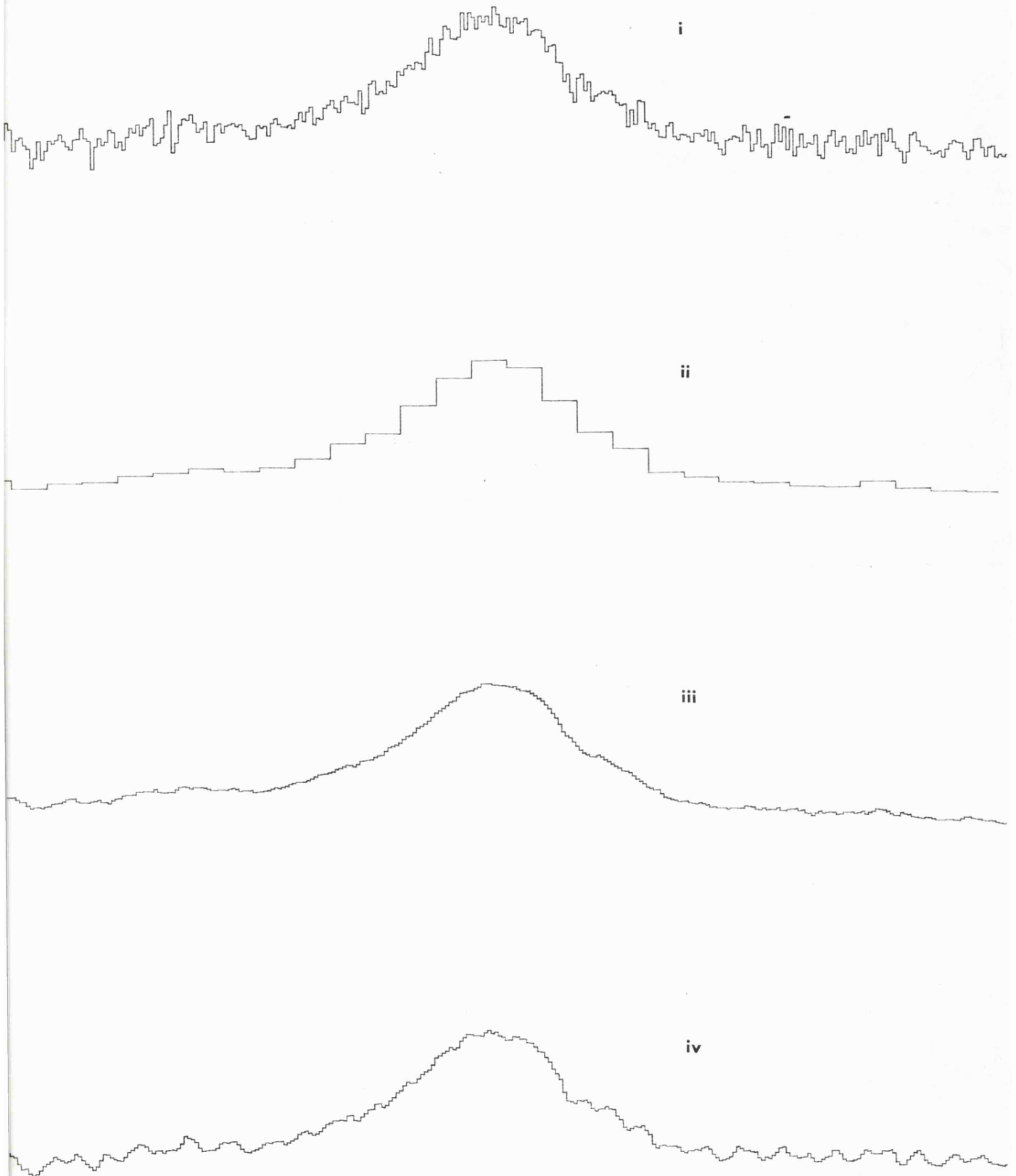


Fig. 2.7: Some of the various plotting options (see text for details)

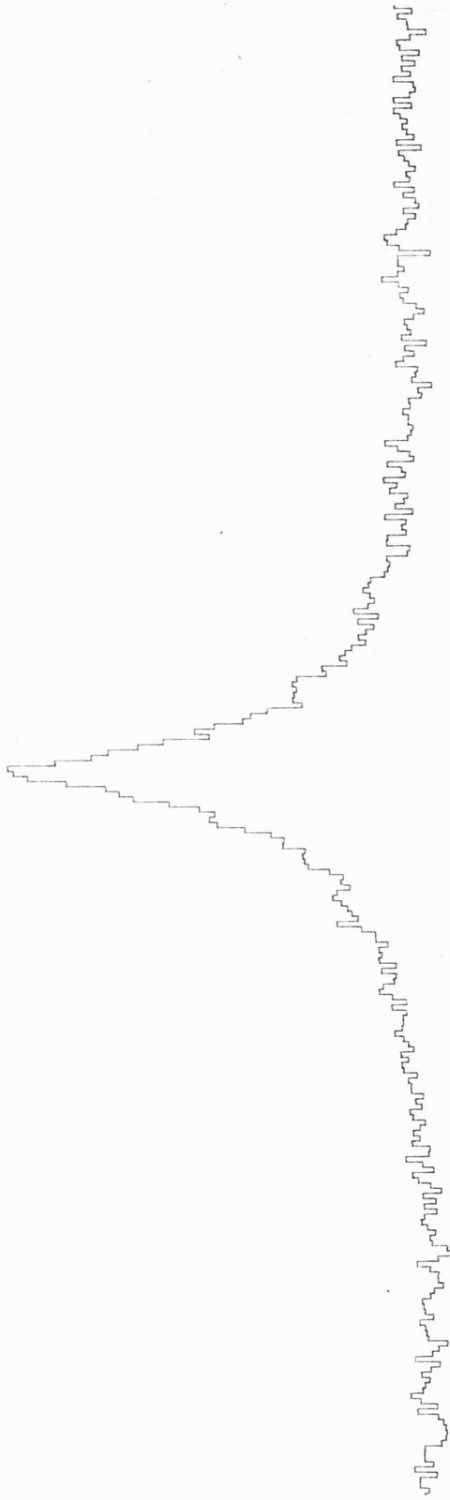


Fig. 2.8: Profile from an R.A. Scan of M31

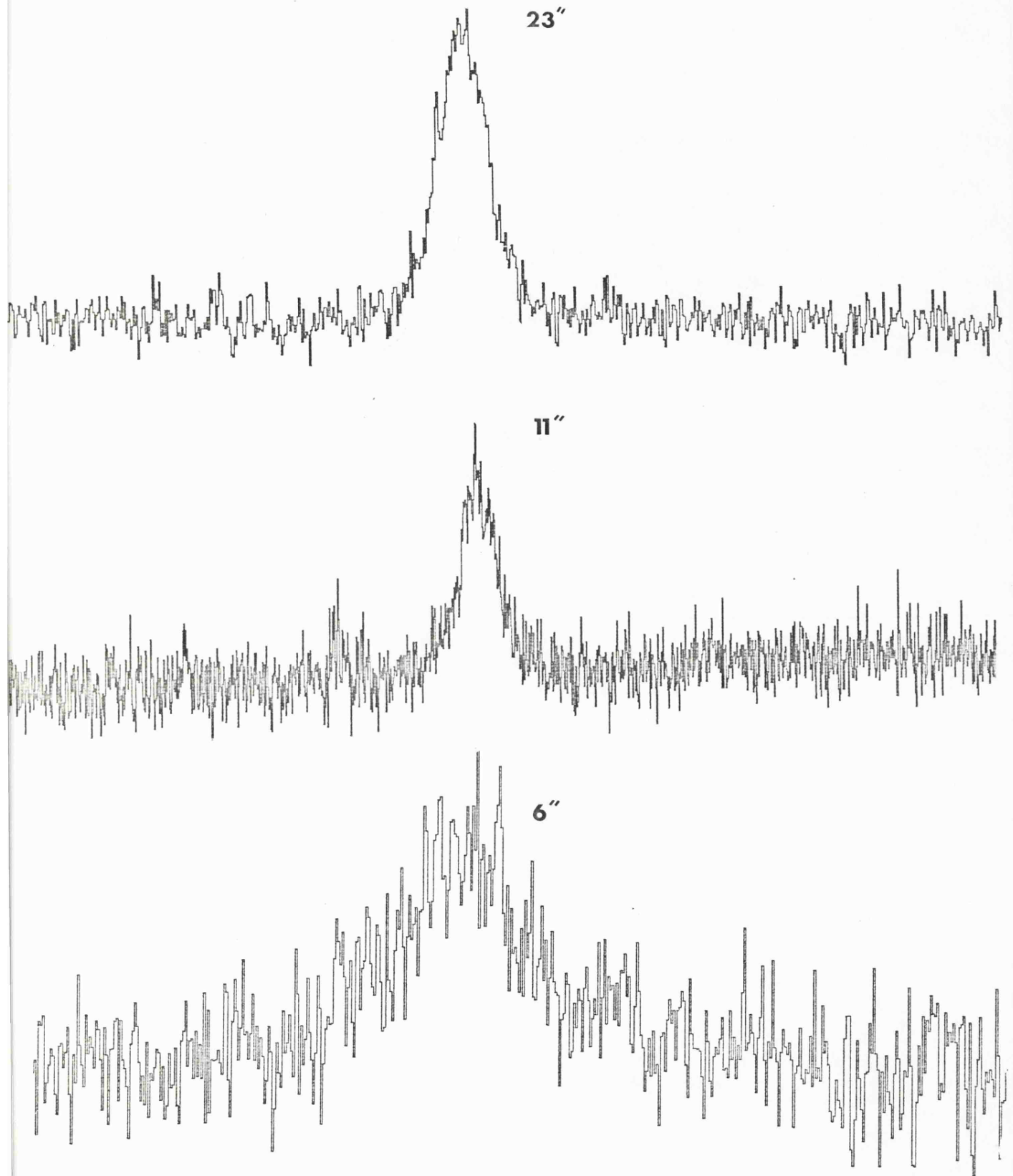


Fig. 2.9: Profiles from scans through M82 with various apertures

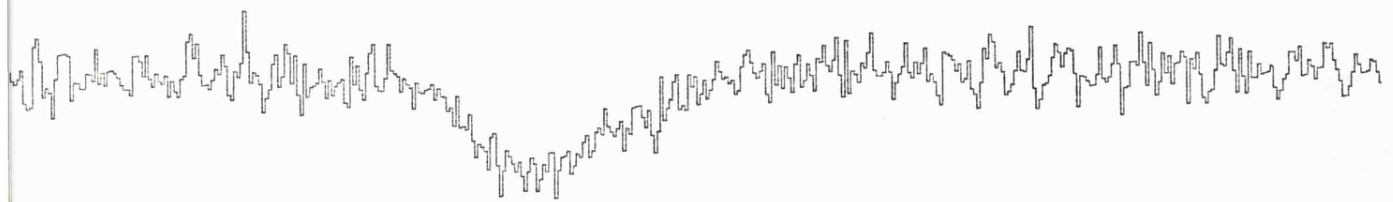
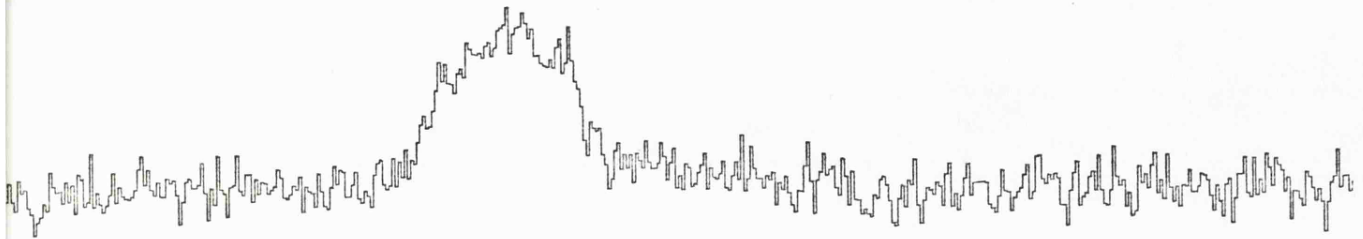


Fig. 2.10: Examples of NGC 972 Mapping Profiles

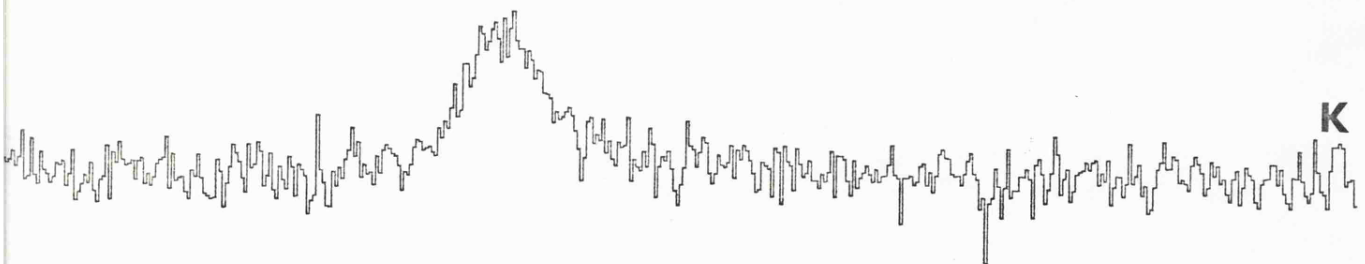
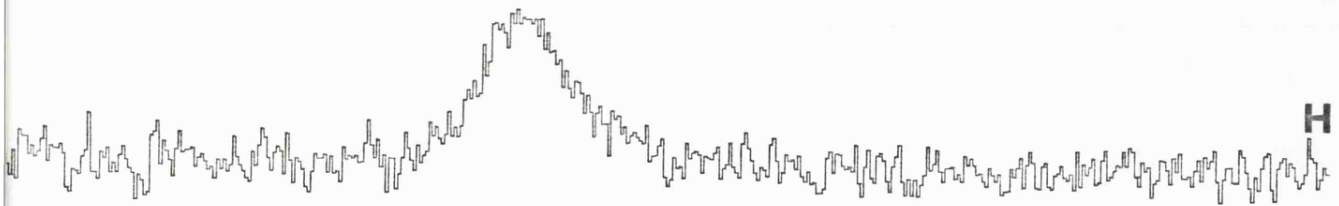
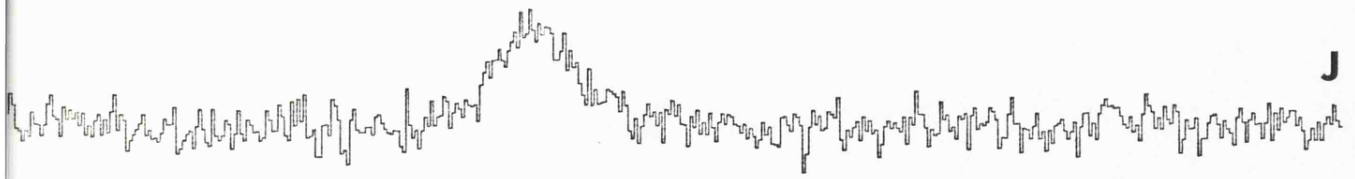
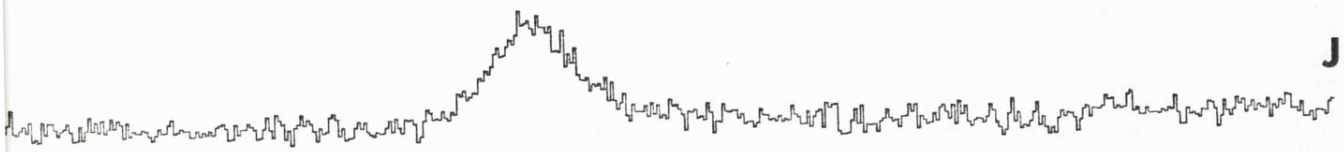
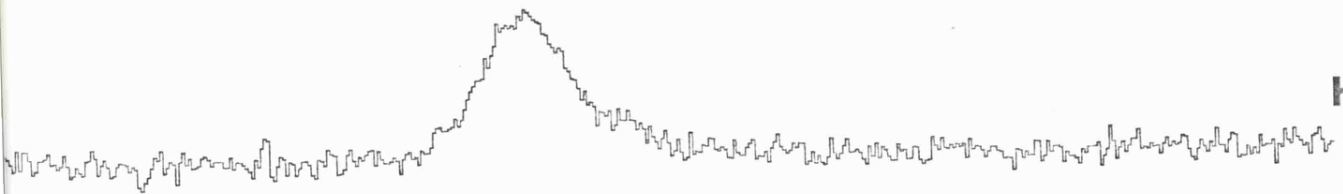


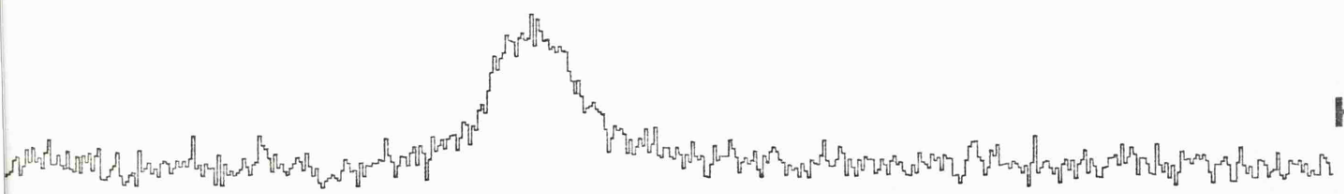
Fig. 2.11a: Examples of NGC 972 Slit Aperture Profiles



**J**



**H**



**K**

Fig. 2.11b: NGC 972 Slit Profiles: S/N improved by adding profiles (3x)

Table 2.3 : Observed Vs Theoretical Noise Limits

Site and Date	System Used	Observed Noise Limits on a 1.5 m Telescope ( $1\sigma$ in 1 sec)		
		J	H	K
Tenerife Summer 1976	Version I Photometer, b.b. chopper Barnes InSb, 770K	-	-	8.6
Tenerife Autumn 1977	Version II Photometer, Wide throw chopper SBRC InSb, 63°K	-	-	11.8
Sussex March 1977 and August 1978	Hatfield Polarimeter SBRC InSb, 63°K	-	-	8.4-8.7
Tenerife Winter 1978/79	Version I Photometer, Vibrating mirror chopper, SBRC InSb 63°K	12.5	12.4	11.9
Tenerife* Summer 1979	Version I Photometer, Vibrating mirror chopper, SBRC InSb 63°K	12.5	-	11.9
Tenerife MacGregor Report 1977	Imperial College System	12.2	12.5	12.5
-	Theoretical InSb Limits $T = 63^{\circ}\text{K}, \eta = 0.5, R = 5 \times 10^9$	13.2	12.4	12.7
Tenerife	Sky shotnoise limits	13.0	15.5	14.0

\* Data provided by M. Sherrington

agreement. At J and H these limits are also very close to the observed limits of MacGregor, and at J the observed noise compares well with the sky shot noise limit. At K however the observed limits of the Leicester system consistently fall short of the observed limits of MacGregor and therefore also of the theoretical limit for a detector with  $R = 5 \times 10^9 \Omega$  and  $\eta = 0.5$ . The detector system is known to be poor at  $3.5 \mu\text{m}$ , probably due to inadequate baffling against background emission, which should not be important at J and H but may begin to have an effect at K.

### CALIBRATION

Throughout this project calibration has been with respect to stars from the Johnson list of standards (Johnson et al. 1966). Any selected star is first checked for possible variability by reference to the Catalogue of Bright Stars. Any star suspected of being a variable is discarded as a possible standard. The primary criteria for selecting standards are (a) the star should lie as near in the sky as possible to the galaxy of interest and (b) that the star be as close as possible in brightness to the galaxy of interest to avoid possible systematic error introduced by any non-linearity in the amplifiers. As infrared standard stars are relatively few in number and are generally relatively bright, the star(s) selected often do not satisfy the above criteria well but are always an optimum selection. A calibration observation consists of a scan through the star executed in a manner exactly similar to that in the scans through the galaxy, i.e. same rate, direction and aperture. The times of all galaxy and calibration star measurements are always noted so that atmospheric extinction corrections can be made.

After correcting the measured signals for atmospheric extinction, conversion to magnitudes is achieved by application of the well known formula:

Table 2.4: Absolute Calibration of Photometry

Filter band	$\lambda_0$ ( $\mu$ m)	$F_\nu$ ( $W m^{-2} Hz^{-1}$ ) (for mag = 0.0)
V	0.55	$3.81 \times 10^{-23}$
J	1.25	$1.77 \times 10^{-23}$
H	1.65	$1.16 \times 10^{-23}$ *
K	2.22	$6.3 \times 10^{-24}$

\* Interpolation of Johnson's (1966) calibration.

$$m_g(\lambda) = m_s(\lambda) - 2.5 \log_{10} \left( \frac{s_g(\lambda)}{s_s(\lambda)} \right)$$

where  $m_g(\lambda)$ ,  $m_s(\lambda)$  are the magnitudes of the standard star and galaxy at wavelength,  $\lambda$  and  $s_g(\lambda)$ ,  $s_s(\lambda)$  are the measured signals at  $\lambda$ . Conversion to flux units follows the absolute calibration of Johnson 1966 (Table 2.4).

### CORRECTIONS

It is frequently necessary to correct observed data to compensate for other effects which may alter the intrinsic colours and magnitudes of the object of interest:

#### i) ATMOSPHERIC EXTINCTION

Extinction of starlight in the Earth's atmosphere is caused by scattering and absorption of light by the various constituents of the atmosphere. The apparent magnitude  $m(\lambda)$  is a function of airmass  $M(z)$  at zenith angle,  $z$ ,

$$m(\lambda) = m_0(\lambda) + \Delta m_0(\lambda) M(z)$$

where  $m_0(\lambda)$  is the magnitude which would be observed outside the Earth's atmosphere, and  $\Delta m_0(\lambda)$  is the magnitude loss at the zenith and equals  $2.5 D(0)$  where  $D(0)$  represents the optical density of the atmosphere for one airmass ( $z = 0$ ). The airmass can be expressed in a simple form when the atmosphere is assumed to have a plane parallel structure and the zenith angle of the star is less than  $60^\circ$ , i.e.  $M(z) = \sec z$ . More involved formulae apply when  $z > 60^\circ$ . The usual practice to correct for atmospheric extinction effects is to plot a graph of  $\log_{10}$  (observed signal), at zenith angle  $z$ , against  $\sec z$  for the calibration star(s). Any deviations from a straight line can then be seen as changes of the atmospheric extinction with time.

Magnitudes of the object of interest can then be obtained directly by using the calibration star signal extrapolated to the appropriate airmass.

#### ii) GALACTIC ABSORPTION

Light propagating in the Galaxy will be scattered and absorbed by interstellar dust particles. This interstellar matter is concentrated in the plane of the Galaxy and therefore absorption decreases towards the Galactic Poles. The necessary corrections to observed magnitudes and colours have been extensively investigated and are well described in a famous review by Johnson (1968). Various correction factors are discussed by Johnson but the most widely used correction law is that based upon the extinction versus wavelength curve no. 15 of van de Hulst (1949). The particular corrections given by Johnson and corresponding to van de Hulst's curve 15 are:  $E_{V-K}/A_V = 0.91$ ,  $E_{J-H}/A_V = 0.1$  and  $E_{H-K}/A_V = 0.06$ , where  $E$  = colour excess and  $A_V$  = magnitudes of visible extinction given by  $A_V = 0.15 \operatorname{cosec} b$ , where  $b$  = Galactic latitude. More recently Sandage (1973) has shown that the obscuration in the galaxy is probably less than previously supposed, particularly towards the poles. In his "absorption-free polar cap model" Sandage suggests the dependence of extinction on Galactic latitude is as follows:

$$A_V = 0.10 (\operatorname{cosec} b - 1); \quad |b| \leq 50^\circ$$

$$A_V = 0; \quad |b| > 50^\circ .$$

#### ABSORPTION WITHIN OTHER GALAXIES

After correcting for (i) and (ii) the colours of the galaxy may still appear incompatible with its expected stellar content. This might be due to an unusual population of stars or perhaps to the presence of one of the non-stellar sources discussed in chapter 1. Alternatively,

it may simply be due to obscuration within the galaxy itself. The first order correction to compensate for internal obscuration is simply to apply the van de Hulst extinction law as in (ii) above. This however implicitly assumes the source to lie behind a veil of obscuring matter, whereas in reality the emission from external galaxies is the sum of millions of discrete sources, some or all of which may be randomly intermingled with the obscuring matter. In such cases corrections can only be based upon a model of source distribution within the obscuring dust clouse (see chapter 4).

### iii) THE "K-CORRECTION"

This correction is necessary to magnitudes and colours because the part of the galaxy's spectrum intercepted by the standard photometric filters obviously changes with galaxy redshift. Correction factors for the near infrared region have been discussed by Frogel et al. 1978. Corrections to magnitudes and colours are as follows:

$K_K = -3.25z$ ,  $K_{J-H} = 0.5z$ ,  $K_{H-K} = 3.6z$ . For M82 and M31 ( $z < 0.001$ ) the K corrections are negligible, and even for NGC 972 ( $z = 0.006$ ) they are very small;  $K_K = -0.02$ ,  $K_{J-H} = 0.003$  and  $K_{H-K} = 0.02$ . These corrections are of the order, or much less than, the statistical accuracy of the data obtained in the observations of NGC 972 described in chapter 5 and have therefore been neglected.

### CONTOUR PLOTTING

After the profiles from a set of mapping scans have been calibrated, the necessary correction factors have been applied and where possible duplicate scans have been summed to improve the signal-to-noise, the processed data set is filed on computer as a matrix representing the surface brightness distribution of the galaxy observed. Software has been developed to reproduce such a matrix in the form of

an isophotal contour map. For the actual contour plotting the software used relies heavily on the graphics package "CGHOST" available at the Leicester University Computer Laboratory, although data manipulation routines to prepare the matrix have been developed by members of the infrared group. In common with the profile plots discussed earlier the contour maps can be drawn from binned or smoothed data. The contour maps of M82 and NGC 972 are shown in chapters 4 and 5 respectively.

## REFERENCES

- Aaronson, M. 1978, Ph.D. Thesis, Harvard University.
- Akinci, R. 1978, Ph.D. Thesis, Leicester University.
- Baddiley, C.J. and Ring, J. 1977, *Infrared Physics*, 17, 405.
- Becklin, E. and Neugebauer, G. 1968, *Ap. J.*, 151, 145.
- Becklin, E. and Neugebauer, G. 1978, *P.A.S.P.*, 90, 657.
- Cox, L.J., Hough, J.H. and McCall, A. 1978, *M.N.*, 185, 199.
- Frogel, J.A., Persson, S.E., Aaronson, M. and Matthews, K. 1978,  
*Ap. J.*, 220, 75.
- Hall, D.N.B., Aikens, R.S., Joyce, R. and McCurnin, T.W. 1975, *Applied Optics*, 14, 450.
- Hudson, D.H. *Infrared Systems Engineering* 1969, Wiley Interscience.
- Johnson, H.L. 1966, *Ann. Rev. Astron. and Ap.*, 4, 193.
- Johnson, H.L. 1968, in *Stars and Stellar Systems*, Vol. VII, 167.
- Johnson, H.L., Mitchell, R.I., Iriarte, B. and Wisniewski, W.Z. 1966,  
*Ariz. Uni. Lunar planet. Lab. Comms.*, 4, 99.
- Longmore, A. 1975 , Ph.D. Thesis, Leicester University.
- MacGregor, A. 1977, *ICST Detector Testing Contract: Final Report*.
- McCall, A. 1979, Ph.D. Thesis, Hatfield Polytechnic.
- Sandage, A. 1973, *Ap. J.*, 183, 711.
- Savitzky, A. and Golay, M.J.E. 1964, *Analytical Chemistry*, 36, 1627.
- Strom, K.M., Strom, S.E. and Wells, D.C. 1978, *Ap. J.*, 220, 62.
- Van de Hulst, H.C. 1949, *Rech. astr. Obs. Utrecht*, 11, 1.
- Wolfe, W.L. (Ed.) 1965, *Handbook of Military Infrared Technology*,  
Office of Naval Research, Washington.

Two Micron observations of the Nuclear Bulge of M31

### 3.1 INTRODUCTION

M31 was the first galaxy for which the group attempted any serious work. The choice was an obvious one for the first venture into a new field for three simple reasons: it is the brightest extragalactic source at  $2.2 \mu\text{m}$ , some reliable infrared data already existed (Johnson 1966, Sandage et al. 1969) against which we could check our initial results, and finally, and this was the most important influencing factor, there seemed to be scope to extend the previous work of others without modification of the group's existing equipment. The general case for making infrared observations of galaxies such as M31, which appear to be absolutely "normal" at optical wavelengths, has been described by Sandage et al. (1969) and is as follows: (a) to search for any central non-thermal excess (i.e. akin to Seyfert activity) which is not apparent in the visible waveband, (b) to provide long wavelength constraints for stellar synthesis modelling since optical data alone are insufficient to determine the luminosity function for late type stars and (c) to investigate the comparative radial distribution of infrared and visible light since an observed colour gradient would provide further data relating to the way in which stellar population changes with increasing radius. It was the problem of radial distribution of light which interested us (and eventually became the topic of this thesis). Sandage et al. (1969) measured the  $2.2 \mu\text{m}$  brightness distribution in the central  $\pm 2$  arcmins ( $\pm 400$  pc) of M31 to determine if there was any significant difference between the population in the nucleus ( $r \lesssim 10''$  arc) and the immediately adjacent region of the bulge component. The aim in extending their study was two-fold: first to see how closely, if at all, the  $2.2 \mu\text{m}$  distribution followed the  $r^{-\frac{1}{4}}$  law within the spheroidal bulge as a whole, and to check for any contribution from the disc component, and secondly to measure

the V-K gradient over as much of this region as our sensitivity permitted. Independently, and at the time unbeknown to us, Japanese Infrared Astronomy groups at Nagoya and Tokyo Universities were jointly working on a similar project. The independent results of the Leicester and Japanese groups are compared below.

### 3.2 Previous Infrared Observations of M31

M31 was first observed at wavelengths  $\lambda > 1 \mu\text{m}$  by Johnson who included it in his early survey of the infrared colours of galaxies (Johnson, 1966). His results and those of the more extensive UBVRIHKL multiaperture photometry of Sandage et al. (1969) showed that although a "mean nucleus" of KOIII stars provided an adequate model of the observed ultra-violet through visible continuum, stars of a much later spectral type must be present to account for the observed continuum longward of  $1 \mu\text{m}$ , (see fig. 1.1b and section 1.4). Stellar synthesis models of the nucleus ( $r \lesssim 10''$  arc) based upon optical narrow band data and the available broad band infrared data (Spinrad and Taylor 1971, Faber 1972) were in disagreement over the question of whether the light of dwarfs (Spinrad and Taylor) or of giants (Faber) dominated the integrated infrared light. The CO absorption band photometry of Baldwin et al. (1973) provided the first direct observational evidence that suggested giant stars were the principal contributors. Although the broad-band data alone failed to give a definite answer to the cool star luminosity function problem, the presence of a non-thermal excess was ruled out by the HKL photometry (Sandage et al.) and the observed absence of a ten micron excess (Kleinmann and Low, 1970).

The  $2.2 \mu\text{m}$  brightness distribution inwards of  $r = 40$  arcsecs was found to be the same as that for the B, V and R wavebands to within ten percent, although a significant gradient in the U-B colour index

was observed. No data relating to the V-K gradient or brightness distribution of  $2.2 \mu\text{m}$  light, over the whole bulge region existed prior to the observations described below. Such data is necessary to ascertain whether the dominating population at infrared wavelengths is distributed within the bulge in the same way as that which dominates the visible light. The gradient/distribution observed must be accounted for by any theoretical models of galactic structure and evolution.

### 3.3 Observations and Results

The observations were made in June and September 1976 and August 1978 with the Cabezon Observatory  $1.5 \text{ m}$  flux collector and the photometer described in Chapter 2 fitted with the black body chopper. The 1976 observations were made with the Barnes InSb detector operated at  $77^\circ\text{K}$  and unflashed as this process was unknown to us at the time. The 1978 observations were made with the SBRC InSb detector and although it was flashed the operating temperature was again only  $77^\circ\text{K}$  as the vacuum pump was faulty. The initial observations consisted simply of  $2.2 \mu\text{m}$  surface photometry along E-W and N-S lines passing through the nucleus of the galaxy. Three scans in each direction were obtained which traversed the whole of the spheroidal bulge of the galaxy; the scan paths are indicated in fig. 1 by the black lines superimposed on the Hubble Atlas print of M31. In the 1978 work the V-K gradient was measured directly by making simultaneous common-photometer observations in the V and K bands. This method avoids the possible error introduced when subtracting two steeply varying profiles.

Examples of the raw data have been shown in Chapter 2; the reduced data from the 1976 and 1978 work are summarised in figs. 3.2 and 3.3 respectively. Fig.3.2a shows the N-S and E-W profiles in comparison with the beam profile, and fig. 3.3 shows  $\Delta(V-K)$  vs  $r$  in

Fig. 3.1 (Overleaf) :

R.A. and Dec. scan channels superimposed  
on the Hubble Atlas print of M31.

(The region of the galaxy detected at 2.2  $\mu\text{m}$   
is indicated by the tick marks. The small  
black circle represents the beam size.)

10'



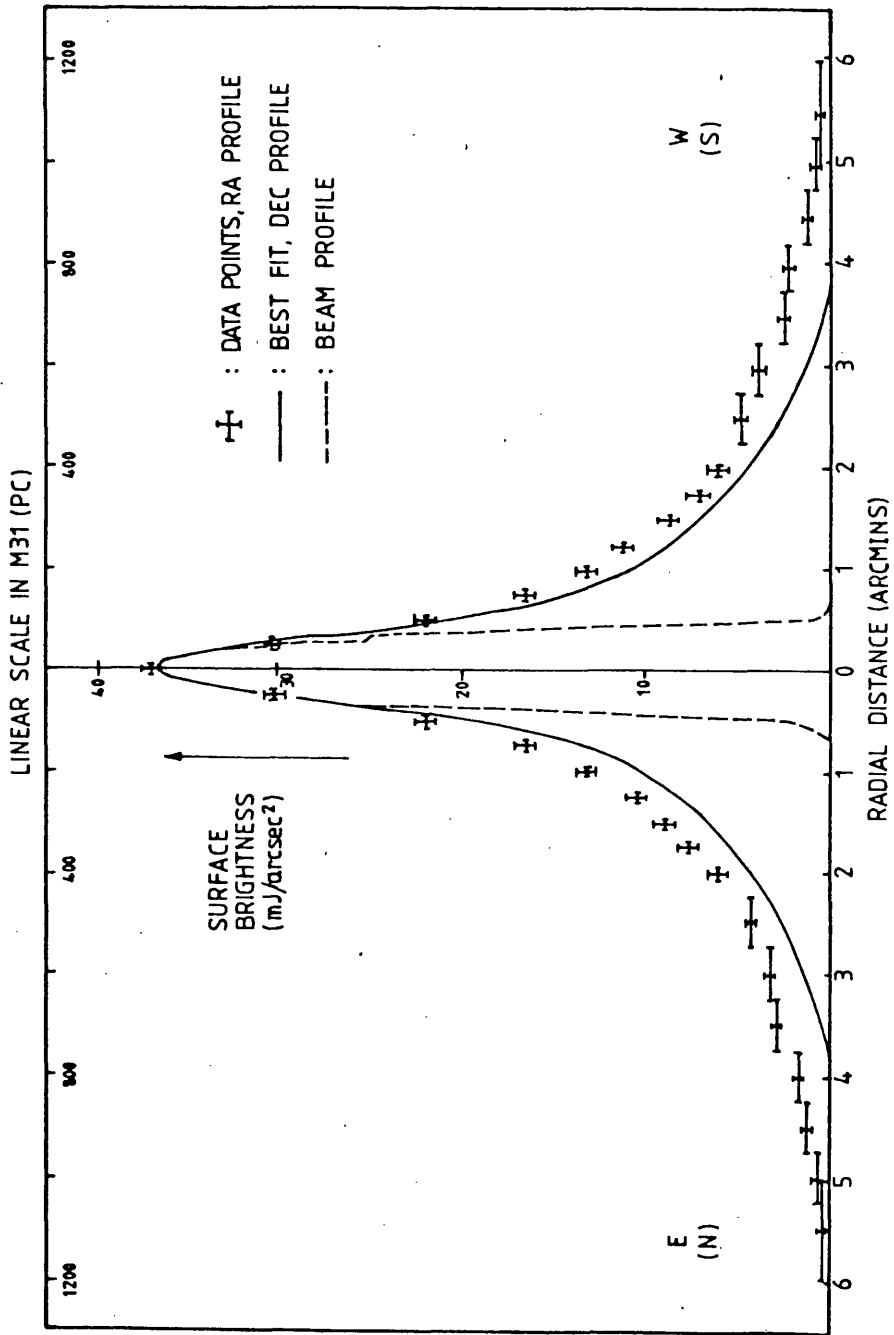


Fig. 3.2a : 2.2  $\mu$ m Brightness Distribution in M31

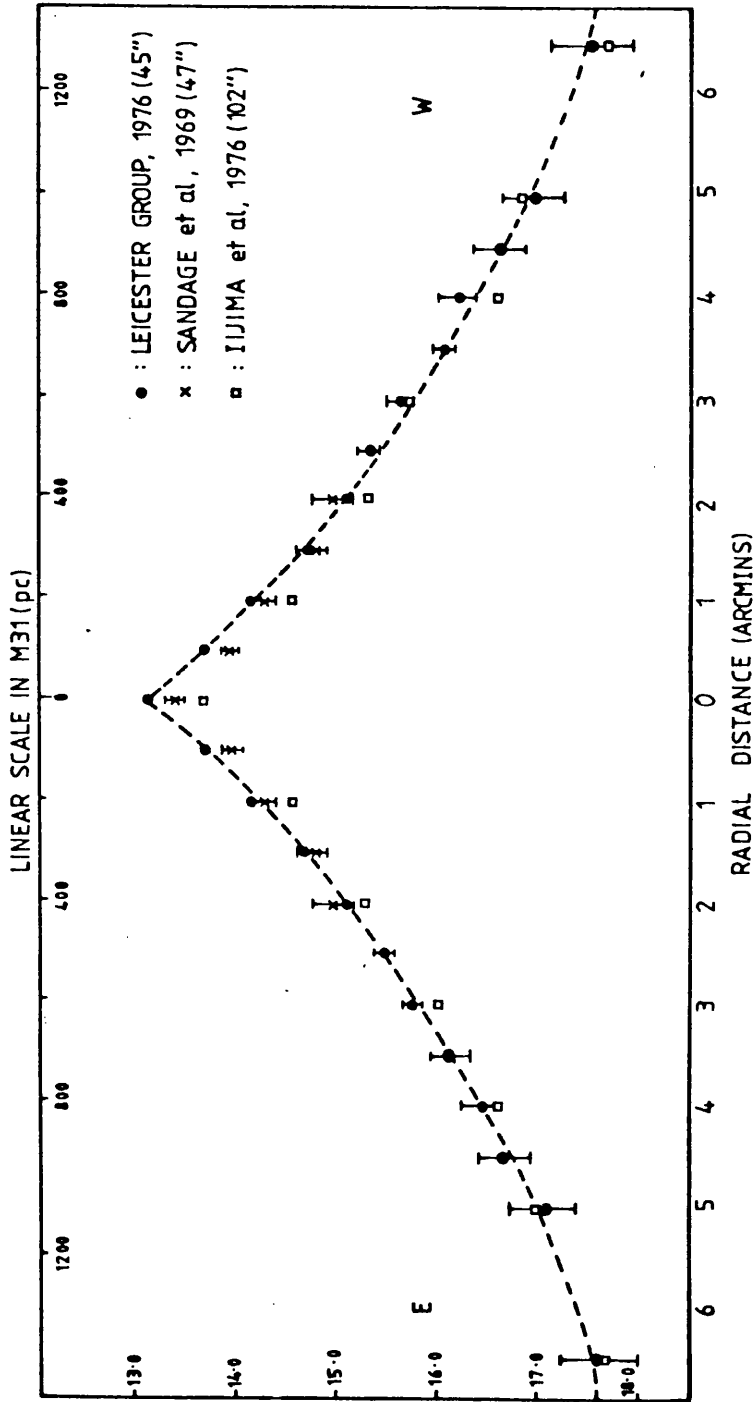


Fig. 3.2b:  $m_K / \square''$  Vs  $r$

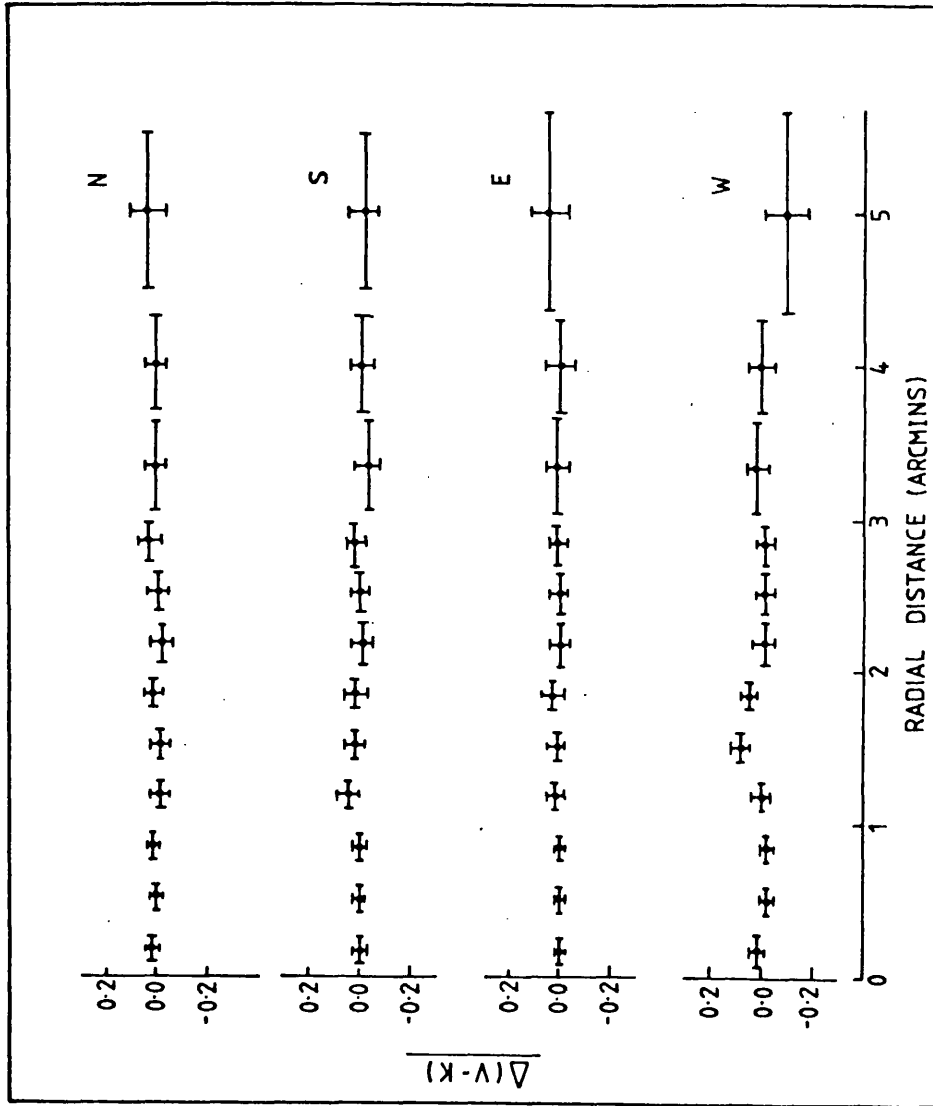


Fig. 3.3 :  $\Delta(V-K)$  Vs r

the central  $\pm 5$  arcmins. In all the M31 observations the sky-projected aperture size was 45 arcsecs FWHM. The error bars on the abscissae indicate the bin width over which the raw data was averaged, and those on the ordinates indicate the one sigma scatter in the particular bin. The E-W profile has been corrected in the central three bins to compensate for the nucleus being missed by  $\sim 10''$  arc in each of the R.A. scans. This problem was due to the telescope drifting slightly in declination during these scans. As drifting did not occur during the declination scans the R.A. profile was corrected by replacing the original three central bins by the corresponding bins from the declination profile. In the central part of the galaxy ( $r \lesssim 45''$ ) the isophotal eccentricity is  $\lesssim 0.9$  (Sandage et al. 1969) and so any error introduced by the correction procedure will be minimal.

"Thermal drifting" of the background (datum) level was a problem in half the scans made in 1976. The drifts were assumed to be linear with time, and so their effect could be removed by subtracting the least-squares best-fit straight line to the background from each of the profiles concerned. This procedure has been used by others when working with black body choppers (see Chapter 2).

Calibration was with respect to  $v$ -And ( $m_K = 4.90$ ) which had in turn been calibrated against the Johnson standards  $\epsilon$ -And and  $\theta$ -Oph. The data presented have been corrected for atmospheric extinction but not for galactic absorption, however according to Aaronson (1978) the necessary correction factors are  $A_K \sim 0.01$ ,  $A_V = 0.17$  and  $E_{(V-K)} = 0.16$ . These corrections will have no effect on the discussion and conclusions presented since (a)  $A_K$  is less than the statistical accuracy of the data, and (b) we are primarily interested in radial changes in the V-K index, rather than the exact absolute value at a given position.

### 3.4 Discussion

#### a) 2.2 $\mu\text{m}$ Brightness Distribution

The most obvious characteristic of the brightness profiles in fig.3.2a is the overall symmetry, both N-S and E-W. In contrast the blue waveband E-W profile is somewhat steeper on the west side (de Vaucouleurs, 1958). As the west side is the near side for us, and as the plane of the galaxy is inclined at only twelve degrees to the line of sight, obscuration by dust in the disk is probably responsible for the asymmetry in the blue light contours. As the 2.2  $\mu\text{m}$  profile is symmetric it can be concluded that interstellar extinction within this region of M31 is negligible at infrared wavelengths. This is in fact to be expected as the asymmetry in the blue profile is slight. There is, furthermore, no indication of asymmetry in the V profiles obtained in the 1978 observations, which confirms that dust obscuration is minimal.

Fig.3.2b shows the E-W surface brightness profile,  $m_K/\text{arcsec}^2$  versus  $r$ . It is a composite picture of all the available large-scale 2.2  $\mu\text{m}$  brightness-distribution data, and includes the results of Sandage et al. (1969), 47 arcsec aperture, and the results of Iijima et al. (1976), 102 arcsec aperture, as well as the data of the Leicester group (presented linearly in fig.3.2a) 45 arcsec aperture. Apart from the expected deviations due to instrumental broadening, which are apparent in the central Japanese data, all the data sets are in reasonable agreement, particularly the data presented for the first time here and that of Sandage et al. obtained with an approximately equivalent aperture. It was explained earlier that the main objective of the 1976 work was to see if the observed 2.2  $\mu\text{m}$  brightness distribution in the bulge followed the  $r^{-\frac{1}{4}}$  law observed for blue light. To test this the logarithm of observed brightness ( $B_K$ ) was plotted against  $r_c^{\frac{1}{4}}$ , where  $r_c$

is the position along the major axis corresponding to the position  $r$  on the E-W line through the nucleus, i.e. this effectively transforms the E-W profile into the major axis profile, by (a) assuming elliptical isophotes and (b) estimating values for the axial ratio ( $b/a$ ) by the procedure described below. One form of the expression relating  $r$ , the radius vector of an ellipse to the semi major axis,  $a$  (i.e.  $r_c$  here)

is: 
$$\frac{r}{a} = \left( \frac{(b/a)^2}{\sin^2 \theta + \frac{\cos^2 \theta}{(b/a)^2}} \right)^{\frac{1}{2}},$$
 where  $b$  is the semi-minor axis and  $\theta$

is the angle made by  $r$  and  $a$ . Inward of  $a = 2$  arcmins the axial ratio ( $b/a$ ) data of Sandage et al. for  $2.2 \mu\text{m}$  were used and at greater radial distances the estimates for ( $b/a$ ) were interpolations based upon the data of Sandage et al. and the value of ( $b/a$ ) at  $a = 16$  arcmins from the blue light contour map of de Vaucouleurs. Fig. 3.4 shows the plot of  $\log B_K$  versus  $r_c^{\frac{1}{4}}$  for  $r = 1$  arcsec to  $r \sim 5.5$  arcmin,  $r_c \sim 12.5$  arcmins. To overcome discrepancy due to instrumental broadening, the high resolution data of Sandage et al. (5 arcsec aperture) was used for  $r < 30$  arcsecs, but at greater radial distances the Leicester data was used. (The profiles of Sandage et al. for  $r < 1$  arcmin show that the high resolution profile merges smoothly with their lower resolution profile (47 arcsec aperture) at  $r \sim 30$  arcsecs). The value taken for  $\theta$ , the angle made by the E-W line along which our scans were made and the major axis, is  $52.5^\circ$ , and assumes the  $2.2 \mu\text{m}$  major axis to be co-linear with the major axis given in de Vaucouleurs (1958).

From fig. 3.4 it is concluded that for  $r_c \lesssim 12$  arcmins the  $2.2 \mu\text{m}$  brightness distribution is adequately described by the  $r^{\frac{1}{4}}$  law, and within this region there is no evidence in our data which suggests the presence of a contribution to the  $2.2 \mu\text{m}$  emission from the galaxy's disk component, since any additional contributions would result in a (+ve) deviation from the straight line in the  $\log B_K$  versus  $r_c^{\frac{1}{4}}$  plot.

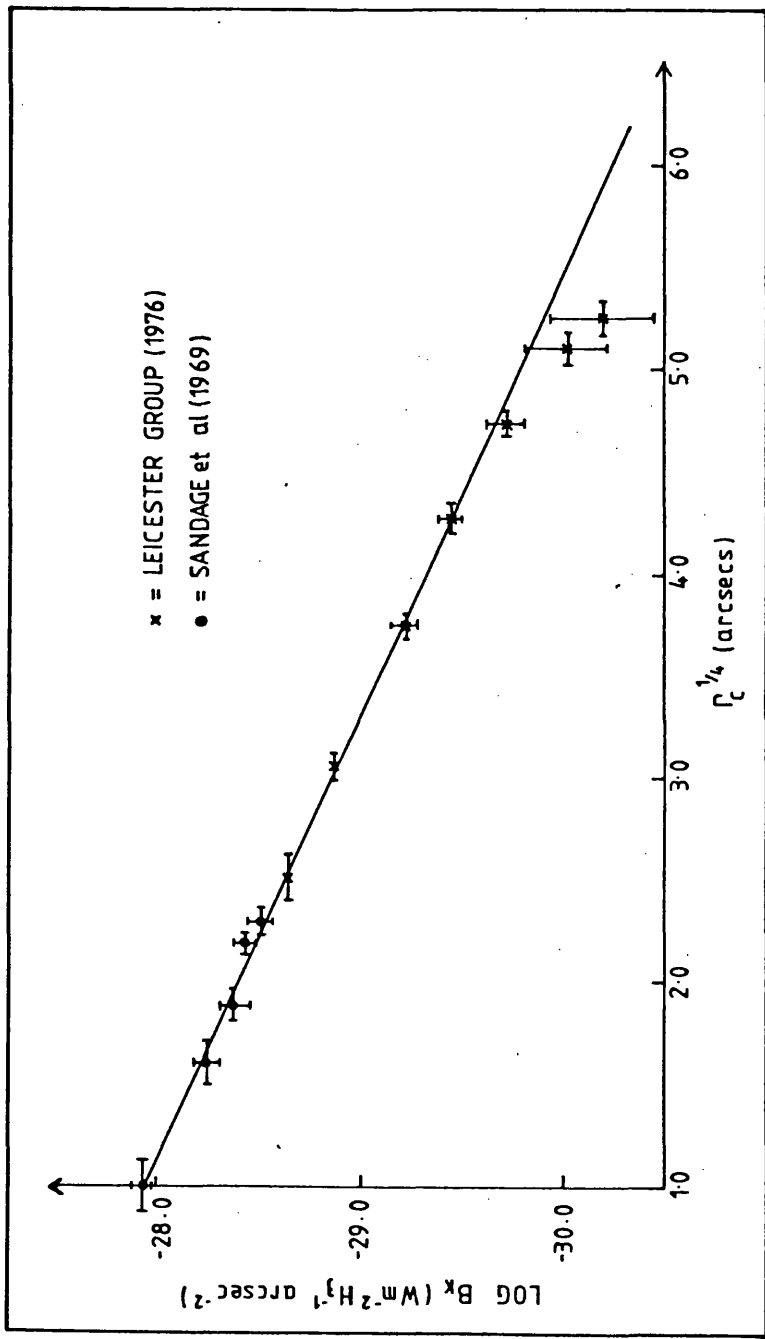


Fig. 3.4 :  $\text{Log } B_K$  Vs  $r_c^{1/4}$

The data of de Vaucouleurs (1958) shows the disk contribution to the integrated B light of M31 to be minimal at  $r = 10$  arcmins and negligible for  $r < 8$  arcmins, but for  $10 \text{ arcmins} < r < 15 \text{ arcmins}$  the disk component begins to have a significant effect and for  $r > 15$  arcmins the disk component dominates the integrated blue light. Clearly then it is within the annular region between  $r = 10$  arcmins and  $r = 15$  arcmins (major axis) that the change between a dominating bulge component and a dominating disk component takes place for the integrated blue light. Unfortunately it is precisely in this region that the available  $2.2 \mu\text{m}$  data finishes. It would therefore be worthwhile to re-observe M31, concentrating on this area, with the sensitive SBRC InSb detector (flashed and operated at  $63^\circ\text{K}$ ) fitted in the Leicester Version II photometer with wide-angle chopper. This would give us the full benefits of the new sensitive InSb systems while avoiding the difficulties involved with black-body chopping. The expected surface brightness in the region concerned, with conservative extrapolation of the data available, should be  $\sim 18\text{-}19 \text{ m}_K$  per square arcsecond. The observations of NGC 972 (Chapter 5) have shown that with the group's SBRC InSb detector in the Version I photometer it is possible to measure down to surface brightnesses  $\sim 18.5 \text{ m}_K/\text{arcsec}^2$ , at the  $3\sigma$  level, with a 22 arcsec aperture in 20 seconds. Thus, if we use apertures  $\sim 45$  arcsecs again, and integrate for  $t \gtrsim 40$  secs, we can optimistically expect to successfully observe this "blue-light changeover region" to check if a similar phenomenon occurs at  $2.2 \mu\text{m}$ . If this is the case there will probably be an associated change in the mean stellar population which will be reflected in the broad band colours. The relative changes in the B-V, V-K, H-K and J-H indices in this region would then be obviously of great interest.

Following the analysis of the 1976 observations Matsumoto et al. (1977) published a  $2.2 \mu\text{m}$  contour map of the central bulge region of

M31 with 102 arcsec resolution. The map reaches  $\sim 12.5$  arcmins along the major axis and is in agreement with our conclusions that the brightness distribution follows the  $r^{\frac{1}{2}}$  law, and that no significant disk contribution is present. Unfortunately here again a relatively insensitive (PbS) detector was used, and despite the much larger aperture employed the data on which the contour map is based are very limited for  $r \gtrsim 8$  arcmins, and so, in common with the Leicester data, are insensitive to small contributions from the disk component. The map is reproduced in fig. 3.5 in order to bring together in one place all the available data on this topic.

#### b) Colour Gradients in the Bulge

Generally speaking colour gradients could be due to a radial change in either the mean spectral type or in the stellar metal abundance. If a metal abundance variation is the dominant factor, then gradients in the U-B index will show a greater relative change than the redder indices since it is more strongly affected by line blanketing changes produced by the said metal abundance variation. High resolution observations over the central  $\pm 40$  arcsecs of M31 (Sandage et al., 1969) showed no sensible variation in B-V, V-R or V-K but revealed a considerable radial variation in U-B. Presumably therefore this change is due primarily to a corresponding variation in metallicity. Although the B-V and V-R indices show no significant variation over the relatively small nuclear region, variation in these colours has been seen, in M31 and elsewhere, over a much larger area by de Vaucouleurs (1961) and Tifft (1963) who measured colour changes across a selection of E, SO, Sa and Sb galaxies. These changes are more likely to be due to a variation in the mean spectral type since they relate more to the galaxy as a whole (Morgan and Osterbrock, 1969). The Leicester V-K

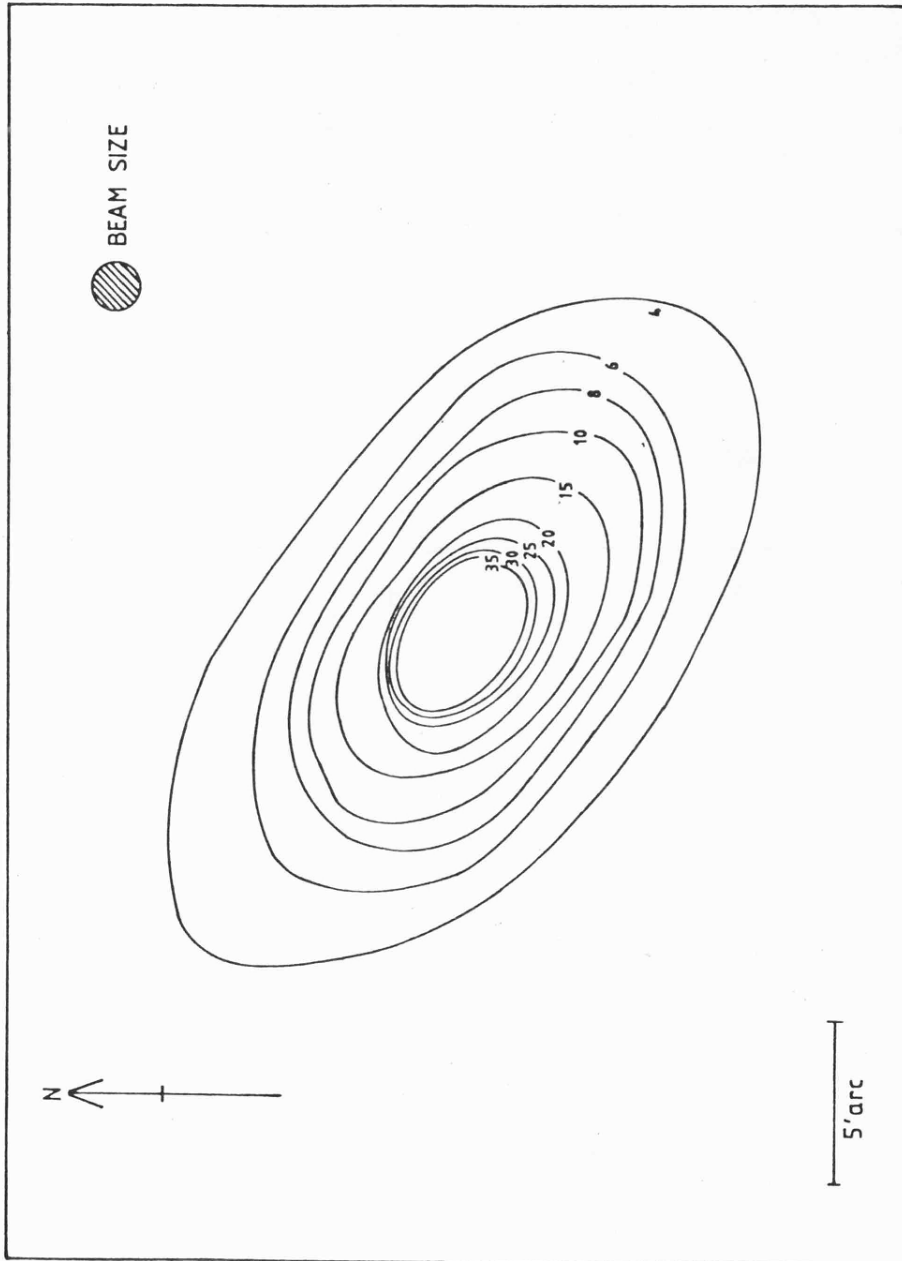


Fig. 3.5 : Matsumoto et al. 2.2  $\mu\text{m}$  Map of M31 bulge region.

observations and the  $\overline{1 \mu m}$ -K observations of Iijima et al. (1976) fall, in terms of scale, approximately midway between the types of observation mentioned above, and have produced conflicting results.

The Leicester data, shown in fig. 3.3 indicate that inward of 5 arcminutes (along an E-W line through the nucleus) there is no evidence of a radial gradient outside the limit:  $|\Delta(V-K)| < 0.1$ . In contrast, Iijima et al. claim there is an approximately linear radial variation in the  $\overline{1 \mu m}$ -K index amounting to  $0.3^m$  at a radius of 5 arcmins along the same E-W line. (At greater radial distances both sets of data become dominated by noise and so no further estimates of colour variation may be made.) It is emphasised that these conflicting results cannot be reconciled as there is no astrophysically plausible stellar model which would produce a radial decrease in the  $\overline{1 \mu m}$ -K colour while at the same time producing the corresponding increase in  $V-\overline{1 \mu m}$  necessary to result in an approximately constant V-K colour. Furthermore, the HKL photometry (Sandage et al. 1969),  $10 \mu m$  photometry (Kleinmann and Low 1970) and more recently the zero result in the  $2.2 \mu m$  polarization measurements of Jameson and Hough (1977), rule out the possible existence of non-stellar sources which might feasibly have accounted for the discrepant results. (Though it is also difficult to imagine any non stellar sources(s) which might explain the results.)

Any real colour variation in this region would have considerable implications in regard to both the ideas on radial distribution of the dominating stellar component and the (related) dynamical structure of the galaxy. For example, Iijima et al. used their data to estimate that the effective radius,  $r_e(\lambda)^*$ , is significantly smaller at  $2.2 \mu m$

---

\*  $r_e(\lambda)$ , is the radius, at  $\lambda$ , within which half the total luminosity of the galaxy is emitted.

( $r_e \sim 7.5$  arcmins) than at  $1 \mu m$  ( $r_e \sim 11$  arcminutes). No similar conclusion can be drawn from our data. Instead, however, we would conclude that although it is probable, given the composite disk-bulge morphology of M31, that the effective radius will decrease with increasing wavelength, the V-K data suggest that the differences in  $r_e$  only become apparent at greater radial distances. Thus, it is important to determine which of the two data sets is correct. This, of course, can only be achieved with any degree of certainty by re-observing. However for the purposes of this discussion we will (a) consider possible sources of systematic error which would invalidate one or other of the data sets, and (b) examine available data of a similar nature to see if it supports either of the observations made.

In their observational procedure Iijima et al. used the sky-chopping technique, and since the chopping-axis was parallel to the scan direction the profiles obtained were of the standard "peak-trough" type common in infrared astronomy. Retrieval of the true (i.e. "single-beam") profile of the galaxy requires deconvolution of the profiles obtained. Even for perfectly "standard" instrumental profiles such as gaussians or top-hats, the process of deconvolution is non-trivial. If the instrumental profile is at all irregular unavoidable errors will be introduced unless the deconvolution technique used is very sophisticated. Furthermore, if the  $1 \mu m$  and  $2.2 \mu m$  instrumental profiles have slightly different shapes additional systematic error may be introduced. In their paper Iijima et al. gloss over the deconvolution process rapidly and so the suspicions of the reader are aroused. Secondly, since their observations did not incorporate simultaneous measurements at the two wavelengths concerned, further systematic error may have been introduced when subtracting the two steeply varying profiles. Clearly neither of these two possible sources

of systematic error could be present in the Leicester data. Since the 1978 V-K observations, unlike the 1976 2.2  $\mu\text{m}$  observations, were not troubled with thermal drifting or telescope tracking problems, they are thought to be free of systematic error. (There was no significant difference between the beam profile at K and that at V in either R.A. or declination directions.)

The only infrared data on M31 which has subsequently become available is the multiaperture photometry of Aaronson (1978), which, for the sake of completeness, is summarised in Table 3.1. Although this data shows no sign of radial colour gradients, and so apparently supports the Leicester data, it relates in fact to a smaller region of the galaxy than that with which we are currently concerned. However Aaronson has also collected similar data for a large number of other normal spiral galaxies, most of which are at much greater distances than M31, and so the multiaperture photometry relates to scales similar to that in M31 with which we are concerned. His data imply that in Sb galaxies radial J-K gradients are much smaller than the  $\overline{1 \mu\text{m}}/\text{K}$  gradient reported by Iijima et al. Furthermore the V-K gradients in Sb galaxies implied by Aaronson's multiaperture data do not conflict with the limit set by the Leicester V-K observations of M31.

The only additional large scale, infrared, surface photometry of external galaxies is that of Strom et al. (1977) who measured the radial variation of the V-K index in the E5 galaxy NGC 2768 and in the SO galaxy NGC 3115. The observations were made along the minor axes of the two systems and reached to relatively much greater radial distances than the observation of M31 made by ourselves and by Iijima et al. The observed colour difference between the nucleus and the outer regions of the galaxy was  $\Delta(V-K) \sim -0.4 \pm 0.15$ . The radial distances involved were  $r/r(a) \sim 0.6 - 0.9$  (where  $r(a) \equiv D(\rho)/2$ ) compared to  $r/r(a) \sim 0.06$

Table 1.1: Aaronson's Photometry of M31 etc.

Aperture (arcsecs)	A/D(0)	$M_K$ ( $\pm 0.01$ )	V-K	J-M ( $\pm 0.03$ )	H-K ( $\pm 0.02$ )	J-K ( $\pm 0.05$ )
13.7	0.002	6.95	$3.42 \pm 0.2$	0.78	0.24	1.02
27.4	0.004	5.81	$3.44 \pm 0.1$	0.76	0.23	0.99
47.5	0.006	4.83	$3.55 \pm 0.2$	0.79	0.23	1.02
53.3	0.0063	4.71	$3.46 \pm 0.1$	0.77	0.22	0.99
107.1	0.013	3.72	$3.37 \pm 0.1$	0.78	0.22	1.00

Abolins and Adams (1978), 45" aperture:

$$M_K = 4.92 \pm 0.04 \text{ (mean of peak in 4 scans)}$$

$$M_V = 8.48 \pm 0.03 \quad " \quad " \quad " \quad " \quad "$$

$$V-K = 3.48 \pm 0.07$$

Sandage et al. (1969), 5" aperture:

$$M_K = 8.57 \pm 0.12$$

$$M_H = 8.88 \pm 0.15$$

$$M_V = 12.03$$

$$V-K = 3.46 \pm 0.12$$

for the radial distance corresponding to the Iijima et al. figure of

$$\Delta(\overline{1 \mu m} - \overline{K}) = 0.3.$$

### 3.5 Conclusions

Independent observations (Leicester, Tokyo-Nagoya) of the spheroidal bulge of M31 have shown that the  $2.2 \mu m$  brightness distribution for  $r \lesssim 10$  arcmins (major axis) does follow the de Vaucouleurs  $r^{-1/4}$  law. This implies that the dynamical forces which govern the gross distribution of the dominant population at visible wavelengths are also responsible for the gross distribution of the dominant  $2.2 \mu m$  population, a result which could not be assumed a priori. Conflicting results have however been obtained for infrared colour gradients within the bulge: the observations of Iijima et al. (1976) indicate a steep  $\overline{1 \mu m} - \overline{K}$  colour gradient within the spheroidal bulge of M31 whereas the multiaperture photometry of spiral galaxies generally (Aaronson 1978) suggests that any gradient in the purely infrared colours of these galaxies is negligible. The simultaneous V and K observations made by the Leicester group place an upper limit  $\sim 0.1$  on the radial change in V-K at the radial distance Iijima et al. claim a change  $\Delta(\overline{1 \mu m} - \overline{K}) \sim 0.3$ . The Leicester result is in better agreement with the available comparable data of others, but since these are not directly equivalent and as multiaperture data are not ideally suited to the measurement of colour gradients, re-observation is necessary to confirm the Leicester result.

## REFERENCES

- Aaronson, M. 1978, Ph.D. Thesis, Harvard University.
- Baldwin, J.R., Danziger, I.J., Frogel, J.A. and Persson, S.E. 1973,  
Ast. L., 14, 1.
- Faber, S.M. 1972, Astron. and Ap., 20, 361.
- Iijima, T., Ito, K., Matsumoto, T. and Uyama, K. 1976, P.A.S.J., 28, 27.
- Jameson, R.F. and Hough, J. 1977, M.N., 182, 179.
- Johnson, H.L. 1966, Ap. J., 143, 187.
- Kleinmann, D.E. and Low, F.J. 1970, Ap. J., 159, L165.
- Matsumoto, T., Murakami, H. and Hamajima, M. 1977, P.A.S.J., 29, 583.
- Morgan, W.W. and Osterbrock, D.E. 1969, A.J., 74, 515.
- Sandage, A.R., Becklin, E.E. and Neugebauer, G. 1969, Ap. J., 157, 55.
- Spinrad, H., Taylor, B.J. 1971, Ap. J. Suppl. S., 22, 445.
- Strom, K.M., Strom, S.E. and Wells, D.C. 1978, Ap. J., 220, 62.
- Tift, W.G. 1963, A.J., 68, 302.
- Vaucouleurs, G. de. 1958, Ap. J., 128, 465.
- Vaucouleurs, G. de. 1961, Ap. J. Suppl. S., 5, 233.

# 4

Mapping of the Core and Inner Disk of M82 at  $2.2\ \mu\text{m}$

#### 4.1 M82 - AN OVERVIEW

M82 (NGC 3034, 3C 231, Arp 337) is the archetypal class II irregular or IO galaxy (Holmberg 1958, Sandage 1961, de Vaucouleurs 1964), lying 3.2 Mpc distant (Tammann and Sandage 1968) in the small M81 group of galaxies. Its chaotic, dust curdled main image has chameleon like qualities, its appearance changing with wavelength and plate exposure time. Fig. 4.1 shows the Hubble Atlas prints which illustrate this well (Sandage 1961). The shortest exposure shows a bright central area, of dimensions  $130'' \times 35''$ , split by a dense dust lane. This region is surrounded by another of similar shape, but much fainter and measuring  $4.6' \times 0.9'$ . The latter region is seen better in the middle plate. The longest exposure shows that the (now greatly overexposed) main body is surrounded by a much fainter halo region measuring  $\sim 7' \times 2.2'$ . By combining several photographic plates, Sandage and Miller (1964) found that the full extent of the faint outer structure, which appears to be composed of a maze of filaments, is approximately  $13.4' \times 8.5'$ .

Apart from its unusual appearance, M82 is an average galaxy in terms of size and mass (Mayall 1960, Sandage 1961), and is dwarfed by giant galaxies such as M31. Although the properties described above marked it as a curious object it was not until the early sixties that it "hit the headlines". At about the time that quasars and high energy phenomena were coming very much into vogue Lynds (1961) identified M82 as the optical counterpart of 3C 231, Elvius (1962) discovered highly polarized blue light (quasar-like) in the outer structure of the galaxy and Lynds and Sandage (1963) found evidence for gas velocities in M82 of order  $10^3 \text{ km s}^{-1}$  and a total energy of  $10^{56}$  ergs. These three pieces of observational data were taken by many as the evidence which proved that M82 had suffered a recent ( $\sim 1-2 \times 10^6$  years ago)

Fig. 4.1 (overleaf) :

The Hubble Atlas print of M82.



explosion in its nucleus.  $H\alpha$  filter photographs presented in Lynds and Sandage, 1963, and Sandage and Miller, 1964, revealed a highly explosive looking M82 and probably provided the single most persuasive argument for the widespread acceptance of the explosion hypothesis. In these articles the blue polarized light was interpreted as synchrotron radiation produced by an explosion debris of relativistic electrons gyrating in the explosion-expanded magnetic field of the galaxy. It was the synchrotron radiation which was seen as the energy source exciting the  $H\alpha$  emission. Mayall (1960) had found that the rotation curve of the underlying galaxy was quite normal; this was the only real doubt hanging over the explosion model. Wouldn't the explosion affect internal motions in some measurable way? After a more thorough and accurate investigation of the system dynamics, Burbidge et al. confirmed Mayall's discovery as a first order result but showed also that there was a core of high velocity gas expanding in a direction perpendicular to the plane of the galaxy. This obviously supported the explosion theory and tied in nicely with the  $H\alpha$  appearance of M82.

Solinger (1969) suggested that the explosion was possibly related to hidden Seyfert activity. There followed several photographic-infrared searches for a hidden point-like nucleus (Bertola et al. 1969, Raff 1969, van den Bergh 1969). No evidence supporting Solinger's hypothesis was found, indeed van den Bergh's red-end spectrum (5800 $\overset{\circ}{\text{A}}$  - 6600 $\overset{\circ}{\text{A}}$ ) showed that emission lines in this waveband, notably  $H\alpha$  and  $\overline{[NII]}$ , were quite definitely narrow and unlike their very broad Seyfert counterparts. The final nail was driven into the Seyfert coffin by Kleinmann and Low (1970b) who showed that M82, unlike the Seyferts, has extended 10  $\mu\text{m}$  emission.

Although the photographic infrared search failed to reveal any Seyfert activity it focussed attention upon a previously overlooked feature of M82, namely the nuclear bright spots. These had previously

been considered merely as regions where the dust obscuration thinned out a little, but van den Bergh (1972) pointed out that the contrast between the bright spots and the galaxy main body increases with increasing wavelength, contrary to the expected behaviour if the bright spots were in fact simply regions which were less heavily veiled by the obscuring matter. The spectroscopic data of Peimbert and Spinrad (1970), Recillas-Cruz and Peimbert (1970), O'Connell (1970) and van den Bergh (1972) proved that there was an unusually large population of hot, young, blue stars in the hot spot region, which van den Bergh interpreted as the product of a very recent burst of star formation, triggered by a shock front or density wave initiated by the famous explosion, and probably currently continuing. Thus the bright spots were interpreted as dense clusters of such stars. The intensity of the star formation can be appreciated from the results of Recillas-Cruz and Peimbert (1970) who showed that two giant HII regions, dubbed M82I and M82II, were each about twenty times more luminous than W49A, one of the brightest Galactic HII regions. It was estimated that  $\sim 8 \times 10^3$  stars were necessary to maintain the emission line flux in these HII regions, whereas Roberts (1957) suggests there are only about  $6 \times 10^3$  of these stars in our entire Galaxy. These HII regions are closely related to van den Bergh's (1972) "superclusters" which he believes are a hundred times brighter than the brightest Galactic clusters.

The region most densely populated with hot spots is just to the west of the very dense, galaxy splitting dust lane, close to the geometrical centre of the galaxy; this corresponds closely both in position and size to the extended radio region (McDonald et al., 1968). To study the region more carefully, particularly with a view to identifying radio counterparts of the optical and photographic infrared

hot spots, Kronberg et al. (1972) mapped the region at 8085 Mhz with 2" resolution and compared the results with photographic plates with 1" resolution. No correspondence between the discrete radio sources and the optical bright spots was found. This interesting result implied that the radio sources were almost certainly situated deeper in the galaxy, behind more of the obscuring dust.

The star formation was believed by some to be triggered by the explosion, Peimbert and Spinrad (1970) on the other hand had shown that in the central region of the galaxy the synchrotron radiation of the explosion model failed, by at least two orders of magnitude, to explain the observed  $H\alpha$  excitation. This however could be explained by the young, hot stars. The synchrotron contribution to the visible continuum was also shown to be negligible. Now the observations and discussion by Sandage and Co. of explosion-generated synchrotron radiation applied essentially to the outer filaments. Nevertheless, the results of Peimbert and Spinrad cast a shadow over the explosion hypothesis. Sandage and Visvanathan (1972) returned to continue the polarization studies of a decade earlier. New techniques enabled them to measure the polarization of the  $H\alpha$  emission line as well as the continuum. Both the line and continuum polarization were mapped over the outer filamentary structure. The result that the observed polarization is exactly the same, in both degree and direction, for the line and continuum emission destroyed the original explosion model, since there is no way that polarized  $H\alpha$  can be produced in the filaments. The only explanation (Morrison 1979) is that the  $H\alpha$  originates elsewhere - probably in nuclear HII regions - and is scattered by the dust particles in the outer reaches of the galaxy. Thus the scattering process is now seen as the mechanism which introduces polarization in both the line and continuum emission.

Very recently two excellent papers (Solinger, Morrison and Markert 1977 and O'Connell and Mangano 1978) have suggested that the unusual appearance of M82, previously thought to be due to the explosion, can be explained by an interaction between M82 and the M81 group of galaxies. M82, now within the group confines, is seen as an average late type galaxy of the field which, sometime less than 1 Gyr ago, encountered the M81 group. The exact mechanism of the interaction is under debate; Solinger et al. prefer an interaction with a cloud of intergalactic matter (HI and very thin dust) which envelopes the group, while O'Connell and Mangano suggest a tidal encounter with either M81 itself or some invisible dwarf system in the group. Both mechanisms, the authors claim, result in a similar outcome: the unusual appearance of M82, including the chaotic dust distribution and faint outer structure, the termination of peripheral star formation (O'Connell 1970) and the triggering of recent, possibly current, star formation in the central region.

The interaction theories are very convincing and for a while it seemed as though the explosion model was finally dead and buried, but quite recently Axon and Taylor (1978) obtained spectroscopic evidence which they claim forces them to resurrect the explosion ideas. Axon and Taylor describe hollow elliptical emission lines seen previously only in such known explosive objects as the Crab nebula. Morrison (1979) maintains however that "(this line structure) ... is within the competence of the (dust reflection) model". Axon and Taylor refute this (private communication Axon, 1979). The explosion versus interaction debate is probably by no means over, and it is possible that both are involved in the peculiar morphology and properties of M82. Most of the rest of this chapter is not directly concerned with differentiating between the two models, nor with the

faint outer structure, but describes the initial reasons for undertaking a two micron mapping project, and how the results have provided a picture of the inner region of the disc and nucleus which are hidden by dense dust from optical observers. The two micron picture must be included in any model of M82; the O'Connell and Mangano model does seem to explain the observed  $2.2 \mu\text{m}$  emission (see sections 4.7e to 4.7g).

#### 4.2 THE INFRARED EMISSION OF M82

The well known near infrared excess in the nucleus of M82 was discovered by Kleinmann and Low (1970a) in their  $1-20 \mu\text{m}$  "first look" at active and peculiar galaxies. JKL photometry of a region  $50''$  NE of the nucleus showed that no similar colour excess existed in this part of the galaxy. Although the nuclear near infrared excess is strong its significance was overshadowed at the time by the  $5-20 \mu\text{m}$  excess which put the bolometric luminosity of M82 on a par with the Seyferts. Shortly after this initial report an isophotal map of an extended region of  $10 \mu\text{m}$  emission appeared in the literature (Kleinmann and Low, 1970b); a crude  $2.2 \mu\text{m}$  centroid position was the only near infrared spatial information given. M82 has been measured out to  $345 \mu\text{m}$  (Low and Aumann 1970, Joyce et al. 1972, Harper and Low 1973, Kleinmann et al. 1976); the data of Harper and Low suggest a turn-off between  $65 \mu\text{m}$  and  $100 \mu\text{m}$  but Joyce et al.'s  $345 \mu\text{m}$  photometry indicate a continued rise out to that wavelength. However if the  $345 \mu\text{m}$  flux is believed the intervening spectrum required to meet the observed short wavelength radio data must be considerably steeper than the Rayleigh-Jeans tail of a black body peaking at  $345 \mu\text{m}$ . Re-radiation from a dust cloud with a temperature gradient seems to account for the far infrared emission. Despite the continued interest in far infrared photometry, or perhaps

because of it, no further near infrared photometry has been published.

8-13  $\mu\text{m}$  CVF spectrometry centred on the peak of the 10  $\mu\text{m}$  source reveals a spectrum very similar to those of the planetary nebulae (Gillett et al. 1975). As planetary nebulae are generally accepted to be thermal in nature, the source(s) in M82 of the emission in this spectral region is (are) probably likewise so. The spectrum is dominated by a deep silicate absorption feature, indicating that this substance must be an important constituent of the dust in M82. More recent 2-8  $\mu\text{m}$  CVF work centred on the same region (Willner et al. 1978) has again shown strong similarities to planetary nebulae. Furthermore, Br  $\alpha$  and possibly Br  $\gamma$  have been observed indicating the presence of HII regions excited by hot, young stars, but the CO absorption overtone is taken by the authors as evidence which suggests that K and M giants dominate the near infrared emission.

#### 4.3 OPTICAL, INFRARED AND RADIO BRIGHT FEATURES

Fig. 4.2 represents schematically the bright central region of M82, and includes all the prominent optical, infrared and radio features from the literature. The positions of the optical bright spots are the centroids given by Kronberg et al. (1972), as are the discrete radio sources. The outline of the diffuse radio emission is from Hargrave (1974) and represents the approximate FWHM shape of the source. The 10  $\mu\text{m}$  centroid is the position given by Kleinmann et al. (1976) which corrects the position of Kleinmann and Low (1970b). The error bar on this position is an estimate of the likely lower limit on their error bar size. The authors do not quote errors, indeed the position is determined solely from their statement: "the peak position so determined is  $\sim 10''$  SW of the centroid (previously given)". The vague manner in which they present the new centroid position defends

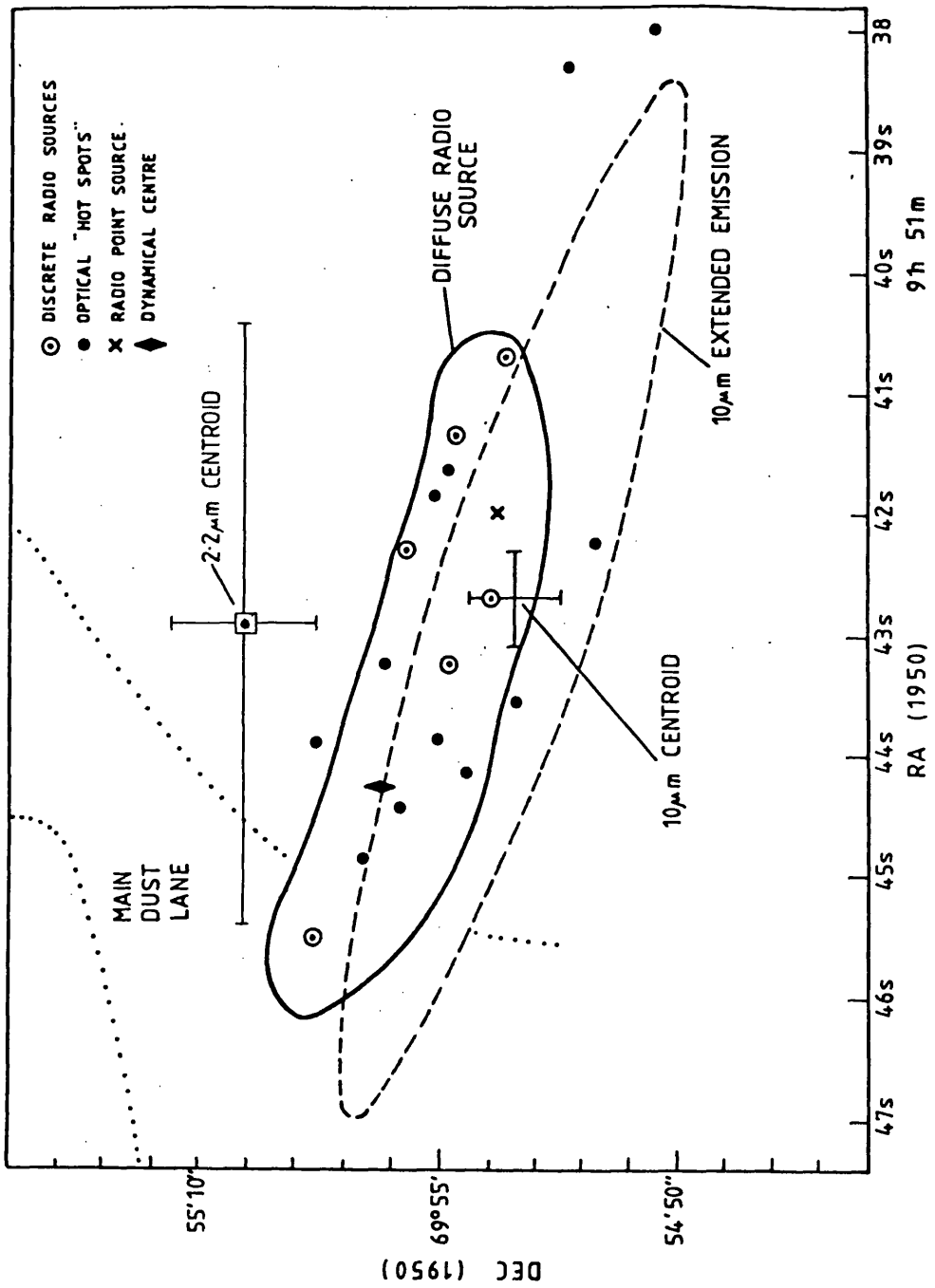


Fig. 4.2 : The centre of M82 (1) - with the old 2.2  $\mu\text{m}$  centroid.

the estimate of error bar size. The size, shape and orientation of the  $10\ \mu\text{m}$  extended source shown in the diagram depicts the FWHM description given by Kleinmann et al. The  $2.2\ \mu\text{m}$  centroid is that given in Kleinmann and Low (1970b). No corrected, nor better, estimate has appeared in the literature. It cannot be assumed that the  $2.2\ \mu\text{m}$  and  $10\ \mu\text{m}$  centroids are coincident. Finally, the dynamical centre is that deduced from the rotation curve by Burbidge et al. (1964).

The position and extent of the diffuse radio emission corresponds closely with the region defined by the optical/photographic infrared bright spots believed to be bright young clusters. Yet, as Kronberg et al. (1972) have emphasised, there is no apparent correspondence between the discrete radio source centroids and the bright cluster centroids, from which it would seem that any optical counterparts to the radio hot spots must be hidden behind a dense dust cloud which in turn lies behind the bright visible clusters. The  $10\ \mu\text{m}$  region as defined by Kleinmann et al. is not exactly concentric with the diffuse radio emission, although the uncertainty in the  $10\ \mu\text{m}$  centroid cannot definitely preclude the possibility that they are so. The  $10\ \mu\text{m}$  centroid is clearly not coincident with any of the bright cluster centroids; this is further circumstantial support for the idea that the latter are foreground objects. The possible coincidence of the  $10\ \mu\text{m}$  centroid and the famous radio "point" source (Hargrave 1974, Kronberg and Wilkinson 1975) is often considered; the new  $10\ \mu\text{m}$  position suggests that the two are not coincident. As the  $10\ \mu\text{m}$  emission is believed to be thermal in nature, and the "point" source is almost certainly non-thermal (Geldzahler et al. 1977, Kronberg and Clarke, 1978) there is little reason for their coincidence to be expected. In fact source B of Hargrave (1974), source no. 5 of Kronberg et al. (1972) is the radio feature in closest proximity to the revised  $10\ \mu\text{m}$  centroid. Any

connection between the two is yet to be discussed in the  $10 \mu\text{m}$  or radio literature.

The major dust lane (outlined in the diagram) seems to be more or less transparent to  $10 \mu\text{m}$  radiation and radio waves yet the visible emission is totally obscured (see photographs). Note especially the asymmetry of the bright spot distribution about the dynamical centre. Although it is feasible that the degree of asymmetry may be exaggerated by a (possibly) erroneous position for the dynamical centre, the close proximity of the dark lane furnishes a more likely explanation for the lack of hot spots to the east of the dynamical centre. Thus, although the nuclear region of the galaxy is seen at  $10 \mu\text{m}$  and longer wavelengths, it is definitely not seen in the visible (or photographic infrared) along the line of sight crossed by the major dust lane, and the circumstantial evidence given above strongly suggests that this is also the case everywhere in the central area. Only bright foreground sources are seen.

#### 4.4 TWO MICRON MAPPING

Given only the data summarised in fig. 4.2, the underlying stellar content of M82 can only be guessed at. The only way to study these underlying stars is by observation at wavelengths,  $\lambda \sim 2 \mu\text{m}$  since the central  $10 \mu\text{m}$  and radio emission come primarily from dust and gas/plasma respectively, not from stars. At near infrared wavelengths however stars are likely to be the main source, and furthermore the expected obscuration is less than a tenth of that in the visible. Hot dust is another possible source at two microns, but to remain hot it must be very close to the stars heating it, and so will not introduce errors into any suggested stellar distribution described by the two micron emission.

The heavy obscuration hiding the nucleus of M82 is estimated to produce extinction,  $A_V \sim 14$  (Gillett et al. 1975). This is much less than the obscuration between the Sun and the Galactic centre,  $A_V \sim 25$ , yet we have no trouble seeing the Galactic centre at  $2.2 \mu\text{m}$ . Consequently, even if the extinction in M82 is comparable, we can confidently expect to see into the heart of the galaxy at  $2.2 \mu\text{m}$ .

It is important to accurately determine the position of the  $2.2 \mu\text{m}$  centroid, since its location relative to the other prominent nuclear features is of obvious astrophysical significance. The position of the  $2.2 \mu\text{m}$  centroid given by Kleinmann and Low (1970b) is almost certainly incorrect, even within the bounds of its error rectangle. (Their  $10 \mu\text{m}$  centroid (1970b) had error bars of  $\pm 3''$ , yet the revised (1976) position is displaced by  $10''$ .) A priori, it is likely that the true  $2.2 \mu\text{m}$  centroid marks the stellar density maximum (i.e. nucleus) of the underlying galaxy, however if the positions of the other prominent nuclear features are accurate then the old  $2.2 \mu\text{m}$  centroid is inconsistent with the idea for two reasons: firstly the nucleus would be coincident with the dynamical centre of the galaxy, the old centroid is not. Secondly the  $10 \mu\text{m}$  centroid and radio point source are likely, by analogy with other galaxies, to be situated close to the nucleus. Since we are looking into the plane of the galaxy, the true separation of these sources from the old  $2.2 \mu\text{m}$  centroid, necessary to account for the apparent separation in fig. 4.2 is so large that they would be near the outskirts of the galaxy if the old  $2.2 \mu\text{m}$  centroid is considered to be the nucleus. These anomalies highlight the need for accurate determination of the position of this important feature.

The discussion above gives the scientific case for mapping M82 at  $2.2 \mu\text{m}$ . We intended to follow the  $2.2 \mu\text{m}$  work with the same at  $1.6 \mu\text{m}$  and  $1.2 \mu\text{m}$  to study the spatial distribution of dust obscuration. Poor weather prevented this.

#### 4.5 OBSERVATIONS

The observations were obtained in July/August 1977 and March 1978 using the Hatfield infrared polarimeter (Cox et al., 1978) at the Cassegrain focus of the 2.5 metre Isaac Newton Telescope. The instrument was operated in photometric mode and the detector was an indium antimonide photodiode operated at 63°K. The use of the polarimeter as a photometer, the reasons for doing so and all practical details, pros and cons etc., have been discussed in Chapter 2. Essentially the technique is exactly similar to using a conventional photometer providing the polarization of the observed source is negligible. This was shown to be the case with M82. Throughout the observations the beam was located on the galaxy by offsetting along a R.A. and declination grid using the AGK star BD 70587 as the origin, and calibration was with respect to the Johnson standard 24 U Maj with cross checks on 22 and 27 U Maj.

Following standard practice in the mapping of extended objects the galaxy was first scanned with the largest available aperture size (23") to determine the overall spatial configuration and the brightness distribution at 2.2  $\mu\text{m}$ . In total eight declination scans were made with this beam size, five in adjacent R.A. channels, approx. one beam width apart, and a further three through the R.A. channel thought to include the brightest region of the galaxy. Two R.A. scans were made along the corresponding declination channel. In all the scans with the 23" aperture, the scan path extended well beyond the optical extremities of the galaxy, and even beyond the outer filamentary structure. By comparing chart recordings of the galaxy profiles with those of a star scanned in exactly the same manner, a first impression was gained of the spatial distribution of the 2.2  $\mu\text{m}$  emission. This was of an extended region, probably aligned with the optical image of the

galaxy, containing a very bright region narrower than the beam size in declination but extending into the two central R.A. channels.

A decision was taken to concentrate upon the bright region discovered. A change to a beam size of  $11''$  was therefore made and with the smaller aperture, and a slower scanning rate, the bright region was covered once in R.A. and once in declination. It was immediately apparent that the region was still small compared to the beam size in the declination direction and not much bigger in R.A. Determination of the surface brightness distribution within an area of this size required the smallest aperture available at the time; this corresponded to a half power width of  $6''$  on the sky. The ideal mapping procedure described in Chapter 2 was to be adopted. However with so small an aperture the poor signal to noise achieved, aggravated by high sky noise, severely reduced the effective time available. This problem coupled with the (usual) bad Sussex weather meant that by the end of the August 1977 observing stint only four good declination profiles in adjacent R.A. channels had been secured. These four channels spanned the whole bright region but were separated by approximately two beam widths from each other, and so we were well short of the half beam width separation necessary for the best contour map.

During the March 1978 observing allocation our aim was to complete the  $2.2 \mu\text{m}$  high resolution, interlaced declination scans, confirm these with R.A. scans and, if possible, scan the bright region at  $1.2 \mu\text{m}$  and  $1.6 \mu\text{m}$ . The declination scans were essentially completed, but again poor weather (one whole and two quarter nights out of seven) prevented most of the additional work from being achieved. Nevertheless some other useful observations were made. The first JHK small aperture photometry centred on the newly determined two micron centroid was completed, and the  $2.2 \mu\text{m}$  polarization at this spot was measured. The

very low degree of polarization confirmed the reliability of the technique used. Three high resolution  $2.2 \mu\text{m}$  R.A. scans through the bright region were also completed. Unfortunately the data obtained on two of the three scans is of limited value due to the long time lapse before calibration and uncertainty in the location of the declination channel in which they were made. The latter problem was discovered at a later date when inconsistencies between the offset guider readings and the INT console readings were noticed in the work log notes. Fortunately one scan was calibrated immediately after its completion and the offset guider readings corresponded exactly with the offset position given by the main console. The R.A. scans were carried out on the last night of the allocation, and although the calibration problem was then appreciated there was no time left to repeat the scans and recalibrate. Full details of the observing procedure and an exact description of the scans made are presented in Table 4.1. This is in effect a copy of the observing log and is reproduced to provide one example of such in the thesis.

#### 4.6 RESULTS

The complete set of processed data is presented in tables 4.2a,b and 4.3, and in the isophotal contour maps in figs. 4.3 and 4.4. Tables 4.2a and 4.2b give the peak values found in each profile, i.e. centroid position and K magnitude, flux and surface brightness, and the contour maps illustrate the spatial information obtained. Table 4.3 gives an "at a glance" synopsis of all the data acquired, including colours, source polarization, source dimensions and integrated magnitudes.

Table 4.2a summarises the results for the declination scans and 4.2b for the R.A. scans; in the latter only the data from the 6"

Table 4.1a: 1977 MB2 Observations

SCAN DESCRIPTION

Date	No.	Aperture Diameter	Direction	Start	Finish	Other Offsets	Rate	Calibrations etc.
30/31 July	-	23"	-	-	-	-	-	Polarization Check on MB2. $\alpha = 9^{\text{h}} 51^{\text{m}} 41.3^{\text{s}}$ ; $\delta = 69^{\circ} 55' 04''$ Calibrate against 24 U Maj.
"	1	23"	Dec	+480"	-240"	+15s RA	1"/sec	
"	2	23"	Dec	-240"	+480"	+15s RA	1"/sec	
"	3	23"	Dec	+480"	-240"	+15s RA	1"/sec	Calibrate against 24 U Maj.
"	4	23"	RA	-60s	+120s	+120" Dec	0.33s/sec	
"	5	23"	RA	+120s	-60s	+120" Dec	0.33s/sec	Calibration scan of 24 U Maj. Calibrate against 22, 24 and 27 U Maj.
"	6	23"	Dec	+480"	-240"	+19s RA	2"/sec	
"	7	23"	Dec	+480"	-240"	+11s RA	2"/sec	
"	8	23"	Dec	+480"	-240"	+23s RA	2"/sec	
"	9	23"	Dec	+480"	-240"	+7s RA	2"/sec	Calibration scans (2) of 24 U Maj. Recheck polarization as above.
31/1 Aug	10	23"	Dec	-60"	+300"	+15s RA	0.5"/sec	Calibration against 22, 24 and 27 U Maj.
"	11	23"	Dec	+300"	-60"	+15s RA	0.5"/sec	
"	12	11"	Dec	+260"	-30"	+16s HA	0.2"/sec	
"	13	11"	RA	-25s	+30s	+120" Dec	0.3s/sec	RA and Dec calibration scans of 24 U Maj.
1/2 Aug	14	6"	Dec	+160"	+90"	+17s RA	0.1"/sec	Calibration scans (2) of 24 U Maj.
"	15	6"	Dec	+140"	+20"	+13s RA	0.1"/sec	Calibrate against 24 U Maj.
2/3 Aug	-	-	-	-	-	-	-	Cloud all night.
3/4 Aug	16	6"	Dec	+140"	+80"	+19s RA	0.1"/sec	Calibrate against 24 U Maj.
"	17	6"	Dec	+160"	+90"	+17s RA	0.1"/sec	
"	18	6"	Dec	+140"	+85"	+17s RA	0.1"/sec	Calibrate against 24 U Maj.
"	19	6"	Dec	+140"	+90"	+19s RA	0.1"/sec	
"	20	6"	Dec	+140"	+85"	+15s RA	0.1"/sec	Calibrate against 24 U Maj.
"	21	6"	Dec	+140"	+85"	+13s RA	0.1"/sec	Calibrate against 24 U Maj.
"	22	6"	Dec	+140"	+90"	+17s RA	0.1"/sec	Calibrate against 24 U Maj.

\* All positions are relative to BD +70 587;  $\alpha = 9^{\text{h}} 51^{\text{m}} 26.3^{\text{s}}$ ,  $\delta = 69^{\circ} 53' 9''$  (1950).

Table 4.1b: 1978 M82 Observations

SCAN DESCRIPTION										
Date	No.	Aperture Diameter	Direction	Start	Finish	Other Offsets	Rate	Calibrations etc.		
23/24 March	-	6"	-	-	-	-	0.1"/sec	4 calibration scans of 24 U Maj.		
"	1	6"	Dec	+90"	+140"	+16.5s RA	0.1"/sec	Calibration scan of 24 U Maj.		
"	2	6"	Dec	+80"	+140"	+16.5s RA	0.1"/sec	"		
"	3	6"	Dec	+80"	+140"	+17.5s RA	0.1"/sec	"		
"	4	6"	Dec	+80"	+140"	+17.5s RA	0.1"/sec	"		
"	5	6"	Dec	+80"	+140"	+15.5s RA	0.1"/sec	"		
"	6	6"	Dec	+80"	+140"	+15.5s RA	0.1"/sec	"		
"	7	6"	Dec	+80"	+140"	+18.5s RA	0.1"/sec	"		
"	8	6"	Dec	+80"	+140"	+18.5s RA	0.1"/sec	"		
24/25	-	-	-	-	-	-	-	Bad weather all night		
25/26	-	6"	-	-	-	-	-	J,H,K Spot photometry on 2.2 $\mu$ m Centroid, 24 U Maj. J,H,K Calibration 2.2 $\mu$ m Polarimetry on Centroid.		
26/27	-	-	-	-	-	-	-	Bad weather all night.		
27/28	-	-	-	-	-	-	-	Bad weather all night.		
28/29	-	-	-	-	-	-	-	Bad weather all night.		
29/30	9	6"	RA	+6s	+24s	+110" ?	0.03s/sec	Calibration scan of 24 U Maj. 2.2 $\mu$ m Polarimetry on Centroid.		
"	10	6"	RA	+6s	+24s	+110" ?	0.03s/sec			
"	11	6"	RA	+6s	+24s	+112.5"	0.03s/sec			

\* All positions are relative to BD +70 567;  $\alpha = 0^h 51^m 26.3s$ ,  $\delta = 69^{\circ} 53' 9''$  (1950).

Table 4.2a. Declination Scans

R.A. Channel ( $\alpha = 9h 51m$ )	Dec. Limits ( $\delta = 69^\circ$ )	Number of Scans	Beam Size (Arcsecs)	Centroid ( $69^\circ$ )	Peak Flux ( $\times 10^{-29}$ $Wm^{-2}Hz^{-1}$ )	Peak K Magnitude	Mean Surface Brightness $m_K/arcsec^2$
33.3 s	50'9";61'9"	1	23	-	$\approx 76$	$\approx 9.8$	$\approx 16.35$
37.3 s	50'9";61'9"	1	23	54'56"±10"	524±48	7.7±0.1	14.25
41.3 s	50'9";61'9"	4	23	55'02"±10"	1582±140	6.5±0.1	13.05
45.3 s	50'9";61'9"	1	23	55'06"±10"	998±90	7.0±0.1	13.55
49.3 s	50'9";61'9"	1	23	55'12"±10"	379±35	8.05±0.1	14.6
41.3 s	52'39";57'29"	1	11	55'04"±7"	830±70	7.2±0.1	12.15
39.3 s	54'29";55'29"	2	6	-	$\approx 76$	$\approx 9.8$	$\approx 13.45$
41.3 s	54'29";55'29"	2	6	54'59"±6"	239±35	8.35±0.1	12.0
41.8 s	54'29";55'29"	2	6	55'00"±2"	346±35	8.15±0.1	11.8
42.8 s	54'29";55'29"	2	6	55'01"±2"	379±35	8.05±0.1	11.7
43.3 s	54'29";56'19"	4	6	55'00"±6"	456±45	7.85±.05	11.5
43.8 s	54'29";55'29"	2	6	55'01"±2"	478±45	7.8±0.1	11.45
44.8 s	54'29";55'29"	2	6	55'03.5"±2"	301±35	8.3±0.1	11.75
45.3 s	54'29";55'29"	1	6	55'01"±6"	173±30	8.9±0.2	12.65

Table 4.2b. R.A. Scans

Dec Channel ( $\delta = 69^\circ$ )	R.A. Limits ( $\alpha = 9h$ )	Number of Scans	Beam Size (Arcsecs)	Centroid ( $\alpha = 9h51m$ )	Peak Flux ( $\times 10^{-29}$ $Wm^{-2}Hz^{-1}$ )	Peak K Magnitude	Mean Surface Brightness $m_K/arcsec^2$
$55^{\circ}09'' \pm 10''$	$50m26.3s;$ $53m26.3s$	2	23	$43.5s \pm 2s$	$1902 \pm 170$	$6.3 \pm 0.1$	12.85
$55^{\circ}09'' \pm 7''$	$51m01.3s;$ $52m31.3s$	1	11	$43.8s \pm 1s$	$793 \pm 60$	$7.25 \pm 0.1$	12.2
$55^{\circ}01.5'' \pm 2''$	$51m32.3;$ $52m50.3s$	1	6	$44.0s \pm .4s$	$478 \pm 45$	$7.8 \pm 0.1$	11.45

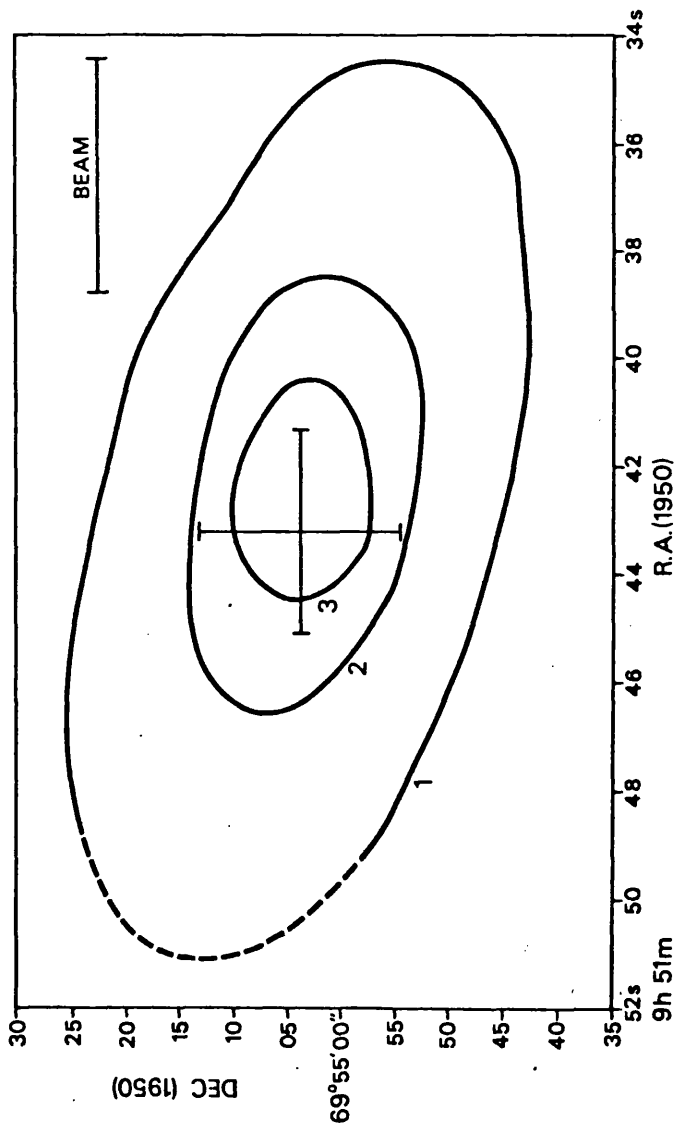
aperture scan for which there exists both adequate calibration and positional certainty is recorded. Whenever a given channel was scanned more than once with the same aperture the values quoted are the means of the parameter concerned. The lengths of repeated scans were not always the same (see Table 4.1), the path lengths given correspond to the outermost limits of the longest scan. Errors quoted on the positions of the profile centroids depend upon the aperture size in use and the precautionary measures prevailing at the time. Briefly, in the August 1977 data the errors correspond to  $\pm \frac{1}{\sqrt{a}}$  quarter of the beam width + backlash error $\sqrt{\quad}$  and in the March 1978 data, when our guidance and backlash avoidance precautions were far more stringent, the errors correspond to the tracking capability of the INT, which is  $\lesssim 2''$ . There is no backlash on the R.A. drive and consequently R.A. channel acquisition was good to within  $\sim 2''$  and possibly better. Errors quoted in the magnitudes and fluxes are those due to statistical uncertainty only. This was rather large since a) the polarimeter technique reduces effective detector sensitivity, b) sky noise was always high compared to better (mountaintop) sites and c) sky brightness and/or transparency changed from hour to hour and extra uncertainty was introduced if the calibration was more than  $\sim 15$ -20 minutes before or after the galaxy observation. During the August 1977 work, calibration took place, on average, after every two or three scans. In March 1978 calibration took place after every scan (except for the R.A. scans). As calibration was so frequent, systematic error due to a difference in intervening air mass was negligible, but in any case the usual extinction-curve correction procedure is invalid under such variable atmospheric conditions so calibration must be as often as possible. The galactic latitude of M82 is  $b^{\text{II}} = 40.6^\circ$ ; this far from the galactic plane interstellar extinction is  $\sim 0.02^{\text{m}}$  at K. As it

is much less than the statistical error this factor has been ignored. Similarly the degree of polarization of the source was shown to be so low that the correction necessary was much less than statistical uncertainty.

In those scans where there was no apparent detection of the galaxy, the sky was always immediately checked for the presence of cloud, and the scan channel positions were checked. If satisfied that neither of these factors was responsible for the non detection, a signal upper limit was assumed corresponding to one sigma in the background noise level of that particular scan. These are given in table 4.2a.

#### Low Resolution Contour Map

The 23" aperture declination scans provided five profiles, each separated from the next by  $\sim 0.9 \times$  the beam width. This is rather worse than the ideal half beam width separation necessary for the best possible map. However, the K surface brightness in the outer detected region changes slowly and the data acquired are sufficient to enable a crude map of the area to be drawn. This is not the case nearer to the centre where the high surface brightness region dominates. As this area fell exactly between two low resolution scan channels, any map constructed without a central profile would give a false impression of the location of the maximum surface brightness. (Note the outer contours would not be affected.) To overcome this a simulated central profile was created by convolving the high resolution data with the 23" beam profile. The contours were drawn from the five observed low resolution profiles and the one simulated profile. The western-most scan showed that there was no signal detected greater than the background noise. This allowed a reliable delineation of the source boundary to the west. On the east side the contour lines were closed by assuming an



The contour levels correspond to  
 $5, 20$  and  $35 \times 10^{-30} \text{ W m}^{-2} \text{ Hz}^{-1}$   
 $\text{arcsec}^{-2}$  respectively.

The cross marks the centroid, and  
indicates the positional uncertainty.

Fig. 4.3 : low resolution  $2.2 \mu\text{m}$  contour map

upper limit similar to that on the west. This assumption is almost certainly valid as an upper limit since the brightness drops off more rapidly on the east side. The finished map is shown in fig. 4.3. The large contour interval reflects the incomplete nature of the data set. In this map the large beam size precludes any further estimate of true surface brightness distribution inward of the central contour, but it is evident from the high resolution data in table 4.2a that there are at least nine more similar contour levels within the innermost shown. The orientation of the map is defined by the centroids of the observed profiles (table 4.2). The simulated profile centroid was assumed to lie centrally on a line connecting the centroids of the two adjacent profiles. Although the data from the two R.A. scans were not directly used in the construction of the map, the profile suggested by the contours agrees well with the observed profile.

#### High Resolution Contour Map

The region within the central contour of the low resolution map was scanned with the 6" aperture as described above. A high resolution map of this area was produced from seven profiles (all but one of which was the sum of data from two or more scans) and an upper limit in an eighth channel west of the other seven. As in the low resolution map the upper limit permitted the delineation of the source boundary on that side. On the eastern side the surface brightness dropped off rapidly and only a small extrapolation was required to close the contour line which remained open; this was made by the curve fitting algorithm in the CGHOST contour plotting routine CONTIL.

The high resolution map was not constructed about the observed centroids of the individual scans, as was the case with the low resolution map, instead the centroids were shifted onto their least

The fine cross (error bars) marks the  $2.2 \mu\text{m}$  centroid and indicates positional uncertainty.

- : old  $2.2 \mu\text{m}$  centroid
- + :  $10 \mu\text{m}$  centroid
- X : radio "point" source

The lowest contour (dotted) and the contour interval represent  $2.8 \times 10^{-29} \text{ W m}^{-2} \text{ Hz}^{-1} \text{ arcsec}^{-2}$

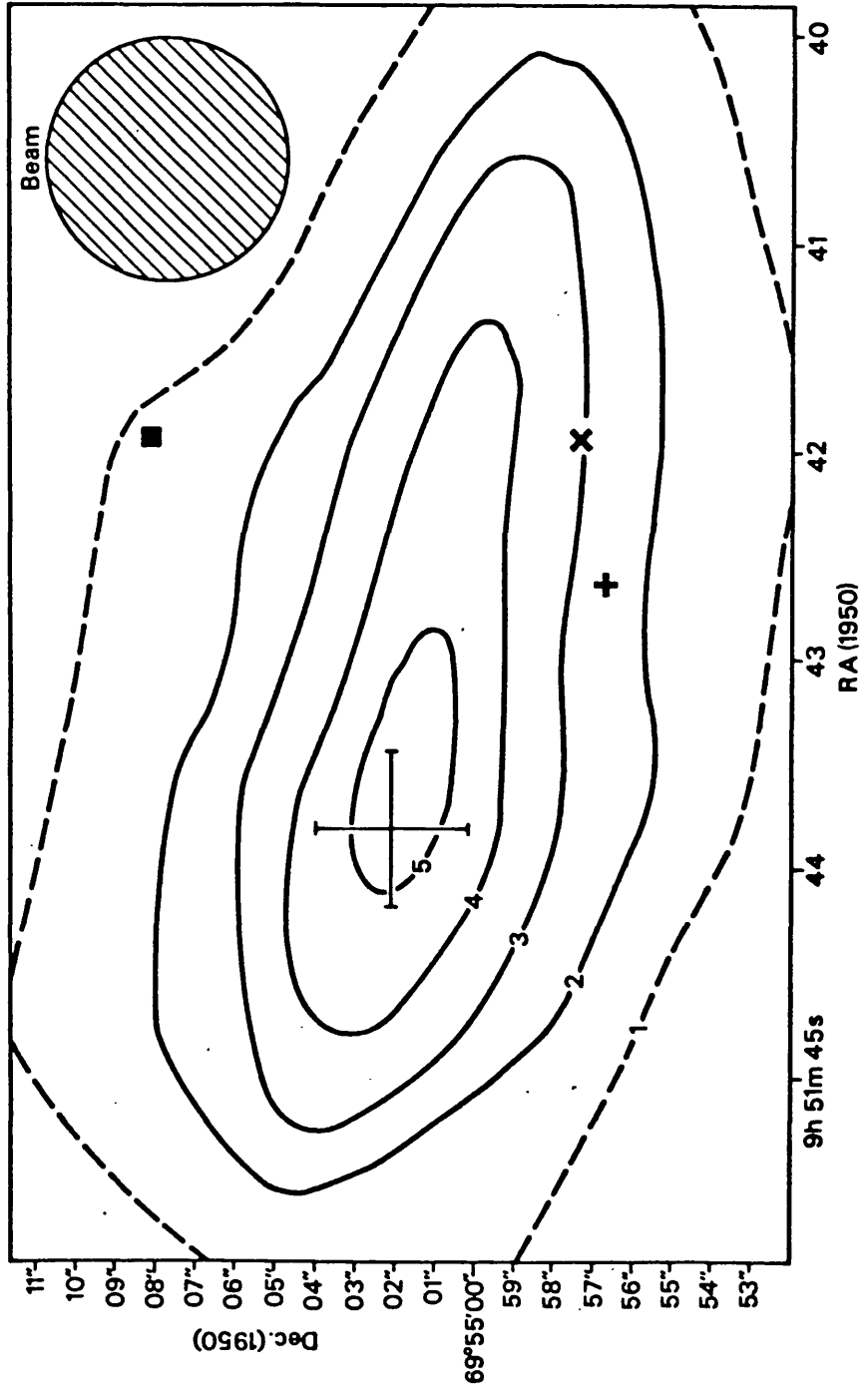


Fig. 4.4 : High resolution  $2.2 \mu\text{m}$  contour map

squares best fit line. As the August 1978 data had the best positional accuracy, only the centroids from these scans were used in the determination of the best fit. The finished map is reproduced in fig. 4.4. The outer contour, shown dotted, may be significantly distorted by noise.

All other data plus certain useful derived quantities are summarised in Table 4.3. The integrated magnitudes were determined using the contour maps.

#### 4.7 DISCUSSION

##### a) Two Micron Morphology

The low resolution contour map shows the region of bright  $2.2 \mu\text{m}$  emission to be an ellipse of dimensions  $\sim 90'' \times 35''$ , or approximately  $1300 \text{ pc} \times 500 \text{ pc}$  at the distance of M82. The size, defined by the outer contour, corresponds roughly to the  $2.5 - 3 \sigma$  level of detection with the infrared system described. As the sensitivity was much less than that usually achieved nowadays, this is smaller than the area detectable with a standard photometer. Note however that as the scans extended beyond the visible bounds of the galaxy and no other signal above the background noise level was detected, it is probable that the two micron brightness drops off uniformly and no other anomalously bright (c.f. visible) infrared source(s) exists in the optically faint outer region of the galaxy and beyond. Lying approximately at the geometrical centre of the  $2 \mu\text{m}$  extended region is an area of much higher surface brightness which measures  $25'' \times 8''$  at FWHM or  $375 \text{ pc} \times 80 \text{ pc}$ , and contains within its bounds the brightest optical/photographic infrared hot spots. This small inner source, which henceforth will be referred to as the two micron core, has approximately the same luminosity, at  $2.2 \mu\text{m}$ , as the much bigger outer

Table 4.3

PROPERTY	OBSERVED VALUE	COMMENTS
"2 $\mu\text{m}$ Core" Colours	J-H = $1.2 \pm 0.1$ H-K = $1.1 \pm 0.1$	$\alpha = 9\text{h}51\text{m}43.8\text{s};$ $\delta = 69^\circ55'01'';$ 6" aperture
Polarization, 23" aperture	$0.4 \pm 0.4\%$	$\alpha = 9\text{h}51\text{m}41.3\text{s};$ $\delta = 69^\circ55'04''$
Polarization, 6" aperture	$0.6 \pm 0.4\%$	$\alpha = 9\text{h}51\text{m}43.8\text{s};$ $\delta = 69^\circ55'01''$
Orientation, 2 $\mu\text{m}$ outer disc	P.A. = $75^\circ \pm 15^\circ$	(from contour map)
Orientation, 2 $\mu\text{m}$ core	P.A. = $77^\circ \pm 15^\circ$	(from contour map)
Total integrated magnitude	$5.7 \pm 0.3$	Not corrected for extinction
Integrated magnitude, 2 $\mu\text{m}$ core	$6.5 \pm 0.2$	FWHM luminosity, not corrected for extinction
2 $\mu\text{m}$ outer disc dimensions	$\sim 90'' \times 35''$ (1350 pc x 525 pc)	At $\sim 2\frac{1}{2} - 3$ level
2 $\mu\text{m}$ core FWHM dimensions	$\sim 25'' \times 8''$	Not corrected for extinction in dark dust lane (see text) or instrumental broadening

disc. If an edge-on disc geometry is assumed for both inner and outer regions (the galaxy's rotation axis is only  $\sim 8^\circ$  out of the plane of the sky) then the inner core region is  $\sim 60$  times more luminous per unit volume than the outer disc. The position angle of the two micron major axis is  $\sim 75^\circ \pm 15^\circ$ . The position angle of the optical major axis is  $65^\circ$  and though the infrared P.A. uncertainty is large enough to accommodate the discrepancy, a real difference between optical and two micron axes cannot be ruled out, although it is unlikely. On both the  $6''$  resolution and  $23''$  resolution maps the beam size is too big to rule out the existence of substructure. Mapping of the outer disc and inner core with beam sizes  $\sim 10''$  and  $2.5''$  respectively would be feasible on a more sensitive system, such as that used for the NGC 972 work, and would probably reveal discrete sources. Certain constraints however can be placed on possible discrete sources: (i) Table 4.2 shows that the flux in beams separated by  $\sim 1$  beam width (i.e. only very slight contamination) along the core axis does not contribute more than a maximum of  $\sim 30 - 35\%$  of the entire core luminosity. Therefore no single discrete source can dominate the two micron luminosity of the core by more than this amount. (ii) Scans with the  $11''$  aperture, one in R.A. and one in declination, centred on the bright core but passing through the entire near infrared outer disc did not reveal any outer substructure, along the channels traversed, brighter than the background noise, i.e.  $m_K \gtrsim 9.5$ , mean surface brightness  $\gtrsim 14.5 m_K \text{ arcsec}^{-2}$ .

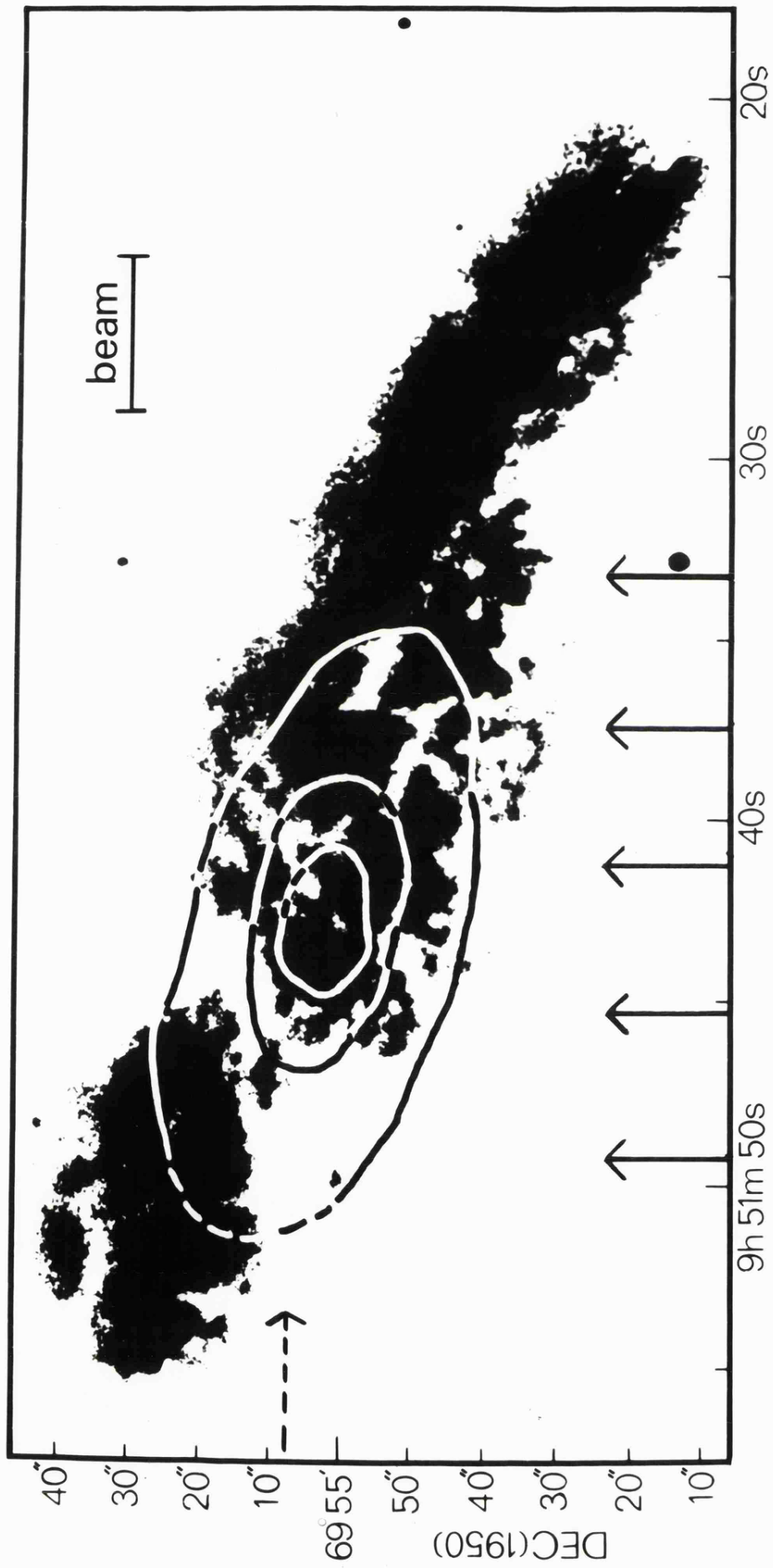
COMPARISON WITH PREVIOUS PHOTOMETRY: The paucity of near infrared data has been mentioned. No small beam photometry ( $\lesssim 25''$ ) has been published for  $\lambda < 10 \mu\text{m}$ . Kleinmann and Low (1970a) have published  $2.2 \mu\text{m}$  spot photometry for the nuclear region and also for a region east of the major dust lane, but unfortunately they did not give

their measuring aperture. Rieke and Low (1972) quote that previous 2.2  $\mu\text{m}$  photometry on M82 used apertures 25" - 35", but do not specify exactly which aperture corresponds to published data. The magnitudes given by Low et al. are  $m_K \sim 6.1$  for beams near the 2.2  $\mu\text{m}$  and 10  $\mu\text{m}$  centroids of 1970. This agrees satisfactorily with the contour map prediction for an aperture size  $\sim 30''$ . The region east of the dust lane for which they found a K magnitude is the HII region of Peimbert and Spinrad (1970), Region B of O'Connell and Mangano (1978). Their mean surface brightness value is  $5.2 \times 10^{-30} \text{ Wm}^{-2} \text{ Hz}^{-1} \text{ arcsec}^{-2}$  if a 35" aperture was used; this assumption is probably correct since the surface brightness here is so low. The region is situated just outside the outer contour of the 23" resolution map and so there is excellent agreement between their value and the map value of  $\sim 5 \times 10^{-30} \text{ Wm}^{-2} \text{ Hz}^{-1} \text{ arcsec}^{-2}$ .

COMPARISON WITH LARGE SCALE OPTICAL MORPHOLOGY: Short/medium exposure photographic plates of M82 show a bright disc measuring approximately 130" x 40" (fig. 4.1, lower two frames), this region corresponds closely in size, shape and position with the outer disc of near infrared emission. This is illustrated in fig. 4.5 which shows the 23" resolution contour map superimposed on a short exposure V plate of M82. (Note however, by comparing figs. 4.1 and 4.5, that in fig. 4.5 the region west of  $\sim 9\text{h } 51\text{m } 33\text{s}$  appears relatively much brighter than it should; this is due to three successive photographic reproductions necessary to obtain the superimposition effect.) The most obvious and dramatic difference between the V and K images is that the visible image is completely split by a wide, dense dust lane whereas the two micron emission is, in comparison, only slightly affected by the lane. Closer examination of the central region however, at higher

Fig. 4.5 (overleaf) :

The low resolution  $2.2 \mu\text{m}$  contour map superimposed  
on a short-exposure V print of M82.



RA (1950)

resolution, shows a marked asymmetry in the  $2.2 \mu\text{m}$  brightness distribution. For dynamical reasons this is unlikely to be due to genuine, intrinsic source structure, and as the more rapid surface brightness decline east of the centroid coincides so closely with the dust lane, increasing obscuration is almost certainly the cause of the asymmetry. The amount of extinction in the dust lane is considered in section d.

b) Two Micron Luminosity of the Central 90 pc

Recent major papers on M82 (Solinger, Morrison and Markert 1977, and O'Connell and Mangano 1978) conclude that the integrated properties of the galaxy, linear dimensions, mass, mass of dust, etc., indicate that the underlying galaxy (i.e. pre interaction or explosion) is an average late type, probably an Sc or Magellanic irregular. A nearby galaxy which fits this description, and is approximately the same size and mass as M82 (Astrophysical Formulae), is the local group ScIII galaxy M33. It would clearly be of interest to compare the relative two micron nuclear luminosity of the two galaxies to see if the near infrared brightness of disturbed M82 can be accounted for by the stars of the nucleus of the possibly normal, underlying galaxy. Penston (1973) measured the K magnitude of the M33 nucleus through a  $28''$  aperture, as the distance ratio  $d_{\text{M82}}/d_{\text{M33}} \sim 4.6$ , Penston's beam size corresponds to the  $6''$  used on M82. The value of  $m_K$  obtained for M33 was 10.9, if M33 was at the distance of M82 the K magnitude would be 14.2, this is a factor of 360 x fainter than the brightest M82 region of the same linear size,  $m_K = 7.8$ . M82 however is almost edge on and M33 is almost face on, and therefore the K magnitude of M33 must be corrected to that which would be measured if the galaxy was viewed edge on. Since the wavelength concerned is  $2.2 \mu\text{m}$  the greater optical path seen by an aperture looking at the system edge on will be considerable

as extinction will be low. Nevertheless the extra  $2.2 \mu\text{m}$  flux seen will be small as the extra stars seen are of the early type disc/spiral arm population, i.e. relatively faint at  $2.2 \mu\text{m}$ . Fig. 4.6 shows a schematic scale diagram of M33 to help illustrate the faintness of the extra component seen by an aperture looking in the plane of the galaxy. The diameter of the galaxy is taken from the 2nd RCBG (de Vaucouleurs et al. 1976) and the disc to bulge ratio from Sandage (1961) and Van den Bergh (1975). It is very difficult to give an accurate estimate for the K magnitude measured through an aperture looking into the plane of the galaxy, however by assuming (a) zero extinction at  $2.2 \mu\text{m}$  and (b) uniform luminosity distribution throughout the galaxy, it is possible to give an upper limit if the K magnitude of the whole galaxy ( $m_{K,TOTAL}$ ) is known. Although the total K magnitude, and so the total K luminosity, has not been measured, there are two methods at hand which enable a good estimate to be made. The first is to use the 2nd RCBG value for  $m_{V,TOTAL}$  and the V-K colour index for late type spirals (Aaronson 1978). The second method involves extrapolation of Penston's photometry using the flux-aperture relation for late-type spirals,  $F \propto D^{1.2}$ , (Aaronson 1978). Both methods suggest  $m_K \sim 4.5$  ( $\pm .5$ ). As the extra volume seen by the beam looking into the plane is  $\sim .00125$  of the total galaxy volume then with assumptions (a) and (b):  $m_K$  (edge on)  $\sim 10.5$ , c.f.  $m_K$  (face on) = 10.9. When adjusted to the value expected at a distance of 3.2 Mpc,  $m_K = 13.8$ , which is still fainter by a factor  $\sim 250$  than the corresponding volume in M82. Thus, if M82 was indeed a simple field galaxy similar to M33, its present day  $2.2 \mu\text{m}$  luminosity must be a result of the activity which has taken place since the event which disrupted the galaxy.

The brightest two micron regions found anywhere in "normal"

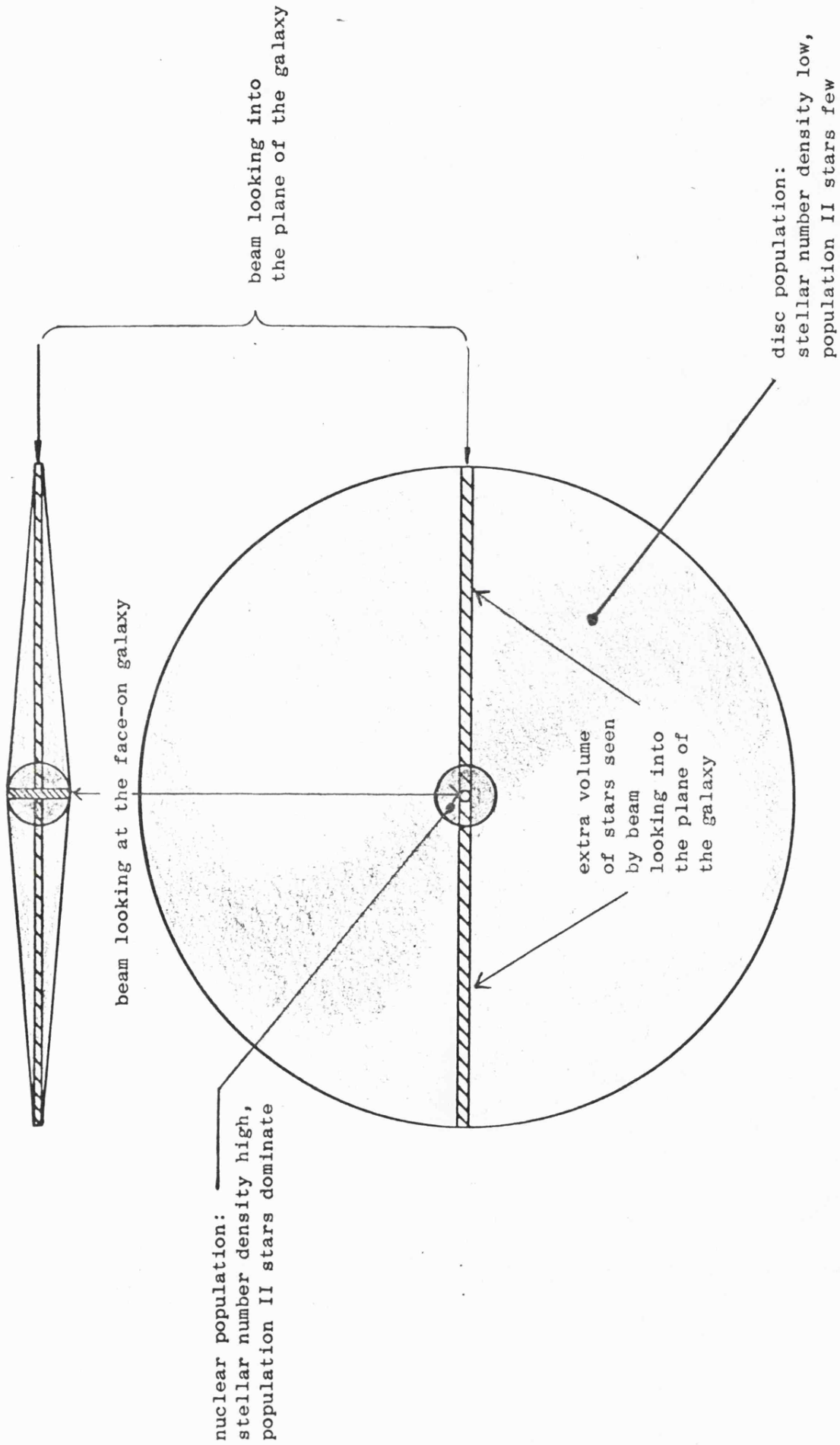


Fig. 4.6: Schematic Diagram of M33-type Galaxy (see text for details)

galaxies are the dense nuclei of Sa/Sb I-II and gE galaxies, since it is here that the number density of late-giants is greatest. The nucleus of M31 is a typical example and has been studied closely (see Chapter 3). We will compare the luminosity in the central 90 pc of M31 with that in M82. The argument this time is straightforward as the rotation axes of M31 and M82 have very similar tilts to the plane of the sky (M31  $\sim 12^\circ$  de Vaucouleurs 1959, M82  $\sim 8^\circ$  Solinger et al. 1977) and so differences due to orientation will be negligible. Using the multiaperture data of Sandage et al. (1969), the central 90 pc of M31 if viewed from 3.2 Mpc would have a K magnitude of  $\sim 9.1$ . So even before the obscuration in M82 is taken into account it is evident that the brightest two micron region in M82 is as bright or brighter than the densely populated, late-type giant dominated, spheroidal components of much more massive galaxies. Finally, in order to see M82 in perspective, its two micron luminosity should be compared to that of a well known active galaxy. NGC 1068, as the prototype of the thermally powered type 2 Seyferts, is a particularly pertinent example. At the distance of NGC 1068 ( $\sim 20$  Mpc, 2nd RCBG) an aperture size of  $\sim 1''$  is equivalent to the  $6''$  (90 pc) aperture used on M82. This is about the size that Becklin et al. (1973) believe the  $10 \mu\text{m}$  source in NGC 1068 to be. Extrapolation of the Neugebauer et al. (1971)  $2.2 \mu\text{m}$  multi-aperture photometry to a beam size of  $1''$  suggest a two micron luminosity  $\sim 20$  x that of M82. Thus, though M82 is certainly anomalously bright in the near infrared, it is an order of magnitude or so fainter than the most active, thermally powered galaxies.

c) Major Axis Surface Brightness Profile

It has been established that the central 90 pc of M82 is surprisingly luminous at  $2.2 \mu\text{m}$ . Furthermore, the contour map shows the

bright region to be extended along the major axis. To determine the full extent of the region over which M82 is unusually bright the major axis  $2.2 \mu\text{m}$  surface brightness profile is compared to that of M31. The M31 profile has been constructed to correspond exactly to that of M82: near the centre ( $r \lesssim 500 \text{ pc}$ ) the data used is that of Sandage et al. (1969) and corresponds to the M82 data obtained using the  $6''$  aperture. At greater radial distances the Japanese (Iijima et al. 1976, Matsumoto et al. 1977) data obtained, with an aperture of  $102''$ , corresponding to the  $23''$  aperture M82 data, is used. Sandage et al. measured the  $2.2 \mu\text{m}$  surface brightness distribution of M31 along an E-W line; to obtain the major axis profile the E-W profile was stretched by a factor  $a/r$  where

$$\frac{a}{r} = \left( \frac{1 - e^2 \cos^2 \theta}{1 - e^2} \right)^{\frac{1}{2}}$$

This is the equation which describes the radius vector length relative to the major axis ( $a$ ) of elliptical isophotes.  $\theta$  is the angle made by the radius vector and the major axis. The eccentricity ( $e$ ) is a function of  $r$ , and the adopted values of the axial ratio  $b/a$  ( $= (1 - e^2)^{\frac{1}{2}}$ ), are those of Sandage et al. (1969) and de Vaucouleurs (1958). This procedure was unnecessary for the Japanese data as it was taken from their contour map. Fig. 4.7 shows the two profiles, with that of M31 corrected to appear as it would if the galaxy was at the same distance as M82. Regardless of the asymmetry in the M82 profile (which is discussed in the next section), the major axis surface brightness distribution of the two systems shows that over the central  $1 - 1.5 \text{ kpc}$  M82 outshines the corresponding region in M31, but at greater radial distances it appears that the  $2.2 \mu\text{m}$  surface brightness of M82 drops off rapidly. This is an extremely interesting result as it shows that M82 is excessively bright not only in the " $2 \mu\text{m}$  core",

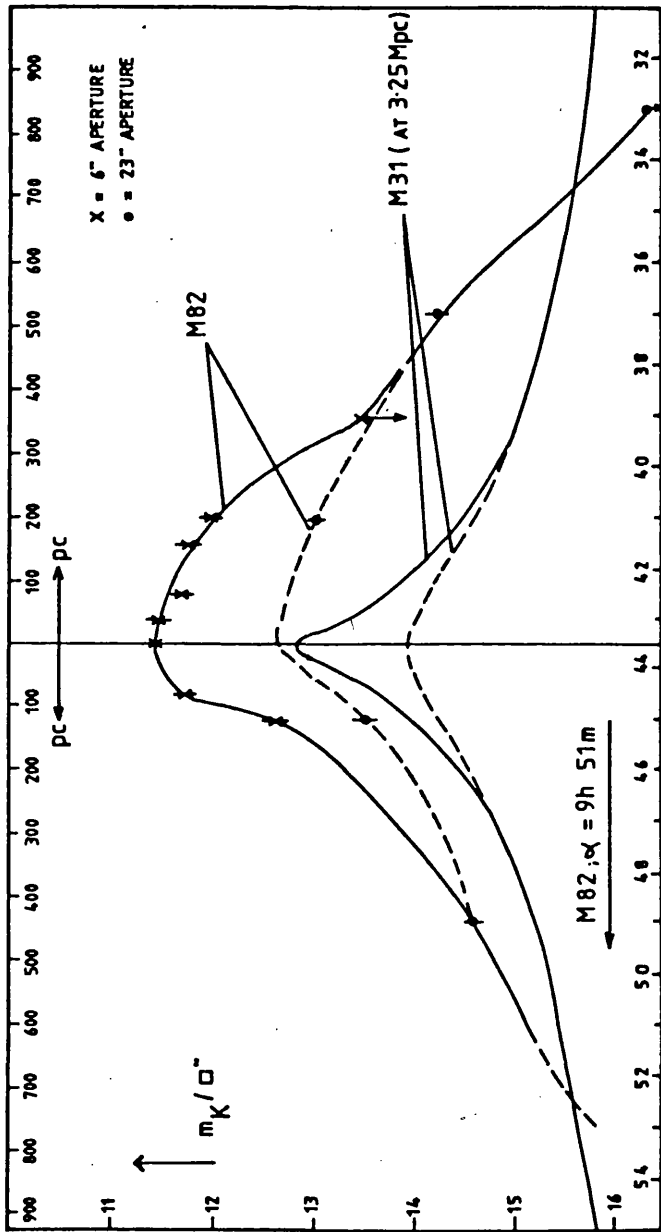


Fig. 4.7 : A Comparison of the M82 and M31 luminosity profiles.

where it is indeed brightest, but also within the entire region encompassed by the outer contour of the low resolution map. It would be interesting to map, with very large apertures ( $\sim 50 - 100''$ ), the low surface brightness region outside  $r \sim 750$  pc ( $50''$ ) to see just how quickly the brightness declines. The surface brightness of late type spirals of luminosity class  $\sim$  II - III decreases exponentially in the disc (Freeman, 1970) and so the profile of M82 would have to show an almost discontinuous decline to reach a surface brightness level similar to that in the disc of an ScIII galaxy. Depending upon the actual value of the upper limit given at the extreme west in fig. 4.7, this could be the case.

d) Extinction in the Major Dust Lane

The contour maps, especially the high resolution core map, and the luminosity profile clearly exhibit considerable asymmetry. The proximity of the dense, apparently galaxy-splitting, dust lane suggests increased obscuration as the cause of the asymmetry. Assuming this to be so, and by assuming that the underlying profile is in fact symmetrical an estimate can be made of the amount of extinction the lane produces. In fig. 4.8 the observed profile is represented by the solid line and the hypothesised, underlying, symmetrical profile is represented by the dashed line. The maximum extinction indicated in this diagram is  $A_K \sim 1.3^m$  or  $A_V \sim 16^m$ , note however that it is not an absolute value, but is the extinction in excess of the mean extinction to the west of the dust lane. The position at which the maximum extinction is determined to occur coincides with the geometrical centre of the dust lane and so lends support to the original assumption. Fig. 4.8 suggests the true diameter of the core source is  $34''$  (FWHM).

It is believed that value given above is the first estimate of

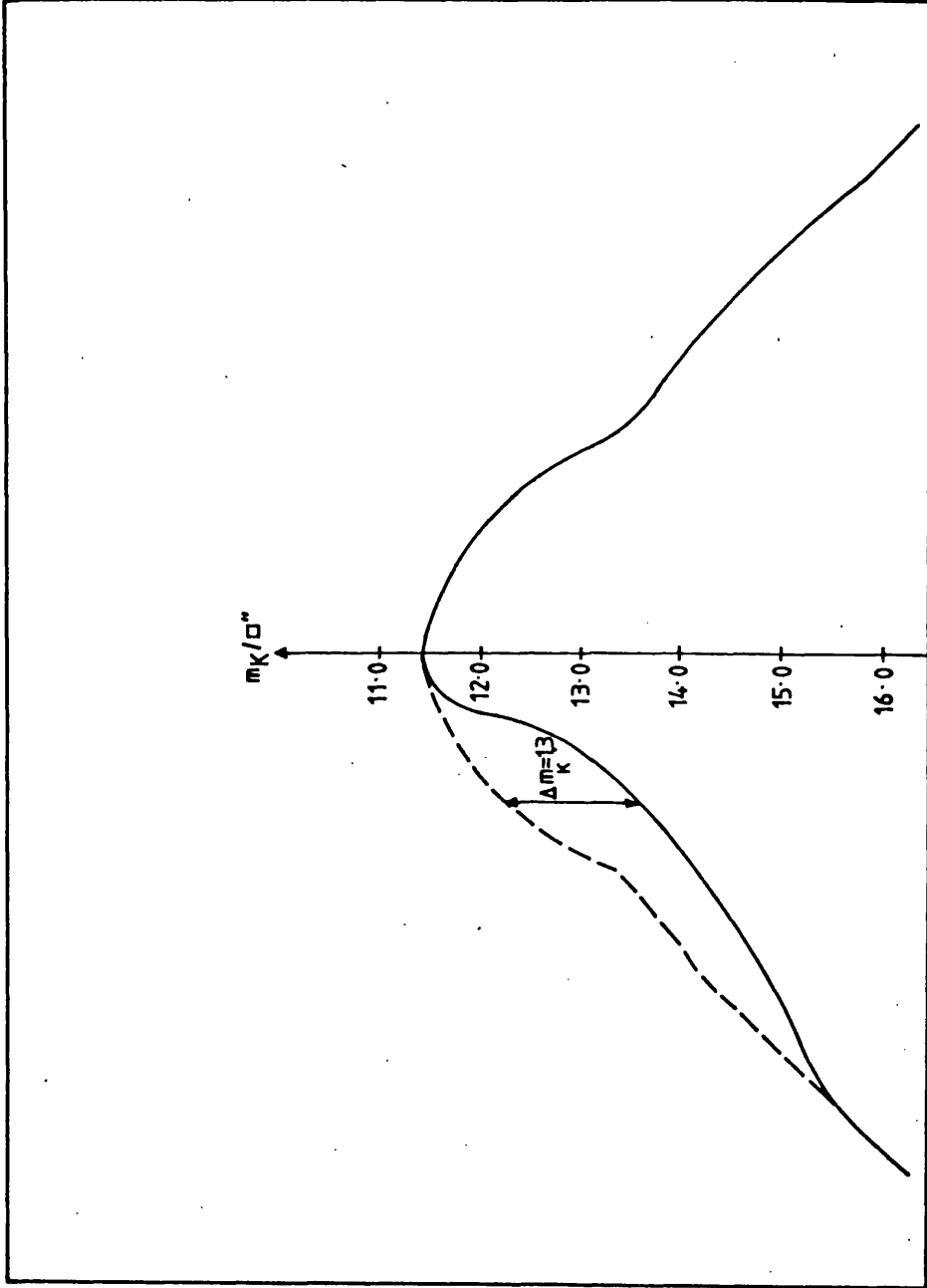


Fig. 4.8 : Extinction in the main dust lane

extinction in the lane based upon observational evidence; it can be confirmed only by observations at  $\lambda \gtrsim 2 \mu\text{m}$ . Measurements of the  $\text{Br}_\alpha / \text{Br}_\gamma$  decrement, assuming the existence of underlying HII regions, would furnish an excellent method of doing so.

e) Two Micron Core in Relation to Other Nuclear Bright Features

Fig. 4.9 shows the revised version of fig. 4.2; the old two micron centroid is removed and the new spatial information is added. Fig. 4.10 shows a superimposition of the main features of fig. 4.9 onto a short exposure visible print. The two parallel lines represent the observed FWHM dimensions of the core source, the dots mark visible hot spots, the + sign marks the  $10 \mu\text{m}$  centroid and the x sign marks the "point" radio source. The two micron core, the diffuse radio emission and the optical core region defined by the hot spot distribution are all remarkably coincident, and probably coextensive if allowance is made for total extinction of the visible light, and partial extinction of the near infrared light by the major dust lane. The ten micron extended source seems to be centred slightly to the south of the region in which the brightest extended emission at other wavelengths arises, but note that uncertainty in the ten micron centroid might allow for emission at all four wavelengths, visible, near infrared, ten micron and radio, to be superimposed, and indeed this is likely to be the case.

The two micron centroid is almost certainly not coincident with the compact radio source, but is very close, within positional error, to the dynamical centre of Burbidge et al. (1964). Geldzahler et al. (1977) believe the compact radio source is similar to the compact sources seen at the centre of other spiral and elliptical galaxies, e.g. M81. Such sources however are usually symmetrically surrounded by diffuse radio emission and lie at the dynamical centre of the galaxy,

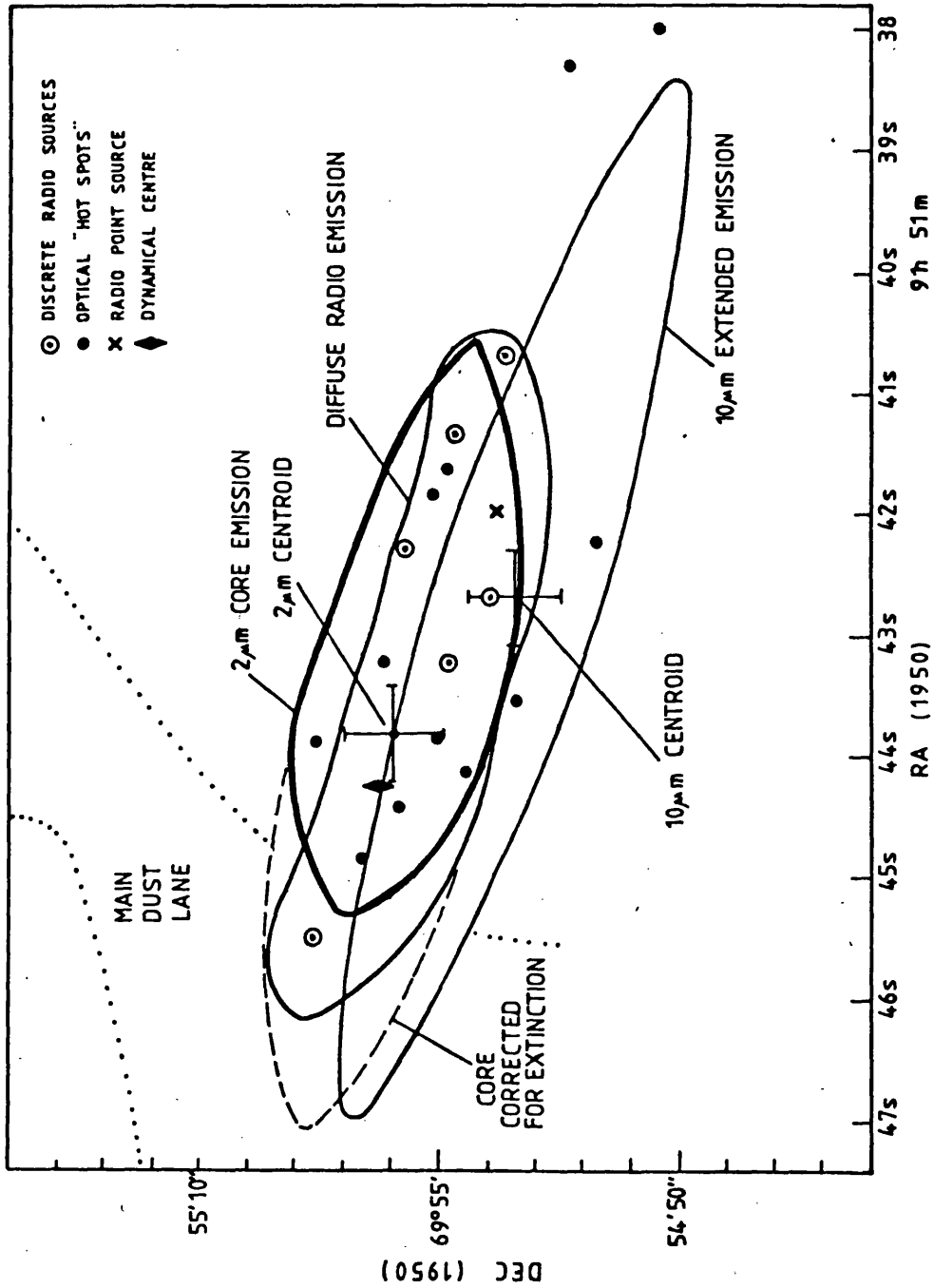
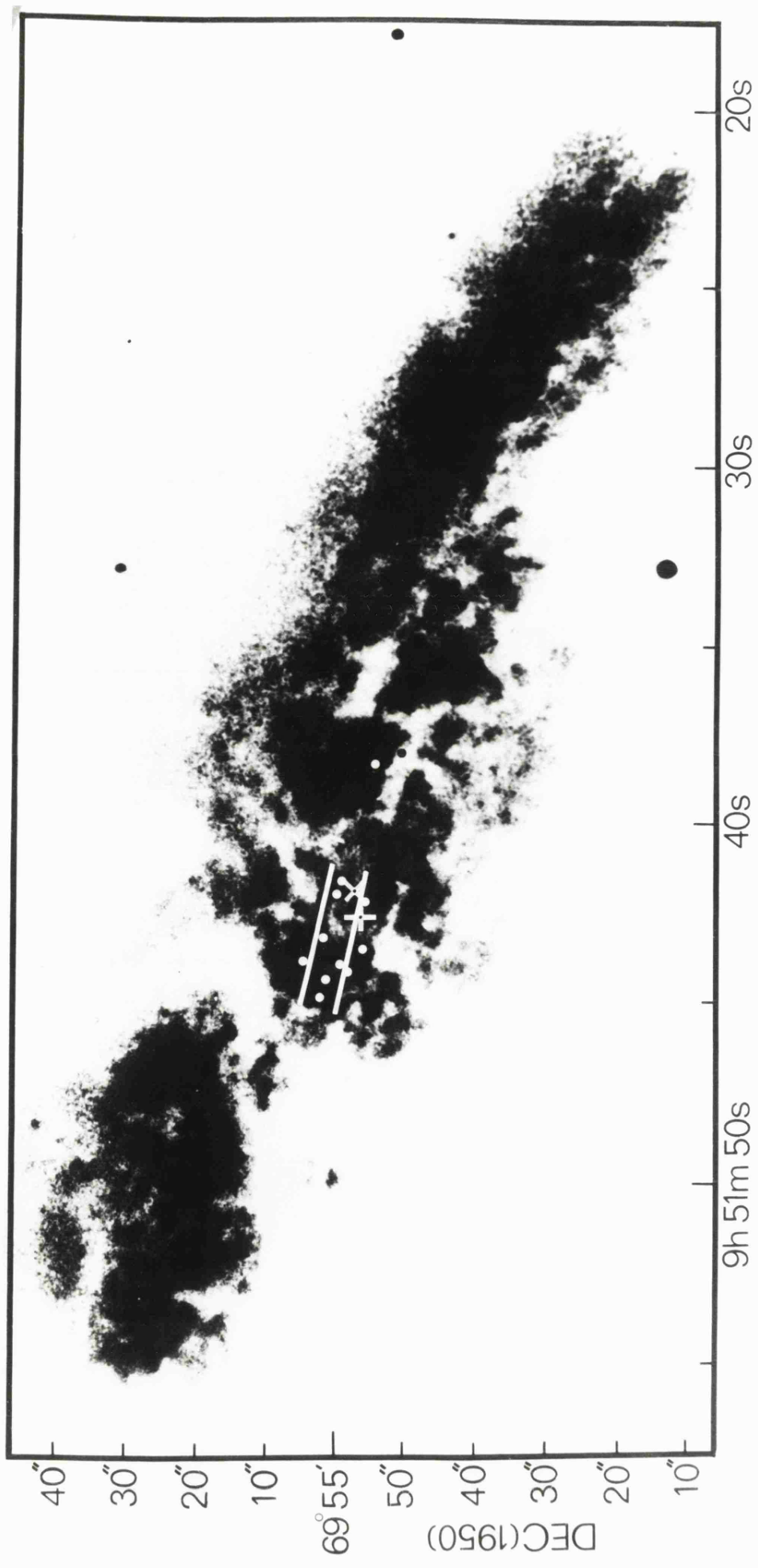


Fig. 4.9 : The centre of M82 (ii) - with the new 2.2 μm mapping data.

Fig. 4.10 (overleaf) :

The prominent features of the centre of M82 superimposed  
on a V print (see text for details).



RA (1950)

9h 51m 50s

20s

30s

40s

40''

30''

20''

10''

69° 55''

50''

DEC (1950)

40''

30''

20''

10''

i.e. the position of the stellar density maximum. Therefore, either the M82 feature is unlike the other compact sources, at least positionally, or the dynamical centre of Burbidge et al. is considerably misplaced, in which case the two micron emission is very asymmetrically distributed about the nucleus if defined by the compact radio source.

The FWHM dimensions of the two micron core source and the ten micron source are  $34'' \times 8''$  (extinction corrected) and  $47'' \times 6''$ . The two micron source has not been corrected for instrumental broadening however, and as both the instrument response and the observed minor axis luminosity profile were almost Gaussian a first order approximation to the intrinsic FWHM size can be made. (Note that as the beam width was  $6''$  the major axis dimension will be hardly effected.) The relationship for Gaussians:  $(FWHM)_{\text{INTRINSIC}}^2 = (FWHM)_{\text{OBSERVED}}^2 - (FWHM)_{\text{BEAM}}^2$ , gives the size of the core source as  $\sim 34'' \times 5.5''$ . Note that this is smaller than the ten micron source; this is a necessary result if warm dust plays any part in the two micron emission.

#### f) Near Infrared/Visible Colour Indices

The near infrared colour indices at the core source centroid, measured through a  $6''$  diameter aperture, are  $J-H = 1.2$ ,  $H-K = 1.1$ . O'Connell (1970) obtained V photometry through a  $7''$  diameter aperture centred  $\sim 1'' - 2''$  from the two micron centroid, which gave  $m_V = 13.04$ , implying  $V-K \sim 5.2$ . This set of colour indices implies a very red source, far redder than the coolest population of normal stars, yet the spectroscopic investigations (O'Connell 1970, Van den Bergh 1972, Peimbert and Spinrad 1970, O'Connell and Mangano 1978) show that the visible light is dominated by hot young stars. Clearly, within dusty M82 interstellar reddening must play a very great role, however, simple reddening laws based upon Van de Hulst curve no. 15 (Johnson 1968)

cannot explain the excesses in the various colour indices for even the reddest possible stellar population, let alone the hot young population. Table 4.4 summarises the situation; the various values of visual extinction,  $A_v$  implied by the colour excesses  $E_{(V-K)}$ ,  $E_{(J-H)}$ ,  $E_{(H-K)}$  are given for two simple models; in the first the mean intrinsic colours are those of an A0 star, i.e. a dominating young population is assumed since it is clear that such stars exist in profusion along the line of sight to the two micron core, and in the second the intrinsic colours are those of a typical late type spiral galaxy (Aaronson 1978). It can be seen immediately that the various values of  $A_v$  are widely disparate, and in particular the H-K excess might equally be attributed to a considerable contribution at  $\lambda \gtrsim 1.5 \mu\text{m}$  from non stellar emission. The environment in M82 however is not so simple as that implicitly assumed when following the standard interstellar reddening laws, i.e. instead of a source(s) situated behind an obscuring cloud, the sources are intimately intermingled with the obscuring matter, and furthermore the appearance of M82 implies that this intermingling is non-homogeneous and non isotropic. It is therefore impossible to take into account all the possible juxtapositions of dense clouds and thin clouds that may lie across the line of sight, obscuring sources within and behind them. Optically thick clouds which may completely obscure visible sources would produce only 1 - 2 magnitudes of extinctions at  $\lambda > 1.5 \mu\text{m}$ , so it is not difficult to imagine a situation where apparently inconsistent values of  $A_v$  obtain from the various colour indices, particularly V-K. There are of course a number of other factors such as grain size, shape and composition which might possibly produce a deviation from the extinction predicted by the standard reddening curves. Nevertheless, as Aaronson (1978) has emphasised, a more straightforward and equally plausible possibility is

TABLE 4.4

Colour Index	Observed Colour	Model 1: Mean A0 Population			Model 2: Late Type Spiral Nucleus		
		Intrinsic Colours	Excess	Implied A <sub>v</sub>	Intrinsic Colours	Excess	Implied A <sub>v</sub>
V-K	5.2	0.0	5.2	5.8	3.0	2.2	2.5
J-H	1.2	0.0	1.2	12.0	0.72	0.48	4.8
H-K	1.1	0.0	1.1	18.3	0.18	0.92	15.3

a contribution from the emission of hot dust, which could account for the H-K excess in particular. In the case of NGC 4631, Aaronson invokes dust at  $T \sim 700^{\circ}\text{K}$  to account for the inconsistent J-H, H-K and K-L excesses he observes; in M82 the excesses are far more extreme and more (hot) dust would be required to account for them. Mapping of the V-K and H-K colour indices within the core (apertures  $\lesssim 3''$ ) may help ascertain whether hot dust is a significant source. As extinction almost certainly varies from place to place across the core changes in the V-K index would reflect this. If hot dust is not a source corresponding changes in H-K would be observed. If however hot dust is a significant source, the H-K index should be approximately constant.

g) Conclusions - the nature of the two micron source

The observed features of the two micron emission of M82 have now been fully described, and pertinent comparisons have been made with a) the two micron emission of various other galaxies and b) the extended emission at other wavelengths of M82 itself. Three major conclusions have been drawn:

1) The  $2\ \mu\text{m}$  surface luminosity over the central 1.5 kpc of M82, but particularly the central  $\sim 500\ \text{pc}$ , is far higher than that expected of its probable original Hubble/DDO form indicated by its other gross properties.

2) The core source is coincident and coextensive with the region defined by the optical bright spots and the diffuse radio emission, and probably with the ten micron source though this is somewhat more extensive than the other regions.

3) The colours of the core source, if typified by the V-K, J-H, and H-K colour indices obtained close to the centroid, are

exceedingly red, and simple interstellar extinction curves (Johnson 1968) cannot explain them. A complex of dense obscuring matter might account for the apparent inconsistency between the extinction implied by the V-K excess and that implied by redder colour indices, but the H-K colour in particular may indicate emission from hot ( $T \sim 700^{\circ}\text{K}$ ) dust. If hot dust is a component of the two micron emission then the emitting region must be smaller than the extended ten micron region which is in turn smaller than the seventy micron source (Kleinmann et al. 1976). The two micron core source has now been observed to be significantly smaller than the ten micron source.

Some further qualification to conclusion (1) is warranted. It is possible that M82 was in fact initially brighter than the particular late type galaxy, M33, chosen to be representative of its (M82's) original two micron luminosity. This galaxy was chosen as it is a perfectly "normal" example of its class, and reliable (and convenient) two micron photometry is available in the literature. Equally possibly M82 may have been an even later (Sd, Sm) spiral or indeed a Magellanic irregular, in which case its original two micron surface brightness would have been less than that of M33. It is however almost certain, given the gross properties of M82, that it was never a galaxy like M31 with a very high surface brightness nuclear bulge. The two micron brightness ratio (current divided by probable "pre-interaction/explosion" brightness) given in section b, and based on M33, was  $\sim 250$ , this should be seen as a plausible mean in an upper and lower limit range of 50-500.

Given that the near infrared luminosity of the core is exceptionally high, and that it is co-spatial with the region of recent intense star formation, it is tentatively concluded that a significant

fraction of the two micron flux from the core must be contributed by the young population and its associated environment. This does not of course preclude cool stars, indeed these have been observed spectroscopically (O'Connell 1970, Willner et al. 1977), but it is unlikely that from within the core there is any significant emission from cool stars other than possible contributions from (a) the young, lower main-sequence, (b) pre main-sequence objects and (c) M supergiants, since O'Connell and Mangano (1978) have shown that the recent burst of star formation is less than  $5 \times 10^7$  years old, and therefore no associated post main-sequence cool giant population will have evolved. (On time scales,  $T \lesssim 5 \times 10^7$  years only those supergiants of mass ~~less than~~ <sup>greater than</sup> five solar masses will have evolved passed the main-sequence.) In apparent contradiction to this, Willner et al. (1977) have seen the CO absorption feature, the signature of late type, i.e. post main sequence, giants, in their CVF spectroscopic study. Furthermore, the strength of this feature, they claim, indicates that the two micron light is dominated by the late type giant emission. This observation can however be reconciled with the hypothesis that the young populations dominate the core. Willner and Co. obtained their spectrum through an aperture of diameter  $30''$  arcsecs roughly centred on the two micron peak, therefore  $\sim 40 - 50\%$  of their flux originated outside the elongated core source, from the disc in fact. In this latter region star formation ceased  $\sim 2 \times 10^7$  years ago, but  $\sim 2 \times 10^8$  years ago (and  $< 10^9$ ) star formation was as prolific as that now observed in the core (Solinger, Morrison, Markert 1977; O'Connell and Mangano 1978). It is the late type giants of this epoch which are likely to be the source of the CO feature. Nevertheless the use of the strength of the CO feature should be applied with caution to regions where star formation has ended only relatively recently, since the

stars of the standard galaxies in this technique (Frogel et al., 1978) are of a much earlier epoch and may therefore have a different abundance of CO in their atmospheres.

The integrated two micron emission of the core as envisaged above is likely to be highly composite with possible contributions from hot, luminous giants, M supergiants, the young, lower main sequence, hot dust, free-free emission and probably, if star formation is currently continuing, some contribution from protostellar objects. A visible - 4  $\mu\text{m}$  spectroscopic investigation with a small aperture ( $\lesssim 6''$ ) is required to determine the relative importance of the various sources involved in this region. Note however that even with small observing apertures there will still be a contribution from the late-type giants of the disk which lay along the line of sight to the core source. Finally, if a significant fraction of the 2.2  $\mu\text{m}$  emission originates in obscured OB stars then the near infrared luminosity is indicative of a much greater bolometric luminosity. If only 10% of the observed 2.2  $\mu\text{m}$  core flux comes from such stars then the total luminosity of the core will be  $2 \times 10^{10} L_{\odot}$ \*; this agrees with the figure obtained by Kleinmann et al. (1976) for the luminosity of the extended 10  $\mu\text{m}$  - 70  $\mu\text{m}$  region of M82 which is approximately concentric with the 2.2  $\mu\text{m}$  core.

---

\*  $m_{K,\text{core}} = 6.5$ ,  $\therefore$  10% of this:  $m_K = 9.0$

assuming  $V-K \sim 0$ ,  $m_V \sim 9.0$

assuming mean BC  $\sim -3.0$  (conservative estimate from A.Q.).

$\therefore m_{\text{bol}} = 6.0$  and  $M_{\text{bol}} = -21.5$  ( $m - M = 27.1$ )

$\therefore L_{\text{core}} \sim 2 \times 10^{10} L_{\odot}$ .

## REFERENCES

- Aaronson, M. 1978, P.A.S.P., 90, 28.
- Axon, D.J. and Taylor, K. 1978, Nature, 274, 37.
- Bertola, F., D'Odorico, S., Ford, W.K. and Rubin, V.C. 1969, Ap. J.,  
157, L27.
- Burbidge, E.M., Burbidge, G.R. and Rubin, V.C. 1964, Ap. J., 140, 914.
- Cox, L.J., Hough, J.H. and McCall, A. 1978, M.N., 185, 199.
- Elvius, A. 1962, Lowell Obs. Bull., 5, 281.
- Geldzahler, B.J., Kellermann, K.I., Shaffer, D.B. and Clark, B.G. 1977,  
Ap. J., 215, L5.
- Hargrave, P.J. 1974, M.N., 168, 491.
- Harper, D.A. and Low, F.J. 1973, Ap. J., 182, L89.
- Holmberg, E. 1958, Medd. Lunds. Astron. Obs. II, 136.
- Joyce, R.R., Gezari, D.Y. and Simon, M. 1972, 171, L67.
- Kleinmann, D.E. and Low, F.J. 1970a, Ap. J., 159, L165.
- Kleinmann, D.E. and Low, F.J. 1970b, Ap. J., 161, L203.
- Kleinmann, D.E., Wright, E.L. and Fazio, G.G. 1976, Centre for Astro-  
physics preprint, 500.
- Kronberg, P.P., Pritchett, C.J. and Van den Bergh, S. 1972, Ap. J., 173, L47.
- Kronberg, P.P. and Wilkinson, P.N. 1975, Ap. J., 200, 430.
- Kronberg, P.P. and Clarke, J.N. 1978, Ap. J., 224, L51.
- Low, F.J. and Aumann, H.H. 1970, Ap. J., 162, L79.
- Lynds, C.R. 1961, Ap. J., 134, 659.
- Lynds, C.R. and Sandage, A. 1963, Ap. J., 137, 1005.
- Mayall, N.U. 1960, Ann. d'Ap., 23, 344.
- McDonald, G.H., Kenderdine, S. and Neville, A.C. 1968, M.N., 138, 259.
- Morrison, P. 1979, Sky and Telescope, January, 26.
- Neugebauer, G., Garmire, G., Rieke, G. and Low, F. 1971, Ap. J., 166, L45.
- O'Connell, R.W. 1970, Ph.D. Thesis, Caltech.
- O'Connell, R.W. and Mangano, J.J. 1978, Ap. J., 221, 62.

- Peimbert, M. and Spinrad, H. 1970, Ap. J., 160, 429.
- Raff, M.I. 1969, Ap. J., 157, L29.
- Recillas-Cruz, E. and Peimbert, M. 1970, Bol. Obs. Tonantzintlay  
Tacubaya, 35, 247.
- Rieke, G.H. and Low, F.J. 1975, Ap. J., 197, 17.
- Roberts, M.S. 1957, P.A.S.P., 69, 59.
- Sandage, A.R. 1961, The Hubble Atlas of Galaxies, Carnegie Institution  
of Washington.
- Sandage, A.R. and Miller, W.C. 1964, Science, 144, 405.
- Sandage, A.R. and Visvanathan, N. 1972, Carnegie Yrb., p.685.
- Solinger, A.B. 1969, Ap. J., 155, 403.
- Solinger, A.B., Morrison, P. and Markert, T. 1977, Ap. J., 211, 707.
- Tammann, A. and Sandage, A.R. 1968, Ap. J., 151, 825.
- Van den Bergh, S. 1969, Ap. J., 156, L19.
- Van den Bergh, S. 1972, Astron. and Ap., 12, 474.
- Van den Bergh, S. 1975, Tercentenary Symposium, RGO, p.95, RGO Bulletins,  
182.
- Vaucouleurs, G. de, and Vaucouleurs, A. de, 1964, Reference Catalogue of  
Bright Galaxies, Univ. of Texas Press, Austin.
- Vaucouleurs, G. de, Vaucouleurs, A. de, and Corwin, H.G. 1976, Second  
Reference Catalogue of Bright Galaxies, Univ. of Texas Press,  
Austin.

Near Infrared Observations of NGC 972

### 5.1 INTRODUCTION

NGC 972 is a dusty, peculiar, field galaxy lying at a distance of 30 Mpc (de Vaucouleurs et al., 1976). The extensive and irregular distribution of dust across the face of the galaxy is seen well in the Hubble Atlas print (Sandage, 1961), reproduced in fig. 5.1. Despite the unusual appearance of the galaxy, Sandage classified it as an Sb, maintaining that a spiral pattern could be traced in the dust lanes, and presumably interpreting the brightest region (fig. 5.1) as a spheroidal bulge. He did however qualify his choice by stating that the galaxy "... contains a great deal of dust" which is "scattered in an almost chaotic manner". De Vaucouleurs (1964) thought these features sufficiently extreme to include the galaxy in his IO, i.e. M82-like, classification, and Krienke and Hodge (1974) included NGC 972 in their list of all IO/IrrII type objects. Apart from the obvious similarity in their dusty optical images, NGC 972 resembles M82 in at least one other major characteristic, namely that the brighter part of NGC 972, i.e. that in the Hubble Atlas print, is surrounded by a far more extensive region of low surface brightness which only becomes apparent on long-exposure photographs. The two-exposure print in Burbidge et al. (1965) shows both regions well, and is reproduced in fig. 5.2. The exposure time for the photograph in fig. 5.1 was roughly half way between those used to produce the print shown in fig. 5.2. (Note that the Burbidge et al. print is mirrored with respect to the Hubble Atlas print.) To use Burbidge's terminology, the "bright main body of the galaxy" measures  $\sim 100 \times 30$  arcseconds, i.e. a diameter of 14 kpc at the distance of NGC 972, making it a rather average galaxy in terms of its linear dimensions. The diameter of the surrounding low surface brightness region is  $\sim 200$  arcseconds, or 28 kpc. In comparison the optical image of M31 shown in Chapter 3 is

25 kpc in diameter, but longer exposures and photoelectric photometry (de Vaucouleurs, 1958) reveal that its full linear extent, at a surface brightness level corresponding to that in the outer structure of NGC 972, is 45 kpc.

Burbidge, Burbidge and Prendergast (1965) studied the dynamics of the system using the  $H_{\alpha}$  emission line to determine the rotation curve. The mass obtained for the whole galaxy was  $1.63 \times 10^{10} M_{\odot}$  and the corresponding mass-to-luminosity, using the integrated magnitude of Humason et al. (1956), was 0.88. (Correcting the Burbidge et al. values to those obtained with  $H_0 = 55 \text{ km sec}^{-1} \text{ Mpc}^{-1}$ ). This is a rather small galactic mass and is certainly much less than the average Sb (Burbidge and Burbidge in "Galaxies and the Universe", Chapter 3). The mass-to-luminosity is also low for an Sb galaxy and indicates that the dominant population in the galaxy is younger than that in M31 for example. This is supported by the mean spectral type of the galaxy which is "a" (Morgan, 1958), but both these values are apparently contradicted by the integrated colour index,  $B-V = 0.85$  (Petit, 1954), which is typical of early type spirals (Sa) and ellipticals. This anomaly is typical of IO galaxies (Krienke and Hodge, 1974) and is interpreted as indicating that a predominantly young stellar population is obscured by dust. The colour excess  $E_{(B-V)} \sim 0.25$  (assuming intrinsic late type spiral colours) implies  $A_V \sim 0.75$  (van de Hulst curve 15, Johnson 1968). The colour of the galaxy given above applies essentially to the galaxy as a whole (since the measuring aperture of Petit (1954) completely encompassed the image of the galaxy) and therefore it may not be representative of any particular smaller region of the galaxy. For instance, in the thick dust lanes obscuration is presumably greater than in the brightest region of the galaxy (see especially the  $H_{\alpha}$  and red photographs, fig. 5.3) and this will be

reflected in the colour indices.

There has been no detailed, modern, photoelectric photometry published for the galaxy, although Bernacca and Bertola (1969) and Blackman (1979) have presented blue-waveband contour maps based on photographic photometry. The earlier map is the more detailed, i.e. higher resolution, but unfortunately no absolute calibration is given. The resolution of Blackman's map is much cruder but it is calibrated. These maps are discussed later.

No detailed spectroscopic data has been published, although Burbidge et al. (1965) have reported the detection of strong  $H\alpha$  and  $\overline{[NII]}$  emission throughout the main body of the galaxy. (Wells, 1972, unpublished Ph.D. Thesis, quoted in de Vaucouleurs et al., 1976, has some spectroscopic data on the galaxy but unfortunately this is not generally available). Lynds (1974) included NGC 972 in her survey of HII regions in galaxies. The  $H\alpha$  and red-continuum narrow-band photographs of NGC 972 she presented are reproduced in fig. 5.3 as they will be frequently referred to. The prints show how predominant  $H\alpha$  emission is in the galaxy. Several very large HII regions are evident as well as extensive diffuse emission. (This may be due to unresolved HII regions as 1 arcsecond  $\cong$  140 pc at the distance of NGC 972, the average size of an HII region is  $\sim$  10 parsecs, and the print scale is  $\sim$  2 arcseconds per mm.) Perhaps the most interesting feature revealed in the Lynds prints is the small, but distinct nucleus, bright in  $H\alpha$ , which lies at the centre of what appears to be a small disk galaxy. The nucleus is not apparent in any broad-band photographs of NGC 972. The shorter exposure print of Burbidge et al. shows four condensations in the brightest part of the galaxy (not distinct in the reproduction in fig. 5.2), but it is not clear if any of these is coincident with the bright nucleus seen in the Lynds print.

Very little work has been done on the galaxy outside the visible window. McCutcheon and Davies (1970) and McCutcheon (1973) have found that the radio continuum spectrum in the  $10^3$ - $10^4$  Mhz region follows a power law of index,  $\alpha = -0.68$ . The galaxy is however a "weak" radio source (i.e.  $L_R < 10^{40}$  erg s<sup>-1</sup>) on the definition of Matthews, Morgan and Schmidt (1964). There have been no previous infrared observations of any kind reported in the literature.

The M82 work described in Chapter 4 kindled an interest in IO/IrrII galaxies generally. Of all the other IO's NGC 972 is perhaps the most similar to M82, particularly morphologically, and for this reason it was put on our observing program. A single north-south scan through the galaxy (July 1977) showed that it was sufficiently bright at  $2.2 \mu\text{m}$  for a mapping project to be undertaken, and revealed an interesting secondary structure in the north-south profile. Thus a serious observing project on the galaxy was planned with two specific aims in mind:

- 1) To see how much of the unusual surface brightness distribution seen in the blue map of Bernacca and Bertola was in fact due to dust. (The  $2.2 \mu\text{m}$  north-south scan mentioned above suggested that perhaps obscuration could not fully account for this).
- 2) To see if the unusual IO-type appearance of NGC 972 was reflected in its  $2.2 \mu\text{m}$  luminosity, as had been the case with M82.

We first attempted to map the galaxy and measure its JHK colours in August 1978. Unfortunately the observations were unsuccessful owing to electronics problems (see Chapter 2) and severe drifting of the telescope during the scans. These problems were eliminated in the successful second attempt which is now described in full.

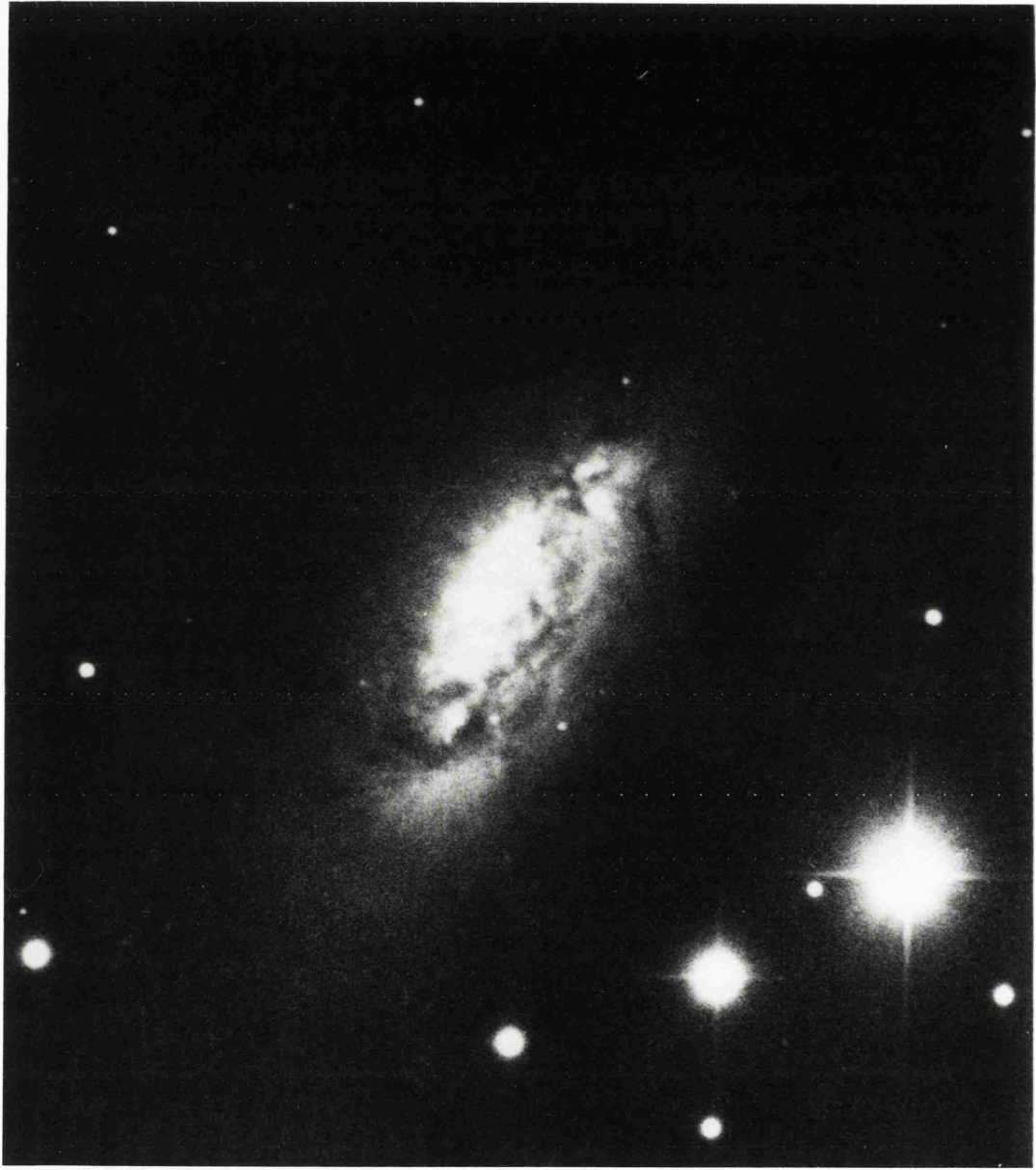
The following three prints are:

Fig. 5.1 : Hubble Atlas print.

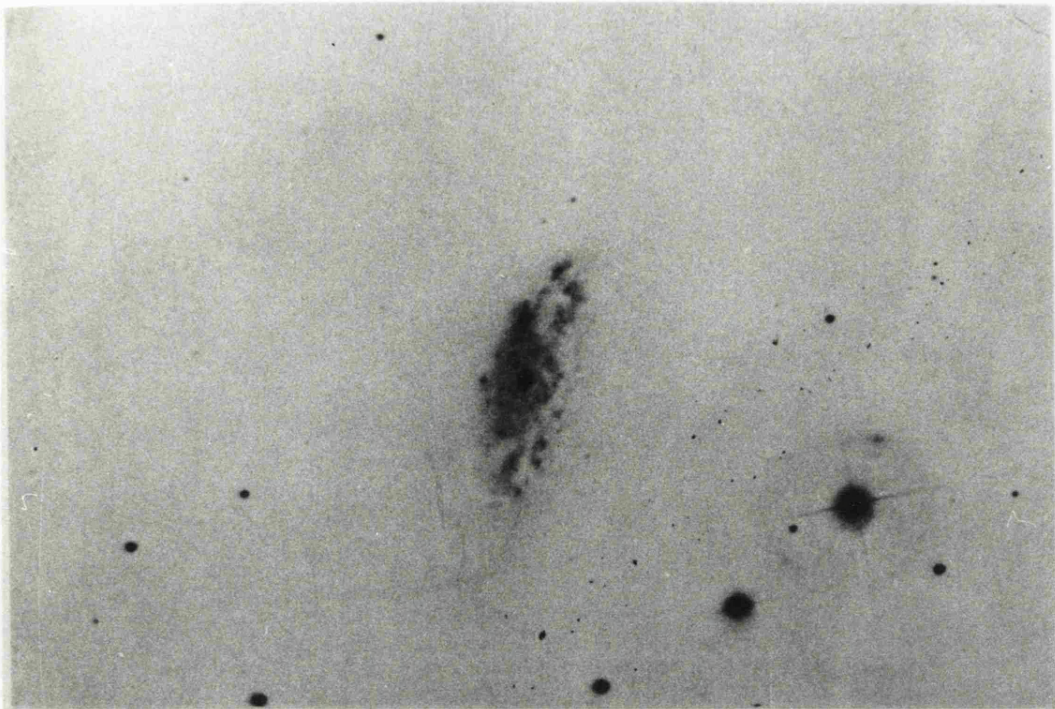
Fig. 5.2 : Burbidge et al. two-exposure print.

Fig. 5.3 : Lynds narrow-band prints.

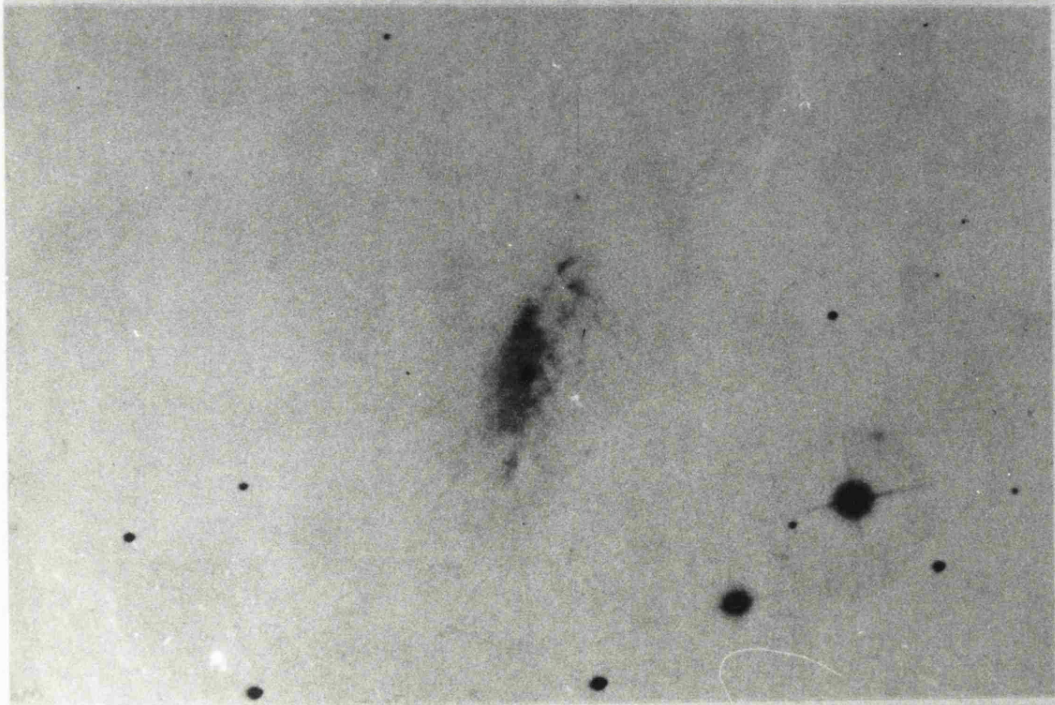
In that order (see text for details).







$\lambda$ 6563



$\lambda$ 6650

NGC 972

## 5.2 OBSERVATIONS

The observations of NGC 972 were made in January 1979 and consisted of (a) a set of  $2.2 \mu\text{m}$  mapping scans and (b) a series of east-west scans through the centre of the galaxy at wavelengths  $1.25 \mu\text{m}$ ,  $1.65 \mu\text{m}$  and  $2.2 \mu\text{m}$  intended to measure any variation in the J-H and H-K colours across the galaxy. Throughout the observations the detector was a "flashed" SBRC InSb photodiode, operated at  $63^\circ\text{K}$ , mounted in the Version I photometer fitted with the Ling vibrating-mirror chopper.

### (a) $2.2 \mu\text{m}$ MAPPING

The mapping observations were made with a sky-projected aperture diameter of twenty-two arcseconds and with the two sky beams separated by thirty arcseconds along the north-south chopping axis. The mapping procedure consisted of scanning the telescope through R.A. in a series of declination channels, each separated by ten arcseconds, i.e. approximately half the beam width. In total fourteen scans were made which gave coverage of the whole galaxy. The details of each scan are listed in Table 5.1 (see also section 5.3), and the channels in which detections of the galaxy were obtained are illustrated in fig. 5.4 which shows them superimposed on the Hubble Atlas print. During the mapping operation the source-beam was located on the galaxy by offsetting from a nearby field star in a manner devised to avoid backlash. (The star is shown arrowed in fig. 5.4 and is at position  $\alpha = 02^{\text{h}} 31^{\text{m}} 10.48^{\text{s}}$ ,  $\delta = 29^\circ 04' 41.0''$ ; epoch 1950. E.D. Clements, RGO, priv. comm.). All scans were made when the zenith angle of the galaxy was less than forty degrees as it was found that under this condition there was no drifting of the telescope from the prescribed path during the scans. Without the drift problem and with possible error due to

Fig. 5.4 (overleaf)

Scan channels in which detections of the galaxy were  
obtained (see text).

9  
8  
7  
6  
5  
4  
3  
2  
1  
0

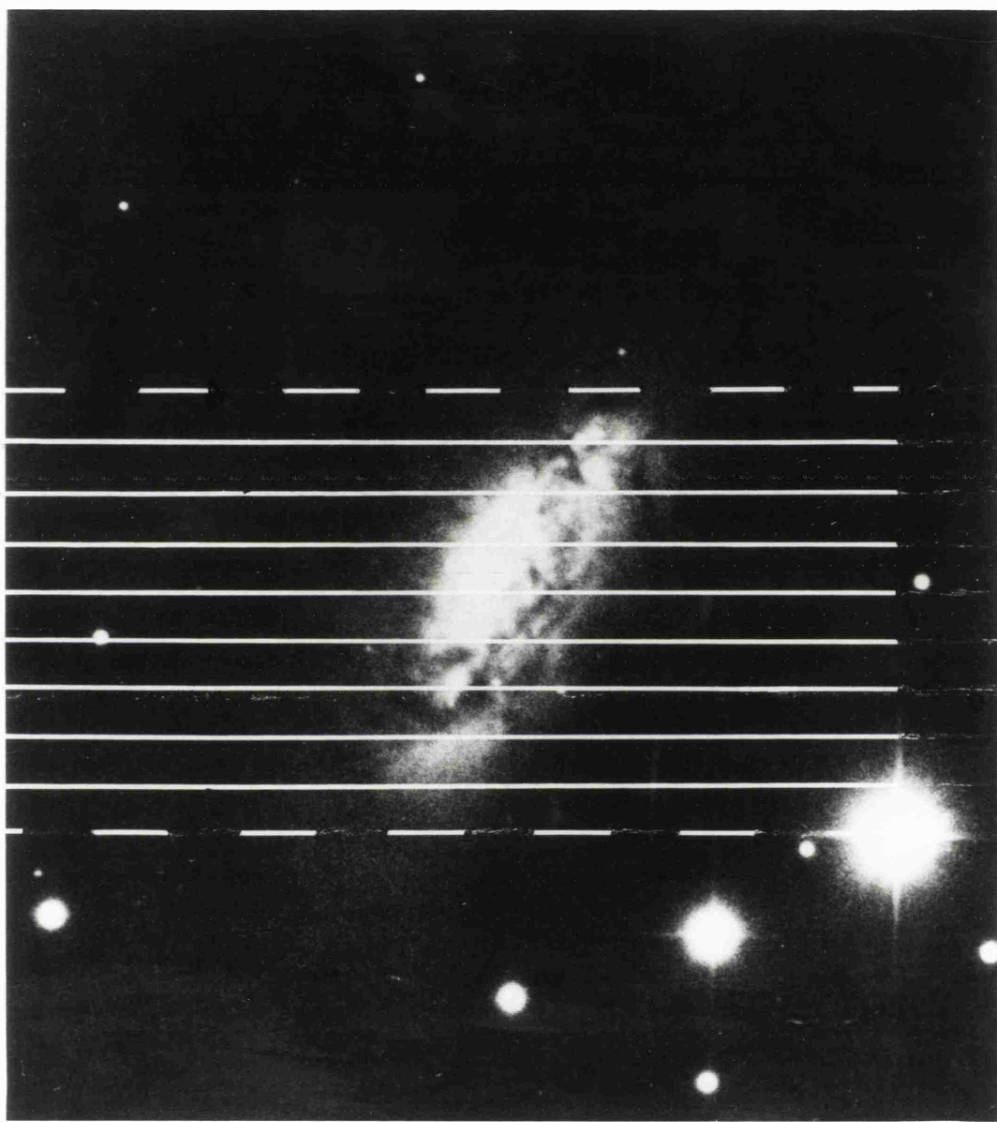


TABLE 5.1: DESCRIPTION OF 2.2  $\mu\text{m}$  MAPPING SCANS

R.A. Extent of Scans : Start : 02h 31m 10.48s ; Finish: 02h 31m 25.15s (Epoch 1950)

Scan Rate : 0.423 arcsec sec<sup>-1</sup>

Scan No.	Declination Channel, of Sky Beams		Source Beam	COMMENTS	Channel No. of Profiles Obtained (see fig. 5.4)
	Northern (-ve)	Southern (+ve)			
1	+0"	-30"	0"	No detection of galaxy. Scans 1 and 2 establish Southern limit of 2.2 $\mu\text{m}$ emission. Two field stars detected.	0
2	+10"	-20"	+10"	Galaxy detected by Northern beam. Profile uncontaminated. Two field stars detected.	1
3	+20"	-10"	+20"	Galaxy detected by Northern beam. Profile uncontaminated. Field star detected.	2
4	+30"	0"	+30"	Galaxy detected by Northern beam. Profile uncontaminated. Field star detected.	3
5	+40"	+10"	+40"	Galaxy detected by both beams. Northern beam on brighter part of galaxy. +40" profile corrected by adding uncontaminated +10" profile (scan 2).	4
6 <sup>+</sup>	+50"	+20"	+50"	Galaxy detected by both beams. Northern beam on brighter part of galaxy. +50" profile corrected by adding uncontaminated +20" profile (scan 3).	5
7 <sup>+</sup>	+60"	+30"	+60"	Galaxy detected by both beams. Northern beam on brighter part of galaxy. +60" profile corrected by adding uncontaminated +30" profile (scan 4).	6
8	+70"	+40"	-	Both beams on equally bright parts of galaxy. Peak-trough profile obtained as galaxy major axis at an angle of $\sim 60^\circ$ to scan direction.	not used

9 <sup>+</sup>	+80"	+50"	+50"	Galaxy detected by both beams. Southern beam on brighter part of galaxy. +50" profile corrected by adding uncontaminated +80" profile (scan 12).	5
10 <sup>+</sup>	+90"	+60"	+60"	Galaxy detected by Southern beam. Profile uncontaminated.	6
11	+100"	+70"	+70"	Galaxy detected by Southern beam. Profile uncontaminated.	7
12	+110"	+80"	+80"	Galaxy detected by Southern beam. Profile uncontaminated.	8
13	+120"	+90"	+90"	Galaxy not detected. Reference beam well north of galaxy. Scans 12 and 13 establish north limit of 2.2 $\mu$ m emission.	9
14	+130"	+100"	+100"	No detection of galaxy. Reference beam well north of galaxy.	not used

\* Declination positions are relative to field star,  $\delta = 29^{\circ}04'41.0''$ .

+ Note that for the dec channels +50" and +60" two profiles were obtained. These were added together to improve S/N.

TABLE 5.2: J H K SLIT SCANS DESCRIPTION

Declination Channel:	29 <sup>o</sup> 05' 36" (1950)
R.A. Extent :	02 <sup>h</sup> 31 <sup>m</sup> 10.48 <sup>s</sup> (1950) (Start)
	02 <sup>h</sup> 31 <sup>m</sup> 25.15 <sup>s</sup> (1950) (Finish)
Scan Rate :	0.423"/sec
Effective Aperture :	30" x 10" (FWHM)
Sky Conditions :	Photometric
No. of Scans :	3 at each wavelength

backlash eliminated it is believed that positional uncertainty is less than four arcseconds (see Chapter 2).

(b) JHK EAST-WEST SCANS

Three scans were made at each wavelength. All the scans traversed an identical path which was designed to pass through the optically brightest part of the galaxy since this was known to be approximately coincident with the brightest  $2.2 \mu\text{m}$  region. (Estimated from the previous  $2.2 \mu\text{m}$  mapping scans). Details of the scans are given in Table 5.2. In these observations a north-south oriented slit aperture of sky-projected dimensions  $40 \times 10$  arcseconds was used. However, as the beam separation was only 30 arcseconds, the effective size of the beam was reduced to  $30 \times 10$  arcseconds. A narrow slit aperture was chosen for this work as it effectively gives better resolution in the direction of the scan without reducing the signal to that received with a circular aperture of diameter equal to the slit width.

Calibration for both the mapping and the slit scans was with respect to the Johnson standard  $\alpha$ -Tri ( $m_K = 2.24$ ,  $m_H = 2.39$ ,  $m_J = 2.53$ ). As sky conditions were "photometric" during all the NGC 972 observations the calibration star was observed approximately once every hour.

### 5.3 DATA REDUCTION AND RESULTS

(a)  $2.2 \mu\text{m}$  MAPPING

In infrared astronomy the "source-beam" is usually the positive channel and the "reference-beam" is the negative channel. In any given mapping scan of NGC 972 either the positive or the negative channel was used as the source-beam depending on which one was pointing at a part of the galaxy. As the beam separation was less than the  $2.2 \mu\text{m}$  extent

of the galaxy, sometimes both beams were situated on its  $2.2 \mu\text{m}$  emission, in which case the source beam was taken as that pointing at the brighter part of the galaxy. Profiles obtained under this circumstance required correction to eliminate "reference-beam contamination".

Table 5.1 specifies which beam was the source-beam in each scan, and summarises where and how corrections were made. In scans 1 and 13 the reference-beam was well south and well north of the galaxy respectively, yet no signal above the background noise was detected in the locality of the galaxy's faint, outer structure along these channels. Thus the northern and southern limits of the system-detectable  $2.2 \mu\text{m}$  emission were established, and consequently it was only necessary to correct profiles from scans where the reference beam was within these limits. The scans in question were numbers 5, 6, 7, 8 and 9. As the beam separation was an exact multiple of the declination separation of adjacent scans, the contaminated profiles could be directly corrected since the flux in the reference-beam had been measured in one of the (uncontaminated) scans across the outer detectable parts of the galaxy. Hence a contaminated profile was corrected by adding the profile seen by the reference beam (see table 5.1). Eight profiles were finally obtained corresponding to the brightness distributions across channels 1 to 8 (see fig. 5.4). These eight and two "zero-profiles" for channels 0 and 9 made up the matrix from which an isophotal contour map of the galaxy could be constructed. The contours were drawn by the Leicester Cyber 73 computer using the CGHOST routine CONTIL. The map is shown in fig. 5.5; dashed contours are at intervals of  $1.9 \times 10^{-31} \text{ W m}^{-2} \text{ Hz}^{-1} \text{ arcsec}^{-1}$ , and the solid contours are at intervals of  $7.6 \times 10^{-31} \text{ W m}^{-2} \text{ Hz}^{-1} \text{ arcsec}^{-2}$ . Dashed contours are omitted from  $7.6 \times 10^{-31} \text{ W m}^{-2} \text{ Hz}^{-1} \text{ arcsec}^{-2}$ . The outermost contour corresponds to  $18.8 \text{ m}_K \text{ arcsec}^{-2}$ , and is the lowest surface brightness mapped to date

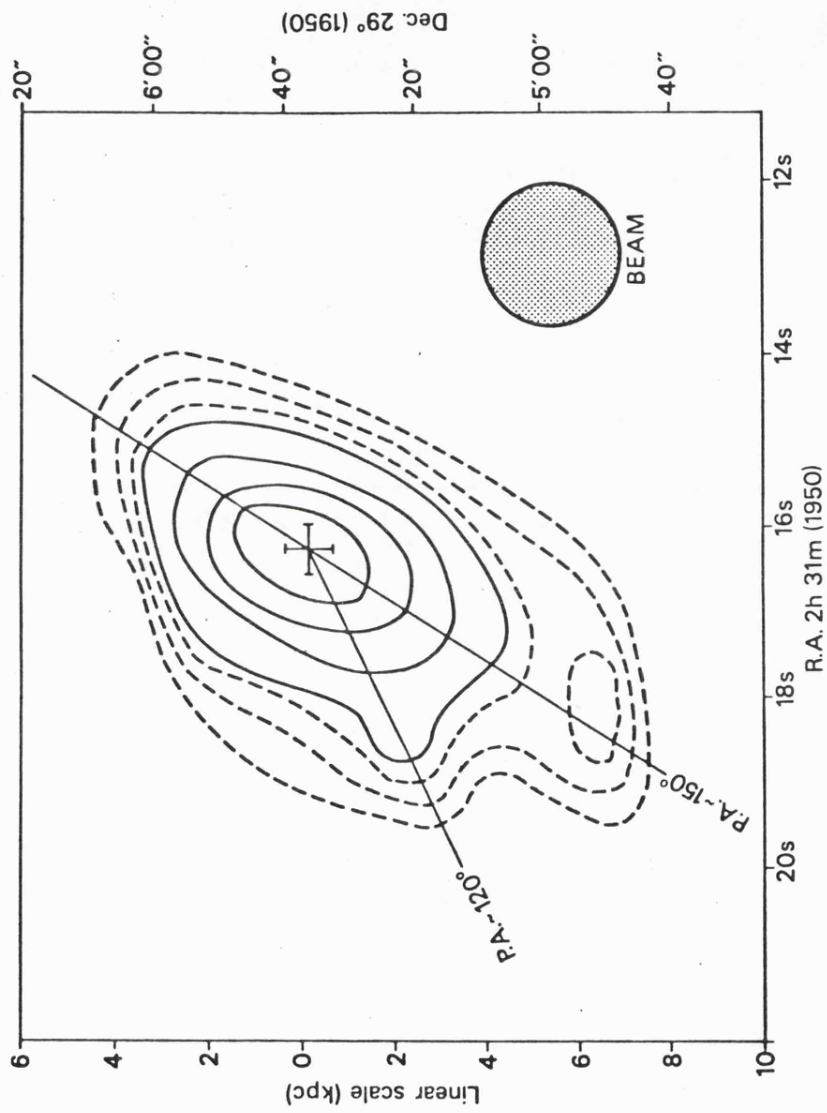


Fig. 5.5 : 2.2  $\mu$ m map of NGC 972

Table 5.3: Slit Scan Data\*

r"	m <sub>J</sub>	m <sub>H</sub>	m <sub>K</sub>	J-H	H-K
15" W	13.8 ± .4	12.34 ± .1	11.86 ± .16	1.46 ± .50	0.48 ± .26
10" W	11.85 ± .08	10.96 ± .04	10.8 ± .07	0.89 ± .12	0.16 ± .11
5" W	10.79 ± .03	10.10 ± .02	9.75 ± .02	0.69 ± .05	0.35 ± .04
0"	10.33 ± .02	9.72 ± .02	9.23 ± .02	0.61 ± .04	0.49 ± .04
5" E	10.70 ± .03	10.14 ± .02	9.59 ± .02	0.56 ± .05	0.55 ± .04
10" E	11.44 ± .05	10.80 ± .04	10.39 ± .04	0.64 ± .09	0.41 ± .08
15" E	12.21 ± .10	11.43 ± .06	11.23 ± .06	0.78 ± .16	0.20 ± .12
20" E	12.81 ± .18	12.22 ± .11	11.83 ± .15	0.59 ± .29	0.39 ± .26

\* Uncorrected for reference beam flux.

in an external galaxy. The error bar at the centroid indicates the positional uncertainty and the shaded circle indicates the beam size.

The map is corrected for atmospheric extinction but not for galactic absorption, however the latter will be small at K,  $A_K \sim 0.03$ , using  $A_K = 0.08 A_V$  and  $A_V = 0.15 \operatorname{cosec} b$ , or even less,  $A_K \sim 0.01$  if we assume the Sandage (1973) absorption-free polar-cap model,  $A_V = 0.10 (\operatorname{cosec} b - 1)$ . The Galactic latitude of NGC 972 is  $b^{\text{II}} = -28.43$ . (Further details of Galactic absorption corrections are given in Chapter 2.)

#### (b) THE JHK SLIT SCANS

The three profiles at each wavelength were added together to improve the signal-to-noise ratio, and the resultant profiles (see Chapter 2) were calibrated against  $\alpha$ -Tri. The usual extinction-curve procedure was used to correct for atmospheric absorption.

The corrected data are listed in Table 5.3, and the observed profiles are shown in Chapter 2.

### 5.4 DISCUSSION

#### (a) GROSS FEATURES OF THE MAP

The  $2.2 \mu\text{m}$  map covers a region approximately equivalent in extent to the optical image of the galaxy seen in the Hubble Atlas print (Sandage, 1961) which in turn corresponds to the "main body" region of Burbidge et al., 1965 (see section 5.1). The scans made extended into the faint outer regions beyond the main body of the galaxy, but no signal brighter than the background noise-level was ever detected, indicating that the faint emission from the outer structure is not unusually bright at  $2.2 \mu\text{m}$  relative to the blue. The position angle of the  $2.2 \mu\text{m}$  major axis is approximately  $150^\circ$ , and so is essentially the

same as the figure of  $149^\circ$  given by Burbidge et al. (1965) from their blue-band photograph. The  $2.2 \mu\text{m}$  centroid is, within the limits of uncertainty, coincident with the small nucleus which is clearly visible on the red and  $\text{H}\alpha$  narrow band photographs of Lynds, 1974. The inner contours are essentially featureless, indicating a smooth, roughly symmetric distribution of  $2.2 \mu\text{m}$  emission. On the eastern edge of the galaxy however there is an extension of emission relative to that on the western side. There is also a definite structure in the  $2.2 \mu\text{m}$  contours along P.A.  $\sim 120^\circ$ . The east-west brightness distribution is quite unlike that suggested by the contours of the blue-waveband maps of Bernacca and Bertola, 1969 (see fig. 5.6) and Blackman (1979) which both show a more rapid decline in surface brightness on the east side, relative to that on the west. The asymmetry is probably due to thicker dust lanes on the east side of the galaxy, which are not so apparent in optical photographic images as those on the west which are conspicuous as they are seen against the bright main body of the galaxy. The exact location of the centroids of the B-maps of Bernacca and Bertola, and of Blackman, are not specified, but it is estimated\* that these are within five arcseconds of the  $2.2 \mu\text{m}$  centroid, and may be coincident. The major axes of the maps are colinear to within  $5^\circ$ .

The structure seen in the  $2.2 \mu\text{m}$  contours along position angle  $120^\circ$  is not clearly evident in the optical image on the Hubble Atlas print, but does have a counterpart in the blue map of Bernacca and Bertola, and is distinguishable on the long exposure print given in Burbidge et al. The feature seems more prominent at the longer wavelength but this could be due simply to greater obscuration of the blue

---

\* Estimated by comparison of the B and K maps with the photographs of Lynds and Sandage, using ruler and protractor.

light. The most obvious similarity in the B and K waveband maps is the outlying bright region situated some fifty arcseconds south of the centre along the major axis. The fact that the feature appears at both wavelengths indicates that the intervening region of lower surface brightness cannot be explained simply by a dense dust lane, i.e. the region (henceforth known as region A) is anomalously bright relative to the (exponential) distribution extrapolated from the inner contours. It is interesting to note that although region A is as bright at  $2.2 \mu\text{m}$  (and in the B-band) as, for instance, the region thirty five arcseconds northwest of the centroid, it is completely devoid of any of the bright  $H\alpha$  features present in the latter region and throughout the rest of the galaxy (Lynds, 1974). This fact strongly suggests that there has been no recent star formation in region A. In this respect region A is markedly different from the rest of the bright part of the galaxy where star formation appears to be continuing vigorously.

Fig. 5.6 shows the  $2.2 \mu\text{m}$  map side-by-side with the B-band map of Bernacca and Bertola, 1969 (contour levels not given by the authors) so allowing a qualitative comparison of the two to be made. Along the major axis the overall luminosity distributions at B and K are very similar, and furthermore Blackman (1979) has shown that the same structure is seen at U, V and R also. As the degree of NW-SE asymmetry in the galaxy's structure is similar at all wavelengths from ultraviolet to infrared, it cannot be due to obscuration by dust. Bernacca and Bertola, and Blackman, have also shown that in the visible the gross distribution of surface brightness along the major axis is essentially exponential, and that no spheroidal component is present. There is not sufficient  $2.2 \mu\text{m}$  data of high signal-to-noise to produce an accurate major axis brightness profile, however the overall similarity in the B and K-band maps strongly suggests purely disc structure exists at  $2.2 \mu\text{m}$  also.

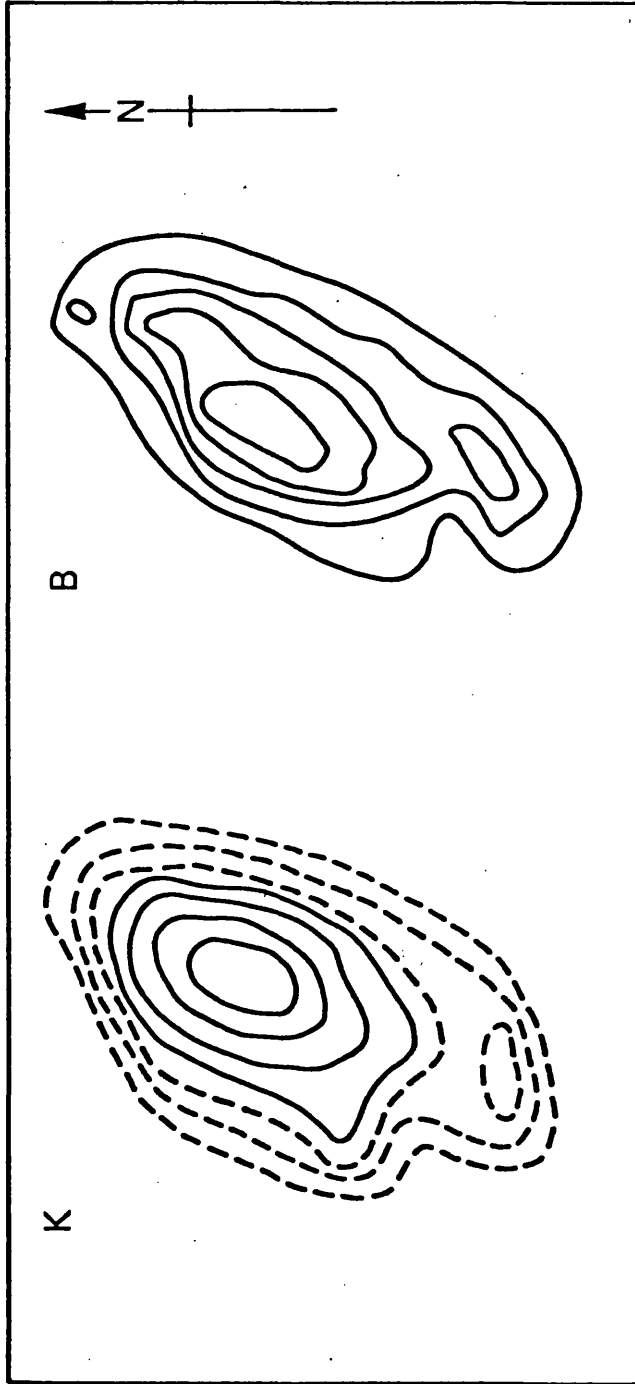


Fig. 5.6 : Comparison of B and K maps of NGC 972

## (b) CLASSIFICATION OF NGC 972

NGC 972 has been variously classified as aI? (Morgan, 1958), Sb (Sandage, 1961), IO (de Vaucouleurs et al., 1964, 1976) and Sbc/Abc (Van den Bergh, 1976). This confusion has been due in part to the chaotic distribution of dust across the galaxy which obscures the underlying morphology, but also to the general uncertainty in the astronomical community over the physical significance of the IO/IrrII classification. In recent years several authors have emphasised that IO and similar galaxies are probably not a physically distinct species, but rather are (previously) normal systems which have undergone some form of interaction or disruption (Krienke and Hodge, 1974; Solinger et al., Cotrell, 1977) which has left their original optical appearance distorted by a veil of irregular dust lanes. On this basis galaxies such as NGC 972 may be considered both as IO systems and as (disturbed) "ordinary" galaxies. We will therefore examine the classifications of Morgan, Sandage and Van den Bergh given above to see how well they describe the underlying galaxy, and then later (section 5.4f) consider the possible mechanisms by which NGC 972 could have been transformed into an IO system.

Morgan's a-type spectral classification is undoubtedly correct, but his "form family" classification, I, is vaguely defined and means simply "not clearly E or S", but on the basis of the broad-band photographic evidence alone it is perhaps valid. However the H $\alpha$  and red narrow band photographs of Lynds show a definite nucleus, and as true irregular (Im) systems do not have a nucleus NGC 972 cannot now be considered as an irregular galaxy of the Magellanic type. Sandage's Sb classification is clearly incorrect if Sb galaxies are considered to be systems which have a definite spheroidal bulge, since the absence of this component in NGC 972 has now been clearly established (see

above). Thus Van den Bergh's selection of the "bc" subcategory is nearest to the mark, but should probably be amended to simply "c". (No Sd or later systems are defined in Van den Bergh's (1976) system.) However his suggestion that NGC 972 is a possible transition system lying between his "normal spirals" (S) and "anemic spirals" (A) is almost certainly incorrect. Van den Bergh defines anemic spirals as objects intermediate between "vigorous gas-rich normal spirals" and "gas-poor SO systems". (SO's are seen now as paralleling spiral galaxies in a "tuning-fork" type diagram, and not as a species intermediate between elliptical and spiral galaxies.) His anemics are objects, found primarily in rich clusters, in which the star formation rate is much lower than in the corresponding normal-type spiral (i.e. Sa, Sb or Sc). NGC 972 however shows strong  $H_{\alpha}$  throughout its main body and is of mean spectral type "a", and so does not fit into the "anemic" definition. Furthermore, NGC 972 is almost certainly a field system and is quite definitely not in a rich cluster. The misclassification may be due to the soft, hazy texture of the photographic image of NGC 972 as this is a characteristic of the spiral arms of anemic galaxies. It is also however a quality of the whole image of all IO galaxies.

On the Hubble/Sandage/de Vaucouleurs system the underlying main body of NGC 972 is probably best described by the Sc/Sd classification, and on the Van den Bergh (1976) system, Sc.

(c) A (B-K) COLOUR GRADIENT?

The available data at B and K are exceedingly inhomogeneous, and therefore a detailed analysis of the colour variation within the galaxy is not warranted. Nevertheless, there does appear to be evidence of a significant colour difference between the centre and the edge of the galaxy, as defined by the outer  $2.2 \mu\text{m}$  contours. From the infrared

data and the calibrated B map of Blackman (1979) it is possible to obtain estimates of the mean B-K colour at easily identifiable locations within the galaxy. In the centre this is  $B-K \sim 4.3 \pm 0.2$  and at the northwest and southeast ends of the K map it is  $B-K \sim 3.2 \pm 0.4$ , indicating the significant difference  $\Delta(B-K) \sim -1.1 \pm 0.6$ . The colour at the centre is significantly redder than that expected from the V-K ( $\sim 3.0$ ) and B-V ( $\sim 0.5$ ) of a late-type spiral. Obscuration by dust seems the most obvious explanation although this could only be confirmed by homogeneous, photoelectric photometry at all wavebands in the optical and near infrared. The colour difference between the centre and edge of the galaxy is difficult to interpret in isolation and in view of the uncertainty involved, but is in qualitative agreement with optical observations of galaxies generally, which show a bluenning of light with increasing radius. The only comparable optical/infrared data is that of Strom et al. (1977) who measured the radial change of the V-K colour index in the E5 galaxy NGC 2768 and the SO galaxy NGC 3115. The colour change seen in these objects amounts to  $\Delta(V-K) \sim -0.35$  at  $r/r(\varrho) \sim 0.6$  ( $r$  is the radial distance,  $r(\varrho) = D(\varrho)/2$ ). This corresponds approximately to the radial distance in NGC 972 at which the colour difference,  $\Delta(B-K) \sim 1.1$  has been found. In the early-type galaxies NGC 2768 and NGC 3115 the colour gradient is interpreted in terms of a radial change in stellar metallicity; the B-K variation in the late-type galaxy NGC 972 is probably due to the combined effect of radial changes in metallicity, mean spectral type and dust obscuration, although the presence of a very red, non-stellar source at the nucleus cannot be dismissed at this stage.

(d) THE 2.2  $\mu$ m LUMINOSITY OF NGC 972

The luminosity of the central  $\sim 3$  kpc of NGC 972 (22 arcsec

aperture,  $R = 30 \text{ Mpc}$ ,  $H_0 = 55 \text{ km s}^{-1} \text{ Mpc}^{-1}$ ) can be obtained from our data ( $m_K = 9.2$ ), and it is interesting to compare this to the  $2.2 \mu\text{m}$  luminosity of the equivalent central region of M31. The  $2.2 \mu\text{m}$  luminosity of the corresponding region in M31 was determined by integration of the  $2.2 \mu\text{m}$  map of Matsumoto et al. (1977), within a radius of 7.85 arcminutes, assuming M31 to be at a distance of 0.7 Mpc. The  $2.2 \mu\text{m}$  luminosity is somewhat greater in NGC 972,  $M_K = -23.2$ , compared to  $M_K = -22.5$  for M31. The result is notable since in M31 the region concerned is within the spheroidal bulge which has mean spectral type  $gk/k$  (Morgan 1958, de Vaucouleurs et al. 1976) and is rich in K and M giants, whereas the centre of NGC 972 is of mean spectral type  $af/a$  and has no spheroidal component. Integration of the  $2.2 \mu\text{m}$  map of NGC 972 yields  $m_{(K,\text{total})} \sim 8.3 \pm 0.2$ , or  $M_{(K,\text{total})} \sim -24.1$ . Blackman (1979) gives  $M_{(B,\text{total})} = -20.56$  for NGC 972, and Bernacca and Bertola give  $M_{(B,\text{total})} = -20.15$ . In comparison, de Vaucouleurs (1958) gives  $M_{(B,\text{total})} = -19.9$  for M31. Assuming the total integrated B-K colour for M31  $\sim 4.0$ , then  $M_{(K,\text{total})} = -23.9$ . This is again a surprising result since it shows that the total B and K luminosities of NGC 972 are also comparable to those of M31, yet the mass ratio of the galaxies, mass of M31-to-mass of NGC 972, is about fifteen. (Burbidge and Burbidge, Chapter 3 in "Galaxies and the Universe"). It follows that the mass to luminosity in NGC 972 is one fifteenth that in M31 at B and K. The widespread presence of strong  $H\alpha$  in NGC 972 implies a large and extensive population of hot, young stars which might in themselves account for the relatively high B luminosity, yet to do so either their number density must be much greater than in M31 or their luminosity function must be quite different from that in M31, i.e. more massive stars must dominate. These hot, young stars could not however account for the high  $2.2 \mu\text{m}$  luminosity of NGC 972, and so alternative sources must be considered. Since the low mass, early spectral type

and disc morphology of the galaxy rule out the presence of a sufficiently large population of K and M giants the only remaining possible stellar source would be a large number of M supergiants, otherwise non-stellar sources must be invoked. The widespread  $H\alpha$  emission and the dusty appearance of the galaxy suggest that free-free emission and radiation from heated dust are the most likely non-stellar sources.

(e) SLIT SCANS - JHK COLOURS

Direct quantitative comparison of the slit scan and mapping data cannot be made as the former is not corrected for reference beam flux, and as the apertures used were of different size and shape. There is however a clear qualitative agreement between the east-west brightness distributions implied by the two data sets. In particular the eastern extension of  $2.2\ \mu\text{m}$  emission suggested by the contour map is confirmed and is clearly present at  $1.65\ \mu\text{m}$  and  $1.25\ \mu\text{m}$  also.

Table 5.3 shows that the H-K colour near the centre of the galaxy is significantly redder than that of a normal late-type galaxy, whereas the J-H index is significantly bluer. Obviously this cannot be accounted for by obscuration as this would result in greater reddening of the J-H index. Similarly an unusually large population of M supergiants - remnants of possible recent massive star formation - would lead to both indices being redder than normal. The various astrophysically common non-stellar sources are discussed in section 1.5, and of these only free-free emission could contaminate the colours of a normal galaxy in the way observed.

Fig. 5.7a shows the radial variation of the J-H and H-K colours along the central east-west line, and fig. 5.7b shows the corresponding positions of the slit axis (and reference beam axis), for each data point, superimposed on the contour map. Away from the centre the colours

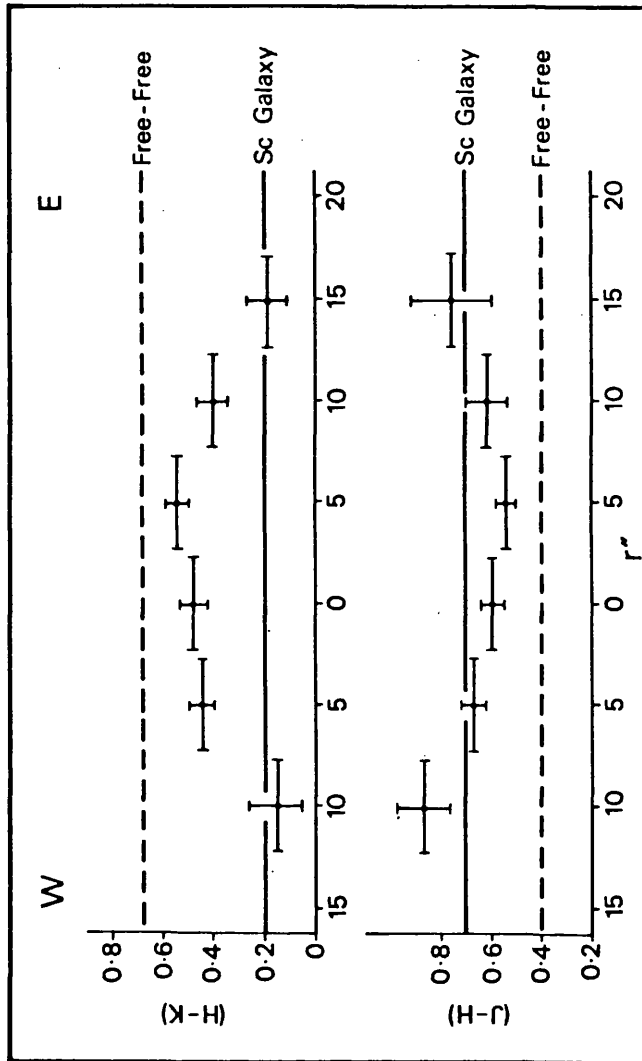


Fig. 5.7a: Radial variation of colour indices in NGC 972

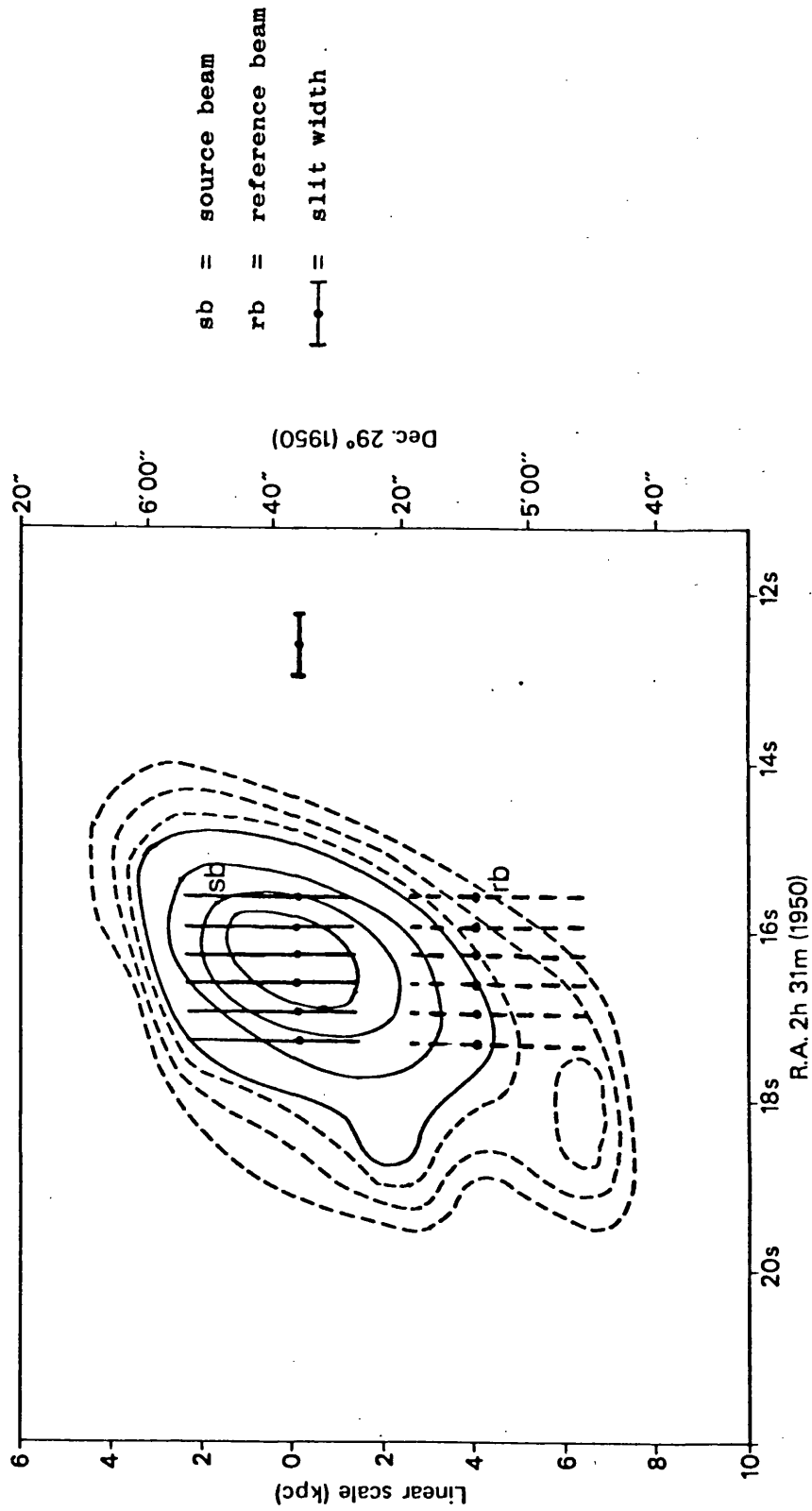


Fig. 5.7b : Slit positions corresponding to fig. 5.7a.

tend towards those of a normal late-type galaxy which implies that the radial colour variation is not due to unusual colours in the reference beam. The anomalous colours do however appear to arise in an extended region which seems asymmetrically distributed about the centre of the galaxy. The H-K index appears to be more contaminated by a free-free component, but this could be due to greater reddening of the J-H index, or alternatively by the H-K index being pushed further away from the late-type galaxy line by a warm dust component which would not greatly change the J-H index.

Table 5.4 gives the colours of a late-type galaxy as it becomes increasingly contaminated by optically thin free-free emission. The colours observed in the slit scans of NGC 972 do not exactly fit in with any of those in the simple late-type galaxy/free-free model, although precise agreement cannot be expected since dust obscuration, and possibly dust emission, will affect the colours of this galaxy. However if free-free is assumed to be the dominant non-stellar source, it is clear from tables 5.4 and 5.3 that  $\sim 50\%$  of the  $2.2 \mu\text{m}$  flux must be from free-free emission to account for the observed near infrared colours close to the centre.

No infrared data at longer wavelengths has been reported in the literature, so to investigate the free-free hypothesis further we must examine the radio data. The only results available are those of McCutcheon and Davies (1970) and McCutcheon (1973). These however suggest the radio emission is the standard power law type common in normal spirals. Fig. 5.8 summarises the data relating to the hypothesis that free-free emission may be a significant component in the  $2.2 \mu\text{m}$  flux of NGC 972. In the diagram the crosses represent the observed radio points, the filled circle is the observed  $2.2 \mu\text{m}$  point and the empty circle indicates the fraction of the observed  $2.2 \mu\text{m}$  flux that

Table 5.4: Late-Type Spiral/Free-Free\* Mixtures

% Free-Free in 2.2 $\mu\text{m}$ Flux	J-H	H-K
0	0.73	0.21
10	0.71	0.25
20	0.68	0.29
30	0.66	0.34
40	0.63	0.38
50	0.60	0.42
60	0.58	0.47
70	0.54	0.52
80	0.51	0.58
90	0.47	0.64
100	0.43	0.70

\* Fiducial Colours from Aaronson, 1978.

(Free colours for  $T_e \sim 8000^{\circ}\text{K}$ )

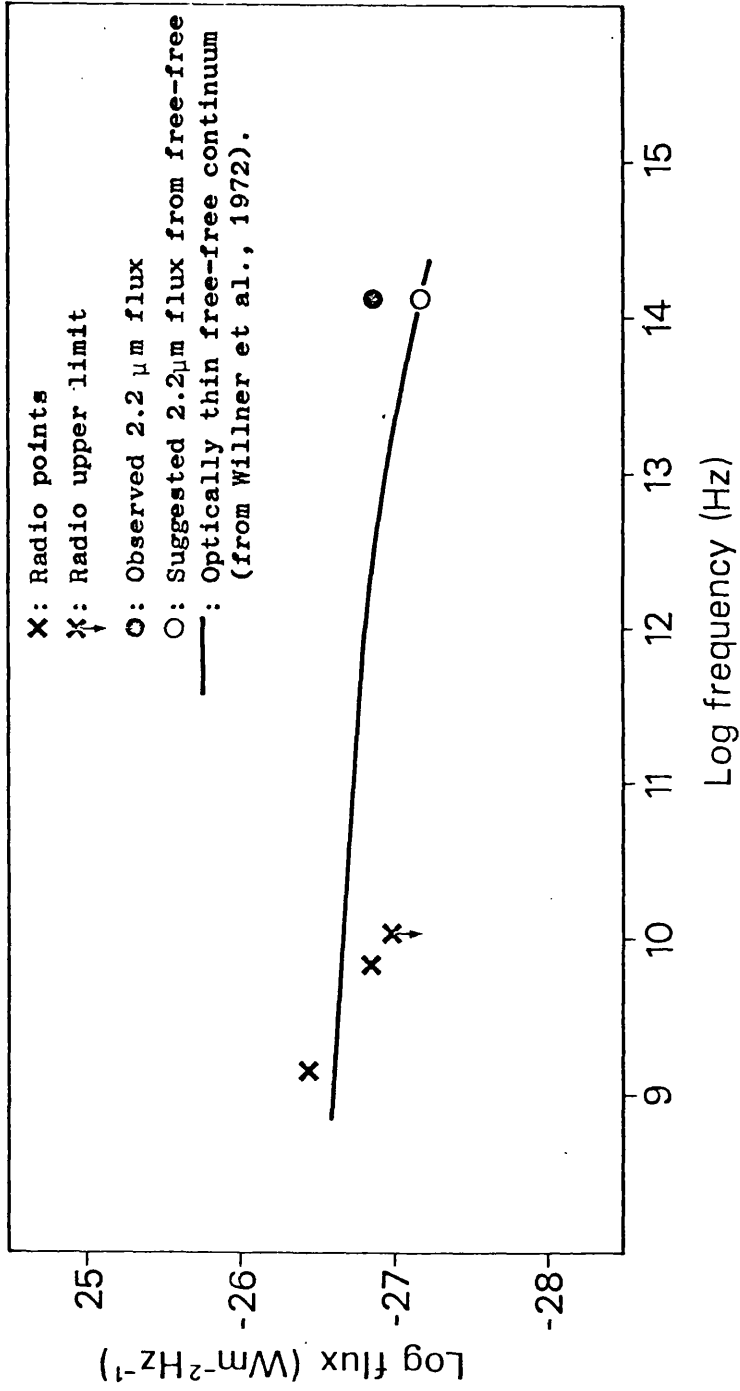


Fig. 5.8 : Free-free emission from NGC 972 ?

must be due to optically thin free-free emission if this is to account for the observed near infrared colours. The black curve represents the optically thin, radio to infrared, free-free continuum (as determined by Willner et al., 1972) extended from the necessary  $2.2 \mu\text{m}$  point. Thus it can be seen from fig. 5.8 that if  $\sim 50\%$  of the  $2.2 \mu\text{m}$  flux is due to free-free emission, then the free-free source must become optically thick shortward of  $\sim 10^{10.6}$  Hz. Further observations at J,H,K,L and  $10 \mu\text{m}$  are required to confirm the presence of a free-free component in the infrared emission of NGC 972.

(f) NGC 972 AS AN IO GALAXY

Of the twelve or so IO systems known, only three are apparently isolated; NGC 972 is one of these. Cottrell (1977) suggests that all IO galaxies have undergone an interaction of some description, past or present. In some cases, such as NGC 5195, it is a close gravitational interaction between two galaxies, and in others such as M82 the interaction is with the tenuous intergalactic medium associated with small groups of galaxies. Until recently violent internal disruptions were seen as another possible disturbing influence in IO galaxies, but this mechanism is currently out of favour (see chapter 4). Nevertheless, if NGC 972 is an isolated system then an internal disturbance must be invoked to account for its unusual characteristics, unless NGC 972 has escaped the confines of the small group, or pair, of galaxies of which it was once a member. This remains as a possibility, but, as an alternative explanation, it is now tentatively suggested that NGC 972 may in fact be a pair of interacting galaxies, where the primary member is the Sc/Sd system, discussed in section 5.4b, which is seen as the main body of the NGC 972 system, and the secondary member is a small/dwarf galaxy which is seen as region A in the  $2.2 \mu\text{m}$  map. This

suggestion is based upon the following three points:

- i) Region A has now been shown to be separate from the main body, and not just an artefact of a dense dust lane.
- ii) It is unlikely that region A is an anomalously bright part of a spiral arm since it is completely devoid of any of the  $H\alpha$  emission (characteristic of bright spiral arms) seen in other regions of the main body of comparable surface brightness (B or K).
- iii) The total, absolute K magnitude of region A,  $M_K \sim -20.5$ , is typical of that of a small galaxy,  $M_V \sim 16-18$ , assuming the integrated V-K index of such systems is  $\lesssim 3.0$ , and is rather brighter than M32 or the SMC for instance.

The secondary galaxy could be a small elliptical, or a Magellanic irregular in which star formation has been terminated by a mechanism similar to that which terminated star formation in the disc of M82, following its interaction with the M81 group (O'Connell and Mangano, 1978). The interacting pair hypothesis offers an explanation of the considerable northwest-southeast asymmetry in NGC 972, and the extensive low surface brightness emission which envelopes the brighter central part of the system is presumably qualitatively similar to that which surrounds the M51 system.

(g) COMPARISON OF THE M82 AND NGC 972 OBSERVATIONS

The observations of NGC 972 were quite different, in terms of scale, than those of M82 (chapter 4). In the latter an area of 1500 pc diameter was mapped with a best resolution equivalent to 90 pc in M82, whereas in the observations of NGC 972 a region of 14 kpc diameter was mapped with a resolution equivalent to 3 kpc in NGC 972; i.e. the observations of NGC 972 covered the whole galaxy to ascertain its

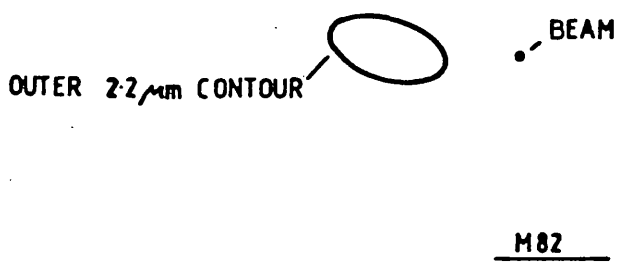
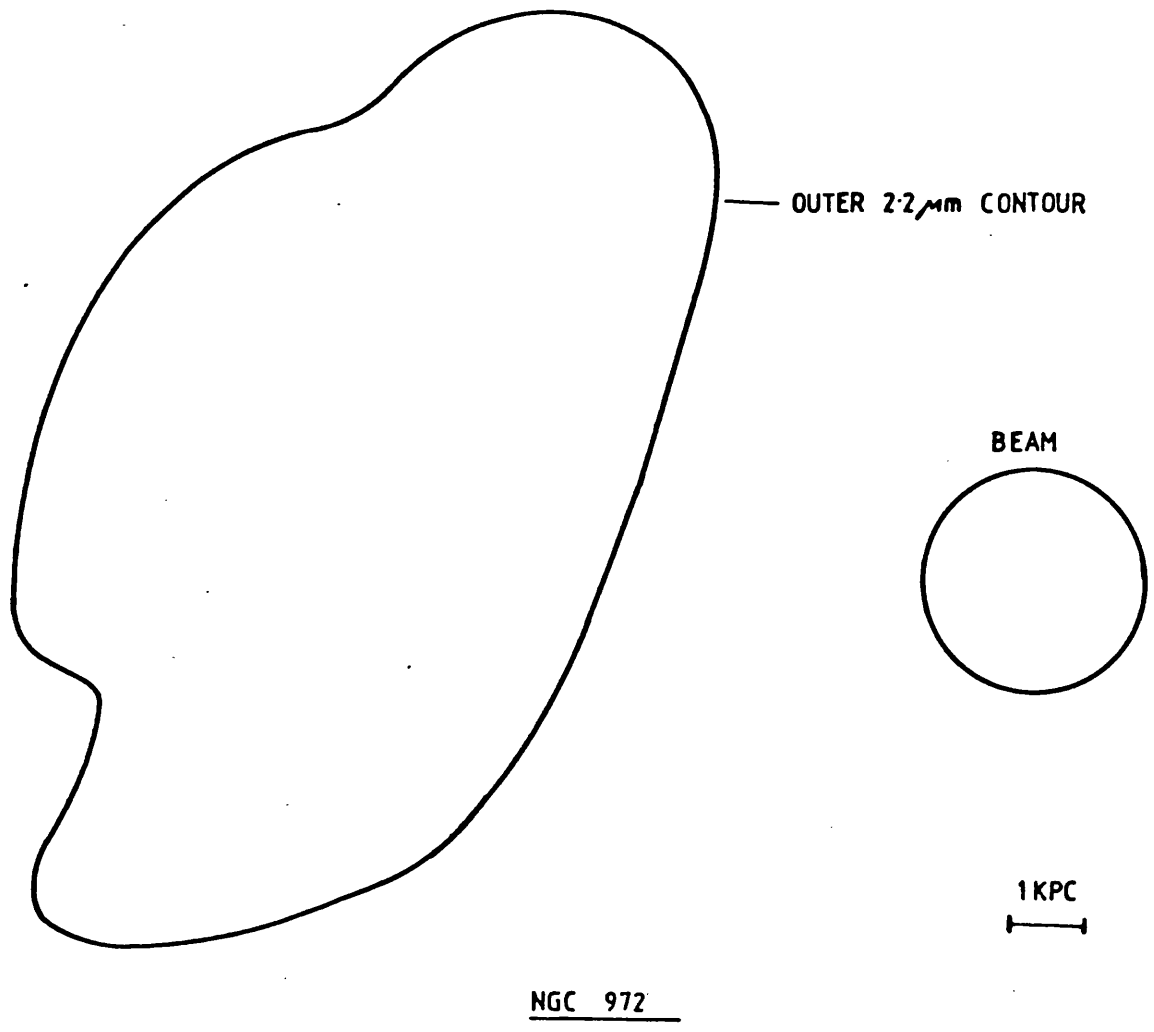


Fig. 5.9 : Relative scales of the NGC 972 and M82 observations

gross  $2.2 \mu\text{m}$  structure, whereas those of M82 were intended to make a detailed study of the  $2.2 \mu\text{m}$  distribution within a relatively small region of high surface brightness. Fig. 5.9 illustrates the linear scales involved in the two projects.

Despite the large difference in relative beam size, comparison of the luminosities of equivalent regions of the two systems can be made by extrapolation of the available data for M82. The observed K magnitude for the centre of M82 with various apertures between 6 and 105 arcseconds diameter ( $d$ ) (this thesis & Aaronson, 1978) fits the power law,  $m_K(d) = 10.15d^{-0.15}$  very closely (coefficient of determination,  $r^2 = 0.99$ ). For a beam of 200 arcseconds diameter ( $\approx 3 \text{ kpc}$ ) this magnitude-aperture relation predicts  $m_K = 4.6$ , or  $M_K = -22.9$ . The corresponding figure for the central 3 kpc of NGC 972 has been shown to be  $M_K = -23.2$  (section 5.4d), and thus it is apparent that the central regions of the two galaxies are of comparable  $2.2 \mu\text{m}$  luminosity. Both of these two IO systems have the gross properties, i.e. mass, disc morphology and mean spectral type, of late-type spirals of D.D.O. class II-III, such as M33, and it is now apparent that both are at least an order of magnitude more luminous at K than normal late-type systems of this D.D.O. class if typified by M33.\* This is believed to be due to enhanced star formation triggered by the interaction responsible for the IO-type appearance of the galaxies. A closer comparison of the luminosity and colour indices in NGC 972 and M82 could be made by observing NGC 972 with apertures of diameter  $\sim 5$  and 10 arcseconds, which would correspond closely to the JHK observations of M82 by Aaronson with apertures of 41 and 105 arcseconds. This would be difficult from Tenerife with the 1.5 m flux-collector, especially with a 5 arcsecond aperture, but would be easily possible from Hawaii with UKIRT.

\* (Penston, 1973 and Aaronson, 1978)

## CONCLUSIONS

The gross surface brightness distribution at  $2.2 \mu\text{m}$  in the galaxy NGC 972 has been mapped; except for an extension of emission to the east, which is clearly apparent at  $1.25 \mu\text{m}$  and  $1.65 \mu\text{m}$  also, the overall structure at this wavelength is remarkably similar to that seen in optical, broad-band photographs of the galaxy. The similarity suggests that the main features of the visible appearance of the galaxy, namely the considerable northwest-southeast asymmetry, and the apparent separation of the bright southern region (region A) from the "main body" of the galaxy, are not simply artefacts of dense dust lanes - as previously assumed. The brightness of region A at  $2.2 \mu\text{m}$ , its lack of  $\text{H}\alpha$  emission (common in the rest of the galaxy) and its (now established) separation from the main body suggest that it may be a small/dwarf galaxy whose interaction with the latter has resulted in the IO-type appearance of the system. The  $2.2 \mu\text{m}$  luminosity of the main body is at least an order of magnitude greater than that of other disk galaxies of similar mass and mean spectral type, if typified by M33. The observed near infrared colours suggest that free-free emission may be responsible for some of the  $2.2 \mu\text{m}$  luminosity, however further, homogeneous photometric observations at J,H,K,L and  $10 \mu\text{m}$  are required for confirmation of this, and to check for the presence of other non-stellar components.

## REFERENCES

- Aaronson, M. 1978, Ph.D. Thesis, Harvard University.
- Bernacca, P.L. and Bertola, F. 1969, Mem. Soc. astr. Ital., 40, 133.
- Blackman, C.P. 1979, M.N., 188, 93.
- Burbidge, E.M., Burbidge, G.R. and Prendergast, K.H. 1965, Ap. J., 142, 649.
- Cotrell, G.A. 1978, M.N., 184, 259.
- Freeman, K.C. 1970, Ap. J., 160, 811.
- Frogel, J.A., Persson, S.E., Aaronson, M. and Matthews, K. 1978, Ap. J., 220, 75.
- Humason, M.L., Mayall, N.U. and Sandage, A.R. 1956, A.J., 61, 97.
- Johnson, H.L., Mitchell, R.I., Iriarte, B. and Wisniewski, W.Z. 1966, Ariz. Univ. Lunar. Planet. Lab. Comms, 4, 99.
- Krienke, O.K. and Hodge, P.W. 1974, A.J., 79, 1242.
- Lynds, B.T. 1974, Ap. J., Suppl. S., 28, 391.
- Matthews, T.A., Morgan, W.W. and Schmidt, M. 1964, Ap. J., 140, 35.
- Matsumoto, T., Murakami, H. and Hamajima, K. 1977, P.A.S.J., 29, 583.
- McCutcheon, W.H. and Davies, R.D. 1970, M.N., 150, 337.
- McCutcheon, W.H. 1973, A.J., 78, 18.
- Morgan, W.W. 1958, P.A.S.P., 70, 364.
- O'Connell, R.W. and Mangano, J.J. 1978, Ap. J., 221, 62.
- Penston, M.W. 1973, M.N., 162, 359.
- Petit, E. 1954, Ap. J., 120, 413.
- Sandage, A.R. 1961, "The Hubble Atlas of Galaxies" (Carnegie Inst., Washington).
- Sandage, A.R., Becklin, E.E. and Neugebauer, G. 1969, Ap. J., 157, 55.
- Sandage, A.R., Sandage, M. and Kristian, J. (Eds.), "Galaxies and the Universe" (Univ. of Chicago Press).

- Solinger, A., Morrison, P. and Markert, T. 1977, Ap. J., 211, 707.
- Strom, K.N., Strom, S.E. and Wells, D.C. 1978, Ap. J., 220, 62.
- Van den Bergh, S. 1976, Ap. J., 206, 883.
- Vaucouleurs, G. de, 1958, Ap. J., 128, 465.
- Vaucouleurs, G. de, and Vaucouleurs, A. de, 1964, Reference Catalogue  
of Bright Galaxies, Univ. of Texas Press, Austin.
- Vaucouleurs, G. de, Vaucouleurs, A. de, and Corwin, H.G. 1976, Second  
Reference Catalogue of Bright Galaxies, Univ. of Texas Press,  
Austin.
- Willner, S.P., Becklin, E.E. and Visvanathan, N. 1972, Ap. J., 175, 699.

**APPENDIX**

**(A published paper reporting part of the M82 work)**

## Detection of a bright ridge in the 2.2- $\mu\text{m}$ emission of M82

J. A. Abolins, D. J. Adams and R. F. Jameson

*Astronomy Department, University of Leicester*

J. H. Hough *School of Natural Sciences, Hatfield Polytechnic*

D. J. Axon *Astronomy Centre, University of Sussex*

Received 1978 October 31

**Summary.** Photometric scans through the central region of M82, with a resolution of 6 arcsec reveal that the 2.2- $\mu\text{m}$  emission source has a compact ridge structure which is approximately aligned ( $\pm 10^\circ$ ) with the major axis of the galaxy. The source has an integrated  $K$  magnitude of 6.5 and dimensions of  $300 \times 75$  pc, corresponding to  $20 \times 5$  arcsec on the sky. The 2.2- $\mu\text{m}$  ridge embraces the bright visible knots A and E and lies close to the centre of the 10- $\mu\text{m}$  emission region and the sub-arcsecond radio source.

### Introduction

Two of the more unusual features of the galaxy M82 are that it shows a strong 10- $\mu\text{m}$  infrared excess (Kleinmann & Low 1970a) and that its optical image is surrounded by a faint but highly polarized halo (Bingham *et al.* 1976). Both features suggest that it contains a bright or 'active' nucleus. Such a nucleus is not apparent on visible and near-infrared photographs, which show instead a complex of bright knots and dark dust lanes presumably obscuring the nuclear region from view. Numerous attempts have been made to locate 'the missing nucleus' of M82, which has been variously attributed to the brightest optical features (Peimbert & Spinrad 1970), to hidden components such as the VLBI radio source (Geldzahler *et al.* 1977) or to the centre of symmetry of the optical polarization pattern (Solinger & Markert 1975). In an attempt to obtain a clearer picture of the underlying stellar structure of the central region of M82, we have made photometric scans across the galaxy at 2.2  $\mu\text{m}$ , at which wavelength the dust obscuration is likely to be only a tenth of that in the visible. Although M82 has previously been detected at 2.2  $\mu\text{m}$  by Kleinmann & Low (1970b) who report a flux of  $2.3 \pm 0.1 \times 10^{-26} \text{ W m}^{-2} \text{ Hz}^{-1}$ , these observations are the first high resolution surface photometry at this wavelength.

### Observations

The observations were obtained in 1977 July and 1978 March using the Hatfield infrared polarimeter (Cox, Hough & McCall 1978) at the Cassegrain focus of the 2.5-m Isaac Newton

telescope at Herstmonceux, Sussex. The instrument was operated as a single beam photometer by introducing a fixed HR Polaroid element in front of the rotating Polaroid element. The detector used was an Indium Antimonide photodiode, operated at 63 K. The advantages of this technique are that it avoids the problems of scanning an extended object with a sky chopping photometer, and that it minimizes the thermal drift problems encountered when using room temperature single beam choppers. The disadvantages are a loss in sensitivity, and the need to make corrections for the polarization of the source observed. In the case of M82, the observed  $2.2\text{-}\mu\text{m}$  polarization was so small ( $0.6 \pm 0.4$  per cent through a 6-arcsec aperture on the brightest region) that corrections for polarization were negligible. Photometric calibrations were derived from observations of the star 24 UMa with  $V = 4.57$  and  $K = 2.68$  (Johnson *et al.* 1966). The beam was located on the galaxy by offsetting the telescope from the star BD + 70 587 (RA  $9^{\text{h}} 51^{\text{m}} 26^{\text{s}}.3$ , dec  $69^{\circ} 53' 9''$  1950.0) in a manner devised to minimize the effects of backlash. The beam registration was checked with an off-axis guider, enabling us to keep within a positional uncertainty of  $\pm 2$  arcsec.

A 2-arcmin square field centred on the compact VLBI source was surveyed by scanning in both right ascension and declination with 23 and 11 arcsec beams. The data showed evidence of a strong source extended  $\sim 30$  arcsec in right ascension but unresolved in declination, superimposed on faint diffuse background emission. A high resolution map of this source was obtained from declination scans made at 3 arcsec intervals in right ascension using a 6-arcsec beam. No detection was recorded in the two extreme scans, thus enabling us to delineate the boundaries of the source. The contour map of Fig. 1 was constructed from the average of two scans in each of the remaining spatial channels. The general source morphology and location was confirmed from single right ascension scans in adjacent declination channels. However, since these scans had inferior signal/noise to the declination data they were not utilized in constructing the map of Fig. 1. The lowest contour, shown dotted in Fig. 1 may in any case be significantly distorted by noise.

The orientation of the source was determined by linear least-square fits through the peak signal in each right ascension channel and is aligned with the major axis of the galaxy within

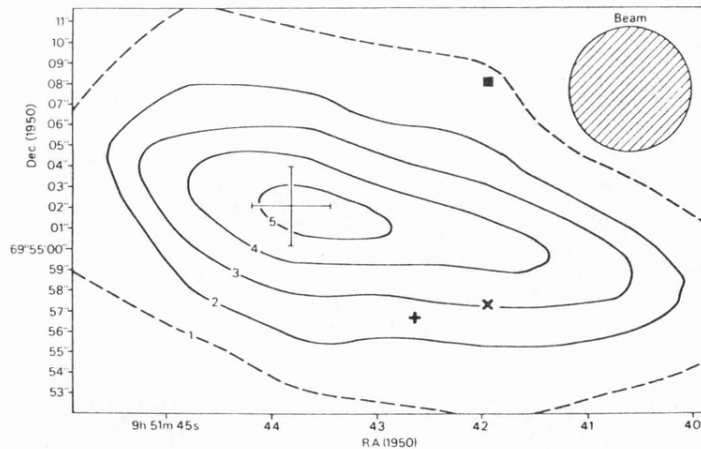


Figure 1. Two-micron contour map of M82. The lowest contour (shown dotted) is at  $2.8 \times 10^{-29} \text{ W m}^{-2} \text{ Hz}^{-1} \text{ arcsec}^{-2}$  and the contour interval is the same. The position of the  $2.2\text{-}\mu\text{m}$  peak is marked by a fine cross whose size indicates the positional uncertainty. Also marked are the centre of the  $2.2\text{-}\mu\text{m}$  emission due to Kleinmann & Low (1970b), the VLBI radio source  $\times$  and the  $10\text{-}\mu\text{m}$  centroid  $+$ .

an error of  $\pm 10^\circ$ . The source is clearly resolved as an extended object in the right ascension direction and if account is taken of the instrumental broadening the FWHM size of the source is approximately  $20 \times 5$  arcsec. The elongated shape of the feature leads us to describe it as a 'ridge'; however, with the present resolution a source morphology consisting of several stellar or semi-stellar objects cannot be ruled out. One of the most striking aspects of the source, which is visible in Fig. 1, is its marked east–west asymmetry, which was also apparent in the right ascension profiles. The integrated  $K$  magnitude of the ridge is  $6.5 \pm 0.2$  which is in reasonable agreement with the large beam spot photometry of M82 obtained by both Kleinmann & Low (1970b) and Willner *et al.* (1977). Photometry with the 6-arcsec aperture centred on the peak of the ridge emission was obtained at 2.2 ( $K$ ), 1.6 ( $H$ ) and 1.2 ( $J$ )  $\mu\text{m}$  and yielded colour indices of  $H-K = 1.1$  and  $J-K = 2.3$ .

### Discussion

The position of the 2.2- $\mu\text{m}$  ridge is shown superimposed on an optical photograph of M82 in Fig. 2, the parallel lines indicating the FWHM extent of the source. There is a close correspondence between the ridge and the visible 0.9  $\mu\text{m}$  bright spots, which are marked as dots from the data of Kronberg, Pritchett & van den Bergh (1972). In particular the 2.2- $\mu\text{m}$  ridge embraces the bright visible regions A and E which have been convincingly interpreted as bright star clusters by O'Connell & Mangano (1978). A great deal of confused discussion about the identity of these various knots has been generated in the literature and there appears to be a general misconception that the 0.9  $\mu\text{m}$  and visible knots are distinct features. However, as O'Connell & Mangano (1978) have pointed out, they are, in the case of all of the knots engulfed by the 2.2- $\mu\text{m}$  ridge, the same physical entities. We have also marked the bright 10- $\mu\text{m}$  region investigated by Kleinmann, Wright & Fazio (1976) on Fig. 2 and, given the large uncertainty in its position, it may well be coincident with the 2.2- $\mu\text{m}$  ridge. The bright sub-arcsecond radio source is shown using the position from Kronberg & Wilkinson (1975). For the sake of clarity we have refrained from marking the centre of symmetry of the optical polarization pattern on Fig. 2 but its position is given by Bingham *et al.* (1976) as  $9^{\text{h}} 51^{\text{m}} 41^{\text{s}}.65, 69^\circ 55' 7''$  with an error of a few arcseconds.

The data on the reddening of the ridge are difficult to interpret properly in the absence of detailed information on the relative distribution of stars and dust. Using the Perseus curve of Johnson (1965), a  $J-K$  value of 2.3 implies a visible extinction of 10–15 mag, while Willner *et al.* (1977) derived a visible extinction of 25 mag from their Brackett line data. An extinction of  $\sim 20$  mag at  $V$  and 2 mag at  $K$  is not unreasonable and leads to a corrected absolute  $K$  magnitude for the ridge of  $-23$ . Obscuration variations across the ridge offer a ready explanation of the E–W asymmetry of the source.

The coincidence of the bright knots with the ridge leads naturally to the suspicion that the features may be associated. On the assumption that there are  $\sim 10$  star clusters similar to knots A and E the stellar models of O'Connell & Mangano (1978) give results compatible with the observed ridge luminosity, and offer a plausible explanation of the source. In such circumstances the 2.3- $\mu\text{m}$  CO signature observed by Willner *et al.* (1977) would be accounted for by the dominance of cool stars at this wavelength and the surrounding dusty medium may be sufficiently heated by the stellar continua to explain the 10–100- $\mu\text{m}$  luminosity.

Other explanations of the ridge are obviously not precluded and bearing in mind the 30 arcsec beam size used in the CO observations it is not even certain that this feature originates in the ridge. Clearly, higher resolution 2.2- $\mu\text{m}$  observations are required to resolve the detailed structure of this interesting source and small beam spectroscopy (6 arcsec or less) in the 2.0 and 2.4  $\mu\text{m}$  region is necessary if the emitting mechanism is to be established.

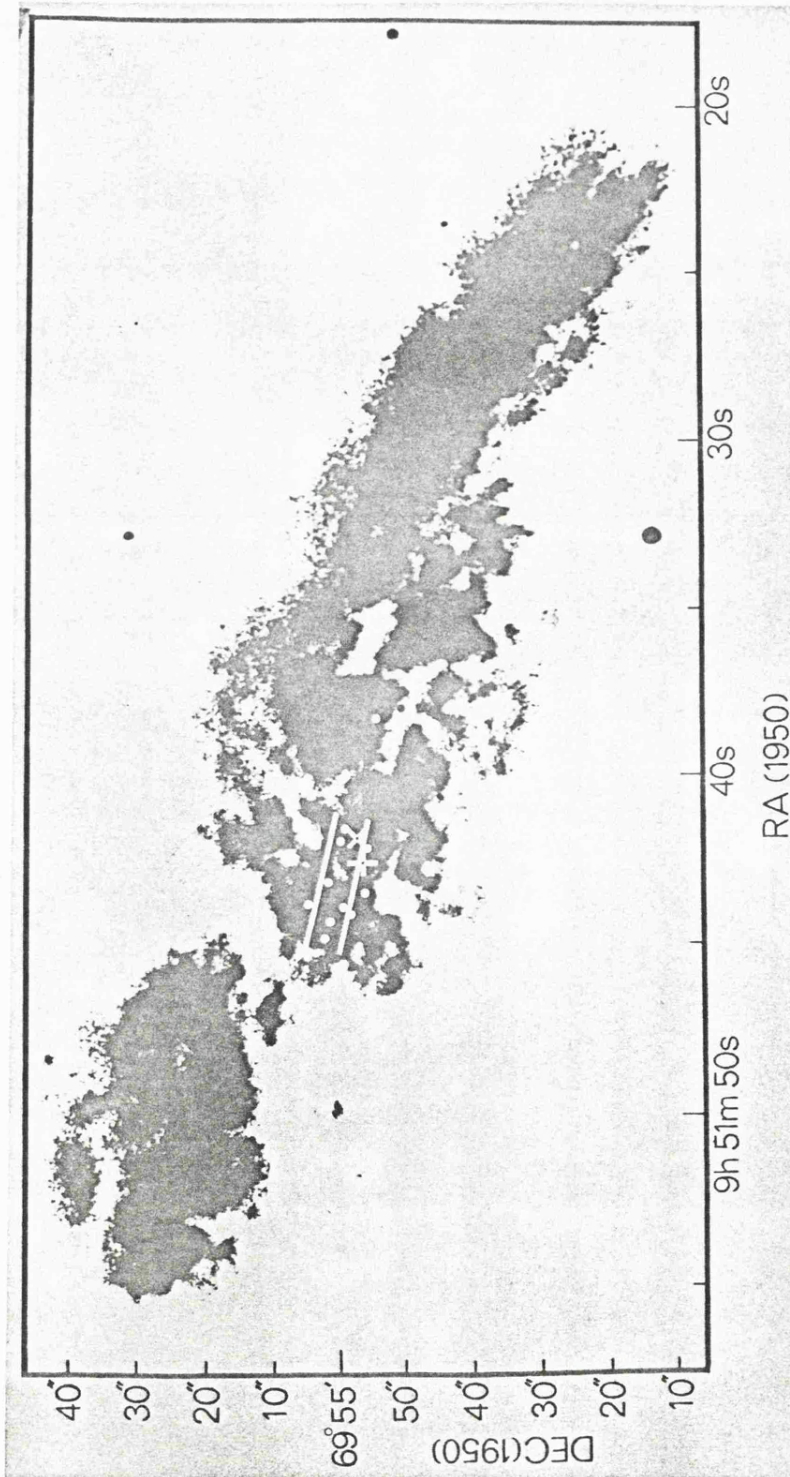


Figure 2. The 2- $\mu$ m ridge shown superimposed on a visible photograph of M82. White lines show the position and extent of the 2- $\mu$ m ridge (see text). Dots mark the various hot spots or bright spots listed by Kronberg & Wilkinson. + marks the 10- $\mu$ m centroid and X marks the VLBI source.

### Acknowledgments

We are grateful to Drs K. Taylor and R. C. Smith for many useful discussions and for suggestions for improving the presentation of our paper. We wish to thank PATT for allocation of telescope time and the staff of the Royal Greenwich Observatory for technical assistance. Financial support for this work was provided by the SRC, and one of us (JAA) is in receipt of a SRC Research Studentship.

### References

- Bingham, R. G., McMullan, D., Pallister, W. S., White, C., Axon, D. J. & Scarrott, S. M., 1976. *Nature*, **259**, 463.
- Cox, L. J., Hough, J. H. & McCall, A., 1978. *Mon. Not. R. astr. Soc.*, **185**, 199.
- Geldzahler, B. J., Kellermann, K. I., Shaffer, D. B. & Clark, B. G., 1977. *Astrophys. J.*, **215**, L5.
- Johnson, H. L., 1965. *Astrophys. J.*, **141**, 923.
- Johnson, H. L., Mitchell, R. I., Iriarte, B. & Wisniewski, W. Z., 1966. *Ariz. Uni. Lunar planet. Lab. Comms*, **4**, 99.
- Kleinmann, D. E. & Low, F. J., 1970a. *Astrophys. J.*, **161**, L203.
- Kleinmann, D. E. & Low, F. J., 1970b. *Astrophys. J.*, **159**, L165.
- Kleinmann, D. E., Wright, E. L. & Fazio, G. G., 1976. Preprint.
- Kronberg, P. P., Pritchett, C. J. & van den Bergh, S., 1972. *Astrophys. J.*, **173**, L47.
- Kronberg, P. P. & Wilkinson, P. N., 1975. *Astrophys. J.*, **200**, 430.
- O'Connell, R. W. & Mangano, J. J., 1978. *Astrophys. J.*, **221**, 62.
- Peimbert, M. & Spinrad, H., 1970. *Astrophys. J.*, **160**, 429.
- Solinger, A. B. & Markert, T., 1975. *Astrophys. J.*, **197**, 309.
- Willner, S. P., Soifer, B. T., Russell, R. W., Joyce, R. R. & Gillett, F. C., 1977. *Astrophys. J.*, **217**, L121.

### ACKNOWLEDGEMENTS

I would like to take the opportunity to extend my thanks to the many people who have helped me during my research work at Leicester. To my supervisor Dr. Dave Adams who initiated the work on galaxies at Leicester and with whom I have worked closely during the last three years, to Dr. Richard Jameson who has also given much support and encouragement, to Dr. Barry Giles for his excellent technical help in the winter 78/79 observations, to Phil Lawson for interfacing the tape-deck to Cyber and to Mandy Sherrington and Nick Eaton for help with the observations. I would also like to give a special thank you to Norma Corby for putting up with my excessive typing demands. Finally to my wife Clare whose selfless patience and constant encouragement have seen me through the last, long year.

## ABSTRACT

NEAR-INFRARED PHOTOMETRIC SCANNING OF GALAXIES

J. A. Abolins

Near-infrared surface-photometric observations of the galaxies M31, M82 and NGC 972 are described, and the results discussed in the light of other, recent literature. The techniques of near-infrared surface photometry are described and, as an introduction, a detailed review of near-infrared extragalactic astronomy is given.

Scans through the centre of M31 show the  $2.2 \mu\text{m}$  surface brightness distribution in the nuclear bulge follows the de Vaucouleurs' law and that the V-K gradient with the central  $\pm 5'$  arc is small,  $\Delta(V-K)_{r=5'} < 0.1$ . Comparisons are made with other published data.

Mapping of the active, central region of M82 reveals a  $2.2 \mu\text{m}$  "core" source ( $\sim 25'' \times 8''$ ) of very high surface brightness surrounded by a larger disk ( $\sim 90'' \times 35''$ ), which, though of lower surface brightness, is still brighter than the corresponding region in other normal, disk systems. Contour maps of the two regions are presented. The core source is approximately coincident and co-extensive with the diffuse radio emission and the visible "hot-spot" region, and is probably associated with a burst of star formation near the centre of the galaxy.

Two micron scans through NGC 972 yield a low resolution map of the whole galaxy which is similar in some respects to published blue-waveband maps and suggests that much of the unusual structure seen at shorter wavelengths cannot be due to dust obscuration as was previously assumed. An exciting possibility arising from this work is that the secondary feature in the southeast of the map may be a small, previously unsuspected, interacting galaxy, which might account for the IO-type appearance of NGC 972. The  $2.2 \mu\text{m}$  luminosity of NGC 972 is comparable to that of M82. The JHK colour indices suggest a free-free source near the galaxy's centre. These are the first reported observations of NGC 972 at infrared wavelengths.